

APPENDIX 2A
ILLUSTRATIVE EXAMPLES

Problem 2A-1. Free-Air Burst

Problem: Determine incident blast wave parameters for a point of interest in the air for a free air burst.

Procedure:

Step 1. Determine the charge weight and height of burst H_c . Select point of interest in the air relative to the charge.

Step 2. Apply a 20% safety factor to the charge weight.

Step 3. For the point of interest, calculate slant distance R and scaled slant distance Z:

$$Z = R/W^{1/3}$$

Step 4. Determine incident blast wave parameters from Figures 2-7 and 2-8 for the calculated value of the scaled slant distance Z.

From Figure 2-7 read:

Peak positive incident pressure P_{s0}

Shock front velocity U

Scaled unit positive incident impulse $i_s/W^{1/3}$

Scaled positive phase duration $t_o/W^{1/3}$

Scaled arrival time $t_A/W^{1/3}$

Scaled wave length of positive phase $L_w/W^{1/3}$

From Figure 2-8 Read:

Peak negative incident pressure P_{s0}^-

Scaled unit negative incident impulse $i_s^- /W^{1/3}$

Scaled negative phase duration $t_o^- /W^{1/3}$

Scaled wave length of negative phase $L_w^- /W^{1/3}$

Multiply scaled values by $W^{1/3}$ to obtain absolute values.

Example 2A-1. Free-Air Burst

Required: Incident blast wave parameters P_{s0} , P_{s0}^- , U , i_s , i_s^- , t_0 , t_0^- , t_A , L_w^- at a point 30 ft. below and 45 ft. away in the air from an air burst of 290 lbs. at a height of burst of 60 ft. above the ground.

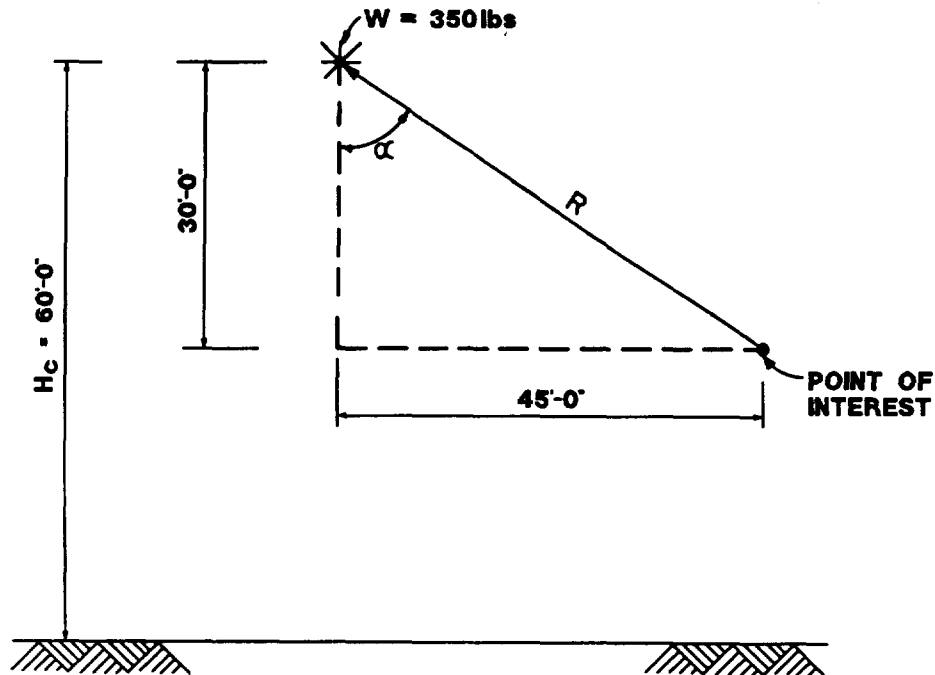


Figure 2A-1

Solution:

Step 1. Given: Charge weight = 290 lbs., $H_c = 60$ ft.

Step 2. $W = 1.2 (290) = 350$ lbs.

Step 3. For the point of interest:

$$R = \left[(45)^2 + (30)^2 \right]^{1/2} = 54.1 \text{ ft.}$$

$$Z = \frac{R}{W^{1/3}} = \frac{54.1}{(350)^{1/3}} = 7.67 \text{ ft./lb}^{1/3}$$

Step 4. Determine incident blast wave parameters for

$$Z = 7.67 \text{ ft./lb}^{1/3}$$

From Figure 2-7:

$$P_{so} = 11.2 \text{ psi}$$

$$U = 1.34 \text{ ft./ms}$$

$$i_s / W^{1/3} = 7.0 \text{ psi-ms/lb}^{1/3}, \quad i_s = 7.0 (350)^{1/3} = 49.3 \text{ psi-ms}$$

$$t_o / W^{1/3} = 2.05 \text{ ms/lb}^{1/3}, \quad t_o = 2.05 (350)^{1/3} = 14.45 \text{ ms.}$$

$$t_A / W^{1/3} = 3.15 \text{ ms/lb}^{1/3}, \quad t_A = 3.15 (350)^{1/3} = 22.2 \text{ ms}$$

$$L_w / W^{1/3} = 2.0 \text{ ft/lb}^{1/3}, \quad L_w = 14.09 \text{ ft}$$

From Figure 2-8:

$$P_{so} = 1.63 \text{ psi}$$

$$i_s^- / W^{1/3} = 7.2 \text{ psi-ms/lb}^{1/3}, \quad i_s^- = 7.2 (350)^{1/3} = 50.74 \text{ psi-ms}$$

$$t_o^- / W^{1/3} = 8.4 \text{ ms/lb}^{1/3}, \quad t_o^- = 8.4 (350)^{1/3} = 59.20 \text{ ms}$$

$$L_w^- / W^{1/3} = 5.8 \text{ ft/lb}^{1/3}, \quad L_w^- = 5.8 (350)^{1/3} = 40.87 \text{ ft.}$$

Problem 2A-2. Air Burst

Problem: Determine free-field blast wave parameters at a point on the ground for an air burst.

Procedure:

- Step 1. Select point of interest on the ground relative to the charge. Determine the charge weight, height of burst H_C , and ground distance R_C .
- Step 2. Apply a 20% safety factor to the charge weight.
- Step 3. Calculate scaled height of burst and angle of incidence α :

$$H_c / W^{1/3}$$

$$\alpha = \tan^{-1} (R_G/H_C)$$

Step 4. Determine peak reflected pressure $P_{r\alpha}$ and scaled unit positive reflected impulse $i_{r\alpha}/W^{1/3}$ in Mach front from Figures 2-9 and 2-10, respectively, for corresponding scaled height of burst and angle of incidence α :

Read $P_{r\alpha}$ and $i_{r\alpha}/W^{1/3}$

Multiply scaled value by $W^{1/3}$ to obtain absolute value.

Step 5. Read scaled distance Z from Figure 2-7 for corresponding peak incident pressure $P_{so} = P_{r\alpha}$ in the Mach front.

Step 6. Determine shock front velocity U and scaled time of arrival of blast wave $t_A/W^{1/3}$ from Figure 2-7 for value Z from step 5. Multiply scaled value of $W^{1/3}$ to obtain absolute value.

Step 7. Read scaled distance Z from Figure 2-7 for corresponding scaled unit positive incident impulse $i_s/W^{1/3} = i_{r\alpha}/W^{1/3}$ in the Mach front.

Step 8. Determine scaled positive duration of positive phase from Figure 2-7 for the value of Z from step 7. Multiply scaled value of $W^{1/3}$ to obtain absolute value.

Example 2A-2. Air Burst

Required: Free-field blast wave parameters P_{so} , U , i_s , t_o , t_A for an air burst of 20,800 lbs. at a ground distance of 300 ft. and a height of burst of 90 ft.

Solution:

Step 1. Given: Charge weight = 20,800 lb. $R_G = 300$ ft, $H_C = 90$ ft.

Step 2. $W = 1.20 (20,800) = 25,000$ lbs.

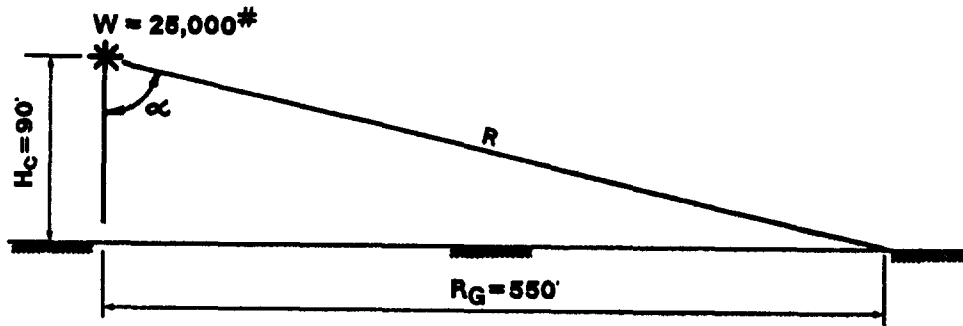


Figure 2A-2

Step 3. For point of interest

$$H_c/W^{1/3} = 90/(25,000)^{1/3} = 3.08 \text{ ft/lb}^{1/3}$$

$$\alpha = \tan^{-1} \left[\frac{R_G}{H_c} \right] = \tan^{-1}[300/90] = 73.3'$$

Step 4. Determine reflected pressure $P_{r\alpha}$ and reflected impulse in the Mach front from Figure 2-9 and 2-10.

$$H_c/W^{1/3} = 3.08 \text{ ft/lb}^{1/3} \text{ and } \alpha = 73.3'$$

$$P_{r\alpha} = 10.1 \text{ psi}$$

$$\frac{i_{r\alpha}}{W^{1/3}} = 9.2 \text{ psi-ms/lb}^{1/3}, \quad i_{r\alpha} = 9.2 (25,000)^{1/3} = 269.0 \text{ psi-ms}$$

Step 5. Read scaled distance Z from Figure 2-7 corresponding to $P_{so} = P_{r\alpha} = 10.1 \text{ psi}$

$$Z = 7.8 \text{ ft/lb}^{1/3}$$

Step 6. Determine U and $t_A/W^{1/3}$ from Figure 2-7 corresponding to Z

$$= 7.8 \text{ ft/lb}^{1/3}.$$

$$U = 1.38 \text{ ft/ms}$$

$$t_A/W^{1/3} = 300 \text{ ms/lb}^{1/3}, \quad t_A = 300 (25,000)^{1/3} = 8772.05 \text{ ms.}$$

Step 7. Read scaled distance Z from Fig. 2-7 corresponding to
 $i_s/W^{1/3} = i_{r\alpha}/W^{1/3} = 9.2 \text{ psi-ms/lb}^{1/3}$
 $Z = 5.7 \text{ ft/lb}^{1/3}$

Step 8. Determine $t_o/W^{1/3}$ from Figure 2-7 corresponding to
 $Z = 5.7 \text{ ft/lb}^{1/3}$
 $t_o/W^{1/3} = 155 \text{ ms/lb}^{1/3}$, $t_o = 155(25,000)^{1/3} = 4532.23 \text{ ms}$

Problem 2A-3. Surface Burst

Problem: Determine free-field blast wave parameters for a surface burst.

Procedure:

Step 1. Select point of interest on the ground relative to the charge. Determine the charge weight, and ground distance R_G .

Step 2. Apply a 20% safety factor to the charge weight.

Step 3. Calculate scaled ground distance Z_G :

$$Z_G = \frac{R_G}{W^{1/3}}$$

Step 4. Determine free-field blast wave parameters from Figure 2-15 for corresponding scaled ground distance Z_G :

Read:

Peak positive incident pressure P_{so}

Shock front velocity U

Scaled unit positive incident impulse $i_s/W^{1/3}$

Scaled positive phase duration $t_o/W^{1/3}$

Scaled arrival time $t_A/W^{1/3}$

Multiply scaled values by $W^{1/3}$ to obtain absolute values.

Example 2A-3. Surface Burst

Required: Free-field blast wave parameters P_{so} , U , i_s , t_o , t_A for a surface burst of 20,800 lbs at a distance of 530 ft.

Solution:

Step 1: Given: Charge weight = 20,800 lb. $R_G = 530$ ft.

Step 2. $W = 1.20 (20,800) = 25,000$ lbs.

Step 3. For point of interest:

$$Z_G = \frac{R_G}{W^{1/3}} = \frac{530}{(25,000)^{1/3}} = 18.1 \text{ ft/lb}^{1/3}$$

Step 4. Determine blast wave parameters from Figure 2-15 for

$$Z_G = 18.1 \text{ ft/lb}^{1/3}$$

$$P_{so} = 3.45 \text{ psi}$$

$$U = 1.22 \text{ ft/ms}$$

$$\frac{i_s}{W^{1/3}} = 4.7 \text{ psi-ms/lb}^{1/3}, i_s = 4.7(25,000)^{1/3} = 137.4 \text{ psi-ms}$$

$$\frac{t_o}{W^{1/3}} = 3.3 \text{ ms/lb}^{1/3}, t_o = 3.3(25,000)^{1/3} = 96.5 \text{ ms}$$

$$\frac{t_A}{W^{1/3}} = 10.6 \text{ ms/lb}^{1/3}, t_A = 10.6(25,000)^{1/3} = 310 \text{ ms}$$

Problem 2A-4 Shock Loads on Cubicle Walls

Problem: Determine the average peak reflected pressure and average scaled reflected impulse acting on the wall of a cubicle from an internal explosion. The cubicle is fully vented.

Procedure:

Step 1. Select from Figure 2-51 the structural configuration which will define the number N and location of effective reflecting surfaces for the wall of the structure in question. Determine the charge weight, and, as defined by the structural configuration chosen above, the charge location parameters R_A , h , l and the structural parameters L , H .

Step 2. Apply a 20% safety factor to the charge weight.

Step 3. Calculate the chart parameters $\frac{h}{H}$, $\frac{l}{L}$, $\frac{L}{R_A}$, and the scaled distance Z_A .

Note:

Use of the average pressure and impulse charts may require interpolation in many cases. Interpolation may be achieved by inspection for the scaled distance Z_A and by a graphical procedure for the chart parameters L/H , l/L , and h/H using 2 cycle x 2 cycle logarithmic graph paper. The following procedure will illustrate the interpolation of all three chart parameters.

Step 4. From table 2-3 determine the appropriate pressure and impulse charts for the number of adjacent reflecting surfaces N . Determine and tabulate the values of the average pressure P_r and average scaled impulse $i_r/W^{1/3}$ from these charts for the required L/R_A and Z_A and the following variables:

$L/H = 0.625, 1.25, 2.50, \text{ and } 5.00$

$l/L = 0.10, 0.25, 0.50, \text{ and } 0.75$

$h/H = 0.10, 0.25, 0.50, \text{ and } 0.75$

Step 5. a. Prepare four 2-cycle log-log charts with L/H as the lower abscissa, l/L as the upper abscissa, and P_r as the ordinate (one chart for each of the h/H ratios). On each chart for constant h/H and Z_A , plot i_b versus L/H for all l/L values.

Repeat with the ordinate labeled as $i_r/W^{1/3}$.

b. Using chart for $h/H = 0.10$, read values of P_r and $i_r/W^{1/3}$ versus l/L for required L/H . Tabulate results.

- c. Repeat step 5b for charts $h/H = 0.25, 0.50, \text{ and } 0.75$. Tabulate results.
 - d. On each h/H chart, plot P_r and $i_r/W^{1/3}$ versus l/L from steps 5b and 5c.
 - e. On each h/H chart, read P_r and $i_r/W^{1/3}$ for required l/L ratio.
 - f. On a fifth chart, plot P_r and $i_r/W^{1/3}$ from step 5e versus h/H .
- Step 6. For required h/H ratio, read P_r and $i_r/W^{1/3}$ from chart of step 5f.
- Step 7. Calculate duration of load on element from equation 2-2.

Example 2A-4 (A) Shock Loads on Cubicle Walls

Required: Average peak reflected pressure and average scaled reflected impulse on the side wall of a three-wall cubicle from an explosive charge of 205 lbs. The cubicle is fully vented.

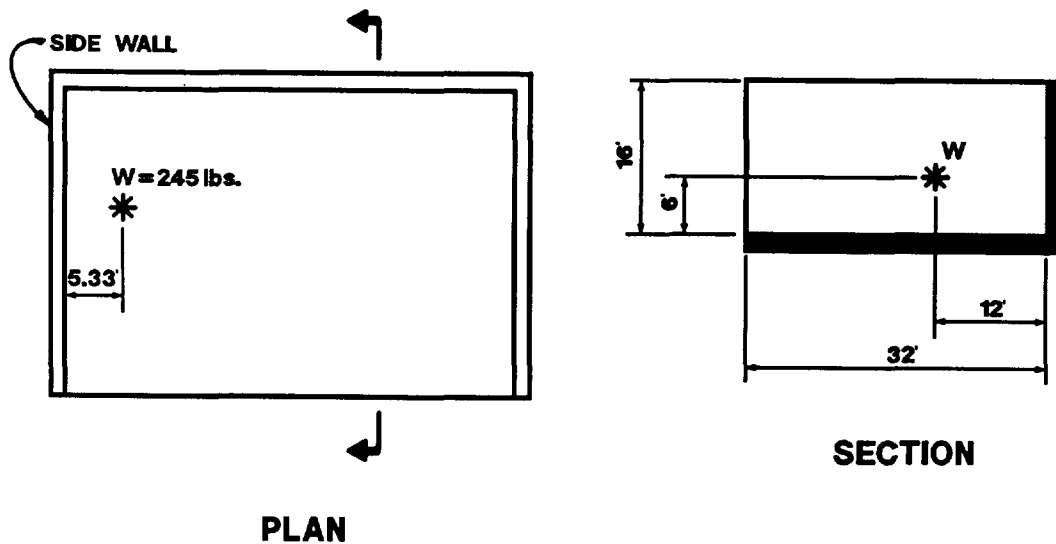


Figure 2A-3

Solution:

- | | | | |
|---------|----------------------|----------------------|--------------------------|
| Step 1. | $H = 16 \text{ ft.}$ | $L = 32 \text{ ft.}$ | Charge Weight = 205 lbs. |
| | $h = 6 \text{ ft.}$ | $l = 12 \text{ ft.}$ | $R_A = 5.33 \text{ ft.}$ |

Note:

For definition of terms, see Figure 2-51 (side wall of three wall cubicle, $N = 2$).

Step 2. $W = 1.20 (205) = 245$ lbs.

Step 3. $h/H = 0.375$ $1/L = 0.375$ $L/R_A = 6.00$ $L/H = 2.00$

$$Z_A = \frac{R_A}{W^{1/3}} = \frac{5.33}{(245)^{1/3}} = 0.85 \text{ ft/lb}^{1/3}$$

Interpolation is required for Z_A , L/H , $1/L$, and h/H .

Step 4. Determine and tabulate the values of P_r and $i_r/W^{1/3}$ from pressure and impulse charts (see table 2-3 for $N = 2$) for:

$$L/R_A = 6.00, \quad Z_A = 0.85$$

(interpolate by inspection) and for values given for L/H , $1/L$ and h/H . The results are tabulated in tables 2A-1 and 2A-2.

- Step 5.
- a. Plot P_r and $i_r/W^{1/3}$ versus L/H for the values of $1/L$ and constant h/H (fig. 2A-4 and 2A-5).
 - b. Determine P_r and $i_r/W^{1/3}$ for $L/H = 2.00$, $h/H = 0.10$, and various $1/L$ ratios by entering Figure 2A-4a and 2A-5a with $L/H = 2.00$
 - c. Repeat above step for $h/H = 0.25$, 0.50 , and 0.75 by entering Figures 2A-4b through d and 2A-5b through d with $L/H = 2.00$ (tabulation of results not shown).
 - d. On each h/H chart, plot P_r and $i_r/W^{1/3}$ (steps 5b and 5c) versus $1/L$ (upper abscissa of Figures 2A-4a through d and 2A-5a through d).
 - e. Determine P_r and $i_r/W^{1/3}$ for $1/L = 0.375$ on each h/H chart of Figures 2A-4 and 2A-5 with $1/L = 0.375$ and reading curves plotted in step 5d.

**Table 2A-1 Average Pressure
(Part 1)**

h/H	0.10				0.25			
1/L	0.10	0.25	0.50	0.75	0.10	0.25	0.50	0.75
L/H 0.625	462	569	598	569	533	665	701	665
1.25	749	932	980	932	943	1178	1238	1178
2.50	1200	1488	1562	1488	1432	1796	1881	1796
5.00	2032	2519	2635	2519	1870	2334	2437	2334
Fig.	2-64	2-65	2-66	2-67	2-68	2-69	2-70	2-71

**Table 2A-1 Average Pressure
(Part 2)**

h/H	0.50				0.75			
1/L	0.10	0.25	0.50	0.75	0.10	0.25	0.50	0.75
L/H 0.625	546	681	718	681	533	665	701	665
1.25	1017	1267	1333	1267	943	1178	1238	1178
2.50	1609	2028	2120	2028	1432	1796	1881	1796
5.00	1987	2456	2563	2456	2623	3119	3210	3119
Fig.	2-72	2-73	2-74	2-75	2-76	2-77	2-78	2-79

**Table 2A-2 Average Unit Impulses
(Part 1)**

h/H	0.10				0.25			
1/L	0.10	0.25	0.50	0.75	0.10	0.25	0.50	0.75
L/H 0.625	73	71	70	66	65	61	59	55
1.25	96	92	90	84	96	92	90	83
2.50	126	121	121	111	139	131	129	120
5.00	172	164	164	153	167	153	154	143
Fig.	2-113	2-114	2-115	2-116	2-117	2-118	2-119	2-120

**Table 2A-2 Average Unit Impulses
(Part 2)**

h/H	0.50				0.75			
1/L	0.10	0.25	0.50	0.75	0.10	0.25	0.50	0.75
L/H 0.625	64	61	58	54	59	56	53	49
1.25	93	87	83	76	87	79	76	70
2.50	129	120	118	109	117	106	103	95
5.00	186	168	168	158	201	189	189	179
Fig.	2-121	2-122	2-123	2-124	2-125	2-126	2-127	2-128

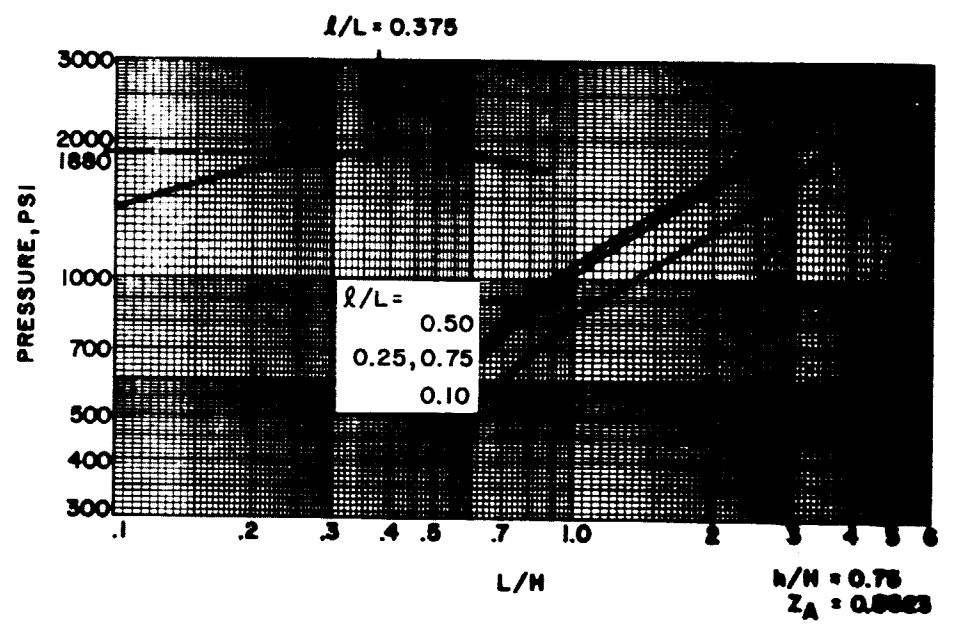
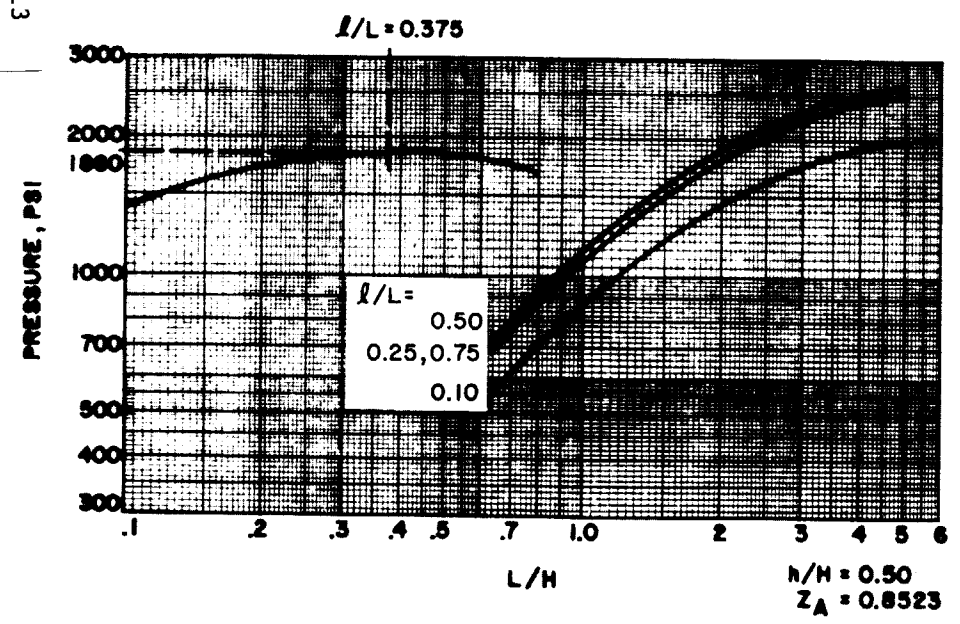
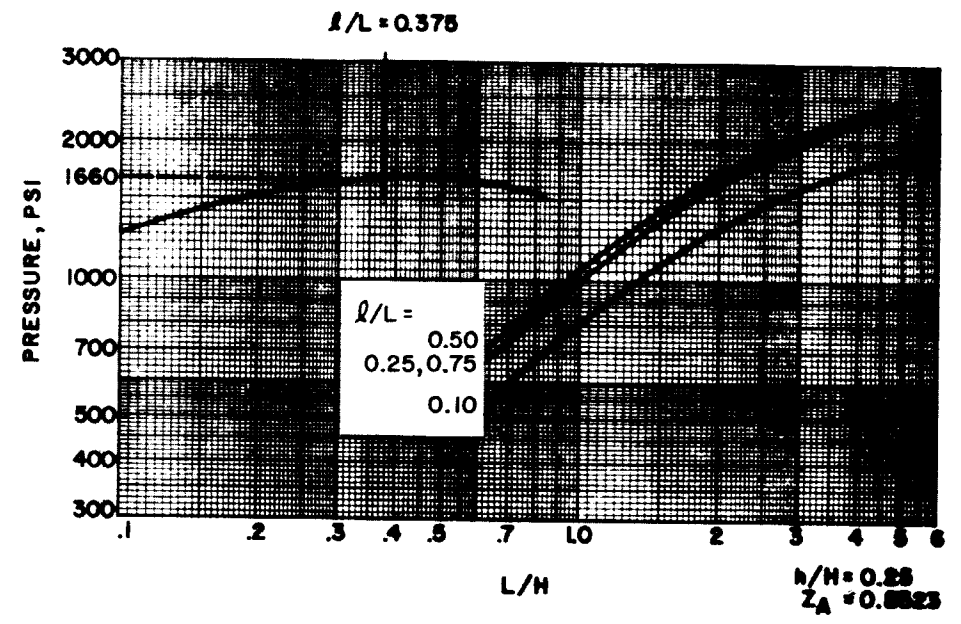
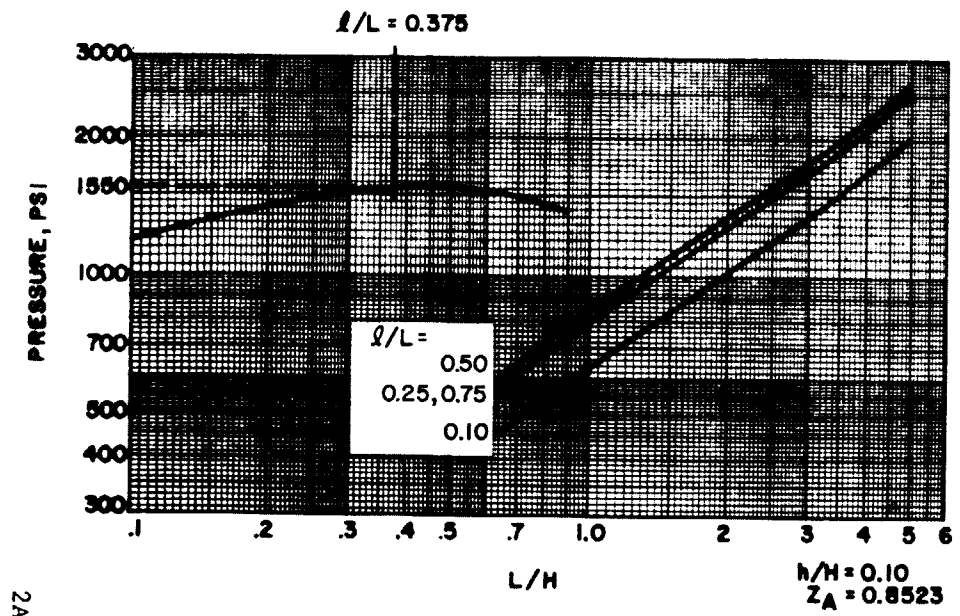
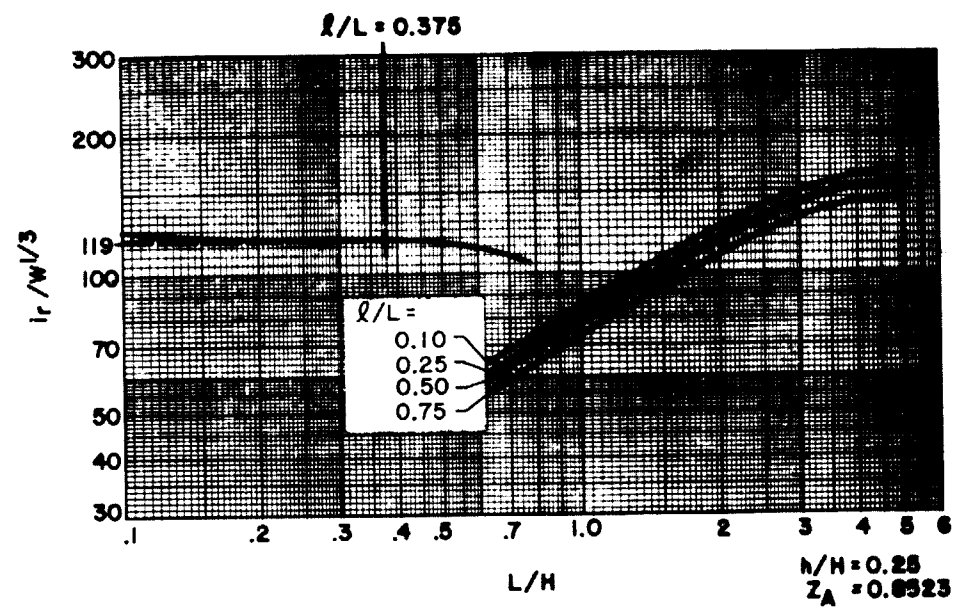
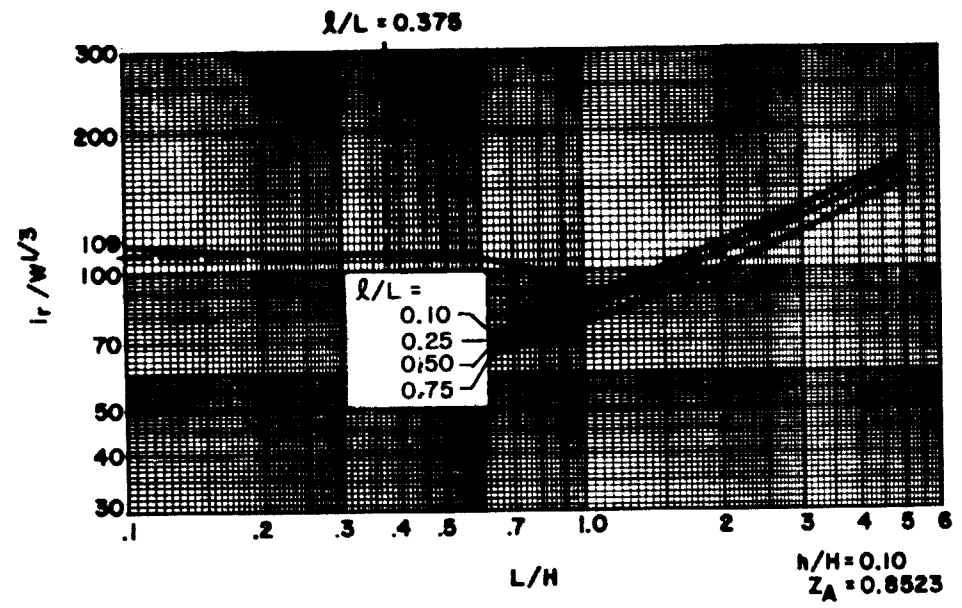


FIGURE 2A-4

2A-13



2A-14

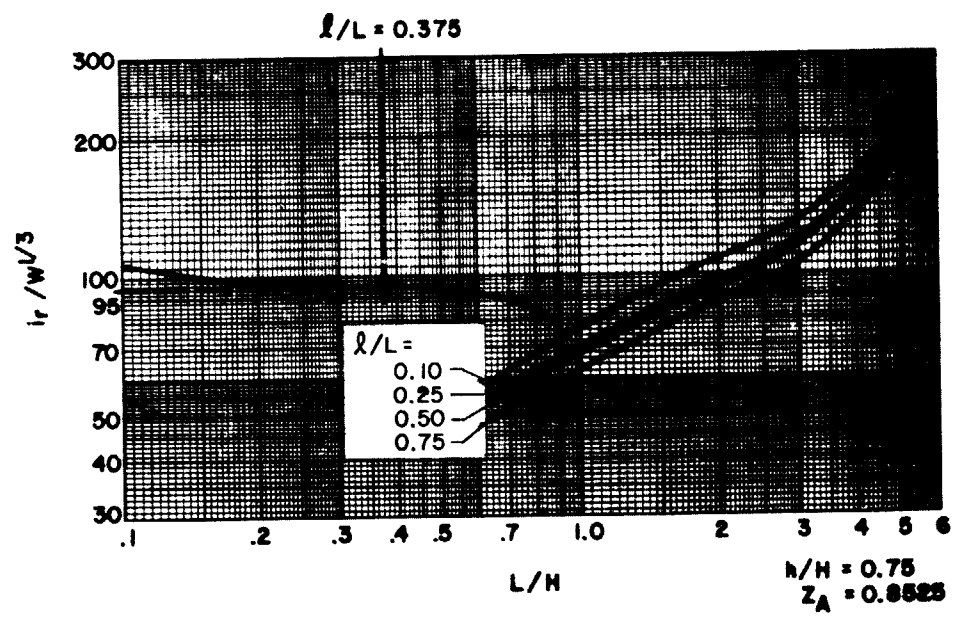
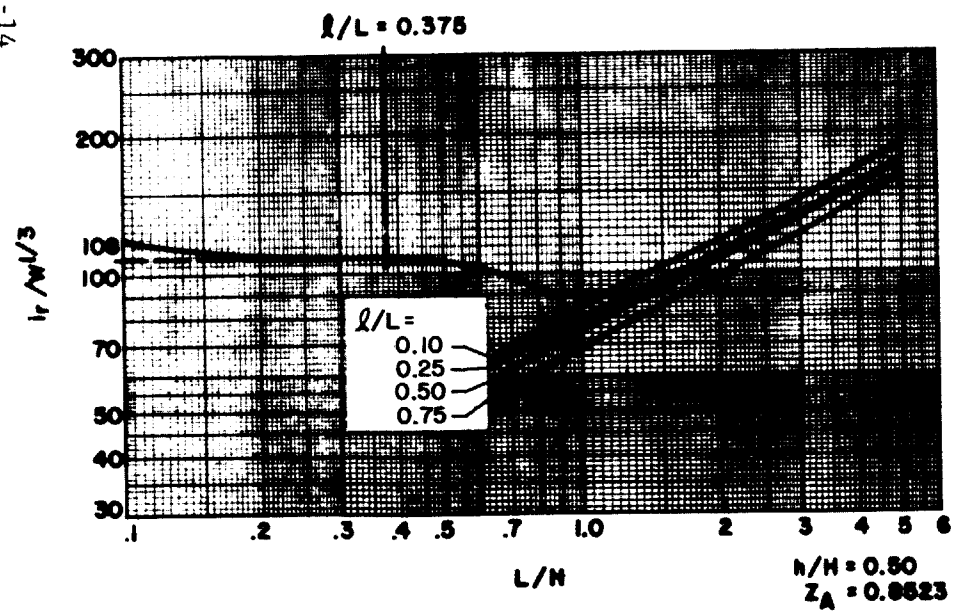


FIGURE 2A-5

h/H	P_r	$i_r/W^{1/3}$
0.10	1550	109
0.25	1660	119
0.50	1860	108
0.75	1880	95

f. Plot P_r and $i_r/W^{1/3}$ (step 5e) versus h/H (fig.2A-7).

Step 6. For $h/H = 0.375$ read $P_r = 1800$ psi on Figure 2A-7 and read $i_r/W^{1/3} = 115$ psi-ms/lb^{1/3} on Figure 2A-7

Step 7. Calculate duration of load on wall.

$$\tau_o = 2(i_r/W^{1/3}) (W)^{1/3} / P_r = 2 (115) (245)^{1/3} / 1800 = 0.80 \text{ ms}$$

Example 2A-4(B). Shock Loads on Cubicle Walls

Required: Average peak reflected pressure and average scaled reflected impulse on the back wall of a three-wall cubicle from an explosive charge of 3,750 lbs. The cubicle is fully vented and shown in Figure 2A-6.

Solution:

Step 1. H = 16 ft. L = 36 ft. Charge weight = 3,750 lbs.
 h = 4 ft. l = 9 ft. $R_A = 16.5$ ft.

Note:

For definition of terms, see Figure 2-51 (back wall of three-wall cubicle, N = 3).

Step 2. W = 1.20 (3,750) = 4,500 lbs.

Step 3. h/H = 0.25 l/L = 0.25 L/ R_A = 2.18 L/H = 2.25

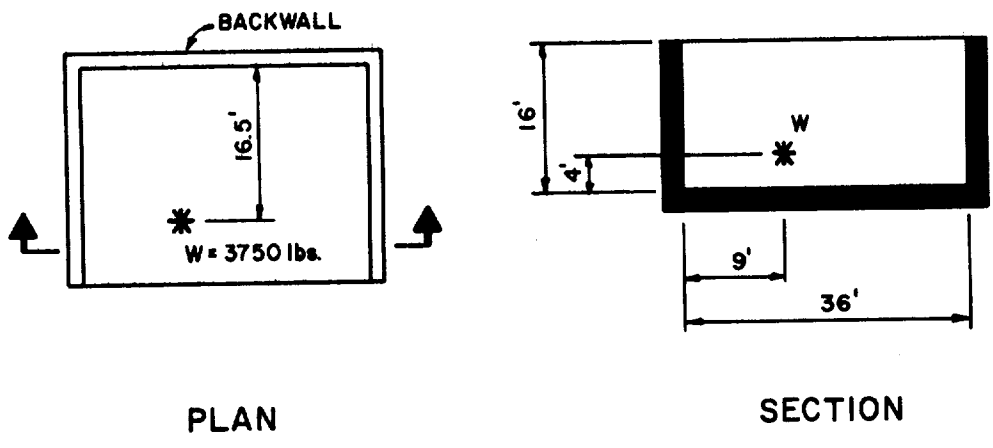
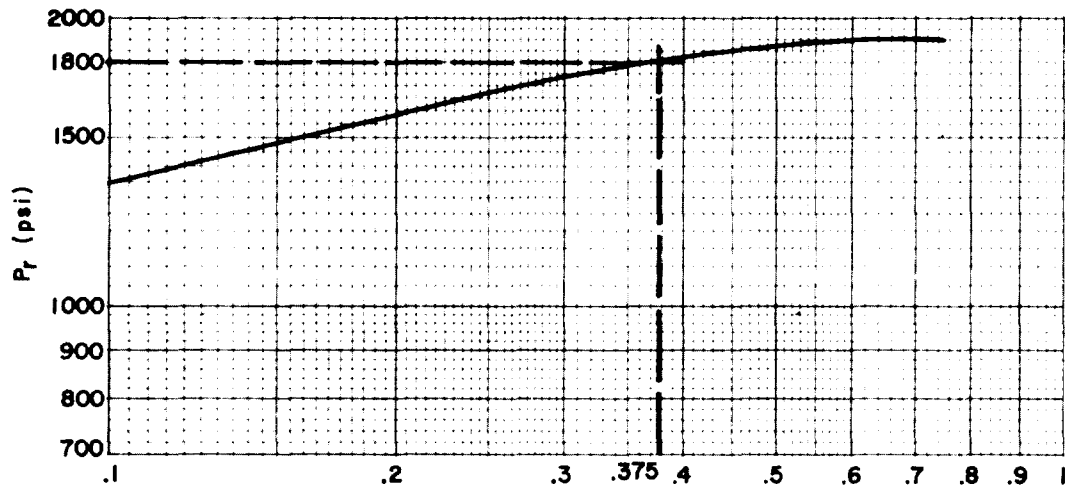
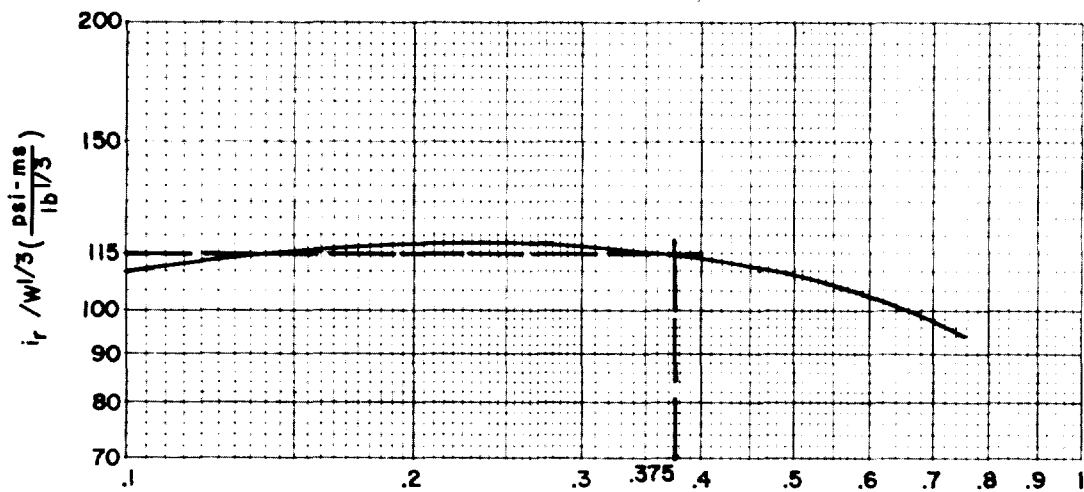


FIGURE 2A-6



h/H

(a)



h/H

(b)

R/A = 4.0	L/H = 2.0
L/R = 6.0	l/L = 0.375
Z/A = 0.85	h/H = 0.375

FIGURE 2A-7

$$Z_A = \frac{R_A}{W^{1/3}} = \frac{16.5}{(4,500)^{1/3}} = 1.00 \text{ ft/lb}^{1/3}$$

Interpolation is required for L/H

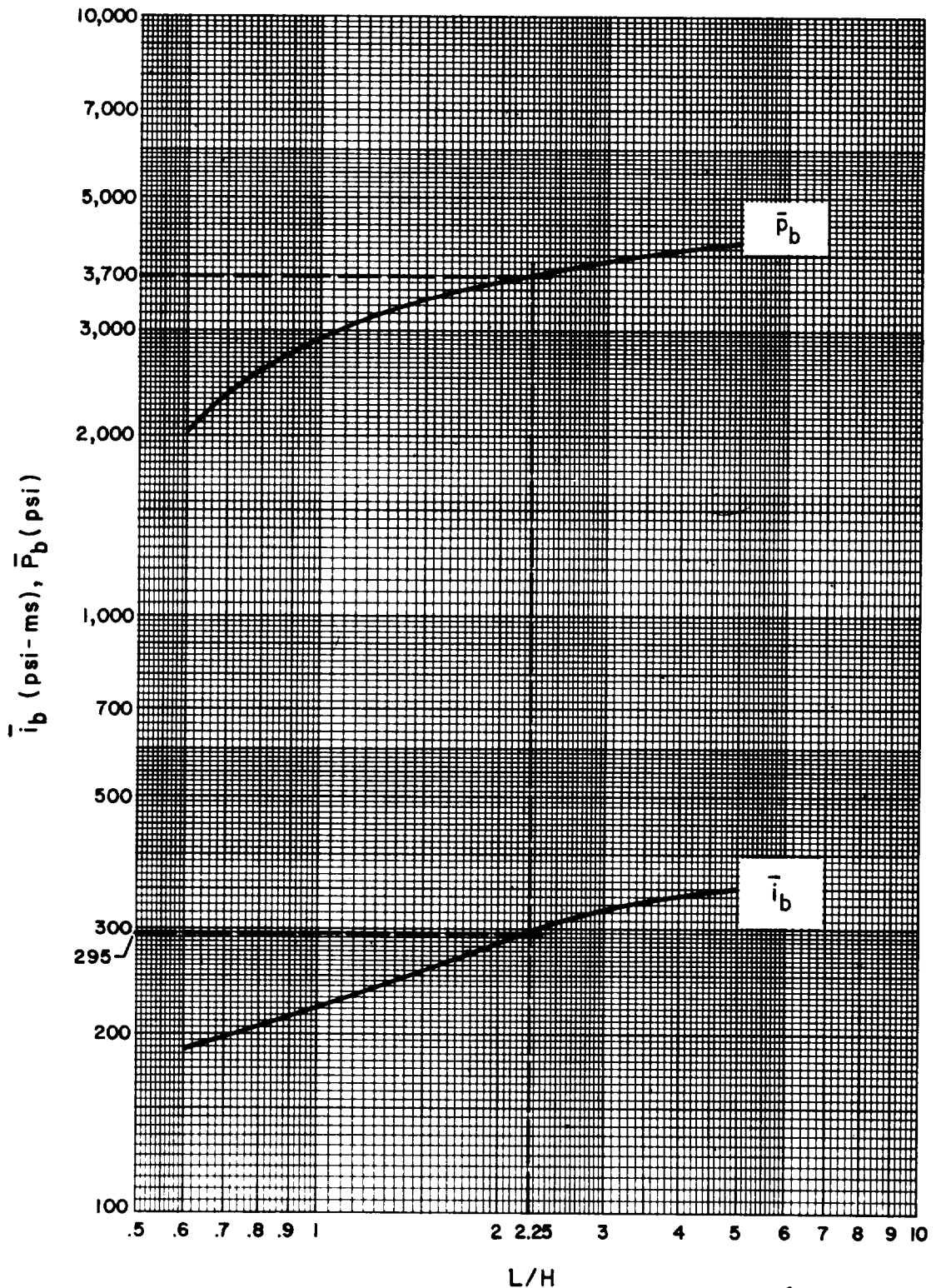
- Step 4. Determine the values of P_r and $i_r/W^{1/3}$ from Figures 2-84 and 2-133 (determined from table 2-3 for $N = 3$, $h/H = 0.25$, $l/L = 0.25$) for L/H ratios of 0.625, 1.25, 2.50 and 5.00.
- Step 5. Plot P_r and $i_r/W^{1/3}$ versus L/H (fig. 2A-8).
- Step 6. For $L/H = 2.25$ read, $P_r = 3700$ psi and $i_r/W^{1/3} = 295$ psi-ms/lb^{1/3} and on Figure 2A-8.
- Step 7. Calculate duration of load on wall (equation 2-2).
- $$t_o = 2(i_r/W^{1/3}) W^{1/3}/P_r = 2 (295) (4500)^{1/3}/3700 = 2.63 \text{ ms}$$

Problem 2A-5 Effect of Frangibility on Shock Loads

Problem: Determine average peak reflected pressure and average reflected impulse acting on the wall of a cubicle due to an internal explosion. One of the reflection surfaces is a frangible wall.

Procedure:

- Step 1. Determine the average peak reflected pressure P_r and the average reflected impulse acting on the element in question according to the procedure in problem 2A-4 assuming that the adjoining frangible element will remain in place and provide full reflection.
- Step 2. Determine the average reflected impulse acting on the element in question according to the procedure in problem A-4 assuming that the adjoining frangible element is not in place.
- Step 3. Subtract the average impulse determined in step 2 from the one in step 1.



$L/H = \ell/L = 0.25$
 $L/R_A = 2.1818$
 $Z_A = \sim 1.0$

FIGURE 2A-8

- Step 4. Calculate unit weight of the frangible element W_F and divide by the sixth root of the charge weight (apply a 20% factor of safety to the charge weight).
- Step 5. Calculate the normal scaled distance Z between the center of the charge and the surface of the frangible element.
- Step 6. Determine the reflection factor f_r from Figure 2-150 for the values of $W_F/W^{1/6}$ from step 4 and Z from step 5. Interpolate for value of Z if required.
- Step 7. Determine the magnitude of the impulse load reflected from the frangible element to the element in question by multiplying the value of the average impulse from step 3 and f_r from step 6.
- Step 8. a. Determine the total impulse load acting on the element in question by adding the impulse values from steps 2 and 7.
- b. The peak average reflected pressure of the shock load is equal to the value of P_r in step 1.
- c. Determine the duration of the load from equation 2-2.

Example 2A-5 Effect of Frangibility on Shock Loads

Required: Average peak reflected pressure and average reflected impulse on the back wall of the cubicle described in example 2A-4B except the left side wall is a 10 psf frangible element. The charge weight is 3,750 lbs (see Figure 2A-6).

Solution:

- Step 1. Assuming the frangible side wall provides full reflection of the blast wave, P_r and i_r for the back wall according to the procedure in problem 2A-4 are:
- $P_r = 3700.0$ psi
- $i_r = 4870.3$ psi-ms
- Step 2. Assuming no left side wall, the average reflected impulse on the back wall, according to procedure in problem 2A-4 is:
- $i_r = 3962.3$ psi-ms
- Step 3. Calculate the reflected impulse contributed by the left side wall by subtracting the impulse value of step 2 from step 1.
- $\delta i_r = 4870.3 - 3962.3 = 908.0$ psi-ms

- Step 4.
- a. $W_F = 10 \text{ lb/ft}^2$ (given)
 - b. $W = 3,750 \times 1.20 = 4,500 \text{ lbs}$
 - c. Calculate $W_F/W^{1/6}$ ratio:
 $W_F/W^{1/6} = 10/(4500)^{1/6} = 2.46$

- Step 5.
- a. $R = 9.0 \text{ feet}$ (see Figure 2A-6)
 - b. Calculate normal scale distance Z:

$$Z = \frac{R}{W^{1/3}} = \frac{9}{(4500)^{1/3}} = 0.545 \text{ ft/lb}^{1/3}$$

- Step 6. From Figure 2-150 where $W_F/W^{1/6} = 2.46$ and $Z = 0.545$ read:
 $f_r = 0.68$

- Step 7. Determine the magnitude of the impulse reflected from the frangible left side wall, using $f_r = 0.68$ and the impulse from step 3.

$$i_r \text{ (left side wall)} = 908 (0.68) = 617.4 \text{ psi-ms}$$

- Step 8.
- a. Calculate total reflected impulse on the back wall by adding impulse values from steps 2 and 7.

$$i_r \text{ (back wall)} = 3962.3 + 617.4 = 4579.7 \text{ psi-ms}$$

- b. Peak reflected pressure from step 1:

$$P_r = 3700 \text{ psi}$$

- c. Calculate duration of load on wall:

$$t_o = \frac{2i_r}{P_r} = \frac{2 (4579.7)}{3700} = 2.48 \text{ ms}$$

Problem 2A-6 Shock Loads on Frangible Elements

Problem: Determine the average peak reflected pressure and average reflected impulse acting on the frangible wall of a cubicle due to an internal explosion.

Procedure:

- Step 1. Determine the average peak reflected pressure P_r and the average reflected impulse acting on the element in question according to the procedure in problem 2A-4, assuming that the wall will remain intact.
- Step 2. Calculate the unit weight of the frangible element W_F and divide by the sixth root of the charge weight (apply a 20% factor of safety to the charge weight).
- Step 3. From Figure 2-7 determine the fictitious scaled distance Z which corresponds to the average scaled impulse determined in step 1.
- Step 4. Using the value of $W_F/W^{1/6}$ from step 2 and the Z from step 3, determine the reflection factor f_r from Figure 2-150. Interpolate for value of Z if required.
- Step 5.
 - a. Calculate the value of the average impulse contributing to the translation of the frangible element by multiplying the values of i_r and f_r of steps 1 and 4 respectively.
 - b. The peak average reflected pressure of the shock load is equal to the value of P_r in step 1.
 - c. Determine the duration of the load from equation 2-2.

Example 2A-6 Shock Loads on Frangible Elements

Required: Average peak reflected pressure and average scaled reflected impulse on the back wall of the cubicle described in example 2A-4 except the back wall is a 10 psf frangible wall. The charge weight is 3,750 lbs (see Figure 2A-6).

Solution:

- Step 1. P_r and i_r for the back wall, assuming it is a rigid element, according to procedure in problem 2A-4 are:

$$P_r = 3700.0 \text{ psi}$$

$$i_r/W^{1/3} = 295.0 \text{ psi}\cdot\text{ms}/\text{lb}^{1/3}$$

$$i_r = 4870.3 \text{ psi}\cdot\text{ms}$$

- Step 2. a. $W_F = 10.0 \text{ lb/ft}^2$ (given)
- b. $W = 3.750 \times 1.20 = 4,500 \text{ lbs}$
- c. Calculate $W_F/W^{1/6}$ ratio:
- $W_F/W^{1/6} = 10/(4500)^{1/6} = 2.46$
- Step 3. Read the fictitious scaled-distance Z corresponding to $i_r/W^{1/3} = 295$ from Figure 2-7.
- $Z = 0.82 \text{ ft/lb}^{1/3}$
- Step 4. From Figure 2-150 where $W_F/W^{1/6} = 2.46$ and $Z = 0.82$ read:
- $f_r = 0.74$
- Step 5. a. Calculate reflected impulse on the frangible back wall by multiplying the value of impulse from step 1 and $f_r = 0.74$
- i_r (frangible back wall) - $4870.3 (0.74) = 3604.0 \text{ psi-ms}$
- b. Peak reflected pressure from step 1.
- $P_r = 3700 \text{ psi}$
- c. Calculate duration of load on wall.
- $t_o = \frac{2i_r}{P_r} = \frac{2 (3604.0)}{3700} = 1.95 \text{ ms}$

Problem 2A-7 Gas Pressure

Problem: Determine the gas pressure-time loading inside a cubicle, with a small vent opening, due to an internal explosion. The vent opening may be sealed or unsealed with a frangible panel or cover.

Procedure:

- Step 1. Apply a 20% factor of safety to the charge weight.

- Step 2. Calculate the free volume inside the cubicle V_f .
- Step 3. Determine the charge weight to free volume ratio W/V_f .
- Step 4. Determine the peak gas pressure P_g from Figure 2-152 using the value of W/V_f from step 3.
- Step 5. Determine vent area A .
- Step 6. Determine scaled value of the vent area $A/V^{2/3}$.
- Step 7. a. Calculate the unit weight of the frangible panel W_F , if any.
- b. Calculate the scaled unit weight of the frangible panel or cover $W_F/W^{1/3}$. Use $W_F/W^{1/3} = 0$ for no cover.
- Step 8. Determine the scaled average reflected impulse on the element containing the vent opening with no cover according to the procedure outlined in Problem 2A-4 or on the frangible panel (cover) using the procedure of Problem 2A-6.
- Step 9. Determine the scaled gas impulse from Figures 2-153 to 2-164. Use the values of W/V_f from step 3, $W_F/W^{1/3}$ from step 7, $A/V^{2/3}$ from step 6 and $i_r/W^{1/3}$ from step 8. Interpolate for values of W/V_f and $i_r/W^{1/3}$ if required. Multiply by $W^{1/3}$ to calculate gas impulse.
- Step 10. Calculate the fictitious gas duration using equation 2-4 and values of P_g and i_g from steps 4 and 9 respectively.

Example 2A-7 (A) Gas Pressure (Small Vent Opening)

Required: Gas pressure-time loading inside a 10' x 10' x 10' cubicle with a 2' x 2' vent opening on the rear wall. The charge weight is 833.3 pounds.

Solution:

- Step 1. Charge weight:
- $$W = 833.3 \times 1.20 = 1,000 \text{ lbs}$$
- Step 2. Free volume inside the structure:
- $$V_f = 10' \times 10' \times 10' = 1,000 \text{ ft}^3$$

Step 3. Charge weight to free volume ratio:

$$W/V_f = 1000.0/1000.0 = 1.0$$

Step 4. Read P_g from fig. 2-152 for $W/V_f = 1.0$.

$$P_g = 2,650 \text{ psi}$$

Step 5. Vent area of 2' x 2' opening:

$$A = 2' \times 2' = 4 \text{ ft}^2$$

Step 6. Calculate scaled vent area:

$$A/V^{2/3} = 4/1000^{2/3} = .04 \text{ ft}^2/\text{ft}^2$$

Step 7. a. Vent has no cover.

b. Scaled weight of the cover:

$$W_F/W^{1/3} = 0$$

Step 8. Scaled average reflected impulse of the rear wall from procedure outlined in problem 2A-4:

$$i_r/W^{1/3} = 1225 \text{ psi-ms/lb}^{1/3}$$

Step 9. Read scaled gas impulse from Figures 2-162 to 2-164 for $A/V^{2/3} = 0.04$ and $W_F/W^{1/3} = 0.0$. Interpolate for scaled impulse of

$$i_r/W^{1/3} = 1225.$$

$$i_g/W^{1/3} = 7500 \text{ psi-ms/lb}^{1/3}$$

$$\therefore i_g = 7,500 \times 1,000^{1/3} = 75,000.0 \text{ psi-ms}$$

Step 10. Calculate fictitious duration of gas load from equation 2-4.

$$t_g = \frac{2i_g}{P_g} = \frac{2 \times 75,000.0}{2,650} = 56.6 \text{ ms}$$

Example 2A-7 (B) Gas Pressure (Frangible Wall)

Required: Gas pressure-time loading inside a 10' x 10' x 10' cubicle with a frangible wall of 10 psf as the rear wall. The charge weight is 833.3 pounds.

Solution:

Step 1. Charge weight:

$$W = 833.3 \times 1.2 = 1,000 \text{ lbs}$$

Step 2. Free volume inside the structure:

$$V_f = 10' \times 10' \times 10' = 1,000 \text{ ft}^3$$

Step 3. Charge weight to free volume ratio:

$$W/V_f = 1000/1000 = 1.0$$

Step 4. Read P_g from fig. 2-152 for $W/V_f = 1.0$.

$$P_g = 2650 \text{ psi}$$

Step 5. Vent area of frangible wall:

$$A = 10' \times 10' = 100 \text{ ft}^2$$

Step 6. Calculate scaled vent area:

$$A/V^{2/3} = 100/1000^{2/3} = 1.0 \text{ ft}^2/\text{ft}^2$$

Step 7. a. Unit density of the frangible wall:

$$W_F = 10.0 \text{ lbs}/\text{ft}^2 \text{ (given)}$$

b. Scaled weight of the frangible wall:

$$W_F/W^{1/3} = 10/1000^{1/3} = 1.0$$

Step 8. Scaled average reflected impulse of the rear frangible wall from procedure outlined in problem 2A-6:

$$i_r/W^{1/3} = 784 \text{ psi-ms}/\text{lb}^{1/3}$$

- Step 9. Read scaled gas impulse from Figures 2-162 to 2-164 for $A/V^{2/3} = 1.0$ and $W_F/W^{1/3} = 1.0$. Interpolate for scaled impulse of $i_r/W^{1/3} = 784$.

$$i_g/W^{1/3} = 400.0 \text{ psi-ms/lb}^{1/3}$$

$$\therefore i_g = 400.0 \times 1000^{1/3} = 4000 \text{ psi-ms}$$

- Step 10. Calculate fictitious duration of gas load from equation 2-4.

$$t_g = \frac{2i_g}{P_g} = \frac{2 \times 4000}{2650} = 3.02 \text{ ms}$$

Problem 2A-8 Leakage Pressures from Fully Vented Three Wall Cubicle

Problem: Determine free-field blast wave parameters at a distance from a fully vented explosion inside a three wall cubicle.

Procedure:

- Step 1. Determine charge weight, distance in the desired direction and volume of structure.
- Step 2. Apply a 20% safety factor to the charge weight.
- Step 3. Calculate scaled distance and W/V ratio.
- Step 4. Determine peak positive pressures using Figures 2-168 or 2-169.
- Step 5. Determine maximum peak pressure for side and back directions from Figure 2-170 using W/V ratio.
- Step 6. For W/V ratio determine scaled positive impulses using Figures 2-171 to 2-182. Multiply by $W^{1/3}$ to calculate actual value of impulses.
- Step 7. Determine shock parameters from Figure 2-15 corresponding to the peak pressure from step 4, except for the normal reflected impulse where the scaled impulse from step 6 should be used.

Example 2A-8 Leakage Pressures from Fully Vented Three Wall Cubicle

Required: Blast wave parameters at a distance of 200 ft. from an explosion located at the center of a three wall cubicle with no roof. The charge weight is 833.3 lbs. and the interior dimensions of the cubicle are 17.5 ft. x 17.5 ft. x 13 ft. high. Calculate the parameters at the front, side and back of the cubicle.

Solution:

Step 1. Given:

- a. Charge weight = 833.3 lbs.
- b. R = 200 ft. in all directions.
- c. $V = 17.5 \times 17.5 \times 13 = 3.980 \text{ ft}^3$

Step 2. Calculate W:

$$W = 1.20 \times \text{Charge Weight} = 1.20 \times 833.3 = 1000 \text{ lbs.}$$

Step 3. Calculate:

- a. Scaled distance Z,

$$Z = \frac{R}{W^{1/3}} = \frac{200}{(1000)^{1/3}} = 20 \text{ ft/lbs}^{1/3}$$

- b. W/V ratio,

$$W/V = 1000/3.980 = 0.25 \text{ lbs/ft}^3$$

Step 4. Determine peak incident pressure from Figure 2-168:

$$P_{so} \text{ (front)} = 5.5 \text{ psi}$$

$$P_{so} \text{ (side)} = 4.0 \text{ psi}$$

$$P_{so} \text{ (back)} = 2.8 \text{ psi}$$

Step 5. For $W/V = 0.25$, read the maximum peak incident pressures from Figure 2-170:

$$(P_{so})_{\text{max}} \text{ (back and side)} = 47.0 \text{ psi} > 4.0 > 2.8$$

Step 6. Scaled positive impulse, for $Z = 20 \text{ ft/lb}^{1/3}$ and $W/V = 0.25 \text{ lbs/ft}^3$

$$i_s/W^{1/3} \text{ (front)} = 5.5 \text{ psi-ms/lb}^{1/3} \quad \text{Figure 2-171}$$

$$i_s \text{ (front)} = 5.5 \times 1000^{1/3} = 55 \text{ psi-ms}$$

$$i_s/W^{1/3} \text{ (side)} = 4.5 \text{ psi-ms/lb}^{1/3} \quad \text{Figure 2-173}$$

$$i_s \text{ (side)} = 4.5 \times 1000^{1/3} = 45 \text{ psi-ms}$$

$$i_s/W^{1/3} \text{ (back)} = 3.8 \text{ psi-ms/lb}^{1/3} \quad \text{Figure 2-175}$$

$$i_s \text{ (back)} = 3.8 \times 1000^{1/3} = 38 \text{ psi-ms}$$

Step 7. For peak positive pressures (P_{s0}) read shock parameters from Figure 2-15 at front, side and back directions.

a. For P_{s0} (front) = 5.5 psi (Step 4)

$$U = 1.28 \text{ ft/ms}$$

$$t_o/W^{1/3} = 2.95 \text{ ms/lb}^{1/3}$$

$$t_o = 2.95 \times 1000^{1/3} = 29.5 \text{ ms}$$

$$t_A/W^{1/3} = 7.00 \text{ ms/lb}^{1/3}$$

$$t_A = 7.00 \times 1000^{1/3} = 70.0 \text{ ms}$$

b. For P_{s0} (side) = 4.0 psi (Step 4)

$$U = 1.24 \text{ ft/ms}$$

$$t_o/W^{1/3} = 3.20 \text{ ms/lb}^{1/3}$$

$$t_o = 3.2 \times 1000^{1/3} = 32.0 \text{ ms}$$

$$t_A/W^{1/3} = 9.30 \text{ ms/lb}^{1/3}$$

$$t_A = 9.3 \times 1000^{1/3} = 93.0 \text{ ms}$$

c. For P_{so} (back) = 2.8 psi

$$U = 1.20 \text{ ft/ms}$$

$$t_o/W^{1/3} = 3.45 \text{ ms/lb}^{1/3}$$

$$t_o = 3.45 \times 1000^{1/3} = 34.5 \text{ ms}$$

$$t_A/W^{1/3} = 12.90 \text{ ms/lb}^{1/3}$$

$$t_A = 12.9 \times 1000^{1/3} = 129.0 \text{ ms}$$

**Problem 2A-9 Leakage Pressure from Partially Vented
Four Wall Cubicle**

Problem: Determine free-field blast wave parameters at a distance from a partially vented explosion inside a four wall cubicle.

Procedure:

- Step 1. Determine charge weight, distance to point in question, vent area and volume of structure.
- Step 2. Apply a 20% safety factor to the charge weight.
- Step 3. Calculate distance Z , $A/V^{2/3}$ ratio and $AW^{1/3}/V$ ratio.
- Step 4. Determine peak positive pressure using Figure 2-184.
- Step 5. Determine scaled positive impulses using Figure 2-185. Multiply by $W^{1/3}$ to calculate actual value of impulses.

- Step 6. Determine shock parameters from Figure 2-15. Use the peak pressure from step 4, except for normal reflected impulse where the scaled impulse(s) from step 5 should be used.

Example 2A-9 Leakage Pressure from Partially Vented Four Wall Cubicle

Required: Blast wave parameters at distance of 200 ft. from a charge located in an above ground four wall cubicle. The circular vent is located at the center of the roof and has a diameter of 4 ft. The charge is 833.3 lbs and located at the center of 17.5' x 17.5' x 13' cubicle. Top of the roof is 15 feet above the ground level.

Solution:

- Step 1. Given (see Figure 2-183b for parameters):

a. Charge weight = 833.3 lbs.

b. $R = 200$ ft., $h = 15$ ft.

$$d_1 = \left[(4/2)^2 + (15 - 13/2)^2 \right]^{1/2} = 8.73 \text{ ft.}$$

$$d_2 = (17.5 - 4)/2 = 6.75 \text{ ft.}$$

$$d_3 = \left[(15)^2 + (200 - 4/2 - 6.75 - 15)^2 \right]^{1/2} = 176.89 \text{ ft.}$$

$$R' = d_1 + d_2 + h + d_3 = 8.73 + 6.75 + 15 + 176.89 = 207.37 \text{ ft.}$$

c. $A = \pi(2)^2 = 12.57 \text{ ft}^2$

d. $V = 17.5 \times 17.5 \times 13 = 3,980 \text{ ft}^3$

- Step 2. Calculate W:

$$W = 1.20 \times \text{charge weight} = 1.20 \times 833.3 = 1000 \text{ lbs.}$$

- Step 3. Calculate:

a. Scaled distance Z.

$$Z = \frac{R'}{W^{1/3}} = \frac{207.37}{1000^{1/3}} = 20.7 \text{ ft/lb}^{1/3}$$

b. $A/V^{2/3} = 12.57/(3980)^{2/3} = 0.05$

c. $AW^{1/3}/V = 12.57 (1000)^{1/3} / 3,980 = 0.0316 \text{ lb}^{1/3}/\text{ft}$

Step 4. Peak positive pressure from Figure 2-184 for $Z = 20.7$ and $A/V^{2/3} = .050$.

$\therefore P_{so} = 0.95 \text{ psi}$

Step 5. Peak positive pressure impulse from Figure 2-185 for $Z = 20.7$ and

$AW^{1/3}/V = .0316$.

$i_s/W^{1/3} = 1.80 \text{ psi-ms/lb}^{1/3}$

$i_s = 1.8 \times 1000^{1/3} = 18.0 \text{ psi-ms}$

Step 6. For peak positive pressure $P_{so} = .95 \text{ psi}$, read shock parameters from Figure 2-15.

$U = 1.12 \text{ ft/ms}$

$t_o/W^{1/3} = 4.5 \text{ ms/lb}^{1/3}$

$t_o = 4.5 \times 1000^{1/3} = 45.0 \text{ ms}$

$t_A/W^{1/3} = 35.0 \text{ ms/lb}^{1/3}$

$t_A = 35.0 \times 1000^{1/3} = 350.0 \text{ ms}$

Problem 2A-10 External Blast Loads on Structures

Problem: Determine the pressure-time blast loading curves on a rectangular structure from an external explosion.

Procedure:

- Step 1. Determine the charge weight, ground distance R_G , height of burst H_c (for air burst) and structure dimensions.
- Step 2. Apply a 20% safety factor to the charge weight.
- Step 3. Select several points on the structure (front wall, roof, rear wall, etc.) and determine free-field blast wave parameters for each point. For air burst, follow the procedure outlined in problem 2A-2; a surface burst, problem 2A-3; and leakage pressures, problem 2A-8 or 2A-9.

Step 4. For the front wall:

- a. Calculate peak positive reflected pressure $P_{r\alpha} = C_{r\alpha} \times P_{so}$. Read value of $C_{r\alpha}$ for P_{so} and α from Figure 2-193.
- b. Read scaled unit positive reflected impulse $i_{r\alpha}/W^{1/3}$ from Figure 2-194 for P_{so} and α . Multiply scaled value by $W^{1/3}$ to obtain absolute value.

Note: If wave front is not plane, use average values.

Step 5. Determine positive phase of front wall loading.

- a. Determine sound velocity in reflected overpressure region C_r from Figure 2-192 for peak-incident pressure P_{so} .
- b. Calculate clearing time t_c :

$$t_c = \frac{4S}{(1 + R) C_r} \text{ (ms)} \quad \text{(eq. 2-3)}$$

where:

S = height of front wall or one-half its width, whichever is smaller.

G = maximum of wall height or one-half its width

R = S/G

- c. Calculate fictitious positive phase duration t_{of} :

$$t_{of} = \frac{2i_s}{P_{so}} \quad \text{(eq. 2-6)}$$

- d. Determine peak dynamic pressure q_0 from Figure 2-3 for P_{so} .

- e. Calculate $P_{so} + C_D q_0$. Obtain C_D from paragraph 2-15.3.2.
- f. Calculate fictitious duration t_{rf} of the reflected pressure.

$$t_{rf} = \frac{2i_{r\alpha}}{P_{r\alpha}} \quad (\text{eq. 2-11})$$

- g. Construct the positive pressure-time curve of the front wall similar to Figure 2-191. The actual loading is the smaller of the impulse (area under curve) due to reflected pressure or cleared reflected pressure plus incident pressure.

Step 6. Determine negative phase of the front wall loading.

- a. Read the values of Z from Figure 2-15 for the value of $P_{r\alpha}$ from step 4a and $i_{r\alpha}/W^{1/3}$ from step 4b.
- b. Determine $P_{r\alpha}^-$ and $i_{r\alpha}^-/W^{1/3}$ from Figure 2-16 for the corresponding values of Z from step 6a. Multiply scaled value of the negative impulse by $W^{1/3}$ to obtain absolute value.
- c. Calculate the fictitious duration of the negative reflected pressure.

$$t_{rf}^- = 2i_{r\alpha}^-/P_{r\alpha} \quad (\text{eq. 2-7})$$

- d. Calculate rise time of the negative pressure by multiplying t_{rf}^- by 0.27 (Section 2-15.3.2).
- e. Construct the negative pressure-time curve similar to Figure 2-191.

Step 7. Determine positive phase of side wall loading.

- a. Calculate the wave length to span length ratio L_{wf}/L at front of the span.
- b. Read values of C_E , $t_d/W^{1/3}$ and $t_{of}/W^{1/3}$ from Figures 2-196, 2-197 and 2-198 respectively.
- c. Calculate P_R , t_r and t_o .
- d. Determine dynamic pressure q_0 from Figure 2-3 for P_R .
- e. Calculate $P_R = C_E P_{sof} + C_D q_0$ (eq. 2-12). Obtain C_D from paragraph ???
- f. Construct positive phase pressure-time curve similar to Figure 2-195.

- Step 8. Determine negative phase of side wall loading.
- Determine value of C_E^- and $t_{of}^-/W^{1/3}$ for the value of L_{wf}/L from step 7a from Figures 2-196 and 2-198 respectively.
 - Calculate $P_r = C_E \times P_{sof}$ and t_{of} .
 - Calculate rise time of negative phase equal to $0.27 t_{of}$ (section 2-15.3.2).
 - Construct the negative pressure-time curve similar to Figure 2-195.
- Step 9. Determine roof loading. Follow procedure outlined for side wall loading.
- Step 10. Determine rear wall loading. Follow procedure outlined for side wall loading. For the purpose of calculations, assume that the back wall is rotated to a horizontal position (see Figure 2-199).

Example 2A-10 External Blast Loads on Structures

Required: Determine pressure-time blast loading curves for the front wall, roof, rear half of the side walls and rear wall of the structure shown in Figure 2A-9 for a surface burst of 5,000 lbs. at a distance from the front wall of 155 ft. Structure width is 30 ft. and the shock front is plane.

- Step 1. Given: Charge weight = 5,000 lbs., $R_G = 155$ ft.
- Step 2. $W = 1.2 (5,000) = 6,000$ lbs.
- Step 3. Determine free-field blast wave parameters P_{so} , t_A , L_w and t_o at points 1 through 3 and i_s at point 1.

For point 1:

a.
$$Z_G = \frac{R_G}{W^{1/3}} = \frac{155}{6000^{1/3}} = 8.53 \text{ ft/lb}^{1/3}$$

- b. Determine free-field blast wave parameters from Figure 2-15 for $Z_G = 8.53 \text{ ft/lb}^{1/3}$

$P_{so} = 12.8 \text{ psi}$

$t_A/W^{1/3} = 3.35 \text{ ms/lb}^{1/3} \therefore t_A = 3.35 (6000)^{1/3} = 60.9 \text{ ms}$

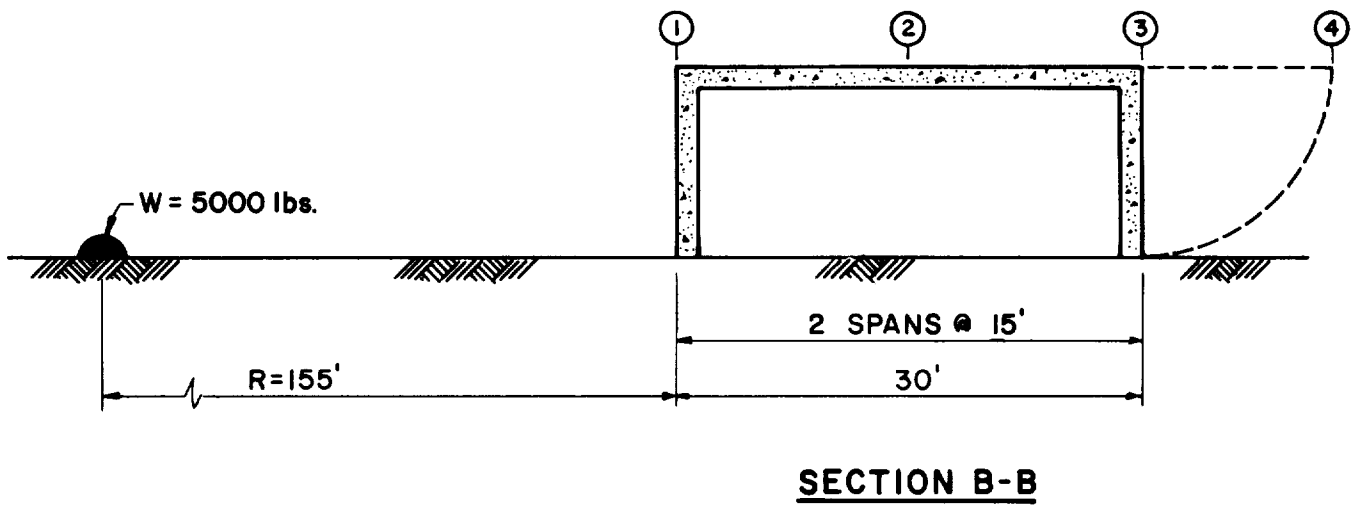
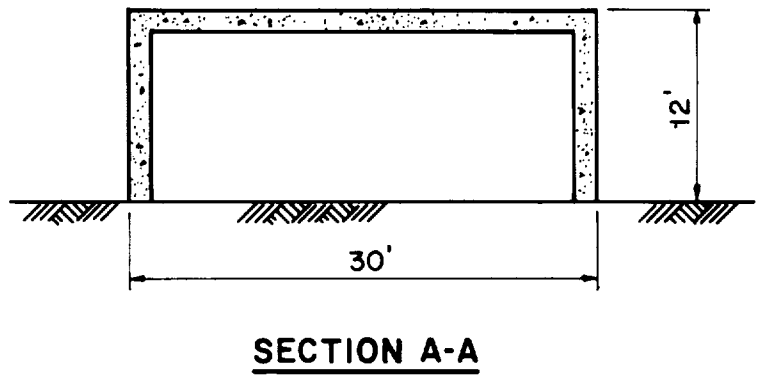
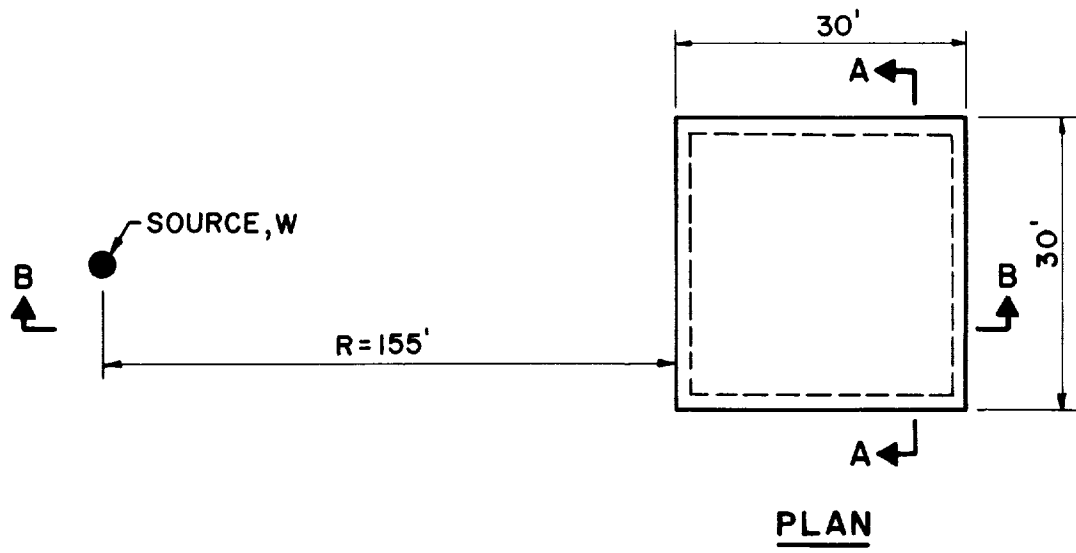


FIGURE 2A-9

$$L_w/W^{1/3} = 2.10 \text{ ft/lb}^{1/3} \therefore L_w = 2.10 (6000)^{1/3} = 38.2 \text{ ft}$$

$$t_o/W^{1/3} = 2.35 \text{ ms/lb}^{1/3} \therefore t_o = 2.35 (6000)^{1/3} = 42.7 \text{ ms}$$

- c. Determine incident impulse from Figure 2-15 for $Z_G = 8.53 \text{ ft/lb}^{1/3}$.

$$\frac{i_s}{W^{1/3}} = 9.0 \text{ psi-ms/lb}^{1/3} \therefore i_s = 9.0 (6000)^{1/3} = 163.5 \text{ psi-ms}$$

- d. Repeat steps 3a and 3b for points 2 and 3. Results are tabulated below.

Point No.	R_G (ft)	Z_G (ft/lb ^{1/3})	P_{so} (psi)	$t_A/W^{1/3}$ (ms/lb ^{1/3})	t_A (ms)
1	155.0	8.53	12.8	3.35	60.9
2	170.0	9.35	10.8	3.90	70.9
3	185.0	10.18	9.0	4.60	83.6

$L_w/W^{1/3}$ (ft/lb ^{1/3})	L_w (ft)	$t_o/W^{1/3}$ (ms/lb ^{1/3})	t_o (ms)	$i_s/W^{1/3}$ (psi-ms/lb ^{1/3})	i_s (psi-ms)
2.10	38.2	2.35	42.7	9.00	163.5
2.24	40.7	2.48	45.1	-	-
2.35	42.7	2.62	47.6	-	-

- Step 4. Determine front wall reflected pressure and impulse.

- a. Read $C_{r\alpha}$ for $P_{so} = 12.8 \text{ psi}$ and $\alpha = 0^\circ$ from Figure 2-193 for point 1.

$$C_{r\alpha} = 2.70 \text{ then } P_{r\alpha} = C_{r\alpha} \times P_{so} = 2.70 \times 12.8 = 34.6 \text{ psi}$$

- b. Read $i_{r\alpha}/W^{1/3}$ for $P_{so} = 12.8 \text{ psi}$ and $\alpha = 0^\circ$ from Figure 2-194 for point 1.

$$i_{r\alpha}/W^{1/3} = 17.0 \text{ then } i_{r\alpha} = 17.0 (6,000)^{1/3} = 308.9 \text{ psi-ms}$$

Step 5. Front wall loading, positive phase.

- a. Calculate sound velocity in reflected overpressure region C_r from Figure 2-192 for $P_{so} = 12.8$ psi.

$$C_r = 1.325 \text{ ft/ms}$$

- b. Calculate clearing time t_c from eq. 2-3:

$$t_c = \frac{4S}{(1 + R)C_r} \quad (\text{eq. 2-3})$$

where:

$$S = 12.0 \text{ ft} < 30./2$$

$$G = 30./2 = 15.0 \text{ ft} > 12.0 \text{ ft.}$$

$$R = S/G = 12./15. = .80$$

then:

$$t_c = \frac{4 \times 12}{(1 + 0.80) 1.325} = 20.1 \text{ ms}$$

- c. Calculate t_{of} from eq. 2-11. Use impulse from step 3c.

$$t_{of} = \frac{2i_s}{P_{so}} = \frac{2 \times 163.5}{12.8} = 25.5 \text{ ms}$$

- d. Determine q_o from Figure 2-3 for $P_{so} = 12.8$ psi.

$$q_o = 3.5 \text{ psi}$$

- e. Calculate $P_{so} + C_D q_o$:

$$C_D = 1.0 \text{ from section 2-15.3.2}$$

then,

$$P_{so} + C_D q_o = 12.8 + (1.0 \times 3.5) = 16.3 \text{ psi}$$

- f. Calculate t_{rf} from eq. 2-11 and results of step 4.

$$t_r = \frac{2i_{r\alpha}}{P_{r\alpha}} = \frac{2 \times 308.9}{34.6} = 17.9 \text{ ms}$$

- g. Construct the pressure time curve. See Figure 2A-10.

Note: The reflected pressure-time curve is used for design since the reflected impulse is less than the impulse produced by the clearing time.

Step 6. Negative phase loading, front wall.

- a. Read the values of Z corresponding to $P_{r\alpha} = 34.6$ (step 4a) and $i_{r\alpha}/W^{1/3} = 17.0$ (step 4b) from Figure 2-15.

$$P_{r\alpha} = 34.6 \quad \text{then,} \quad Z(P_{r\alpha}) = 8.5$$

$$i_{r\alpha}/W^{1/3} = 17.0 \quad \text{then,} \quad Z(i_{r\alpha}/W^{1/3}) = 10.4$$

- b. Using the Z values from step 6a and Figure 2-16 determine values of $P_{r\alpha}^-$ and $i_{r\alpha}^-$ (Peak pressure and impulse in negative phase).

$$Z(P_{r\alpha}) = 8.5 \quad \text{then,} \quad P_{r\alpha} = 3.25 \text{ psi}$$

$$Z(i_{r\alpha}/W^{1/3}) = 10.4 \quad \text{then,} \quad i_{r\alpha}^-/W^{1/3} = 14.6 \text{ psi-ms/lb}^{1/3}$$

and

$$i_{r\alpha} = 14.6 \times (6,000)^{1/3} = 265.3 \text{ psi-ms}$$

- c. Calculate fictitious duration t_{rf}^- .

$$t_{rf}^- = \frac{2 i_{r\alpha}^-}{P_{r\alpha}^-}$$

$$t_{rf}^- = \frac{2 \times 265.3}{3.25} = 163.3 \text{ ms}$$

- d. Calculate negative phase rise time:

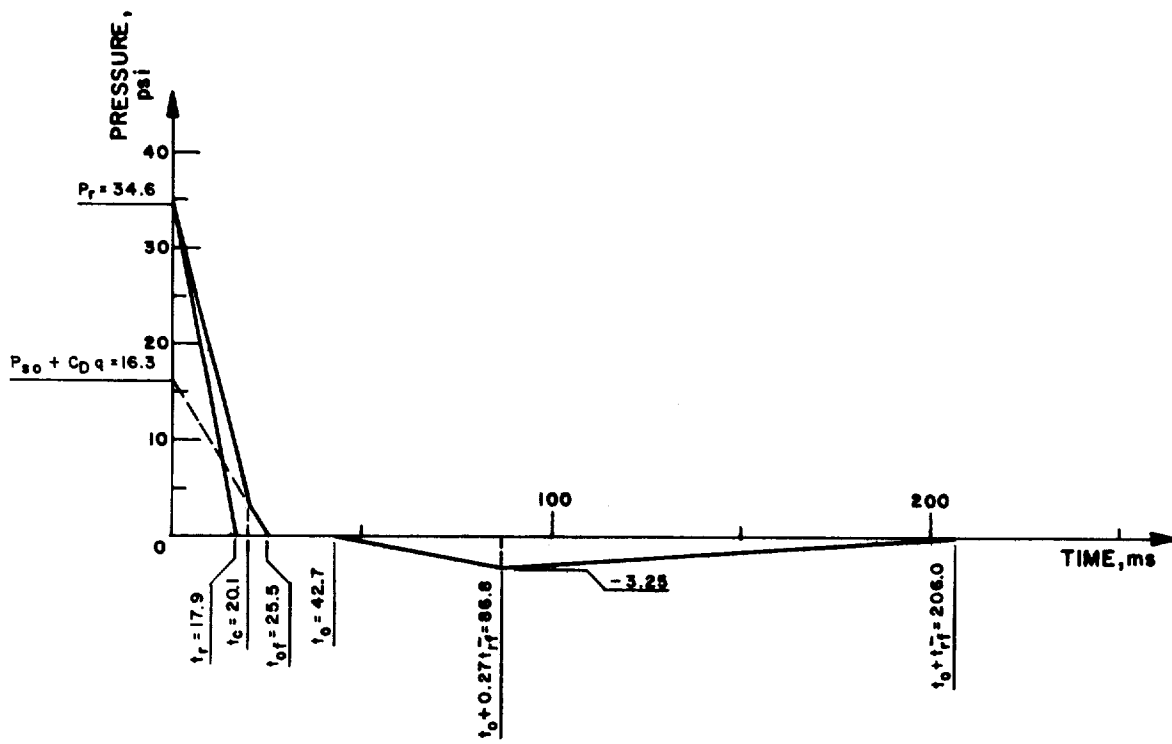


FIGURE 2A-10

$$0.27 \times t_{rf}^- = .27 \times 163.3 = 44.1 \text{ ms}$$

- e. Construct the negative pressure-time curve.

$$t_o = 42.7 \text{ ms (Point 1, step 3d)}$$

$$t_o + 0.27 t_{rf}^- = 42.7 + 44.1 = 86.8 \text{ ms}$$

$$t_o = t_{rf}^- = 42.7 + 163.3 = 206.0 \text{ ms}$$

The negative pressure-time curve is plotted in Figure 2A-10.

- Step 7. Side wall loading, positive phase, calculate the loading on the rear-half of the wall (Point 2 to 3, Figure 2A-9).

- a. Calculate L_{wf}/L ratio:

$$L = 15.0 \text{ ft (Point 2 to 3)}$$

$$L_{wf} = 40.7 \text{ ft (step 3d)}$$

then,

$$L_{wf}/L = 40.7 / 15.0 = 2.71$$

- b. Read $C_E, t_d/W^{1/3}$ and $t_{of}/W^{1/3}$ for $L_{wf}/L = 2.71$ and $P_{sof} = 10.8$ (step 3d, Point 2)

$$C_E = .76 \text{ fig. 2-196}$$

$$t_d/W^{1/3} = .66 \text{ fig. 2-197}$$

$$t_{of}/W^{1/3} = 2.47 \text{ fig. 2-198}$$

- c. Calculate $C_E P_{sof}$, t_d and t_{of} using results of step 7b.

$$C_E P_{sof} = .76 \times 10.8 = 8.2$$

$$\therefore t_r = .66 \times (6,000)^{1/3} = 12.0 \text{ ms}$$

$$\therefore t_{of} = 2.47 \times (6,000)^{1/3} = 44.9 \text{ ms}$$

d. Determine q_o from Figure 2-3 for $C_E P_{sof} = 8.2$ psi.

$$q_o = 1.55 \text{ psi}$$

e. Calculate peak positive pressure from eq. 2-12.

$$C_D = -0.40 \text{ from section 2-15.3.2}$$

$$C_E P_{sof} + C_D q_o = .76 \times 10.8 + (-0.40 \times 1.55) = 7.6 \text{ psi}$$

f. Construct the pressure-time curve.

See Figure 2A-11 below.

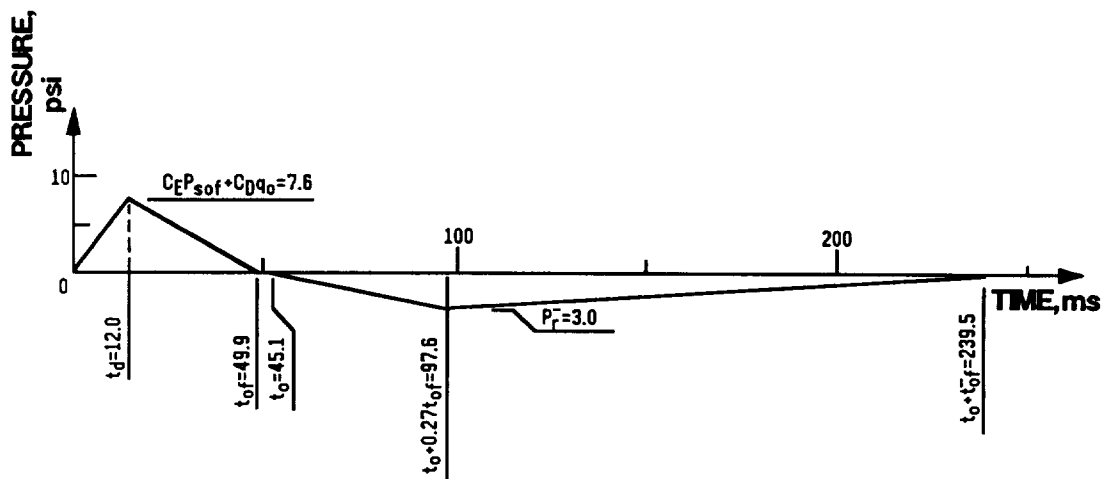


Figure 2A-11

Step 8. Negative phase loading on the rear-half of the side wall.

- a. Read values of C_E^- and $t_{of}^-/W^{1/3}$ for $L_{wf}/L = 2.71$ (Step 7a) from Figures 2-196 and 2-198 respectively.

$$C_E^- = .28$$

$$t_{of}^-/W^{1/3} = 10.7 \text{ ms/lb}^{1/3}$$

- b. Calculate P_r^- and t_{of}^- :

$$P_r^- = C_E^- \times P_{sof} = .28 \times 10.8 = 3.0 \text{ psi}$$

$$t_{of}^- = 10.7 \times (6,000)^{1/3} = 194.4 \text{ ms}$$

- c. Negative phase rise time:

$$0.27 t_{of}^- = .27 \times 194.4 = 52.5 \text{ ms}$$

- d. Construct the negative pressure-time curve.

$$t_o = 45.1 \text{ ms (Point 2, step 3d)}$$

$$t_o + 0.27 t_{of} = 45.1 + 52.5 = 97.6 \text{ ms}$$

$$t_o + t_{of} = 45.1 + 194.4 = 239.5 \text{ ms}$$

The negative pressure-time curve is plotted in Figure 2A-11.

- Step 9. Calculate roof loading. (Point 1 to 3, Figure 2A-9)

- a. Calculate L_{wf}/L ratio:

$$L = 30.0 \text{ ft (Point 1 to 3)}$$

$$L_{wf} = 38.2 \text{ ft (step 3d) then,}$$

$$L_{wf}/L = 38.2/30.0 = 1.27$$

- b. Read C_E , $t_d/w^{1/3}$ and $t_{of}/w^{1/3}$ for $L_{wf}/L = 1.27$ and $P_{sof} = 12.8$ psi (step 3d, Point 1) then,

$$C_E = .52 \quad \text{fig. 2-196}$$

$$t_d/w^{1/3} = 1.25 \quad \text{fig. 2-197}$$

$$t_{of}/w^{1/3} = 3.10 \quad \text{fig. 2-198}$$

- c. Calculate $C_E P_{sof}$, t_d and t_{of} using results of step 9b.

$$C_E P_{sof} = .52 \times 12.8 = 6.66$$

$$t_d = 1.25 \times (6,000)^{1/3} = 22.7 \text{ ms}$$

$$t_{of} = 3.10 \times (6,000)^{1/3} = 56.3 \text{ ms}$$

- d. Determine q_o from Figure 2-3 for $C_E P_{sof} = 6.66$ psi.

$$q_o = 1.05 \text{ psi}$$

- e. Calculate maximum pressure from eq. 2-12:

$$C_D = -0.40 \text{ From section 2-15.3.2}$$

$$C_E P_{sof} + C_D q_o = .52 \times 12.8 + (-0.40 \times 1.05) = 6.24 \text{ psi}$$

- f. Construct the pressure-time curve.

See Figure 2A-12 below.

- g. Read values of C_E^- and $t_{of}^-/w^{1/3}$ for $L_{wf}/L = 1.27$ (step 9a) from Figures 2-196 and 2-198 respectively.

$$C_E^- = .26$$

$$t_{of}^-/w^{1/3} = 11.7 \text{ ms/lb}^{1/3}$$

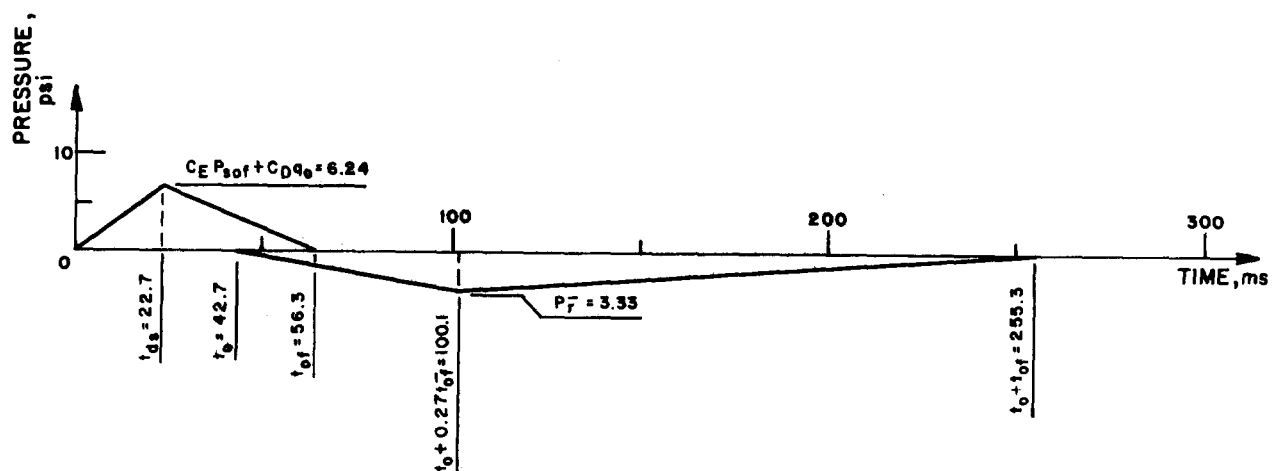


FIGURE 2A-12

- h. Calculate P_r^- and t_{of}^- :

$$P_r^- = C_E^- \times P_{sof} = .26 \times 12.8 = 3.33 \text{ psi}$$

$$t_{of}^- = 11.7 \times (6,000)^{1/3} = 212.6 \text{ ms}$$

- i. Negative phase rise time:

$$0.27 t_{of}^- = .27 \times 212.6 = 57.4 \text{ ms}$$

- j. Construct the negative pressure-time curve.

$$t_o = 42.7 \text{ ms (Point 1, step 3d)}$$

$$t_o + .27 t_{of}^- = 42.7 + 57.4 = 100.1 \text{ ms}$$

$$t_o + t_{of}^- = 42.7 + 212.6 = 255.3 \text{ ms}$$

The negative pressure-time curve is plotted in Figure 2A-12

- Step 10. Calculate rear wall loading (Point 3 to 4, Figure 2A-9). Assume rear wall is rotated to a horizontal position.

- a. Calculate L_{wf}/L ratio:

$$L = 12.0 \text{ ft (Point 3 to 4 or height of the structure)}$$

$$L_{wf} = 42.7 \text{ ft (step 3d), then,}$$

$$L_{wf}/L = 42.7 / 12.0 = 3.56$$

- b. Read C_E , $t_d/w^{1/3}$ and $t_{of}/w^{1/3}$ for $L_{wf}/L = 3.56$ and $P_{sob} = 9.0$ psi (step 3d, point 3).

$$C_E = .83$$

fig. 2-196

$$t_d/w^{1/3} = .51$$

fig. 2-197

$$t_{of}/W^{1/3} = 2.45$$

fig. 2-198

- c. Calculate $C_E P_{sob}$, t_r and t_o using results of step 10b.

$$\therefore C_E P_{sob} = .83 \times 9.0 = 7.47 \text{ psi}$$

$$\therefore t_d = .51 \times (6,000)^{1/3} = 9.3 \text{ ms}$$

$$\therefore t_{of} = 2.45 \times (6,000)^{1/3} = 44.5 \text{ ms}$$

- d. Determine q_o from Figure 2-3 for $C_E P_{sob} = 7.47 \text{ psi}$

$$q_o = 1.30 \text{ psi}$$

- e. Calculate maximum pressure from eq. 2-12:

$$C_D = -0.40 \text{ from section 2-15.3.2}$$

$$C_E P_{sob} + C_D q_o = .83 \times 9.0 + (-0.40 \times 1.30) = 6.95 \text{ psi}$$

- f. Construct the pressure-time curve.

See Figure 2A-13 below.

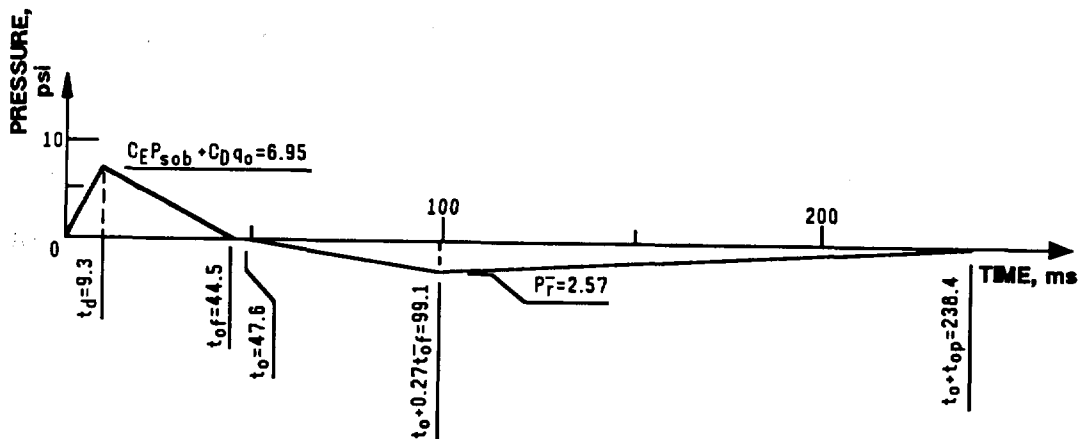


Figure 2A-13

- g. Read values of C_E^- and $t_{of}^-/W^{1/3}$ for $L_{wf}/L = 3.56$ (step 10a) from Figures 2-196 and 2-198 respectively.

$$C_E^- = .285$$

$$t_{of}^-/W^{1/3} = 10.5 \text{ ms/lb}^{1/3}$$

- h. Calculate P_r^- and t_{of}^- :

$$P_r^- = C_E^- \times P_{sob} = .285 \times 9.0 = 2.57 \text{ psi}$$

$$t_{of}^- = 10.5 \times (6,000)^{1/3} = 190.8 \text{ ms}$$

- i. Negative phase rise time:

$$0.27 t_{of}^- = .27 \times 190.8 = 51.5 \text{ ms}$$

- j. Construct the negative pressure-time curve.

$$t_o = 47.6 \text{ ms (Point 3, step 3d)}$$

$$t_o + .27 t_{of}^- = 47.6 + 51.5 = 99.1 \text{ ms}$$

$$t_o + t_{of}^- = 47.6 + 190.8 = 238.4 \text{ ms}$$

The negative pressure-time curve is plotted in Figure 2A-13.

Problem 2A-11 Blast Loads on a Structure with Front Wall Openings

Problem: Determine the pressure-time loads acting on the exterior front wall and all interior surfaces of a rectangular structure with front wall openings due to an external shock load.

Step 1. Charge weight:

- a. Determine TNT equivalent charge weight, W ;
- b. Increase charge weight by 20% safety factor, $W = 1.20 \times W$;
- c. Determine charge weight scaling factor, $W^{1/3}$.

- Step 2. Determine free field blast parameters:
- a. For an air burst, use Problem 2A-2 procedure; for a surface burst, use Problem 2A-3 procedure; for leakage pressures, use Problem 2A-8 or 2A-9 procedures.
 - b. Evaluate the angle of incidence, α , as the angle between the ground distance from the charge to the center of the front wall, and the normal distance from the charge to the front wall.
- Step 3. Front wall idealized pressure-time blast loads:
- A. Exterior Blast Load:
 - a. Determine peak positive reflected pressure, P_r , as a function of P_{SO} and α , using Figure 2-193.
 - b. Determine peak positive reflected scaled unit impulse, $i_{r\alpha}/(W^{1/3})$, as a function of P_{SO} and α , using Figure 2-194.
 - c. Determine the absolute positive reflected impulse by multiplying the scaled unit impulse by $(W^{1/3})$.
 - d. Determine the sound velocity of the reflected pressure wave, C_r , as a function of P_{SO} , using Figure 2-192.
 - e. Determine the reflected pressure clearing time, T'_c , from equation 2-14.
 - f. Construct the exterior blast pressure-time load. Follow the procedure in Problem 2A-10.
 - g. Determine the scaled wave length of the incident wave, $L_w/(W^{1/3})$ as a function of P_{SO} , using Figure 2-15, irrespective of how the external incident wave was created.
 - h. Determine the absolute wave length by multiplying the scaled wave length by $(W^{1/3})$.
 - B. Interior Blast Load:
 - a. Determine the following parameters: L_w/L , L_w/H , A_o/A_w , W/H , and L/H , where A_o is the total area of openings in the front wall, and A_w is the area H by W.

- b. Determine the idealized factored average peak pressure, $(P_{\max} \times (L_w/H))$, as a function of W/H , P_{so} , A_o/A_w , and L_w/H , using Figures 2-203 to 2-206. Calculate $P_{\max} = (P_{\max} \times L_w/H)/(L_w/H)$.
- c. Determine the arrival time, T_1 , as a function of W/H , P_{so} , and A_o/A_w , using Figures 2-207 and 2-208.
- d. Determine the rise time, $T_2 - T_1$, as a function of W/H , P_{so} , and L_w/H , from Figures 2-209 and 2-210.
- e. Determine the duration time, $T_3 - T_1$, as a function of W/H , P_{so} , and L_w/H , from Figures 2-211 and 2-212.
- f. Using times T_1 , $T_2 - T_1$, $T_3 - T_1$, and P_{\max} , construct the idealized pressure-time blast load. See Figure 2-201A for general configuration of this blast load.

Step 4. Side Wall Idealized Interior Pressure-Time Blast Load:

- a. Determine the maximum average sidewall pressure, P_{\max} , from equation 2-15.
- b. Determine the idealized times T_1 and T_2 for W/H , using Figure 2-213.
- c. Determine the idealized times T_3 and T_4 for W/H , using Figures 2-214 to 2-229.
- d. Using times T_1 , T_2 , T_3 , T_4 , and P_{\max} , construct the idealized pressure-time load. See Figure 2-201b for general configuration of this blast load.

Step 5. Back Wall Idealized Interior Pressure-Time Blast Load:

- a. Determine the maximum average positive reflected pressure coefficient, P_{RIB}/P_{so} , as a function of L/H , P_{so} , and A_o/A_w , using Figures 2-233 and 2-234.
- b. Determine the maximum average pressure, P_{RIB} , by multiplying the pressure coefficient, P_{RIB}/P_{so} , by P_{so} .
- c. Determine the idealized time T_1 as a function of W/H , P_{so} , L/H , and A_o/A_w , using Figure 2-230.
- d. Determine the idealized pressure duration, $T_2 - T_1$, as a function of P_{so} , and A_o/A_w , using Figure 2-232.

- e. Using times T_1 , $T_2 - T_1$, and P_{RIB} , construct the idealized pressure-time blast load. See Figure 2-201c for general configuration of this blast load.

Step 6. Roof Idealized Interior Pressure-Time Blast Load:

- a. Determine the W/H ratio for the roof as the inverse of W/H ratio of the side wall.
- b. Repeat Step 4 using the W/H ratio of the roof.

Example 2A-11 Blast Loads on a Structure with Front Wall Openings

Required: For the structure and charge as is shown in Figure 2A-14, determine the idealized positive external blast load on the front wall, and the idealized positive internal blast load on the front wall, side wall, roof and back wall.

Step 1. Charge weight

- a. $W = 5000$ lbs. TNT
- b. $W = 1.20 \times 5000 = 6000$ lbs. TNT
- c. $W^{1/3} = 18.1712$ lbs^{1/3}

Step 2. Free field blast parameters - surface burst

- a. Procedure from Problem 2A-3.

Blast parameters: P_{so} , U , i_s , t_o , t_A , for $W = 6000$ lbs., $R_G = 155'$ $Z_G = R_G/W^{1/3} = 155/18.1712 = 8.53$ (say 8.5)

From Figure 2-15 for hemispherical surface burst

$$P_{so} = f_1(Z_G) = 12.6 \text{ psi}$$

$$U = f_2(Z_G) = 1.46 \text{ ft/ms}$$

$$i_s/W^{1/3} = f_3(Z_G) = 9.0 \text{ psi-ms/lb}^{1/3}, i_s = 163.54 \text{ psi-ms}$$

$$t_o/W^{1/3} = f_4(Z_G) = 2.40 \text{ ms/lb}^{1/3}, t_o = 43.61 \text{ ms}$$

$$t_A/W^{1/3} = f_5(Z_G) = 3.40 \text{ ms/lb}^{1/3}, t_A = 61.78 \text{ ms}$$

- b. Charge to wall center ground distance = 155.0'
Charge to wall normal distance = 155.0'

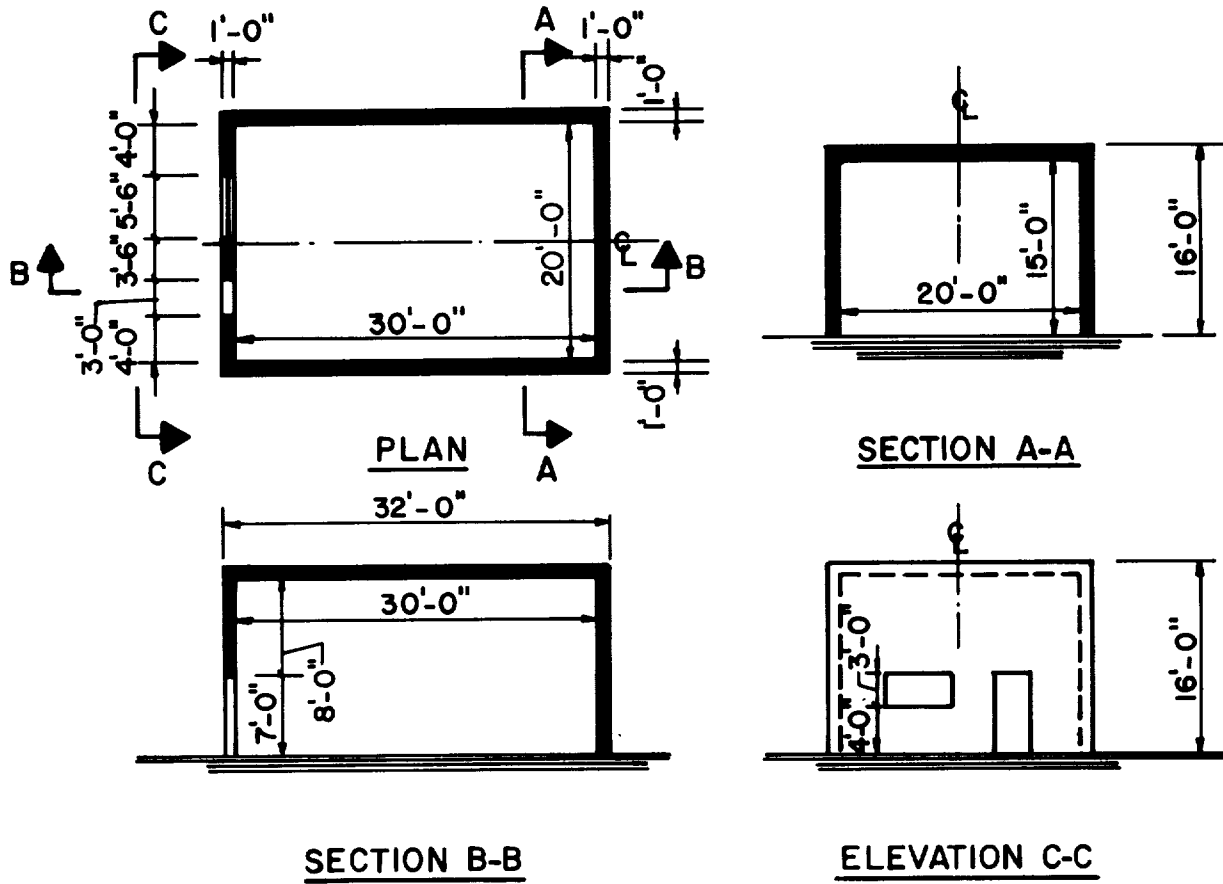
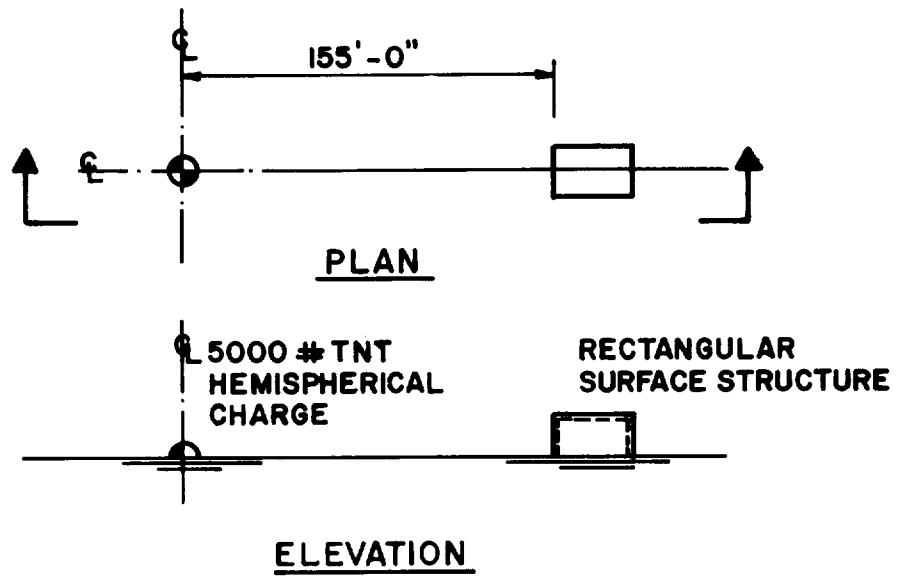
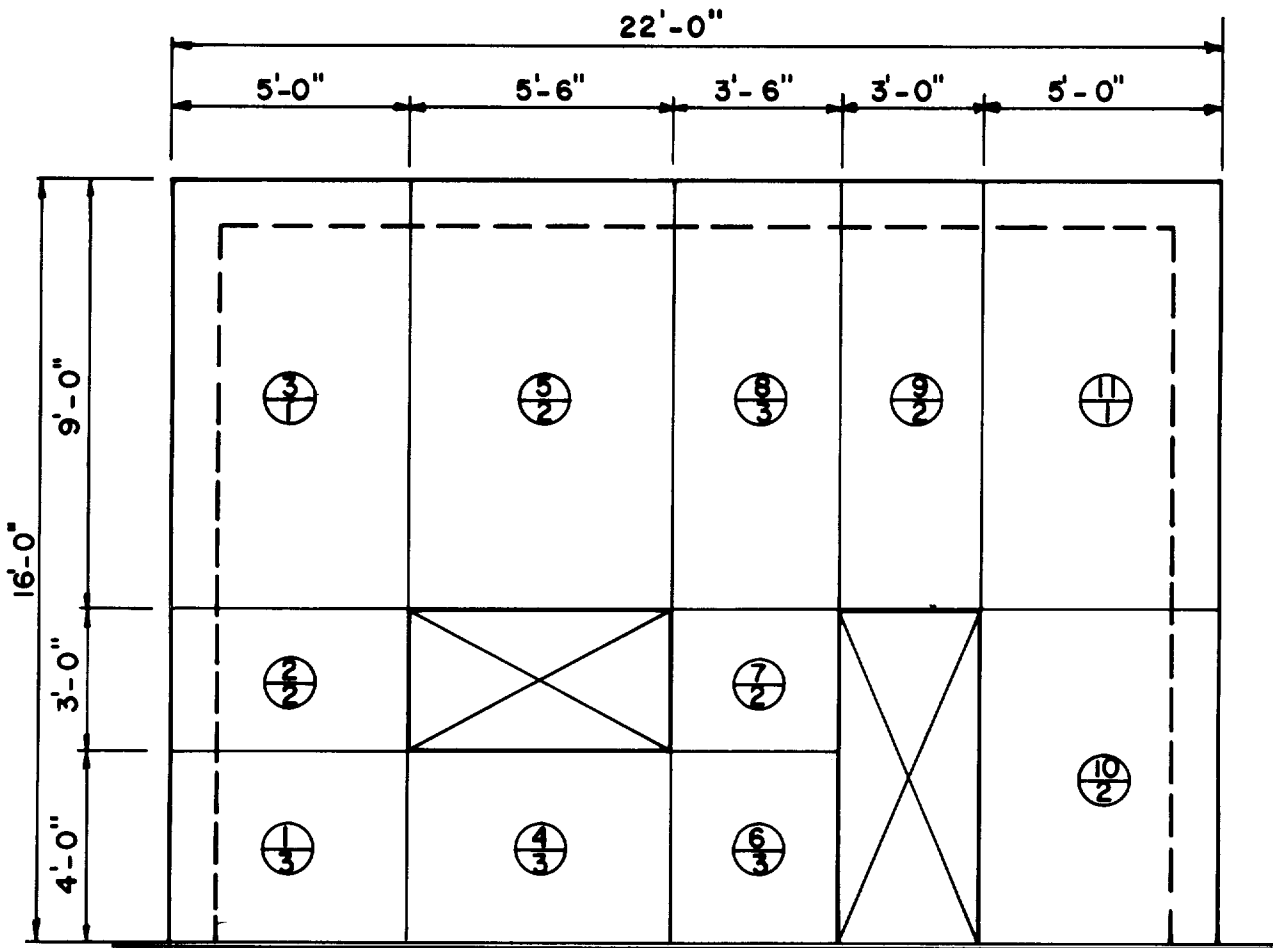
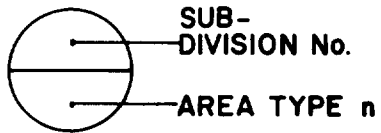


FIGURE 2A-14



ELEVATION



WALL SUB-DIVISION
NOMENCLATURE

FIGURE 2A - 15

$$\alpha = \cos^{-1} (155/155) = 0^\circ$$

Step 3. Front wall idealized pressure-time blast load

A. Exterior Blast Load

a. From Figure 2-193, for $\alpha = 0^\circ$ and $P_{so} = 12.6$ psi, determine

$$C_{r\alpha} = P_{r\alpha}/P_{so}$$

P_{so}	10.0	12.6	20.0
----------	------	------	------

$C_{r\alpha}$	2.40	?	2.90
---------------	------	---	------

$$C_{r\alpha} = (2.9 - 2.4) \times (12.6 - 10.0) / (20.0 - 10.0) + 2.40$$

$$= 0.130 + 2.40 = 2.53$$

$$P_{r\alpha} = C_{r\alpha} \times P_{so} = 2.53 \times 12.6 = 31.878 \text{ psi, say } 31.9 \text{ psi}$$

b. From Figure 2-194, for $\alpha = 0^\circ$, read $i_{r\alpha}/W^{1/3}$ for $P_{so} = 10$ and 20 psi and interpolate for $i_{r\alpha}/W^{1/3}$ at $P_{so} = 12.6$ psi

P_{so}	$i_{r\alpha}/W^{1/3}$
psi	psi-ms/lb ^{1/3}
10	15.2
12.6	?
20	23

$$i_{r\alpha}/W^{1/3} = (23.0 - 15.2) \times (12.6 - 10.0) /$$

$$(20.0 - 10.0) + 15.2 = 2.028$$

$$+ 15.2 = 17.228 \text{ psi-ms/lb}^{1/3}$$

c. Determine absolute impulse,

$$i_{r\alpha} = (i_{r\alpha}/W^{1/3}) \times (W^{1/3}) = 17.228 \times 18.1712 = 313.1 \text{ psi-ms}$$

d. For $P_{so} = 12.6$ psi, $C_r = 1.325$ ft/ms from Figure 2-192.

- e. Using Figure 2A-15 as the front wall sub-divisioning, determine h_n , W_n , δ_n , h'_n , A_n , $\delta_n h'_n A_n$, $\Sigma \delta_n h'_n A_n$, A_f , S' , S , R , and T'_c .

Subdivision	Type	δ_n	h'_n	h_n	W_n	A_n	$\delta_n h'_n A_n$
No.	n	-	ft	ft	ft	ft ²	ft ³
1	3	1.0	5.0	4.0	5.0	20.0	100.0
2	2	0.50	5.0	3.0	5.0	15.0	37.50
3	1	1.0	5.0	9.0	5.0	45.0	225.0
4	3	1.0	4.0	4.0	5.5	22.0	88.0
5	2	0.50	9.0	9.0	5.5	49.50	222.750
6	3	1.0	3.50	4.0	3.5	14.0	49.0
7	2	0.50	3.50	3.0	3.5	10.5	18.375
8	3	1.0	9.0	9.0	3.5	31.5	283.50
9	2	0.50	9.0	9.0	3.0	27.0	121.50
10	2	0.50	5.0	7.0	3.0	35.0	87.50
11	1	1.0	5.0	9.0	3.0	45.0	225.0

$$\Sigma \delta_n h'_n A_n = 1458.125$$

$$A_f = (16 \times 32) - (3 \times 5.5) - (7.0 \times 3.0)$$

$$= 512 - 16.5 - 21.0$$

$$= 512 - 37.5$$

$$= 474.5 \text{ ft}^2$$

$$S' = \left(\frac{\Sigma \delta_n h'_n A_n}{1} \right) / A_f = 1458.1250 / 474.5 = 3.073 \text{ ft}$$

$$H = 15.0', W = 20.0', H < W \dots S = H = 15.0', S' < S \text{ O.K.}$$

$$W > H \dots G = W = 20.0'$$

$$R = S/G = 15.0/20.0 = 0.75; C_T = 1.325 \text{ ft/ms}$$

$$t'_c = 4S' / \langle (1 + R) \times C_T \rangle = (4 \times 3.073) / (1.75 \times 1.325)$$

$$= 5.301 \text{ ms}$$

- f. Following general procedure problem 2A-10, Step 5 required previously determined values are:

$$P_{SO} = 12.6 \text{ psi}$$

$$i_s = 163.5 \text{ psi-ms}$$

$$P_{r\alpha} = 31.9 \text{ psi}$$

$$i_{r\alpha} = 313.1 \text{ psi-ms}$$

Determine

$$t_{of} = 2i_s/P_{so} = 2 \times 163.5/12.6 = 26 \text{ ms, Eq. 2-b,}$$

$$t_{rf} = 2i_{r\alpha}/P_{r\alpha} = 2 \times 313.1/31.9 = 19.6 \text{ ms, eq. 2-11,}$$

$$q_o = f(P_{so}) = 3.4 \text{ psi, Fig. 2-3}$$

$$C_D = 1.0, \text{ Paragraph 2-15.3.2,}$$

$$P_{so} + C_D q_o = 16 \text{ psi, Paragraph 2-15.3.2}$$

Construct infinite surface impulse and theoretic bi-linear actual surface impulse. Minimum value is design impulse.

$$\text{Infinite surface fictitious impulse} = i_{r\alpha} = 313.1 \text{ psi-ms}$$

Bi-linear theoretic actual surface impulse is area under curve $P_{r\alpha}$ to t'_c on line $P_{so} + C_D q_o$ to t_{of}

$$\text{Let } P = (P_{so} + C_D q_o) < 1 - (t'_c/t_{of}) >$$

$$= 16.0 < 1 - (5.3/26) > = 12.7 \text{ psi}$$

$$i_{BL} = [<P_{r\alpha} - P>t'_c/2] + <Pt'_c> + [<t_{of} - t'_c>P/2]$$

$$= [(31.9 - 12.7)(5.3/2)] + (12.7 \times 5.3)$$

$$+ [<26 - 5.3>12.7/2] = 50.9 + 67.3 + 131.4$$

$$= 250 \text{ psi-ms}$$

$i_{BL} < i_{r\alpha}$, use bi-linear pressure-time as design blast load.

See Figure 2A-16

g. For $P_{so} = 12.6 \text{ psi}$, $L_w/W^{1/3} = 2.10 \text{ ft/lb}^{1/3}$, Fig 2-15

h. $L_w = (L_w/W^{1/3})(W^{1/3}) = 2.10 \times 18.1712 = 38.16$, say 38.2 ft.

B. Interior Blast Load

a. From previous steps: $L_w = 38.2 \text{ ft}$, $L = 30 \text{ ft}$, $H = 15 \text{ ft}$, $W = 20 \text{ ft}$.

 FICTICIOUS INFINITE SURFACE IMPULSE

 THEORETIC ACTUAL SURFACE IMPULSE

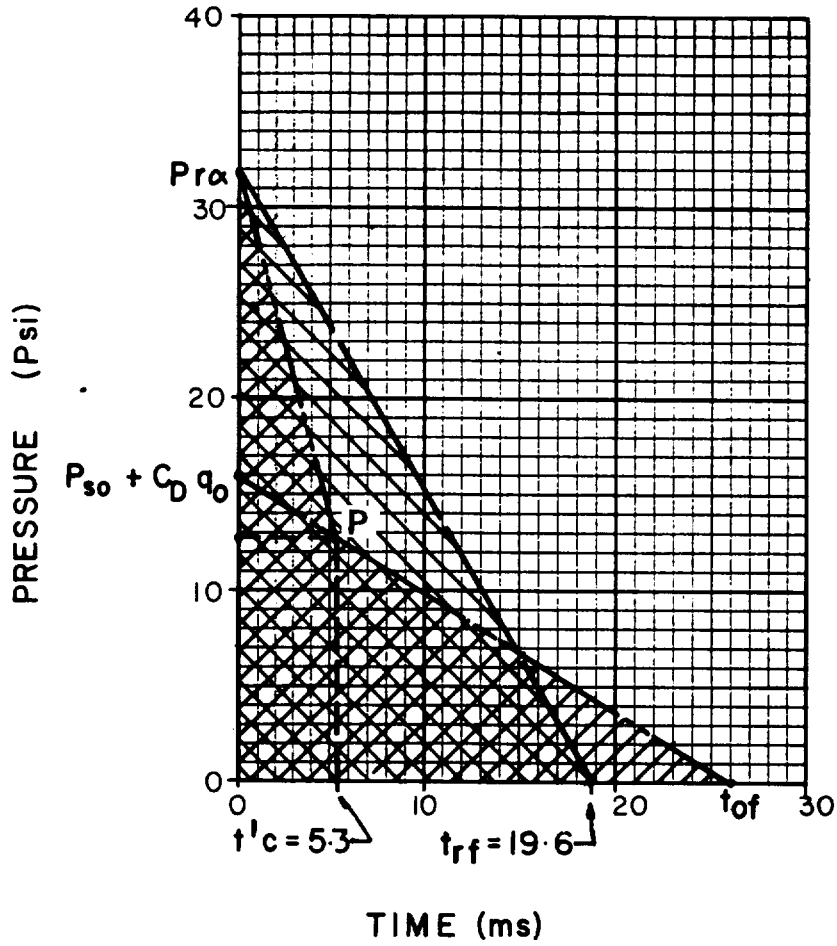


FIGURE 2A-16

A_o = Door opening area + window opening area

$$= (7 \times 3) + (3 \times 5.5) = 37.5 \text{ ft}^2$$

$$A_w = H \times W = 15 \times 20 = 300 \text{ ft}^2$$

$$A_o/A_w = 37.5/300 = 0.125$$

$$L_w/L = 38.2/30 = 1.27$$

$$L_w/H = 38.2/15 = 2.54$$

$$W/H = 20/15 = 1.33$$

$$L/H = 30/15 = 2.00$$

- b. For $W/H = 1.33$, $P_{so} = 12.6$ psi, $A_o/A_w = 0.125$, and $L_w/H = 2.54$ summarize factored maximum average pressure, $P_{max} \times L_w/H$, for W/H and L_w/H equal to .75, 1.5, 3 and 6.

Figure No.	W/H	L_w/H	$P_{max} \times L_w/H$
2-203	0.75	0.75	15.0
		1.50	38.5
		3.0	88.0
		6.0	190.0
2-204	1.50	0.75	4.70
		1.50	17.0
		3.0	55.0
		6.0	131.0
2-205	3.0	0.75	2.0
		1.50	7.0
		3.0	27.0
		6.0	85.0
2-206	6.0	0.75	1.0
		1.50	3.20
		3.0	10.0
		6.0	35.0

Plot Figure 2A-17 (a), and interpolate to determine $P_{\max} \times L_w/H$ at $L_w/H = 2.54$ for $W/H = .75, 1.5, 3$ and 6 .

W/H	.75	1.5	3	6
$P_{\max} \times L_w/H$	74	44	19	7.5

Plot Figure 2A-17 (b) from above values, and interpolate to determine $P_{\max} \times L_w/H = 48$ for $W/H = 1.33$.

Determine $P_{\max} = (P_{\max} \times L_w/H)/(L_w/H) = 48/2.54 = 18.9$ psi.

c. For $P_{so} = 12.6$ psi and $A_o/A_w = 1/8$, determine T_1 for $W/H = .75, 1.5$, and 3 , from Figures 2-207 and 2-208

W/H	.75	1.5	3
T_1	1.25	1.70	2.26

Plot Figure 2A-18 with above values, and determine $T_1 = 1.60$ for $W/H = 1.33$.

d. For $P_{so} = 12.6$ psi, determine $T_2 - T_1$ for W/H and $L_w/H = .75, 1.5$, and 3 , from Figures 2-209 and 2-210

W/H	.75			1.5			3		
L_w/H	.75	1.5	3	.75	1.5	3	.75	1.5	3
$T_2 - T_1$	2.07	2.07	2.07	4.70	6.20	7.0	6.50	10.8	15.0

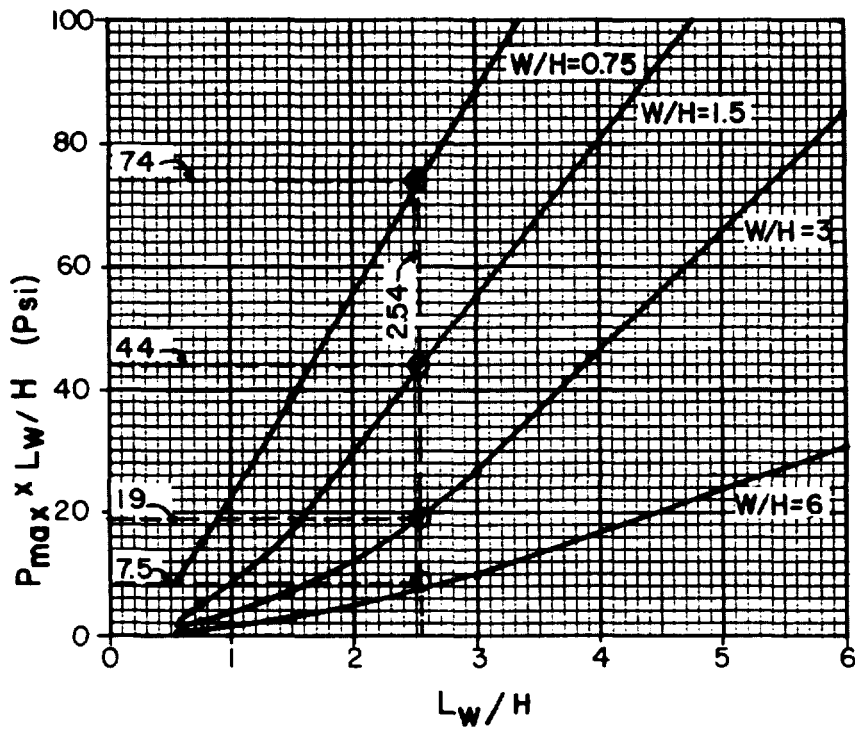
Plot Figure 2A-19 with above values, and interpolate to determine $T_2 - T_1$ at $L_w/H = 2.54$ for $W/H = .75, 1.5$ and 3 , as summarized

below.

W/H	.75	1.5	3
$T_2 - T_1$	2.07	6.75	14.0

Plot Figure 2A-19 with above values, and determine $T_2 - T_1 = 5.80$ ms for $W/H = 1.33$.

e. For $P_{so} = 12.6$ psi, determine $T_3 - T_1$ for $W/H = .75, 1.5$, and 3 , and $L_w/H = .75, 1.5$, and 3 , from Figures 2-211 and 2-212, as summarized below.

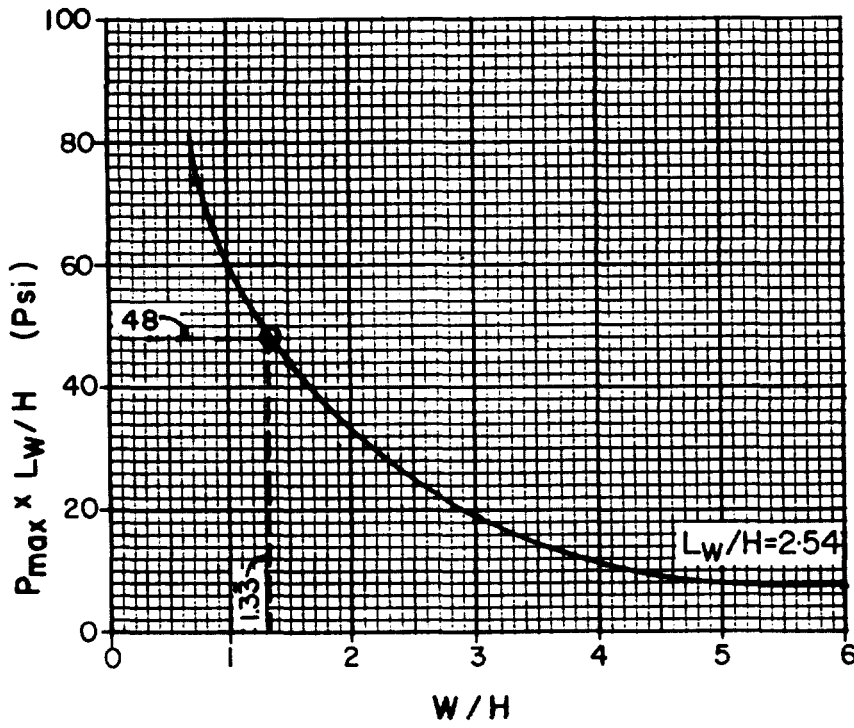


NOTE:
SEE EXAMPLE 2A-11,
STEP 3, PART B, ITEM b

FOR $L_w/H = 2.54$ GRAPHIC
INTERPOLATION YIELDS
 $P_{max} L_w/H = f(W/H)$, AS
SUMMARIZED BELOW.

W/H	$P_{max} L_w/H$
0.75	74
1.5	44
3	19
6	7.5

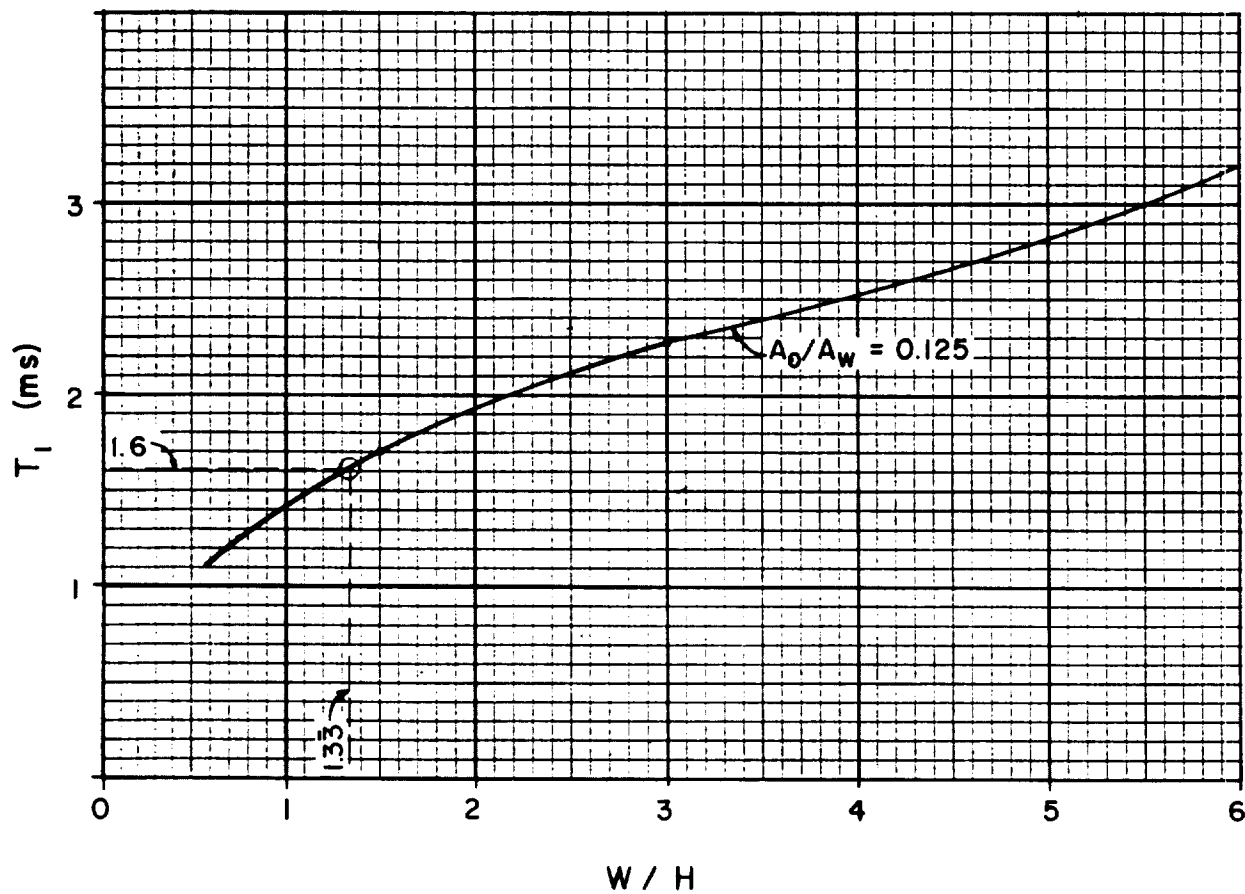
(a)



FOR $L_w/H = 2.54$, AND
 $W/H = 1.33$, GRAPHIC
INTERPOLATION YIELDS
 $P_{max} L_w/H = 48$

(b)

FIGURE 2A-17

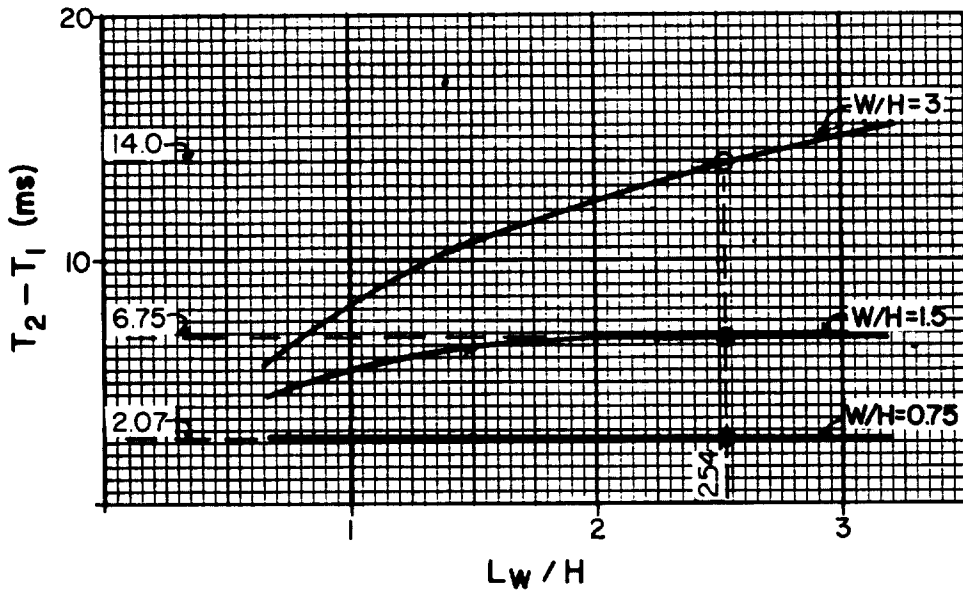


NOTE:

SEE EXAMPLE 2A-II, STEP 3, PART B, ITEM c

FOR $A_0/A_w = 0.125$, FOR $W/H = 1.33$,
 GRAPHIC INTERPOLATION YIELDS $T_1 = 1.60\text{ms}$

FIGURE 2 A -18

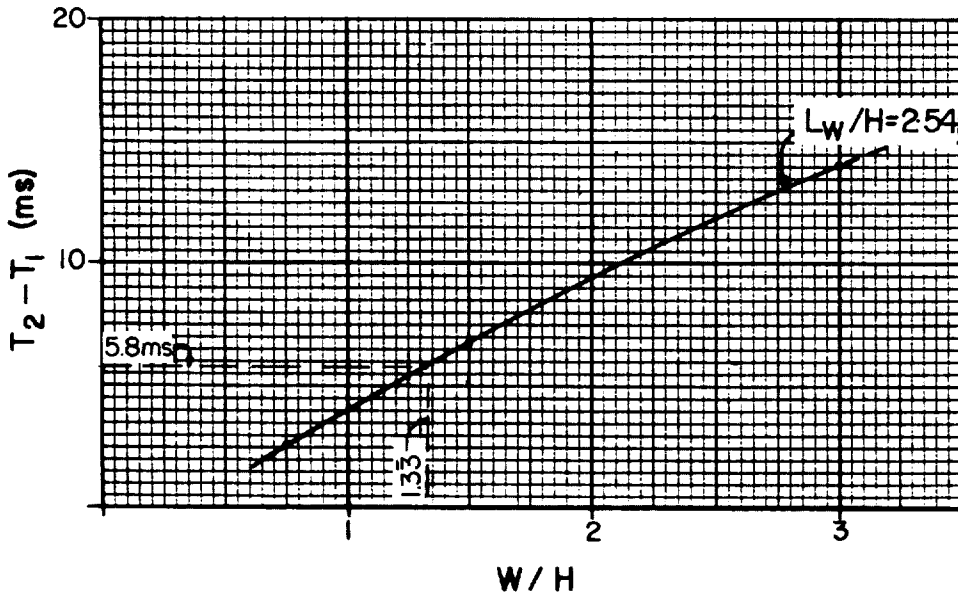


NOTE:

SEE EXAMPLE 2A-II
STEP 3, PART B, ITEM d.
FOR $L_w / H = 2.54$, GRAPHIC
INCORPORATION YIELDS
 $T_2 - T_1$ SUMMARIZED
BELOW

W/H	$T_2 - T_1$
0.75	2.07
1.5	6.75
3	14.0

(a)



NOTE:

FOR $W / H = 1.33$
 $T_2 - T_1 = 5.8$ ms

(b)

FIGURE 2A - 19

W/H	.75			1.5			3		
L_w/H	.75	1.5	3	.75	1.5	3	.75	1.5	3
$T_3 - T_1$	5.2	8.2	14.5	10.0	13.5	19.5	18.6	24.8	34.8

Plot Figure 2A-20 with above values, and graphically interpolate to determine $T_3 - T_1$ at $L_w/H = 2.54$ for $W/H = .75, 1.5,$ and $3,$ as summarized below.

W/H	.75	1.5	3
$T_3 - T_1$	12.8	17.5	31.7

Plot Figure 2A-20 with above values, and determine $T_3 - T_1 = 16.3$ ms at $W/H = 1.33.$

f. Determine times T_2 and T_3 from $T_1, T_2 - T_1,$ and $T_3 - T_1.$

$$T_1 = 1.60 \text{ ms}$$

$$T_2 - T_1 = 5.80 \text{ ms}$$

$$T_3 - T_1 = 16.30 \text{ ms}$$

$$T_2 = 5.80 + 1.60 = 7.40 \text{ ms}$$

$$T_3 = 16.30 + 1.60 = 17.9 \text{ ms}$$

Plot Figure 2A-23 using above values and $P_{max} = 18.9$ psi.

Step 4. Sidewall idealized interior pressure-time blast load.

a. Using equation 2-15, with $P_{so} = 12.6$ psi, $A_o/A_w = 1/8, L_w/L = 1.27, L/H = 2.0,$ solve for P_{max} for $W/H = .75, 1.5,$ and $3.$

$$\text{Equation 2-15: } P_{max} = K / (L_w/L)$$

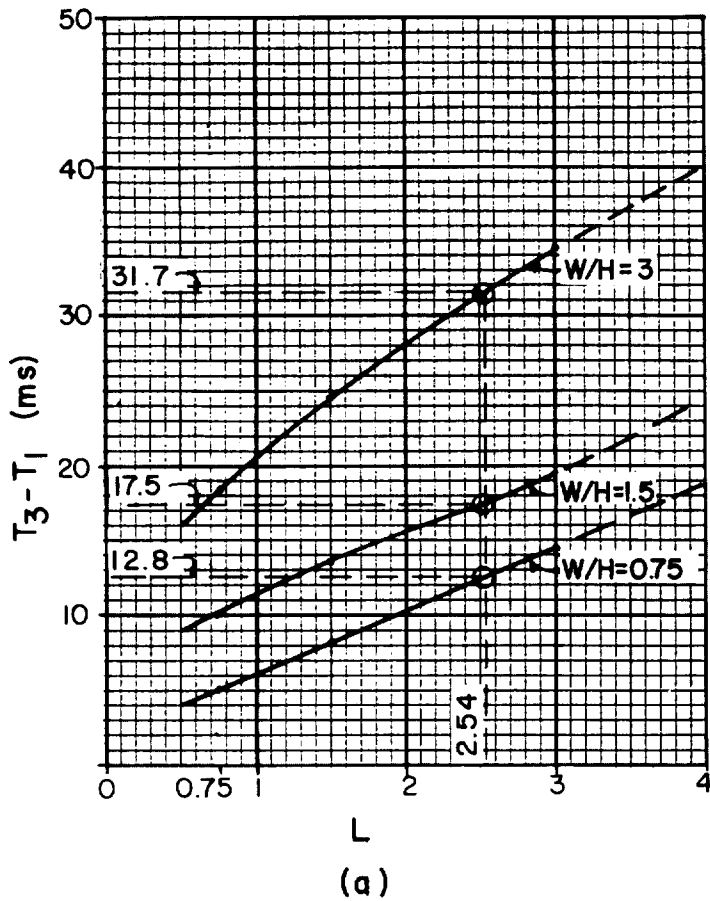
For $W/H = .75, K = A \times B \times C^E \times F^H \times P_{so}^{0.9718},$ where:

$$A = [0.5422 (L_w/L)^{1.2944}] - 0.001829 = 0.7385$$

$$B = [0.654 + 2.616 (A_o/A_w) - 4.928 (A_o/A_w)]^2 \\ \times [2.209 (L/H)^{-0.3451} - 0.739] = 0.9040$$

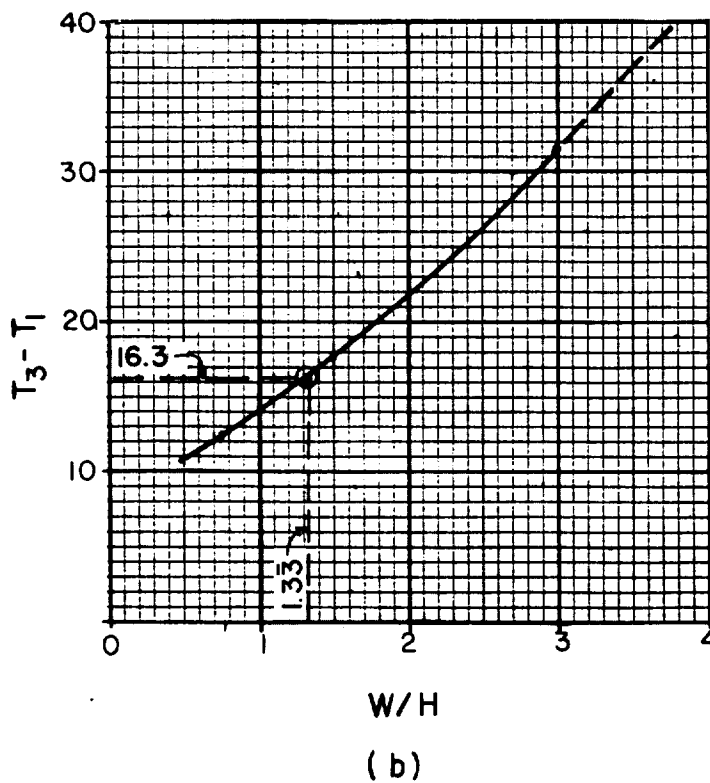
$$C = [0.829 + 0.104 (L_w/L)^{1.6}] + [0.00124 + 0.00414 (L_w/L)^{3.334}] \\ \times [L/H]^D = 1.0388$$

$$D = 2.579 - .0534 (L_w/L)^{3.891} = 2.4428$$



NOTE:
 SEE EXAMPLE 2A-11,
 STEP 3, PART B, ITEM e,
 FOR $L_w/H = 2.54$, GRAPHIC
 INTERPOLATION YIELDS
 $T_3 - T_1$ SUMMARIZED BELOW

W/H	$T_3 - T_1$
0.75	12.8
1.5	17.5
3	31.7
6	56.5



NOTE:
 FOR $W/H = 1.33$
 $T_3 - T_1 \approx 16.3$ ms

FIGURE 2A - 20

$$E = 999 (A_o/A_w)^{9.964} = 0.000001002$$

$$F = 1.468 - 1.6627 (A_o/A_w)^{0.7801} + [1.8692 - 1.1735 (A_o/A_w)^{-0.2226}] \times [L_w/L]^G = 1.1592$$

$$G = 0.2979 (A_o/A_w)^{-1.4872} - 0.8351 = 5.7286$$

$$H = (5.425 \times 10^{-4}) + (1.001 \times 10^{-3}) (L/H)^{9.965} = 0.0005435$$

$$K = 0.7385 \times 0.9040 \times 1.0388^{0.000001002} \times 1.1592^{0.0005435} \times 12.6^{0.9718} = 7.83$$

$$P_{max} = 7.83/1.27 \approx 6.2 \text{ psi, for } W/H = .75$$

$$\text{For } 1.5 \leq W/H \leq 6, K = [A + [B \times (L_w/L)^C]] \times D \times E \times P_{so}^{1.025}$$

where,

$$A = 0.002 (W/H)^{1.4467} - 0.0213$$

$$B = 2.2075 - (1.902 (W/H)^{-0.085})$$

$$C = 1.231 + (0.0008 (W/H)^{2.678})$$

$$D = (2.573 (L/H)^{-0.444}) - 0.3911$$

$$E = 0.4221 + (1.241 (A_o/A_w)^{0.367})$$

For $W/H = 1.5, 3, \text{ and } 6$, determine values for A to E , and K and P_{max} , as summarized below.

W/H	A	B	C	D	E	K	P_{max}
1.5	-0.0177	0.3700	1.2334	1.5003	1.0006	9.6743	7.60
3	-0.0115	0.4751	1.2462	1.5003	1.0006	12.690	9.98

Plot Figure 2A-21 with above values of P_{\max} vs $W/H = .75, 1.5, \text{ and } 3$, and determine $P_{\max} = 7.30 \text{ psi}$ for $W/H = 1.33$.

- b. For $P_{\text{so}} = 12.6 \text{ psi}$, determine T_1 and T_2 for $W/H = .75, 1.5, \text{ and } 3$ from Figure 2-213. as summarized below.

W/H	.75	1.5	3
T_1	1.82	4.95	11.7
T_2	3.20	6.50	12.5

Plot Figure 2A-21 using above values of W/H and T_1 and T_2 , and determine $T_1 = 4.4 \text{ ms}$ and $T_2 = 5.9 \text{ ms}$ for $W/H = 1.33$.

- c. For $P_{\text{so}} = 12.6 \text{ psi}$ and $L/H = 2$, determine T_3 and T_4 for $W/H = .75, 1.5 \text{ and } 3$ and $L_w/L = .75, 1, 1.5, \text{ and } 2$, from Figures 2-218 to 2-221, as summarized below:

Plot Figure 2A-21 with above values, and interpolate to determine T_3 and T_4 , for $L_w/L \approx 1.27$ for $W/H = .75, 1.5, \text{ and } 3$, as summarized below.

W/H	.75	1.5	3
T_3	35	18	24
T_4	71	71	74.5

Plot Figure 2A-21 with above values, and determine $T_3 = 19 \text{ ms}$ and $T_4 = 71 \text{ ms}$, for $W/H = 1.33$.

- d. For $P_{\max} = 7.3 \text{ psi}$, $T_1 = 4.4 \text{ ms}$, $T_2 = 5.9 \text{ ms}$, $T_3 = 19 \text{ ms}$ and $T_4 = 71 \text{ ms}$ plot Figure 2A-23.

Step 5. Back wall idealized interior pressure-time blast load.

- a. For $L/H = 2$, $P_{\text{so}} = 12.6 \text{ psi}$ and $A_o/A_w = 1/8$, determine $P_{\text{RIB}}/P_{\text{so}} = 0.575$ from Figure 2-234.

- b. $P_{\text{RIB}} = (P_{\text{RIB}}/P_{\text{so}}) \times P_{\text{so}} = 0.575 \times 12.6 = 7.5 \text{ psi}$.

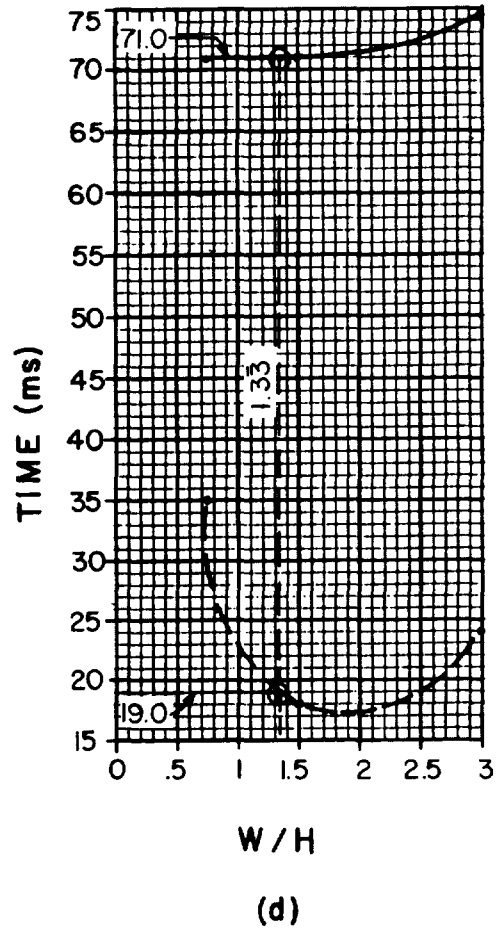
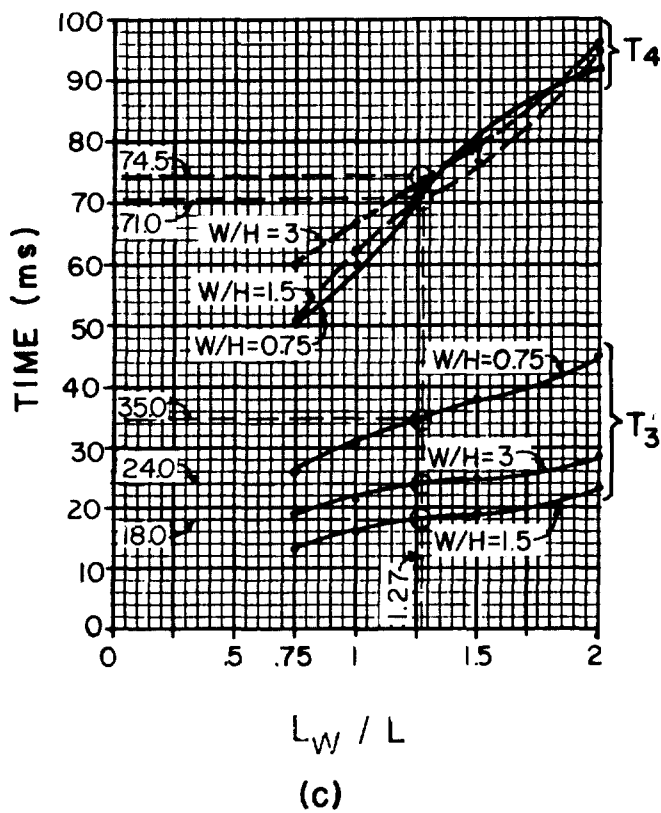
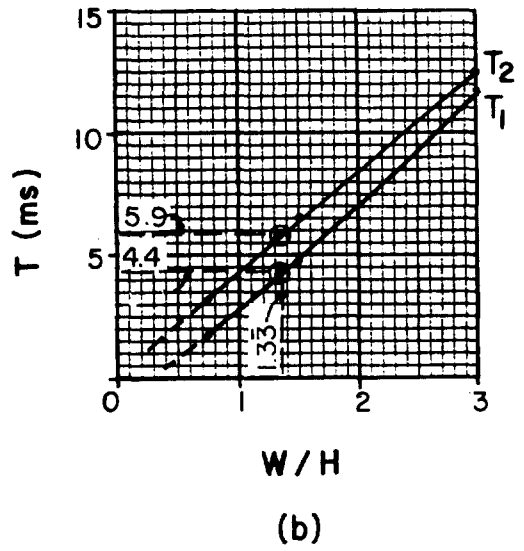
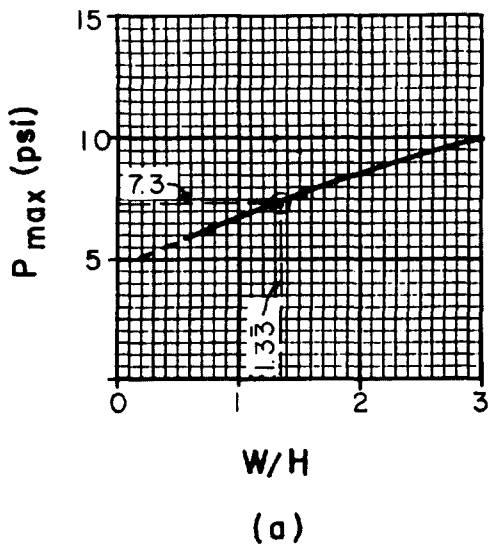


FIGURE 2A-21

- c. For $P_{SO} = 12.6$ psi, $L/H = 2$, and $A_O/A_W = 1/8$, determine T_1 for $W/H = .75, 1.5$ and 3 from Figures 2-230 and 2-231, as is shown below.

W/H	.75	1.5	3
T_1	19.0	21.5	24.0

Plot Figure 2A-22 using above values, and determine $T_1 = 21.1$ ms for $W/H = 1.33$.

- d. For $P_{SO} = 12.6$ psi and $A_O/A_W = 1/8$, determine $T_2 - T_1 = 2.35$ ms from Figure 2-232.

Determine $T_2 = (T_2 - T_1) + T_1 = 2.35$ ms + 21.1 ms = 23.5 ms.

- e. Plot Figure 2A-23 using $P_{RIB} = 7.5$ psi, $T_1 = 21.1$ ms and $T_2 = 23.5$ ms.

Step 6. Roof idealized interior pressure-time blast load

- a. Sidewall $W/H = 1-1/3 = 4/3$

Roof $W/H = 1/(4/3) = 3/4$

- b. Repeat Step 4 with $W/H = 3/4$

For $W/H = 3/4$, $L/H = 2.0$, $A_O/A_W = 1/8$, $L_W/L = 1.272$ and $P_{SO} = 12.6$,

$P_{max} = 6.2$ psi

For $W/H = 3/4$ and $P_{SO} = 12.6$ psi

$T_1 = 1.82$ and $T_2 = 3.20$ ms

For $W/H = 3/4$, $P_{SO} = 12.6$ psi, and $L_W/L = 1.27$

$T_3 = 35$ and $T_4 = 65$ ms

Plot Figure 2A-23 with above values.

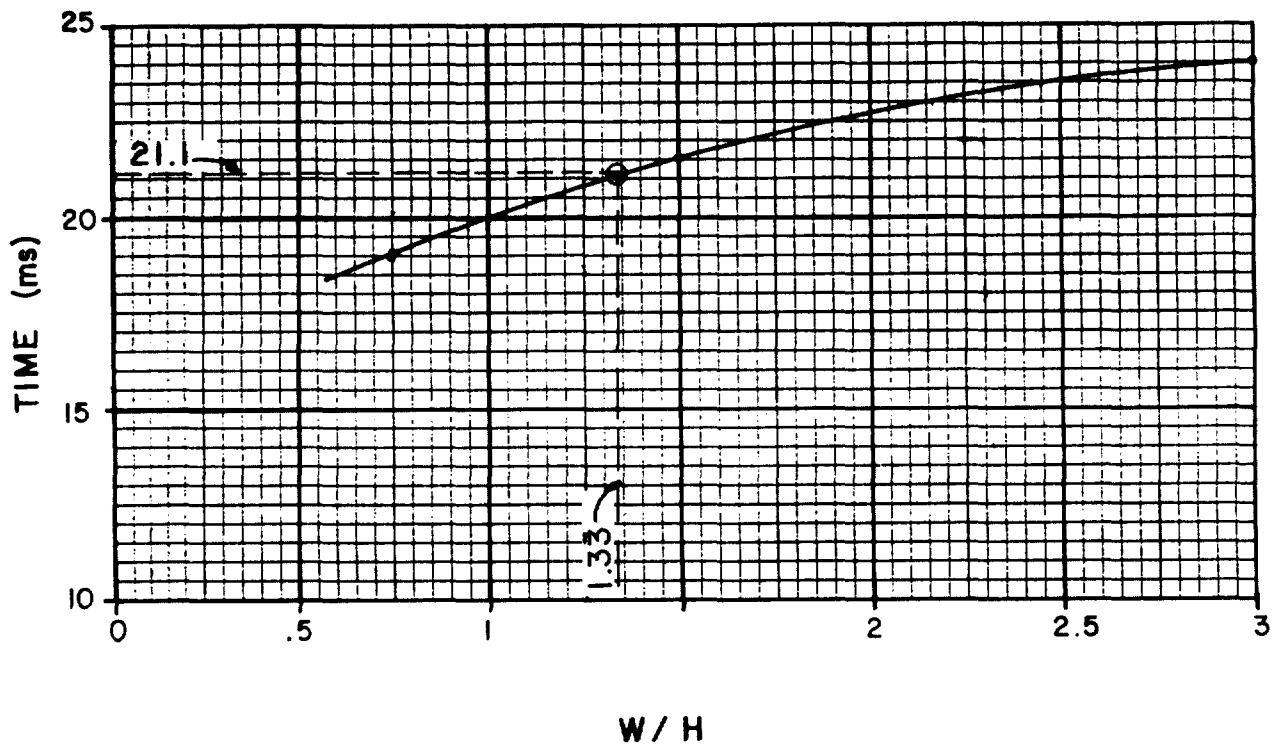
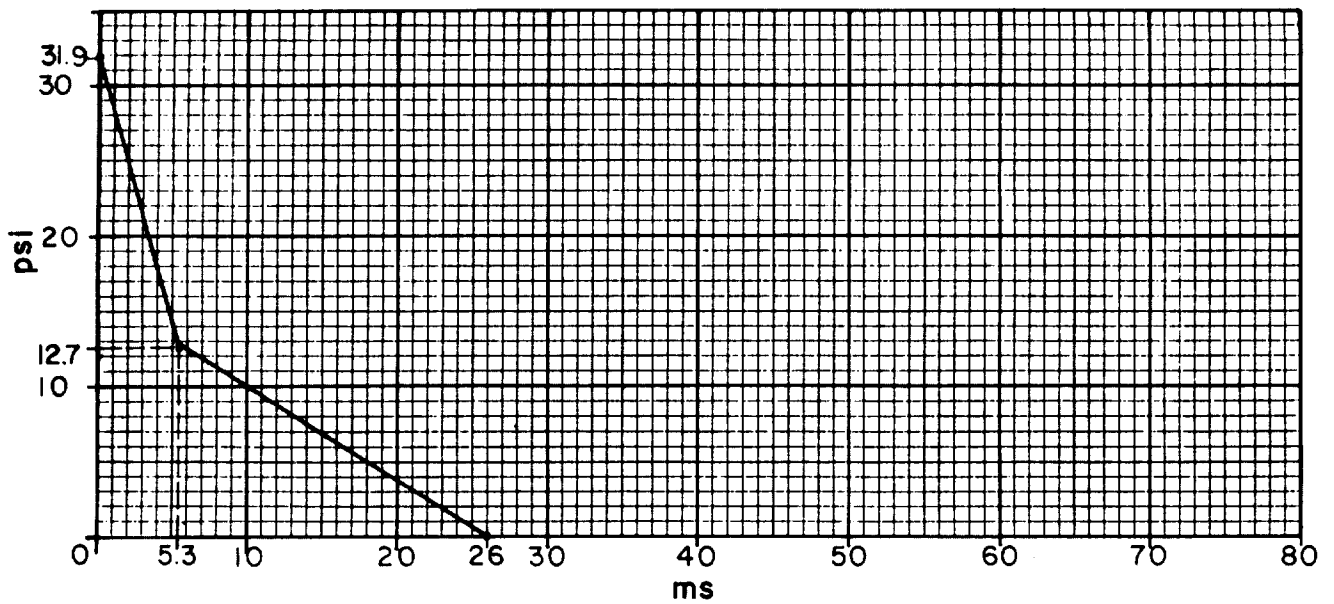
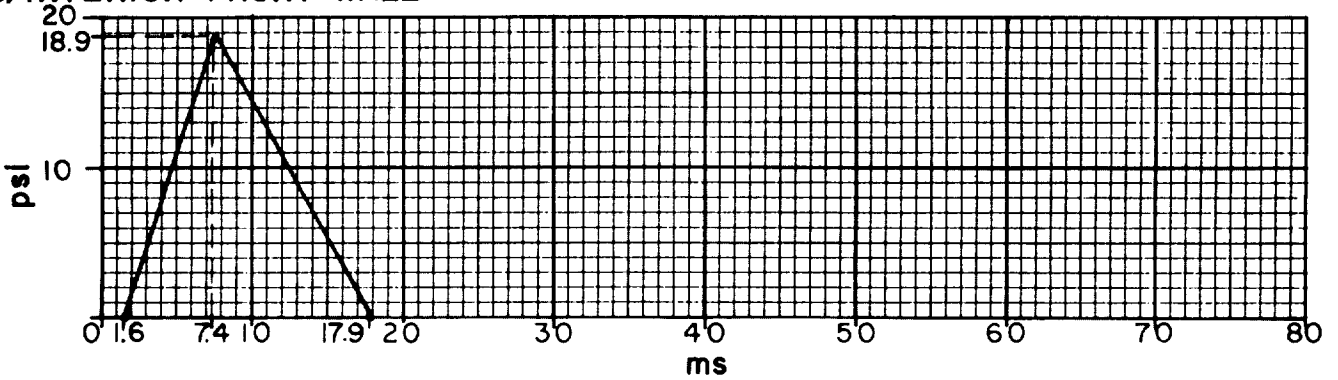


FIGURE 2A-22

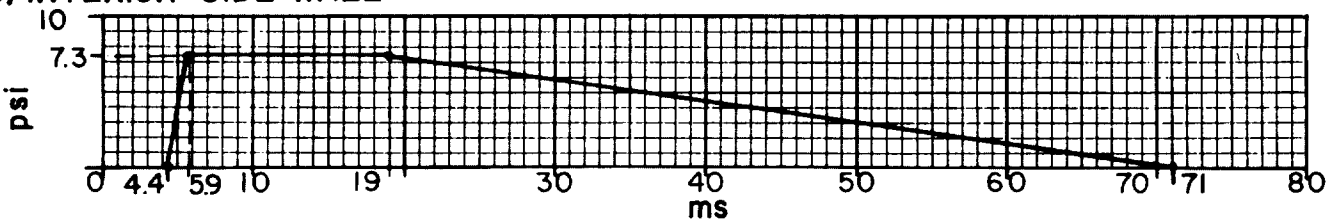
(a) EXTERIOR FRONT WALL



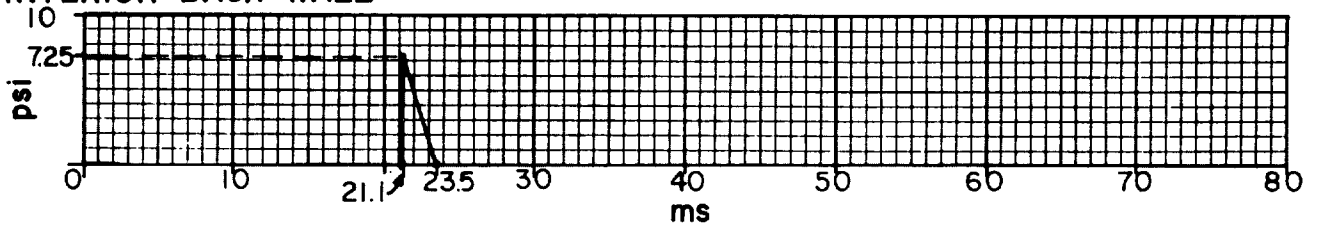
(b) INTERIOR FRONT WALL



(c) INTERIOR SIDE WALL



(d) INTERIOR BACK WALL



(e) INTERIOR ROOF

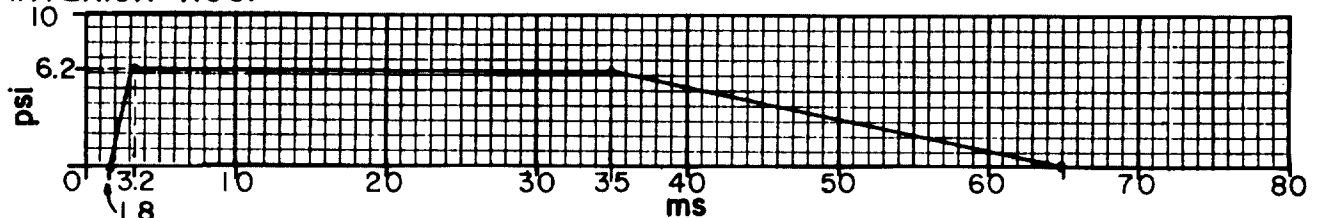


FIGURE 2A-23 BLAST LOAD SUMMARY

Problem 2A-12. Interior Pressure Buildup in a Structure

Problem: Determine the interior pressure-time curve for a structure with an opening in one of its walls and subjected to an applied blast pressure.

Procedure:

- Step 1.** Determine the pressure-time history of the applied blast pressure P acting on the wall surrounding the opening in the structure as presented in problem 2A-10. Also the area of the opening A_o and the volume of the structure V_o must be known.
- Step 2.** Divide the duration t_o of the applied pressure into n equal intervals δt , each interval being approximately $t_o/10$ to $t_o/20$, and determine the pressures at the end of each interval.
- Step 3.** Compute the pressure differential $P-P_i$ where P_i is the interior pressure. Obtain the leakage pressure coefficient C_L for each $P-P_i$ from Figure 2-235.
- Step 4.** Calculate δP_i from

$$\delta P_i = C_L \frac{A_o}{V_o} \delta t \quad (\text{eq. 2-31})$$

using the proper values for C_L and δt . Add δP_i to P_i for the interval being considered to obtain the new value of P_i for the next interval.

- Step 5.** Repeat steps 3 and 4 for each interval using the proper values of P and P_i . Plot curve of pressure buildup.

Note:

When $P-P_i$ becomes negative, the value of C_L must be taken as negative also.

Example 2A-12. Interior Pressure Buildup in a Structure

Required: Interior pressure-time curve for a structure with an opening in one of its walls and subjected to an applied blast pressure.

Solution:

- Step 1.** The curve of the applied blast pressure P for the wall in question is shown in Figure 2A-24. (Only the positive phase of the blast wave is considered in this example.)

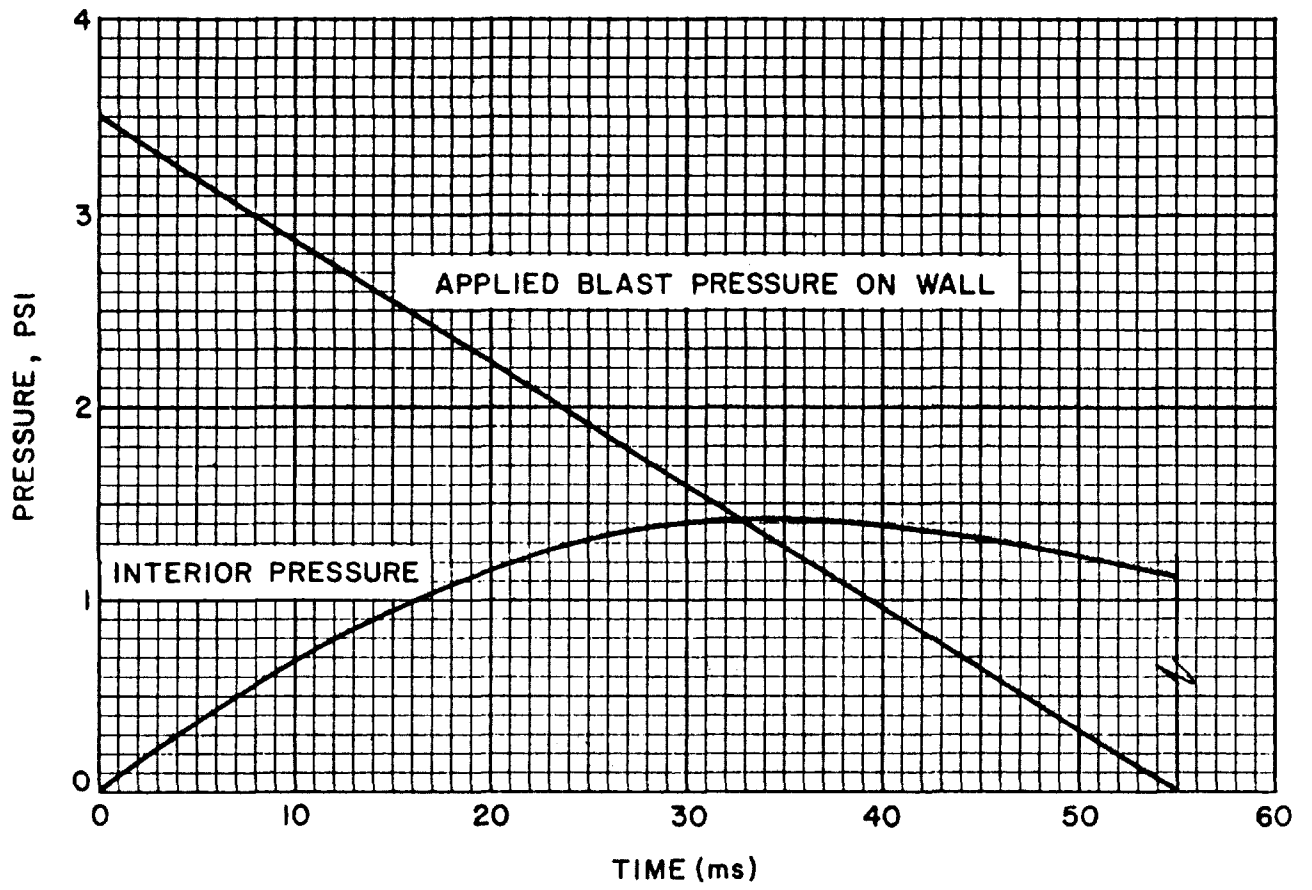


FIGURE 2A-24

Area of opening $A_o = 3' \times 3' = 9 \text{ sq ft.}$

Volume of structure $V_o = 10' \times 10' \times 10'$

$V_o = 1,000 \text{ cu ft}$

Step 2. $t_o = 55 \text{ ms}$

Use $n = 10 \quad \delta t = 5.5 \text{ ms}$

For the first interval, $P = 3.5 \text{ psi at } t = 0$

Step 3. $P_i = 0$ for the first interval

$\therefore P - P_i = 3.50 - 0 = 3.50 \text{ psi}$

$C_L = 8.75$ (fig. 2-235)

Step 4. $\delta P_i = C_L \frac{A_o}{V_o} \delta t$ (eq. 2-31)

$\delta P_i = 8.75 (9.0 / 1000) (5.5) = 0.433 \text{ psi}$

$\therefore \text{new } P_i = 0 + 0.433 = 0.433 \text{ psi}$

Step 5. The remainder of the analysis is presented in tabular form below and the pressure buildup within the structure is plotted in Figure 2A-24.

$t^{(1)}$	P	P_i	$P - P_i$	C_L	δP_i
(ms)	(psi)	(psi)	(psi)	(psi-ft/ms)	(psi)
0.	3.50	0.	3.50	8.75	0.433
5.5	3.15	0.433	2.72	7.00	0.347
11.0	2.80	0.780	2.02	5.45	0.270
16.5	2.45	1.05	1.40	3.78	0.187
22.0	2.10	1.24	0.86	2.32	0.115
27.5	1.75	1.36	0.39	1.05	0.052
33.0	1.40	1.41	-0.01	-0.027	-0.0013
38.5	1.05	1.41	-0.36	-0.972	-0.048
44.0	0.70	1.36	-0.66	-1.78	-0.088
49.5	0.35	1.27	-0.92	-2.48	-0.123
55.0	0.	1.14	-1.14	-3.50	-0.173
60.5	0.	.97	-0.97	-3.00	-0.148
66.0	0.	.82	-0.82	-2.50	-0.124
71.5	0.	.70	-0.70	-2.25	-0.111
77.0	0.	.59	-0.59	-2.00	-0.099
82.5	0.	.49	-0.49	-1.80	-0.089

$t^{(1)}$	P	P_i	$P-P_i$	C_L	δP_i
(ms)	(psi)	(psi)	(psi)	(psi-ft/ms)	(psi)
88.0	0.	.40	-.40	-1.60	-.079
93.5	0.	.32	-.32	-1.45	-.071
99.0	0.	.25	-.25	-1.30	-.064
104.5	0.	.19	-.19	-1.15	-.056
110.0	0.	.13	-.13	-1.0	-.050
115.5	0.	.08	-.08	-.85	-.042
121.0	0.	.04	-.04	-.05	-.025
126.5	0.	.01	-.01	-.2	-.01
132.0	0.	0.	0.	0.	0.

(1) Maximum P_i occurs between $t = 27.5$ and $t = 33.0$ ms

Problem 2A-13 Primary Fragments from Cased Cylindrical Charges

Problem: Determine the average fragment weight for a primary fragment ejected from a uniform cylindrical steel casing; the total number of fragments, the design fragment weight and the number of fragments weighing more than the design fragment.

Procedure:

Step 1. Establish design parameters:

- a. type of explosive.
- b. average casing thickness, t_c .
- c. average inside diameter of casing, d_i .
- d. total casing weight, W_c .
- e. confidence level, C_L .

Step 2. Determine the value of the explosive constant B for the given type of explosive from table 2-6. With this value and the values of t_c and d_i from step 1, calculate the fragment distribution M_A from

$$M_A = B t_c^{5/6} d_i^{1/3} \left[1 + (t_c/d_i) \right] \quad (\text{eq. 2-37})$$

Step 3. With the value of M_A from step 2, calculate the average weight of the fragments from

$$\bar{W}_f = 2M_A^2 \quad (\text{eq. 2-40})$$

Step 4. Calculate the total number of fragments using the value of W_c from step 1d and M_A from step 2 and equation 2-37.

$$N_T = 8W_c/M_A^2 \quad (\text{eq. 2-39})$$

or: With the values of d_i and t_c from step 1, enter Figure 2-241 and determine B^2N_T/W_c . From this value, the value of B from step 2 and W_c from step 1 find N_T .

Step 5. Find the design fragment weight for the confidence level C_L , given in step 1, using the value of M_A and

$$W_f = M_A^2 \ln^2(1 - C_L) \text{ for } C_L \leq 0.9999 \quad (\text{eq. 2-42})$$

or equation 2-43 if $C_L > 0.9999$

Step 6. Using the value of W_c from step 1, M_A from step 2 and W_f from step 5, determine the number of fragments which weigh more than the design fragment from

$$N_f = \frac{8W_c e^{-[(W_f)^{1/2}/M_A]}}{M_A^2} \quad (\text{eq. 2-36})$$

or: Calculate the number of fragments which weigh more than the design fragment using the confidence level of step 1, the total number of fragments from step 4 and equation 2-244.

Example 2A-13 Primary Fragments from Cased Cylindrical Charges

Required: The average fragment weight, the total number of fragments, the design fragment weight and the number of fragments weighing more than the design fragment.

Solution:

Step 1. Given:

- a. type of explosive: Comp B
- b. average casing thickness: $t_c = 0.50$ inch
- c. average inside diameter of casing: $d_i = 12.0$ inches

d. total casing weight: $W_c = 65.0$ lbs

e. confidence level: $C_L = 0.95$

Step 2. For Comp B, $B = 0.22$ (table 2-7)

$$M_A = B t_c^{5/6} d_i^{1/3} (1 + t_c/d_i) \quad (\text{eq. 2-37})$$

$$= 0.22 (0.5)^{5/6} (12)^{1/3} (1 + 0.5/12) = 0.294$$

Step 3. Average weight of fragments.

$$\bar{W}_f = 2M_A^2 = 2 \times (0.294)^2 = 0.17 \text{ oz} \quad (\text{eq. 2-40})$$

Step 4. Total number of fragments.

$$N_T = 8W_c/M_A^2 = 8 \times 65/0.294^2 = 6016 \text{ fragments} \quad (\text{eq. 2-39})$$

or:
$$\frac{B^2 N_T}{W_c} = 0.28 \quad (\text{fig. 2-37})$$

$$N_T = 0.28 \times (65 \times 16)/.22^2 = 6016 \text{ fragments}$$

Step 5. Design fragment weight.

$$W_f = 2M_A^2 \ln^2(1 - C_L) = 0.294^2 \ln^2(1 - 0.95) = 0.78 \text{ oz} \quad (\text{eq. 2-42})$$

Step 6. Number of fragments weighing more than $W_f = 0.78$ oz.

$$N_f = \frac{8W_c e^{-[(W_f)^{1/2}/M_A]} - (8 \times 65) e^{-[(0.78)^{1/2}/0.294]}}{M_A^2} = \frac{(8 \times 65) e^{-[(0.78)^{1/2}/0.294]}}{(0.294)^2}$$

$$= 298 \text{ fragments} \quad (\text{eq. 2-36})$$

or: $C_L = 1 - N_f/N_T$ (eq. 2-44)

$N_f = N_T (1 - C_L) = 6016 (1 - 0.95) = 301$ fragments

Problem 2A-14 Primary Fragment Velocity

Problem: Determine the initial velocity of a primary fragment and its striking velocity.

Procedure:

Step 1. Establish design parameters.

- a. shape of charge
- b. dimensions of charge
- c. type and density of explosive
- d. type and density of casing
- e. distance from center of charge to impact location
- f. weight of fragment

Step 2. Calculate the total weight of the explosive W and increase it 20%. Find the weight of the casing W_c . Also calculate the ratio of the explosive weight to the casing weight W/W_c .

Step 3. Determine the Gurney Energy Constant $(2E')^{1/2}$ for the explosive charge from table 2-5. With this value and the value of W/W_c from step 2, calculate the initial v_o of the primary fragments from the equation chosen from table 2-6.

or: Calculate the casing to charge weight ratio W_c/W . With W_c/W , find the initial velocity from Figure 2-237 for proper shape.

Step 4. For the distance traveled by the fragment R_f , calculate the striking velocity v_s using the initial velocity from step 3, the weight of the fragment from step 1g and

$$v_s = v_o e^{-.004 R_f/W_f^{1/3}} \quad (\text{eq. 2-48})$$

or: With the fragment weight W_f and striking distance R_f from step 1, enter Figure 2-243 and find the ratio of the striking velocity to initial velocity. Multiply the ratio by the initial velocity v_0 from step 3 to find the striking velocity v_s .

Example 2A-14 Primary Fragment Velocity

Required: The initial velocity and striking velocity of a primary fragment.

Solution:

Step 1. Given:

- a. spherical charge
- b. inner diameter of charge: $d_i = 6$ inches
average casing thickness: $t_c = 0.25$ inches
- c. type of explosive TNT
density of explosive = 0.0558 lb/in^3
- d. mild steel casing
density of casing = 0.283 lb/in^3
- e. striking distance $R_f = 35$ ft.
- f. weight of fragment, $W_f = 2$ oz

Step 2.

- a. weight of the explosive
 $W = 4/3 \pi (6/2)^3 \times 0.0558 = 6.31 \text{ lbs}$
- b. Increase weight of explosive 20 percent
 $W = 1.20 \times 6.31 = 7.57 \text{ lb}$
- c. Weight of casing
 $W_c = 4/3 \pi (3.5^3 - 3^3) \times 0.283 = 18.82 \text{ lb}$
- d. Explosive weight to casing weight ratio.
 $W/W_c = 7.57/18.82 = 0.402$

Step 3. For TNT, $(2E')^{1/2} = 8000$ (table 2-5)

Initial velocity from table 2-6

$$v_o = (2E')^{1/2} \left[\frac{W/W_c}{1 + (3W/5W_c)} \right]^{1/2}$$

$$v_o = (8000) \left[\frac{0.40}{1 + 0.40 (3/5)} \right]^{1/2} = 4500 \text{ ft/sec}$$

or: $W_c/W = 18.82/7.57 = 2.49$

from Figure 2-237

$$v_o/(2E')^{1/2} = 0.56$$

$$v_o = 0.56 \times 8000 = 4500 \text{ ft/sec}$$

Step 4. Striking velocity

$$v_s = v_o e^{-0.004 R_f/W_f^{1/3}} = 4500 e^{-0.004 \times (35/2)^{1/3}} \quad (\text{eq. 2-48})$$

$$v_s = 4030 \text{ ft/sec}$$

or: from Figure 2-243

$$v_s/v_o = 0.895$$

$$v_s = 0.895 \times 4500 = 4030 \text{ ft/sec}$$

Problem 2A-15 Unconstrained Secondary Fragments "Close" to a Charge

Problem: Determine the velocity of an unconstrained object close to an explosive charge and its maximum range.

Procedure:

- Step 1. Establish design parameters
- a. weight W and shape of TNT equivalent explosive
 - b. radius of explosive R_e
 - c. shape, dimensions and weight of target
 - d. distance from the center of the explosive charge to the surface of the target, R
 - e. orientation of target with respect to the explosive charge
 - f. mass density of air ρ_o
- Step 2. Calculate the ratio of standoff distance to radius of the explosive R/R_e using the values from step 1.
- Step 3. From Figure 2-249, determine target shape factor, β .
- Step 4.
- a. If R/R_e is less than or equal to 10 for cylindrical charges, or less than equal to 5.0 for spherical charges, determine the specific acquired impulse either from Figure 2-250 or equations 2-60, or 2-61.
 - b. If $10 < R/R_e \leq 20$ for a cylindrical charge, or $5 < R/R_e \leq 20$ for a spherical charge, calculate the scaled standoff distance $Z_A = R/W^{1/3}$. With that value of Z_A , obtain the normal reflected impulse from Figure 2-7. The normal reflected impulse is then used as the specific acquired impulse.
- Step 5. Calculate the mean presented area A of the target and the mass M using the values of step 1.
- Step 6. With the area and mass from step 4, the target shape factor β from step 2 and the impulse from step 3, calculate the velocity from

$$v_o = \frac{1000 A\beta i}{12 M} \quad (\text{eq. 2-59})$$

- Step 7. Determine the drag coefficient C_D from table 2-8. Using that value of C_D , the area and mass of the target from step 5, the velocity from step 6 and the mass density of air from step 1f,

evaluate the term: $12 \rho_o C_D A_D v_o^2 / Mg.$

Step 8. With the term calculated in step 7, enter Figure 2-252 and read the value of $12 \rho_o C_D A_D R/M$ from which the range R is calculated.

Example 2A-15 Unconstrained Secondary Fragments "Close" to a Charge

Required: The velocity and maximum range of a steel tool holder resting on a lathe when a charge being held by the lathe explodes.

Solution:

Step 1. Given:

- a. spherical charge of TNT
W = 15 lbs
- b. radius of explosive: $R_e = 0.33$ ft
- c. cylindrical target; length = 8.0 in
 $R_t = 1.0$ in = 0.083 ft
 $W_t = 7.13$ lb
- d. standoff distance: $R = 1.0$ ft
- e. tool holder is resting so that its longitudinal axis is perpendicular to the radial line from the charge
- f. mass density of air: $\rho_o = 0.115$ lb - ms²/in⁴

Step 2. Ratio of standoff distance to radius of explosive:

$$R/R_e = 1.0/0.33 = 3.03$$

Step 3. Target shape factor.

$$\beta = \pi/4 \text{ from Figure 2-512}$$

Step 4. Determine specific acquired impulse

$$a. \frac{i}{\beta R_{eff}} \left[\frac{R_e}{R_t} \right]^{0.158} = 8000 \frac{\text{psi-ms}}{\text{ft}} \quad (\text{fig 2-250})$$

$$b. R_{eff} = R_e = 0.33 \text{ ft} \quad (\text{eq. 2-61})$$

c. $i = \pi/4 (0.33 \text{ ft}) (0.083/0.33)^{0.158} \times 8000 \text{ psi-ms/ft}$
 $i = 1667 \text{ psi-ms}$

Step 5. Calculate area and mass of target.

a. Mean presented area

$$A = 2.0 \text{ in} \times 8.0 \text{ in} = 16 \text{ in}^2$$

b. Mass

$$M = \frac{W_t}{g} = \frac{7.13 \text{ lb}}{32.2 \times 12 \times 10^{-6} \text{ in/ms}^2} = 18,450 \frac{\text{lb-ms}^2}{\text{in}}$$

Step 6. Find the velocity.

$$v_o = \frac{1000 A \beta i}{12 M} = \frac{1000 \times 16 \times (\pi/4) \times 1667}{12 \times 18450} \quad (\text{eq. 2-59})$$

$$v_o = 95 \text{ ft/sec}$$

Step 7. Evaluate the term $12 \rho_o C_D A_D v_o^2 / Mg$.

a. $C_D = 1.2$ (table 2-8)

b.
$$\frac{12 \rho_o C_D A_D v_o^2}{Mg} = \frac{0.115 (1.2) (16) (95)^2}{18450 \times 32.2} = 0.40$$

Step 8. Calculate the range.

a.
$$\frac{12 \rho_o C_D A_D R}{M} = 0.33 \quad (\text{fig. 2-252})$$

b.
$$R = 0.33M / (12 \rho_o C_D A_D)$$

$$= 0.33 (18450) / [12 (0.115) 1.2 (16)] = 230 \text{ ft.}$$

Problem: 2A-16 Unconstrained Secondary Fragments "Far" from a Charge

Problem: Determine the velocity of an unconstrained object "far" from an explosive charge.

Procedure:

- Step 1. Establish design parameters:
- a. weight W of TNT equivalent explosive
 - b. shape, dimensions and weight of target
 - c. distance from the center of explosive charge to surface of the target
 - d. orientation and location of target with respect to the explosive charge
 - e. velocity of sound in air, a_0
 - f. atmospheric pressure, p_0

- Step 2. Calculate the scaled standoff distance from:

$$Z_A = R_A/W^{1/3}$$

From Figure 2-7. and the scaled distance find the peak incident overpressure and the incident specific impulse.

- Step 3. Determine the drag coefficient C_D from table 2-8 based on the shape and orientation of target (step 1).
- Step 4. Calculate the mass of the target. Determine the distance from the front of the target to the location of its largest cross-sectional area, X . Also, determine the minimum transverse distance of the mean presented area, H , and the presented area.
- Step 5. Determine the constant K , which is equal to 4 if the object is on the ground or reflecting surface. If the target is in the air, K is equal to 2.
- Step 6. With the peak incident overpressure P_{s0} from step 2 and the atmospheric pressure p_0 from step 1f, find P_{s0}/p_0 .

- Step 7. Evaluate the term $12C_D i_s a_o / 10^3 [P_{so}(KH + X)]$ using i_s and P_{so} from step 2, C_D from step 3, a_o from step 1e, K from step 5 and H and X from step 4.
- Step 8. With two terms calculated in steps 6 and 7 enter Figure 2-248 and read $144v_o Ma_o / [10^6 P_o A(KH + X)]$ from which the velocity is calculated.

Example 2A-16 Unconstrained Secondary Fragments "Far" from Charge

Required: The initial velocity of a steel tool holder resting on a nearby table, when a charge explodes.

Solution:

Step 1. Given:

- a. weight of explosive: $W = 15$ lbs of TNT
- b. cylindrical target: length = 8.0 in
 $R_t = 1.0$ in
 $W_t = 7.13$ lb
- c. standoff distance: $R = 10$ ft
- d. tool holder is resting on a table so that its longitudinal axis is perpendicular to the radial line from the charge
- e. velocity of sound in air: $a_o = 1100$ ft/sec
- f. atmospheric pressure: $p_o = 14.7$ psi

Step 2. Find the peak incident overpressure and the incident specific impulse.

a. Scaled distance

$$Z_A = R/W^{1/3} = 10/(15)^{1/3} = 4.05 \text{ ft/lb}^{1/3}$$

b. Peak incident overpressure.

$$P_{so} = 39 \text{ psi} \quad (\text{fig. 2-7})$$

c. Incident specific impulse.

$$i_s/W^{1/3} = 12 \text{ psi-ms/lb}^{1/3} \quad (\text{fig. 2-7})$$

$$i_s = 12 (15)^{1/3} = 29.6 \text{ psi-ms}$$

Step 3. Drag coefficient.

$$C_D = 1 \quad (\text{from table 2-8 for cylinder loaded perpendicular to axis.})$$

Step 4. a. Mass of target.

$$M = \frac{W_t}{g} = \frac{7.13 \text{ lb}}{32.2 \times 12 \times 10^{-6} \text{ in/ms}^2} = 18,450 \frac{\text{lb-ms}^2}{\text{in}}$$

b. Location of largest cross-section.

$$X = 1 \text{ in (radius of object in this case - see fig. 2A-21)}$$

c. Transverse distance of presented area.

$$H = 2.0 \text{ in (diameter of object in this case - see fig. 2A-25).}$$

d. Mean presented area.

$$A = 2 \times 8 = 16 \text{ in}^2$$

Step 5. Reflection constant.

Target is resting on table which is a reflecting surface so:

$$K = 4$$

Step 6. Evaluate P_{SO}/p_o

$$P_{SO}/p_o = 39/14.7 = 2.65$$

Step 7. Evaluate $12C_D i_s a_o / [10^3 P_{SO} (KH + X)]$

$$\frac{12C_D i_s a_o}{10^3 P_{SO} (KH + X)} = \frac{12 (1.2) (29.6) (1100)}{10^3 (39) (2 \times 4 + 1)} = 1.34$$

Step 8. Calculate the velocity.

$$\frac{144 v M_o a_o}{10^6 p A_o (KH + X)} = 6.0 \quad (\text{fig. 2-248})$$

$$v_o = \frac{6.0 p_o A (KH + X) 10^6}{144 M a_o} = \frac{10^6 (6.0)(14.7)(16)(2 \times 4 + 1)}{(144)(18450)(1100)}$$

$$v_o = 4.34 \text{ ft/sec}$$

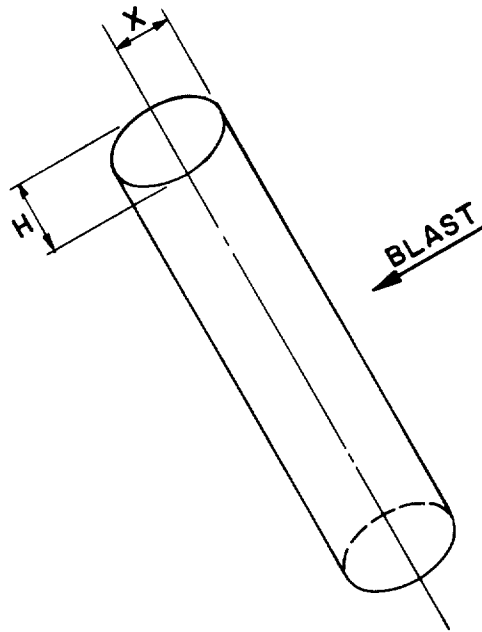


FIGURE 2A - 25

2A-86

Problem 2A-17 Constrained Secondary Fragments

Problem: Determine the velocity of a constrained object close to an exploding charge.

Procedure:

- Step 1. Establish design parameters:
- a. fragment material.
 - b. dimensions of object.
 - c. boundary condition, cantilever or fixed-fixed.
 - d. specific impulse imparted to object.
- Step 2. Determine the fragment toughness T from table 2-9 and the fragment mass density ρ_f .
- Step 3. Calculate the loaded area of the object.
- Step 4. Evaluate the term $ib (2L/b)^{0.3} / [A(\rho_f T)^{0.5}]$, using the specific impulse and object dimensions from step 1, the fragment density and toughness from step 2 and the loaded area from step 3. With this term, enter Figure 2-251 and read the value of $12V/1000 (\rho_f/T)^{0.5}$ from which the velocity is calculated.
- or:
- Using the specific impulse and object dimensions from step 1, the fragment density and toughness from step 2, and the loaded area from step 3, calculate the velocity of the object from equation 2-66.

Example 2A-17 Constrained Secondary Fragments

Required: The velocity of a cylindrical tool holder after it breaks free of its moorings.

Solution:

- Step 1. Given:
- a. fragment material; A36 steel
 - b. dimensions of object: $b = 2.0$ inches
 $L = 8.0$ inches
 - c. boundary conditions; cantilever
 - d. specific impulse: $i = 1667$ psi-ms (see step 4 of example 2A-15).



Step 2.

a. Fragment toughness.

$$T = 12,000 \text{ in-lb/in}^3 \quad (\text{table 2-9})$$

b. Mass density of steel.

$$\rho_f = \frac{490 \text{ lb/ft}^3 (\text{ft}^3/1728 \text{ in}^3)}{32.2 \text{ ft/s}^2 (12 \text{ in/ft})(\text{s}^2/10^6 \text{ ms}^2)} = 734 \frac{\text{lb-ms}^2}{\text{in}^4}$$

Step 3. Loaded area.

$$A = \pi r^2 = \pi (1.0)^2 = 3.14 \text{ in}^2$$

Step 4. Calculate the velocity.

$$\frac{ib}{A(\rho_f T)^{0.5}} \left[\frac{2L}{b} \right]^{0.3} = \frac{1667 \times 2.0}{3.14(734 \times 12,000)^{0.5}} \left[\frac{2 \times 8}{2} \right]^{0.3} = 0.668$$

from Figure 2-251

$$12/1000 [\rho_f/T]^{1/2} v = 0.025$$

so

$$v = \frac{1000}{12} \left[\frac{T}{\rho_f} \right]^{1/2} 0.025 = \frac{1000}{12} \left[\frac{12,000}{734} \right]^{1/2} 0.025 = 8.4 \text{ fps}$$

or from equation 2-66

$$v = \frac{1000}{12} \left[\frac{T}{\rho_f} \right]^{1/2} \left[-.2369 + 0.3931 \left[\frac{ib}{(\rho_f T)^{1/2} A} \right] \left[\frac{2L}{b} \right]^{0.3} \right]$$

$$= \frac{1000}{12} \left[\frac{12,000}{734} \right]^{1/2} (-.2369 + 0.3931 \times 0.668)$$

$$v = 8.6 \text{ fps}$$

Problem 2A-18 Ground Shock Load

Problem: Determine the air blast and direct induced ground shock parameters.

Procedure: Air blast-induced ground shock.

Step 1. Determine the charge weight, ground distance R, height of burst H_c , if any, and structure dimensions.

Step 2. Apply a 20% safety factor to the charge weight.

Step 3. Calculate the scaled distance Z.

Read: From fig. 2-15

a. Peak positive incident pressure P_{so} .

b. Scaled unit positive incident impulse $i_s/W^{1/3}$. Multiply scaled value by $W^{1/3}$ to obtain absolute value.

c. Shock front velocity U.

Step 4. Determine the maximum vertical ground motions.

a. Calculate maximum vertical velocity.

$$V_V = \frac{P_{so}}{\rho C_p} \quad (\text{eq. 2-74})$$

where:

ρ = Mass density of soil (table 2-10)

C_p = Compression wave seismic velocity in the soil (table 2-11)

b. Calculate maximum vertical displacement

$$D_V = \frac{i_s}{1,000 \rho C_p} \quad (\text{eq. 2-74})$$

- c. Calculate maximum vertical acceleration of the ground surface.

$$A_V = \frac{100P_{so}}{\rho C_p g} \quad (\text{eq. 2-76})$$

where:

g = Gravitational constant equal to 32.2 ft/sec²

- Step 5. Determine the maximum horizontal ground motions parameters.

- a. Check $C_p/12000 U > .707$

- b. Calculate maximum horizontal velocity.

$$V_H = V_V \tan [\sin^{-1} (C_p/12,000 U)] \quad (\text{eq. 2-77})$$

- c. Calculate maximum horizontal displacement.

$$D_H = D_V \tan [\sin^{-1} (C_p/12,000 U)] \quad (\text{eq. 2-78})$$

- d. Calculate maximum horizontal acceleration.

$$A_H = A_V \tan [\sin^{-1} (C_p/12,000 U)] \quad (\text{eq. 2-79})$$

- Step 6. Determine arrival time t_A and duration to:

- a. Read from fig. 2-15.

$t_A/W^{1/3}$ scaled time of arrival of blast wave and,

$t_o/W^{1/3}$ scaled duration of positive phase.

- b. Multiply scaled value by $W^{1/3}$ to obtain absolute value.

Direct-Induced Ground Shock

- Step 7. Determine the maximum vertical ground motions.

- a. Calculate maximum vertical displacement.

$$D_V = \frac{0.025 R_G^{1/3} W^{1/3}}{Z_G^{1.3}} \quad (\text{eq. 2-80, rock media})$$

or

$$D_V = \frac{0.17 R_G^{1/3} W^{1/3}}{Z_G^{2.3}} \quad (\text{eq. 2-83, dry or saturated soil})$$

- b. Calculate the maximum vertical velocity.

$$V_V = 150/Z_G^{1.5} \quad (\text{eq. 2-85})$$

- c. Calculate the maximum vertical acceleration.

$$A_V = 10,000/W^{1/3} Z_G^2 \quad (\text{eq. 2-87})$$

Step 8. Determine the maximum horizontal ground motion parameters.

- a. Calculate the maximum horizontal displacement.

$$D_H = 0.5 D_V \quad (\text{eq. 2-82, rock media})$$

or

$$D_H = D_V \quad (\text{eq. 2-84, dry or saturated soil})$$

- b. Calculate the maximum horizontal velocity.

$$V_H = V_V \quad (\text{eq. 2-86, all ground media})$$

- c. Calculate the maximum horizontal acceleration.

$$A_H = 0.5 A_V \quad (\text{eq. 2-88, dry soil})$$

$$A_H = A_V \quad (\text{eq. 2-89, wet soil or rock media})$$

Step 9. Determine arrival time t_{AG} :

$$t_{AG} = 12000 R_G/C_p \quad (\text{eq. 2-92})$$

Example 2A-18 Ground Shock Loads

Required: Maximum acceleration, velocity, and displacement at a point 155 ft. away from a surface burst of 5,000 lbs. Also required are: times of arrival and duration of air-blast induced ground shock.

Solution:

Air blast-induced ground shock.

Step 1. Given: Charge weight = 5,000 lbs., $R = 155$ ft., $H_c = 12$ ft.

Step 2. $W = 1.2 (5,000) = 6,000$ lbs.

Step 3. Calculate the scaled distance Z .

$$Z = \frac{R}{W^{1/3}} = \frac{155}{(6,000)^{1/3}} = 8.53 \text{ ft/lb}^{1/3}$$

Read from Figure 2-15.

a. $P_{so} = 13$ psi

b. $\frac{i_s}{W^{1/3}} = 9 \text{ psi-ms/lb}^{1/3}$

$$i_s = 9 \times W^{1/3} = 9 \times (6,000)^{1/3} = 163.54 \text{ psi-ms}$$

c. $U = 1.5$ ft/ms

Step 4. Determine the maximum vertical ground motion.

a. $V_V = \frac{P_{so}}{\rho C_p} \quad (\text{eq. 2-74})$

$$V_V = \frac{13}{1.65 \times 10^{-4} \times 70,000} = 1.125 \text{ in/sec}$$

b. $D_V = \frac{i_s}{1,000 \rho C_p} \quad (\text{eq. 2-75})$

$$D_V = \frac{163.5}{1,000 (1.65 \times 10^{-4}) 70,000} = 0.0142 \text{ in}$$

c.
$$A_V = \frac{100 P_{so}}{\rho C_p g} \quad (\text{eq. 2-76})$$

$$A_V = \frac{100 \times 12.8}{(1.65 \times 10^{-4}) 70,000 \times 32.2} = 3.44 \text{ g}$$

Step 5. Determine the maximum horizontal ground motion.

a. Check $C_p/12000 U > .707$
 $70,000/12,000 \times 1.5 = 3.89 > .707$

b. $V_H = V_V = 1.125 \text{ in/sec}$

c. $D_H = D_V = 0.0142 \text{ in}$

d. $A_H = A_V = 3.44 \text{ g}$

Step 6. Arrival time t_A

a. Read from Figure 2-15.

$$\frac{t_A}{W^{1/3}} = 3.35 \text{ ms/lb}^{1/3}$$

$$t_o/W^{1/3} = 2.35 \text{ ms/lb}^{1/3}$$

b. $t_A = 3.35 \times W^{1/3} = 3.35 (6,000)^{1/3}$

$$t_A = 60.90 \text{ ms}$$

$$t_o = 2.35 \times W^{1/3} = 2.35 \times (6,000)^{1/3}$$

$$t_0 = 42.70 \text{ ms}$$

Direct-induced ground shock.

Step 7. Maximum vertical ground motions.

$$\begin{aligned} \text{a. } D_V &= \frac{0.17 R_G^{1/3} W^{1/3}}{Z_G^{2.3}} && \text{(eq. 2-83)} \\ &= \frac{0.17 (155)^{1/3} (6,000)^{1/3}}{(8.53)^{2.3}} = 0.1198 \text{ in} \end{aligned}$$

$$\begin{aligned} \text{b. } V_V &= 150/Z_G^{1.5} && \text{(eq. 2-85)} \\ V_V &= 150 / 8.53^{1.5} = 6.020 \text{ in/sec} \end{aligned}$$

$$\begin{aligned} \text{c. } A_V &= 10,000 / W^{1/3} Z_G^2 && \text{(eq. 2-87)} \\ A_V &= 10,000 / [(6,000)^{1/3} (8.53)^2] = 7.56 \text{ g} \end{aligned}$$

Step 8. Horizontal ground motions.

$$\begin{aligned} \text{a. } D_H &= D_V && \text{(eq. 2-84)} \\ D_H &= 0.1198 \text{ in.} \end{aligned}$$

$$\begin{aligned} \text{b. } V_H &= V_V && \text{(eq. 2-86)} \\ V_H &= 6.020 \text{ in/sec} \end{aligned}$$

$$\text{c. } A_H = 0.5 A_V \quad \text{(eq. 2-88)}$$

$$A_H = 0.5 \text{ (7.56)}$$

$$A_H = 3.78 \text{ g}$$

Step 9. Arrival time t_{AG}

$$t_{AG} = 12,000 R_G/C_P = (12,000 \times 155) / 70,000 \quad (\text{eq. 2-92})$$

$$t_{AG} = 26.6 \text{ ms}$$

Problem 2A-19 Structure Motion Due to Air Shock

Problem: Determine the maximum horizontal acceleration, displacement and velocity of an above ground structure subjected to air shock.

Procedure:

- Step 1. Determine external loadings acting on the roof, front and rear walls according to the procedure outlined in problem 2A-10.
- Step 2. Construct the horizontal force-time load curve by combining the front and rear wall loadings from step 1 applied over the area of front and rear walls. Use times of arrival to phase these two loads.
- Step 3. Calculate the dead weight and mass of the structure.
- Step 4. Construct the downward force-time curve by adding the weight of the structure and total roof load. The roof load is the pressure time loading from step 1 applied over the total area of the roof.
- Step 5. Determine the coefficient of friction between soil and the structure from table 2-12.
- Step 6. Determine maximum horizontal acceleration, displacement and velocity using the acceleration impulse extrapolation method outlined in Chapter 3, Article 3-19.2.1.2 of this manual. The resisting force at each time interval is equal to the value of downward force curve of step 4 multiplied by the coefficient of friction determined in step 5. The resisting force is assumed to be effective when the total horizontal movement is equal to or larger than 1/4 inch as mentioned in paragraph

Example 2A-19 Structure Motion Due to Air Shock

Required: Maximum horizontal acceleration, velocity and displacement of the square structure shown in Figure 2A-9 from problem 2A-10 for a surface burst of 5,000 lbs at a distance from the front wall of 155 ft. Assume a coarse and compact soil. Roof, floor slab and side walls are 1 foot thick reinforced concrete slabs and assume a 50 psf of internal dead load for the structure.

Step 1. External loadings on the structure are determined according to the procedure in example 2A-10. See Figures 2A-10, 2A-12 and 2A-13. The arrival time (t_A) for these loads are tabulated in step 3d of example 2A-10.

$$\tau_{Af} \text{ (front wall)} = 60.9 \text{ ms}$$

$$\tau_{Ab} \text{ (rear wall)} = 83.6 \text{ ms}$$

Step 2. a. Calculate area of front and rear walls.

$$\text{Area (front and rear)} = 30 \times 12 \times (12)^2 = 51840 \text{ in}^2$$

b. Calculate the time difference between the rear and front walls from step 1.

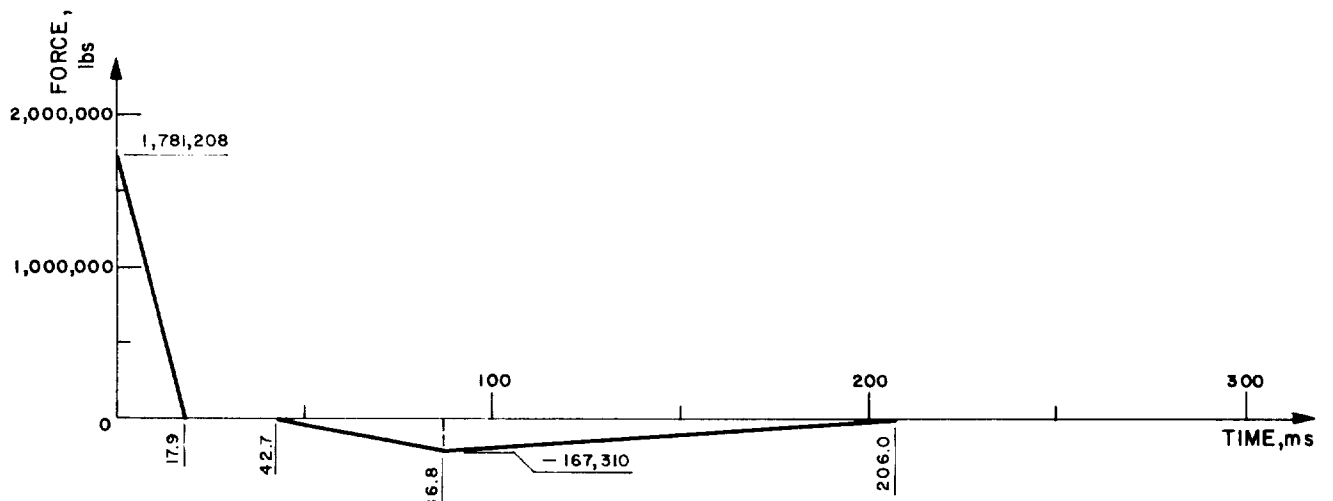
$$\delta t = \tau_{Ab} - \tau_{Af} = 83.6 - 60.9 = 22.7 \text{ ms}$$

c. Construct the horizontal force-time load curve by multiplying the values of the front and rear wall curves from step 1 by the area from step 2a. Rear wall load starts at time equal to $\delta t = 22.7$ from step 2b. See Figure 2A-26.

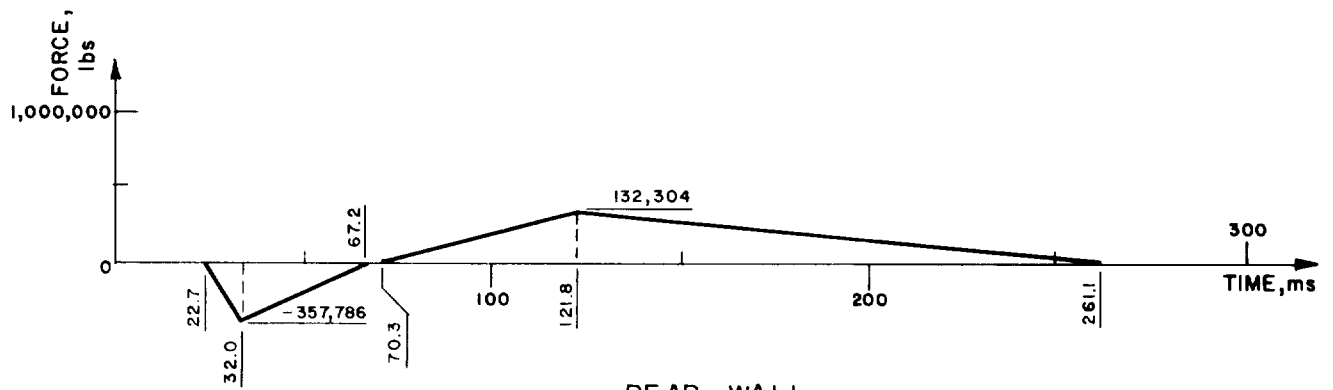
Step 3.

a. Calculate dead weight of structure W_d . Assume concrete weight is 150 psf.

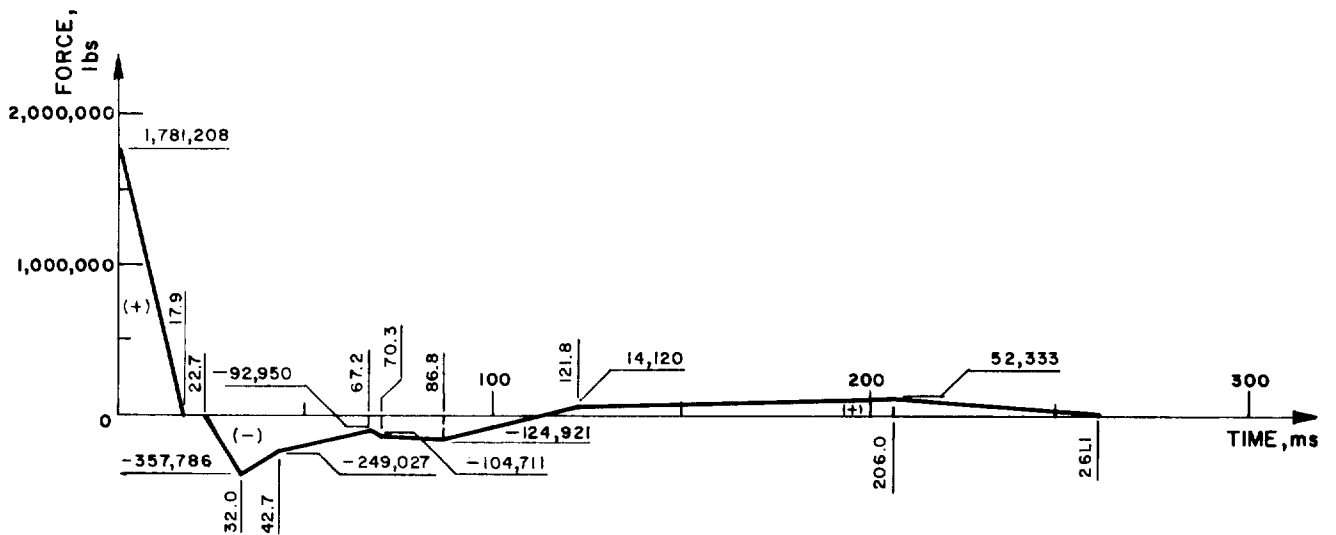
$$W_d = 150 [4 (30 - 1) (12-1) + 2 (30)^2] + 50 (30-2)^2 = 500,600 \text{ lbs}$$



FRONT WALL



REAR WALL



COMBINED

FIGURE 2A-26

b. Calculate total mass.

$$m = \frac{W_d}{g} = \frac{500,600 (1000)^2}{32.2 \times (12)} = 1295.55 \times 10^6 \frac{\text{lb ms}^2}{\text{in}}$$

Step 4. a. Calculate area of the roof.

$$\text{Area (roof)} = 30^2 \times (12)^2 = 129,600 \text{ in}^2$$

b. Construct the downward force-time curve by multiplying the values of the roof curve from step 1 by the roof area from step 4a, and adding the dead weight of structure $W_d = 500,600$ lbs from step 3a. (If the resulting value is negative, assume zero). See Figure 2A-27 below.

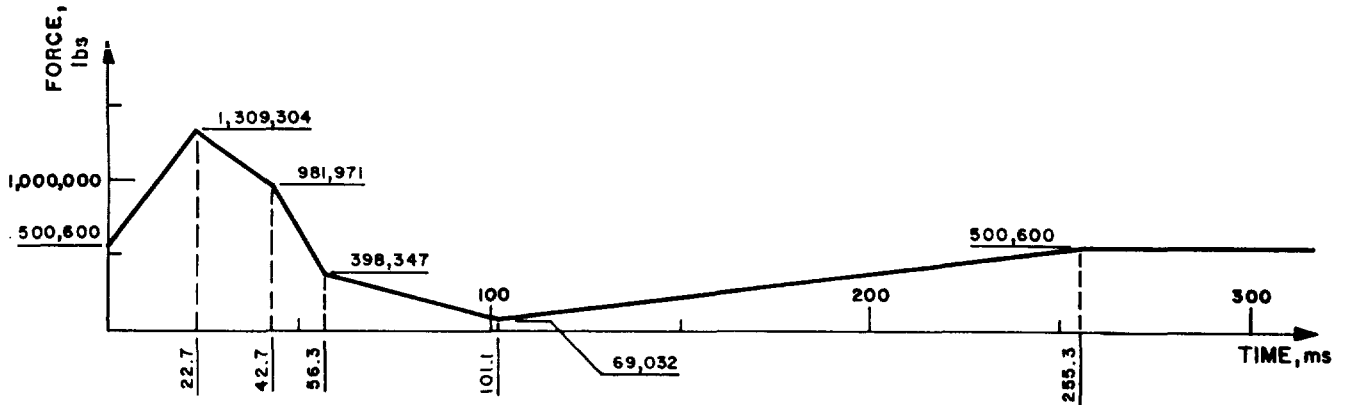


Figure 2A-27

Step 5. Coefficient of friction μ from table 2-12 for coarse and compact soil.

$$\therefore \mu = 0.60$$

Step 6. Using the acceleration impulse extrapolation method from Chapter 3 of this manual determine maximum horizontal acceleration, displacement and velocity of the structure due to load curve (P) from step 2c. Resisting force R is the friction force produced due to the downward load curve F from step 4b after an initial lateral translation of 1/4 inch. Use two ms time intervals for extrapolation. The

$$P_n - R_n = ma_n$$

$$R_n = \mu F_n$$

$$X_{n+1} = 2X_n - X_{n-1} + a_n (\delta t)^2$$

$$V_n = V_{n-1} + a_n (\delta t)$$

where

P_n = Load at time of step n (step 2c)

R_n = Resisting Friction Force at time step n

m = Mass from (step 3b)

a_n = Acceleration at time step n

μ = Friction coefficient (step 5)

F_n = Downward force at time step n (step 4b)

X_n = Deflection at time step n

V_n = Velocity at time step n

The maximum motions from Table 2A-3 are:

$$a_{\max} = .00122 \text{ in/ms}^2 \ll 101.67 \text{ ft/sec}^2 \ll 3.16 \text{ g's}$$

$$V_{\max} = .01231 \text{ in/ms} \ll 1.026 \text{ ft/sec}$$

$$D_{\max} = .355 \text{ in}$$

Problem 2A-20 Shock Response Spectra

Problem: Construct the elastic shock response spectra for the interior components of an above ground structure subject to an external explosion.

Procedure:

Table 2A-3

n	t	P_n lbs	R_n lbs	$P_n - R_n$ lbs	$a_n = (P_n - R_n)/m$ in/ms ²	$a_n(\delta t)^2$ in	$2X_n$ in	X_{n-1} in	X_{n-1} in	$a_n \delta t$ in	V_{n-1} in/ms	V_n in/ms
0	0	1,781,208	0	1,781,208	(.00138)/2	(.00550)/2	0	0	.00275	(.00275)/2	0	.00138
1	2	1,582,190	0	1,582,190	.00122	.00489	.00550	0	.01038	.00244	.00138	.00382
2	4	1,383,173	0	1,383,173	.00107	.00427	.02077	.00275	.02229	.00214	.00382	.00596
3	6	1,184,155	0	1,184,155	.00091	.00366	.04458	.01038	.03786	.00182	.00596	.00778
4	8	985,137	0	985,137	.00076	.00304	.07571	.02229	.05646	.00152	.00778	.00930
5	10	786,120	0	786,120	.00061	.00243	.11292	.03786	.07749	.00122	.00930	.01052
6	12	587,102	0	587,102	.00045	.00181	.15497	.05646	.10032	.00090	.01052	.01142
7	14	388,084	0	388,084	.00030	.00120	.20064	.07749	.12435	.00060	.01142	.01202
8	16	189,067	0	189,067	.00015	.00058	.24870	.10032	.14896	.00029	.01202	.01231
9	18	0	0	0	0	0	.29793	.12435	.17358	0	.01231	.01231
10	20	0	0	0	0	0	.34716	.14896	.19820	0	.01231	.01231
11	22	0	0	0	0	0	.39640	.17358	.22282	0	.01231	.01231
12	24	-50,013	0	-50,013	-.00004	-.00015	.44564	.19820	.24728	-.00008	.01231	.01223
13	26	-126,956	0	-126,956	-.00010	-.00039	.49456	.22282	.27135	-.00020	.01223	.01203
14	28	-203,890	733,536	-937,426	-.00072	-.00289	.54270	.24728	.29253	-.00142	.01203	.01061
15	30	-280,843	713,896	-994,739	-.00077	-.00307	.58505	.27135	.310629	-.00153	.01061	.00908
16	32	-357,786	694,256	-1,052,042	-.00081	-.00325	.62126	.29253	.32548	-.00162	.00908	.00746
17	34	-337,457	674,617	-1,012,074	-.00078	-.00312	.65096	.310629	.33721	-.00156	.00746	.00590
18	36	-317,128	654,977	-972,105	-.00075	-.00300	.67441	.32548	.34593	-.00150	.00590	.00440
19	38	-296,780	635,337	-932,117	-.00072	-.00288	.69186	.33721	.35177	-.00144	.00440	.00296
20	40	-276,471	615,697	-892,168	-.00069	-.00275	.70354	.34593	.35486	-.00138	.00296	.00158
21	42	-256,142	596,057	-852,199	-.00066	-.00263	.70972	.35177	.35532	-.00132	.00158	.00026
22	44	-240,745	555,710	-796,455	-.00061	-.00244	.71064	.35486	.35332	-.00122	.00026	.00096
23	46	-278,004	504,214				.70664	.35532				
24	48	-215,263	452,718				.35332					

- Step 1. Determine maximum acceleration, velocity and displacement due to ground shock according to procedure outlined in Problem 2A-18.
- Step 2. Determine maximum acceleration, velocity and displacement due to air shock according to the procedure outlined in Problems 2A-10 and 2A-19.
- Step 3. Determine if the ground shock is outrunning or superseismic (paragraph 2-23.2). For outrunning ground shock the maximum values of displacement, velocity and acceleration in horizontal and vertical directions are the algebraic summation of the maximum motions from steps 1 and 2. Otherwise proceed to step 4.
- Step 4. For superseismic ground shock the maximum values of displacement, velocity and acceleration are the numerically larger values of direct-induced ground shock or the algebraic sum of the maximum motions from air shock and airburst induced ground shock.
- Step 5. Calculate the magnitude of acceleration, velocity and displacement for response spectra in horizontal and vertical directions by multiplying the maximum values of motions from step 3 or step 4 by their appropriate factor from paragraph 2-24.3.
- Step 6. Draw the horizontal and vertical shock response spectras.

Example 2A-20 Shock Response Spectra

Required: Shock response spectra for the structure defined in Examples 2A-18 and 2A-19.

Solution:

- Step 1. Maximum values of motion in vertical and horizontal directions due to ground shock according to the procedure outlined in Example 2A-18 are:
 - a. Air blast-induced

$$A_H = A_V = 3.44 \text{ g}$$

$$V_H = V_V = 1.125 \text{ in/sec}$$

$$D_H = D_V = .014 \text{ in}$$
 - b. Direct-induced

$$A_H = 3.78 \text{ g}$$

$$A_V = 7.56 \text{ g}$$

$$V_H = V_V = 6.02 \text{ in/sec}$$

$$D_H = D_V = .120 \text{ in}$$

Step 2. Maximum horizontal acceleration, velocity and displacement due to air shock following the procedure outlined in Examples 2A-10 and 2A-19.

$$A_{\max} = 3.16 \text{ g}$$

$$V_{\max} = 12.31 \text{ in/sec}$$

$$D_{\max} = .355 \text{ in}$$

Step 3. a. Check for outrunning ground shock

$$T_{AG} < T_A:$$

From Example 2A-18

$$T_{AG} = 26.6 \text{ ms}$$

$$T_A = 60.9 \text{ ms}$$

∴ $T_{AG} < T_A$ Outrunning ground shock

b. Add the values of maximum motions from step 1 and step 2.

$$∴ A_H \max = 3.16 + 3.44 + 3.78 = 10.38 \text{ g}$$

$$∴ V_H \max = 12.310 + 1.108 + 6.020 = 19.438 \text{ in/sec}$$

$$∴ D_H \max = .355 + .014 + .120 = .489 \text{ in}$$

and

$$\therefore A_V \text{ max} = 3.44 + 7.56 = 11.00 \text{ g}$$

$$\therefore V_V \text{ max} = 1.108 + 6.020 = 7.128 \text{ in/sec}$$

$$\therefore D_V \text{ max} = .014 + .120 = .134 \text{ in}$$

Step 4. Does not apply, the ground shock is not superseismic.

Step 5. Magnitude of the motions for response spectra.

$$A_H = 10.38 \times 2.0 = 20.76 \text{ g}$$

$$V_H = 19.438 \times 1.5 = 29.157 \text{ in/sec}$$

$$D_H = .489 \times 1.0 = .489 \text{ in}$$

and

$$A_V = 11.00 \times 2.0 = 22.00 \text{ g}$$

$$V_V = 7.128 \times 1.5 = 10.692 \text{ in/sec}$$

$$D_V = .134 \times 1.0 = .134 \text{ in}$$

Step 6. See the shock response spectra for the values from step 6 in Figure 2A-28.

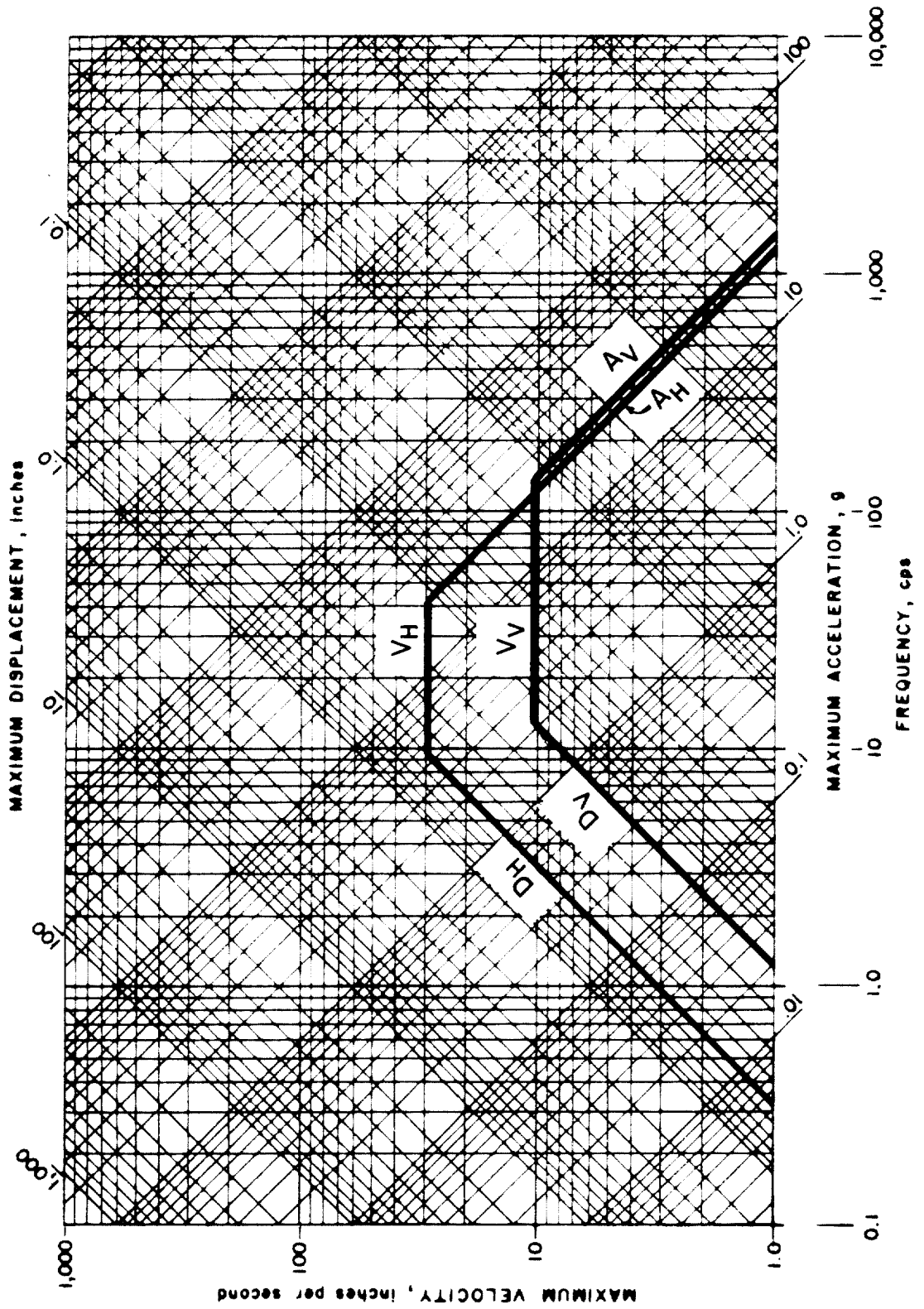


FIGURE 2A - 28

APPENDIX 2B
LIST OF SYMBOLS

a	(1) acceleration (in./ms ²) (2) depth of equivalent rectangular stress block (in.) (3) long span of a panel (in.)
a _o	velocity of sound in air (ft./sec.)
a _x	acceleration in x direction (in./ms ²)
a _y	acceleration in y direction (in./ms ²)
A	(1) area (in. ²) (2) explosive composition factor (oz. ^{1/2} -in. ^{-3/2})
A _a	area of diagonal bars at the support within a width b (in. ²)
A _b	area of reinforcing bar (in. ²)
A _d	(1) door area (in. ²) (2) area of diagonal bars at the support within a width b (in. ²)
A _D	drag area (in. ²)
A _f	net area of wall excluding openings (ft. ²)
A _g	area of gross section (in. ²)
A _H	maximum horizontal acceleration of the ground surface (g's)
A _l	area of longitudinal torsion reinforcement (in. ²)
A _L	lift area (in. ²)
A _n	(1) net area of section (in. ²) (2) area of individual wall subdivision (ft. ²)
A _o	area of openings (ft. ²)
A _{ps}	area of prestressed reinforcement (in. ²)
A _s	area of tension reinforcement within a width b (in. ²)
A _s '	area of compression reinforcement within a width b (in. ²)
A _s ⁻	area of rebound reinforcement (in. ²)
A _{sH}	area of flexural reinforcement within a width b in the horizontal direction on each face (in. ²)*
A _{sp}	area of spiral reinforcement (in. ²)
A _{st}	total area of reinforcing steel (in. ²)
A _{sV}	area of flexural reinforcement within a width b in the vertical direction on each face (in. ²)*

* See note at end of symbols

A_t	area of one leg of a closed tie resisting torsion within a distance s (in. ²)
A_v	total area of stirrups or lacing reinforcement in tension within a distance, s_s or s_l and a width b_s or b_l (in. ²)
A_v	maximum vertical acceleration of the ground surface (g's)
A_w	area of wall (ft. ²)
A_I, A_{II}	area of sector I and II, respectively (in. ²)
b	(1) width of compression face of flexural member (in.) (2) width of concrete strip in which the direct shear stresses at the supports are resisted by diagonal bars (in.) (3) short span of a panel (in.)
b_f	width of fragment (in.)
b_s	width of concrete strip in which the diagonal tension stresses are resisted by stirrups of area A_v (in.)
b_l	width of concrete strip in which the diagonal tension stresses are resisted by lacing of area A_v (in.)
b_o	failure perimeter for punching shear (in.)
b_t	center-to-center dimension of a closed rectangular tie along b (in.)
B	explosive constant defined in table 2-7 (oz. ^{1/2} in. ^{-7/6})
c	(1) distance from the resultant applied load to the axis of rotation (in.) (2) damping coefficient (3) width of column capital (in.)
c_I, c_{II}	distance from the resultant applied load to the axis of rotation for sectors I and II, respectively (in.)
c_s	dilatational velocity of concrete (ft./sec.)
C	(1) shear coefficient (2) deflection coefficient for flat slabs
C_C	deflection coefficient for the center of interior panel of flat slab
C_{cr}	critical damping
C_d	shear coefficient for ultimate shear stress of one-way elements
C_D	drag coefficient
C_{Dq}	drag pressure (psi)

C_{DQ_0}	peak drag pressure (psi)
C_E	equivalent load factor
C_f	post-failure fragment coefficient ($\text{lb.}^2\text{-ms}^4/\text{in.}^8$)
C_H	shear coefficient for ultimate shear stress in horizontal direction for two-way elements*
C_L	(1) leakage pressure coefficient from Figure 2-235
flat	(2) deflection coefficient for midpoint of long side of interior slab panel
	(3) lift coefficient
C_M	maximum shear coefficient
C_m	equivalent moment correction factor
C_p	compression wave seismic velocity in the soil from Table 2-10 (in./sec.)
C_r	sound velocity in reflected region from Figure 2-192 (ft./ms)
C_R	force coefficient for shear at the corners of a window frame
$C_{r\alpha}$	peak reflected pressure coefficient at angle of incidence α
C_s	shear coefficient for ultimate support shear for one-way elements
C_{sH}	shear coefficient for ultimate support shear in horizontal direction for two-way elements*
C_{sV}	shear coefficient for ultimate support shear in vertical direction for two-way elements*
C_S	deflection coefficient for midpoint of short side of interior flat slab panel
C_u	impulse coefficient at deflection X_u ($\text{psi-ms}^2/\text{in.}^2$)
C_u'	impulse coefficient at deflection X_m ($\text{psi-ms}^2/\text{in.}^2$)
C_v	shear coefficient for ultimate shear stress in vertical direction for two-way elements*
C_x	shear coefficient for the ultimate shear along the long side of window frame
C_y	shear coefficient for the ultimate shear along the short side of window frame
C_L	confidence level

* See note at end of symbols

C_1	(1) impulse coefficient at deflection X_1 (psi-ms ² /in. ²) (2) ratio of gas load to shock load
C_1'	impulse coefficient at deflection X_m (psi-ms ² /in. ²)
C_2	ratio of gas load duration to shock load duration
d	(1) distance from extreme compression fiber to centroid of tension reinforcement (in.) (2) diameter (in.) (3) fragment diameter (in.)
d'	distance from extreme compression fiber to centroid of compression reinforcement (in.)
d_b	diameter of reinforcing bar (in.)
d_c	distance between the centroids of the compression and tension reinforcement (in.)
d_{cH}	distance between the centroids of the horizontal compression and tension reinforcement (in.)
d_{co}	diameter of steel core (in.)
d_{cV}	distance between the centroids of the vertical compression and tension reinforcement (in.)
d_e	distance from support and equal to distance d or d_c (in.)
d_i	average inside diameter of explosive casing (in.)
d_i'	adjusted inside diameter of casing (in.)
d_p normal	distance between center lines of adjacent lacing bends measured to flexural reinforcement (in.)
d_p	distance from extreme compression fiber to centroid of prestressed reinforcement (in.)
d_{sp}	depth of spalled concrete (in.)
d_1	diameter of cylindrical portion of primary fragment (in.)
D	(1) unit flexural rigidity (lb-in.) (2) location of shock front for maximum stress (ft.) (3) minimum magazine separation distance (ft.) (4) caliber density (lb/in. ³) (5) overall diameter of circular section (in.) (6) damping force (lb.) (7) displacement of mass from shock load (in.)
D_E	equivalent loaded width of structure for non-planar wave front (ft.)

D_H	maximum horizontal displacement of the ground surface (in.)
DIF	dynamic increase factor
D_s	diameter of the circle through centers of reinforcement arranged in a circular pattern (in.)
D_{sp}	diameter of the spiral measured through the centerline of the spiral bar (in.)
DLF	dynamic load factor
D_V	maximum vertical displacement of the ground surface (in.)
e	(1) base of natural logarithms and equal to 2.71828... (2) distance from centroid of section to centroid of prestressed reinforcement (in.) (3) actual eccentricity of load (in.)
e_b	balanced eccentricity (in.)
$2E'^{1/2}$	Gurney Energy Constant (ft./sec.)
E	(1) modulus of elasticity (2) internal work (in.-lbs.)
E_c	modulus of elasticity of concrete (psi)
E_m	modulus of elasticity of masonry units (psi)
E_s	modulus of elasticity of reinforcement (psi)
f	(1) unit external force (psi) (2) frequency of vibration (cps)
f_c'	static ultimate compressive strength of concrete at 28 days (psi)
f_{dc}'	dynamic ultimate compressive strength of concrete (psi)
f_{dm}'	dynamic ultimate compressive strength of masonry units (psi)
f_{ds}	dynamic design stress for reinforcement (a function of f_y , f_u and θ) (psi)
f_{du}	dynamic ultimate stress of reinforcement (psi)
f_{dy}	dynamic yield stress of reinforcement (psi)
f_m'	static ultimate compressive strength of masonry units (psi)
f_n	natural frequency of vibration (cps)
f_{ps} (psi)	average stress in the prestressed reinforcement at ultimate load

f_{pu}	specified tensile strength of prestressing tendon (psi)
f_{py}	yield stress of prestressing tendon corresponding to a 1 percent elongation (psi)
f_r	reflection factor
f_s	static design stress for reinforcement (psi)
f_{se} all	effective stress in prestressed reinforcement after allowances for prestress losses (psi)
f_u	static ultimate stress of reinforcement (psi)
f_y	static yield stress of reinforcement (psi)
F	(1) total external force (lbs.) (2) coefficient for moment of inertia of cracked section (3) function of C_2 and C_1 for bilinear triangular load
F_o	force in the reinforcing bars (lbs.)
F_E	equivalent external force (lbs.)
F_D	drag force (lbs.)
F_F	frictional force (lbs.)
F_L	lift force (lbs.)
F_N	vertical load supported by foundation (lbs.)
g	acceleration due to gravity (32.2 ft./sec. ²)
G	shear modulus (psi)
h	(1) charge location parameter (ft.) (2) height of masonry wall
h_n	average clearing distance for individual areas of openings from Section 2-15.4.2
h_t	center-to-center dimension of a closed rectangular tie along h (in.)
h'	clear height between floor slab and roof slab
H	(1) span height (in.)* (2) distance between reflecting surface(s) and/or free edge(s) in vertical direction (ft.) (3) minimum transverse dimension of mean presented area of object (ft.)
H_c	height of charge above ground (ft.)

H_s	height of structure (ft.)
H_T	height of triple point (ft.)
H_w	height of wall (ft.)
H_c	heat of combustion (ft.-lb./lb.)
H_d	heat of detonation (ft.-lb./lb.)
i	unit positive impulse (psi-ms)
i_a	sum of blast impulse capacity of the receiver panel and the least impulse absorbed by the sand (psi-ms)
i_{ba}	blast impulse capacity of receiver panel (psi-ms)
i^-	unit negative impulse (psi-ms)
\bar{i}_a	sum of scaled unit blast impulse capacity of receiver panel and scaled unit blast impulse attenuated through concrete and sand in a composite element (psi-ms/lb. ^{1/3})
i_b	unit blast impulse (psi-ms)
\bar{i}_b	scaled unit blast impulse (psi-ms/lb. ^{1/3})
\bar{i}_{ba}	scaled unit blast impulse capacity of receiver panel of composite element (psi-ms/lb. ^{1/3})
\bar{i}_{bd} element	scaled unit blast impulse capacity of donor panel of composite element (psi-ms/lb. ^{1/3})
\bar{i}_{bt}	total scaled unit blast impulse capacity of composite element (psi-ms/lb. ^{1/3})
i_c	impulse capacity of an element (psi-ms)
i_d	total drag and diffraction impulse (psi-ms)
i_e	unit excess blast impulse (psi-ms)
i_{fs}	required impulse capacity of fragment shield (psi-ms)
i_g	gas impulse (psi-ms)
i_r	unit positive normal reflected impulse (psi-ms)
i_r^-	unit negative normal reflected impulse (psi-ms)
$i_{r\alpha}$	peak reflected impulse at angle of incidence α (psi-ms)
i_s	unit positive incident impulse (psi-ms)

i_s^-	unit negative incident impulse (psi-ms)
i_{st}	impulse consumed by fragment support connection (psi-ms)
I	(1) moment of inertia (in. ⁴ /in. for slabs) (in. ⁴ for beams) (2) total impulse applied to fragment
I_a	average of gross and cracked moments of inertia (in. ⁴ /in. for slabs) (in. ⁴ for beams)
I_c	moment of inertia of cracked concrete section (in. ⁴ /in. for slabs) (in. ⁴ for beams)
I_{cH}	moment of inertia of cracked concrete section in horizontal direction (in. ⁴ /in.)*
I_{cV}	moment of inertia of cracked concrete section in vertical direction (in. ⁴ /in.)*
I_g	moment of inertia of gross concrete section (in. ⁴ /in. for slabs) (in. ⁴ for beams)
I_m	mass moment of inertia (lb.-ms ² -in.)
I_n	moment of inertia of net section of masonry unit (in. ⁴)
I_s	gross moment of inertia of slab (in. ⁴ /in.)
I_{st}	impulse consumed by the fragment support connection (psi-ms)
I_w	gross moment of inertia of wall (in. ⁴ /in.)
j	ratio of distance between centroids of compression and tension forces to the depth d
k	(1) constant depending on the casing metal (2) effective length factor
k_v	velocity decay coefficient
K	(1) unit stiffness (psi/in. for slabs) (lb./in./in. for beams) (lb./in. for springs) (2) constant defined in paragraph 2-18.2
K_e	elastic unit stiffness (psi/in. for slabs) (lb./in./in. for beams)
K_{ep}	elasto-plastic unit stiffness (psi/in. for slabs) (lb./in./in. for beams)
K_E	(1) equivalent elastic unit stiffness (psi/in. for slabs) (lb./in./ in. for beams) (2) equivalent spring constant (lb./in.)
K_L	load factor

* See note at end of symbols

K_{LM}	load-mass factor
$(K_{LM})_u$	load-mass factor in the ultimate range
$(K_{LM})_{up}$	load-mass factor in the post-ultimate range
K_M	mass factor
K_R	resistance factor
K_E	kinetic energy
l	charge location parameter (ft.)
l	(1) length of the yield line (in.) (2) width of 1/2 of the column strip (in.)
l_d	basic development length of reinforcing bar (in.)
l_{dh}	development length of hooked bar (in.)
l_c	length of cylindrical explosive (in.)
l_p	spacing of same type of lacing bar (in.)
l_s	span of flat slab panel (in.)
L	(1) span length (in.)* (2) distance between reflecting surface(s) and/or free edge(s) in horizontal direction (ft.)
L_{cyl}	length of cylinder (in.)
L_f	length of fragment (in.)
L_H	clear span in short direction (in.)
L_l	length of lacing bar required in distance s_1 (in.)
L_L	clear span in long direction (in.)
L_o	embedment length of reinforcing bars (in.)
L_u	unsupported length of column (in.)
L_w	wave length of positive pressure phase (ft.)
L_w^-	wave length of negative pressure phase (ft.)
L_x	clear span in long direction (in.)
L_y	clear span in short direction (in.)

L_{wb}, L_{wd}	wave length of positive pressure phase at points b and d, respectively (ft.)
L_1	total length of sector of element normal to axis of rotation (in.)
m	(1) unit mass (psi-ms ² /in. for slabs) [beams, (lb./in-ms ²)/in.] (2) ultimate unit moment (in.-lbs./in.) (3) mass of fragment (lbs.-ms ² /in.)
m_a	average of the effective elastic and plastic unit masses (psi-ms ² /in. for slabs) [beams, (lb./in-ms ²)/in]
m_e	effective unit mass (psi-ms ² /in. for slabs) [beams, (lb/in-ms ²)/in]
m_{sp}	mass of spalled fragments (psi-ms ² /in.)
m_u	effective unit mass in the ultimate range (psi-ms ² /in. for slabs) [beams, (lb/in-ms ²)/in.]
m_{up}	effective unit mass in the post-ultimate range (psi-ms ² /in.)
M beams)	(1) unit bending moment (in.-lbs./in. for slabs) (in.-lbs. for beams) (2) total mass (lb.-ms ² /in.) (3) design moment (in.-lbs.)
M_e	effective total mass (lb.-ms ² /in.)
M_u	ultimate unit resisting moment (in.-lbs./in. for slabs) (in.-lbs. for beams)
M_u^-	ultimate unit rebound moment (in.-lbs./in. for slabs) (in.-lbs. for beams)
M_c	moment of concentrated loads about line of rotation of sector (in.-lbs.)
M_A	fragment distribution factor
M_E	equivalent total mass (lb.-ms ² /in.)
M_{HN}	ultimate unit negative moment capacity in horizontal direction (in.-lbs./in.)*
M_{HP}	ultimate unit positive moment capacity in horizontal direction (in.-lbs./in.)*
M_{OH}, M_{OL}	total panel moment for direction H and L respectively (in.-lbs.)
M_N	ultimate unit negative moment capacity at supports (in.lbs./in. for slabs) (in.-lbs. for beams)
M_P	ultimate unit positive moment capacity at midspan (in.-lbs./in. for slabs) (in.-lbs. for beams)

* See note at end of symbols

M_{VN}	ultimate unit negative moment capacity in vertical direction (in.-lbs./in.)*
M_{VP}	ultimate unit positive moment capacity in vertical direction (in.-lbs./in.)*
M_1	value of smaller end moment on column
M_2	value of larger end moment on column
n	(1) modular ratio (2) number of time intervals (3) number of glass pane tests (4) caliber radius of the tangent ogive of fragment nose
N	(1) number of adjacent reflecting surfaces (2) nose shape factor
N_f	number of primary fragments larger than W_f
N_u	axial load normal to the cross section
N_T	total number of fragments
p	reinforcement ratio equal to A_s/bd or A_s/bd_c
p'	reinforcement ratio equal to A_s'/bd or A_s'/bd_c
p_b strength	reinforcement ratio producing balanced conditions at ultimate strength
p_o	ambient atmospheric pressure (psi)
p_p	prestressed reinforcement ratio equal to A_{ps}/bd_p
p_m	mean pressure in a partially vented chamber (psi)
p_{mo}	peak mean pressure in a partially vented chamber (psi)
p_r	average peak reflected pressure (psi)
p_H	reinforcement ratio in horizontal direction on each face*
p_T	total reinforcement ratio equal to $p_H + p_V$
p_V	reinforcement ratio in vertical direction on each face*
$p(x)$	distributed load per unit length
P	(1) pressure (psi) (2) concentrated load (lbs.)
P^-	negative pressure (psi)
P_c	critical axial load causing buckling (lbs.)

* See note at end of symbols

2B-11

P_g	maximum gas pressure (psi)
P_i	interior pressure within structure (psi)
δP_i	interior pressure increment (psi)
P_f	fictitious peak pressure (psi)
P_{max}	maximum average pressure acting on interior face of wall (psi)
P_o	(1) peak pressure (psi) (2) maximum axial load (lbs.) (3) atmospheric pressure (psi)
P_r	peak positive normal reflected pressure (psi)
P_r^-	peak negative normal reflected pressure (psi)
$P_{r\alpha}$	peak reflected pressure at angle of incidence α (psi)
P_{RIB}	maximum average pressure on backwall (psi)
P_s	positive incident pressure (psi)
P_{sb}, P_{se}	positive incident pressure at points b and e, respectively (psi)
P_{so}	peak positive incident pressure (psi)
P_{so}^-	peak negative incident pressure (psi)
$P_{sob}, P_{sod}, P_{soe}$	peak positive incident pressure at points b, d, and e, respectively (psi)
P_u	ultimate axial load at actual eccentricity c (lbs.)
P_x	ultimate load when eccentricity e_x is present (lbs.)
P_y	ultimate load when eccentricity e_y is present (lbs.)
q	dynamic pressure (psi)
q_b, q_e	dynamic pressure at points b and e, respectively (psi)
q_o	peak dynamic pressure (psi)
q_{ob}, q_{oe}	peak dynamic pressure at points b and e, respectively (psi)
r	(1) unit resistance (psi) (2) radius of spherical TNT [density equals 95 lb./ft. ³] charge (ft.) (3) radius of gyration of cross section of column (in.)
r^-	unit rebound resistance (psi, for slabs) (lb./in. for beams)

r_{avail}	dynamic resistance available (psi)
δr	change in unit resistance (psi, for slabs) (lb./in. for beams)
r_d	radius from center of impulse load to center of door rotation (in.)
r_{DL}	uniform dead load (psi)
r_e	elastic unit resistance (psi, for slabs) (lb./in. for beams)
r_{ep}	elasto-plastic unit resistance (psi, for slabs) (lb./in. for beams)
r_{fs}	ultimate unit resistance of fragment shield (psi)
r_T	tension membrane resistance (psi)
r_u	ultimate unit resistance (psi, for slabs) (lb./in. for beams)
r_{up}	post-ultimate unit resistance (psi)
r_l	radius of hemispherical portion of primary fragment (in.)
R	(1) total internal resistance (lbs.) (2) slant distance (ft.) (3) ratio of S/G (4) standoff distance (ft.)
R_{eff}	effective radius (ft.)
R_f	(1) distance traveled by primary fragment (ft.) (2) distance from center of detonation (ft.)
R_g	uplift force at corners of window frame (lbs.)
R_l	radius of lacing bend (in.)
R_t	target radius (ft.)
R_A	normal distance (ft.)
R_E	equivalent total internal resistance (lbs.)
R_G	ground distance (ft.)
R_u	total ultimate resistance (lb.)
R_I, R_{II}	total internal resistance of sectors I and II, respectively (lbs.)
s	(1) sample standard deviation (2) spacing of torsion reinforcement in a direction parallel to the longitudinal reinforcement (in.) (3) pitch of spiral (in.)

s_s	spacing of stirrups in the direction parallel to the longitudinal reinforcement (in.)
s_l	spacing of lacing in the direction parallel to the longitudinal reinforcement (in.)
S	height of front wall or one-half its width, whichever is smaller (ft.)
S'	weighted average clearing distance with openings (ft.)
SE	strain energy
t	time (ms)
δt	time increment (ms)
t_a	any time (ms)
t_b, t_e, t_f	time of arrival of blast wave at points b, e, and f, respectively (ms)
t_c	(1) clearing time for reflected pressures (ms) (2) average casing thickness of explosive charges (in.)
t_c'	(1) adjusted casing thickness (in.) (2) Clearing time for reflected pressures adjusted for wall openings (ms)
t_d	rise time (ms)
t_E	time to reach maximum elastic deflection (ms)
t_g	fictitious gas duration (ms)
t_m	time at which maximum deflection occurs (ms)
t_o	duration of positive phase of blast pressure (ms)
t_o^-	duration of negative phase of blast pressure (ms)
t_{of}	fictitious positive phase pressure duration (ms)
t_{of}^-	fictitious negative phase pressure duration (ms)
t_r	fictitious reflected pressure duration (ms)
t_u	time at which ultimate deflection occurs (ms)
t_y	time to reach yield (ms)
t_A	time of arrival of blast wave (ms)
t_{AG}	time of arrival of ground shock (ms)

t_1	time at which partial failure occurs (ms)
T	(1) duration of equivalent triangular loading function (ms) (2) thickness of masonry wall (in.) (3) toughness of material (psi-in./in.)
T_c	thickness of concrete section (in.)
\bar{T}_c	scaled thickness of concrete section (ft./lb. ^{1/3})
T_g	thickness of glass (in.)
T_H	force in the continuous reinforcement in the short span direction (lbs.)
T_i	angular impulse load (lb.-ms-in.)
T_L	force in the continuous reinforcement in the long span direction (lbs.)
T_N	effective natural period of vibration (ms)
T_{pf}	minimum thickness of concrete to prevent perforation by a given fragment (in.)
T_r	rise time (ms)
T_s	(1) thickness of sand fill (in.) (2) thickness of slab (in.)
T_{sp}	minimum concrete thickness to prevent spalling (in.)
\bar{T}_s	scaled thickness of sand fill (ft./lb. ^{1/3})
T_u	total torsional moment at critical section (in.-lbs.)
T_w	thickness of wall (in.)
T_y	force of the continuous reinforcement in the short direction (lbs.)
u	particle velocity (ft./ms)
u_u	ultimate flexural or anchorage bond stress (psi)
U	shock front velocity (ft./ms)
U_s	strain energy
v	velocity (in./ms)
v_a	instantaneous velocity at any time (in./ms)
v_b	boundary velocity for primary fragments (ft./sec.)

v_c	ultimate shear stress permitted on an unreinforced web (psi)
v_f	maximum post-failure fragment velocity (in./ms)
$v_f(\text{avg.})$	average post-failure fragment velocity (in./ms)
v_i	velocity at incipient failure deflection (in./ms)
v_o	initial velocity of primary fragment (ft./sec.)
v_r	residual velocity of primary fragment after perforation (ft./sec.)
v_s	striking velocity of primary fragment (ft./sec.)
v_{tc}	maximum torsion capacity of an unreinforced web (psi)
v_{tu}	nominal torsion stress in the direction of v_u (psi)
v_u	ultimate shear stress (psi)
v_{uH}	ultimate shear stress at distance d_e from the horizontal support (psi)*
v_{uV}	ultimate shear stress at distance d_e from the vertical support (psi)*
v_x	velocity in x direction (in./ms.)
v_y	velocity in y direction (in./ms.)
V	(1) volume of partially vented chamber (ft. ³) (2) velocity of compression wave through concrete (in./sec.) (3) velocity of mass under shock load (in./sec.)
V_d	ultimate direct shear capacity of the concrete of width b (lbs.)
V_{dH}	shear at distance d_e from the vertical support on a unit width (lbs./in.)*
V_{dV}	shear at distance d_e from the horizontal support on a unit width (lbs./in.)*
V_f	free volume (ft. ³)
V_H	maximum horizontal velocity of the ground surface (in./sec.)
V_o	volume of structure (ft. ³)
V_s	shear at the support (lb./in., for panels) (lbs. for beam)
V_{sH}	shear at the vertical support on a unit width (lbs./in.)*
V_{sV}	shear at the horizontal support on a unit width (lbs./in.)*
V_u	total shear on a width b (lbs.)

* See note at end of symbols

V_V	maximum vertical velocity of the ground surface (in./sec.)
V_X	unit shear along the long side of window frame (lb./in.)
V_Y	unit shear along the short side of window frame, (lbs./in.)
w	applied uniform load (lbs.-in. ²)
w_c	(1) unit weight (psi, for panels) (lb./in. for beam) (2) weight density of concrete (lbs./ft. ³)
w_s	weight density of sand (lbs./ft. ³)
W	(1) design charge weight (lbs.) (2) external work (in.-lbs.) (3) width of wall (ft.)
W_A	weight of fluid (lbs.)
W_{ACT}	actual quantity of explosives (lbs.)
W_c	total weight of explosive containers (lbs.)
W_E	effective charge weight (lbs.)
W_{EG}	effective charge weight for gas pressure (lb.)
W_{EXP}	weight of explosive in question (lbs.)
W_f	weight of primary fragment (oz.)
\bar{W}_f	average fragment weight (oz.)
W_F	weight of frangible element (lb./ft. ²)
W_{CI}	weight of inner casing (lbs.)
W_{co}	total weight of steel core (lbs.)
W_{CO}	weight of outer casing (lbs.)
W_{c1}, W_{c2}	total weight of plates 1 and 2, respectively (lbs.)
W_s	width of structure (ft.)
W_D	work done
x	yield line location in horizontal direction (in.)*
X	(1) deflection (in.) (2) distance from front of object to location of largest cross section to plane of shock front (ft.)
X_a	any deflection (in.)

* See note at end of symbols

X_c	lateral deflection to which a masonry wall develops no resistance (in.)
X_{DL}	deflection due to dead load (in.)
X_e	elastic deflection (in.)
X_E	equivalent elastic deflection (in.)
X_{ep}	elasto-plastic deflection (in.)
X_F	maximum penetration into concrete of armor-piercing fragments (in.)
X_F'	maximum penetration into concrete of fragments other than armor-piercing (in.)
X_m	maximum transient deflection (in.)
X_p	plastic deflection (in.)
X_s	(1) maximum penetration into sand of armor-piercing fragments (in.) (2) static deflection (in.)
X_u	ultimate deflection (in.)
X_1	(1) partial failure deflection (in.) (2) deflection at maximum ultimate resistance of masonry wall (in.)
y	yield line location in vertical direction (in.)*
y_t	distance from the top of section to centroid (in.)
Z	scaled slant distance (ft./lb. ^{1/3})
Z_A	scaled normal distance (ft./lb. ^{1/3})
Z_G	scaled ground distance (ft./lb. ^{1/3})
α	(1) angle formed by the plane of stirrups, lacing, or diagonal reinforcement and the plane of the longitudinal reinforcement (deg) (2) angle of incidence of the pressure front (deg) (3) acceptance coefficient (4) trajectory angle (deg.)
α_{ec}	ratio of flexural stiffness of exterior wall to flat slab
$\alpha_{ecH}, \alpha_{ecL}$	ratio of flexural stiffness of exterior wall to slab in direction H and L respectively

* See note at end of symbols

β	(1) coefficient for determining elastic and elasto-plastic resistances (2) particular support rotation angle (deg) (3) rejection coefficient (4) target shape factor from Figure 2-212
β_1	factor equal to 0.85 for concrete strengths up to 4,000 psi and is reduced by 0.05 for each 1,000 psi in excess of 4,000 psi
γ	coefficient for determining elastic and elasto-plastic deflections
γ_p	factor for type of prestressing tendon
δ	moment magnifier
δ_n	clearing factor
δ	deflection at sector's displacement (in.)
ϵ_c'	average strain rate for concrete (in./in./ms)
ϵ_m	unit strain in mortar (in./in.)
ϵ_s'	average strain rate for reinforcement (in./in./ms)
ϵ_u	rupture strain (in./in./ms)
θ	(1) support rotation angle (deg) (2) angular acceleration (rad/ms ²)
θ_{max}	maximum support rotation angle (deg)
θ_H	horizontal rotation angle (deg)*
θ_V	vertical rotation angle (deg)*
μ	(1) ductility factor (2) coefficient of friction
ν	Poisson's ratio
ρ	(1) mass density (lbs.-ms. ² /in. ⁴) (2) density of air behind shock front (lbs/ft. ³)
ρ_a	density of air (oz./in. ³)
ρ_c	density of casing (oz./in. ³)
ρ_f	mass density of fragment (oz./in. ³)
ρ_o	mass density of medium (lb.-ms. ² /in. ⁴)
σ_u	fracture strength of concrete (psi)

Σ_o	effective perimeter of reinforcing bars (in.)
ΣM	summation of moments (in.-lbs.)
ΣM_N	sum of the ultimate unit resisting moments acting along the negative yield lines (in.-lbs.)
ΣM_P	sum of the ultimate unit resisting moments acting along the positive yield lines (in.-lbs.)
ϕ	(1) capacity reduction factor (2) bar diameter (in.) (3) TNT conversion factor
ϕ_r	assumed shape function for concentrated loads
$\phi(x)$	assumed shape function for distributed loads free edge
=====	simple support
////////	fixed support
XXXXXX	either fixed, restrained, or simple support

* Note. This symbol was developed for two-way elements which are used as walls. When roof slabs or other horizontal elements are under consideration, this symbol will also be applicable if the element is treated as being rotated into a vertical position.

APPENDIX 2C - BIBLIOGRAPHY

Blast Loads

1. Armendt, B. R., Hippensteel, R. G., Hoffman, A. J., and Keefer, J. H., Project White Tribe: Air Blast From Simultaneously Detonated Large-Scale Explosive Charges, BRL Report 1145, Aberdeen Proving Ground, Maryland, September 1961.
2. Armendt, B. R., Hippensteel, R. G., Hoffman, A. J., and Kingery, C. N., The Air Blast From Simultaneously Detonated Explosive Spheres, BRL Report 1294, Aberdeen Proving Ground, Maryland, August 1960.
3. Armendt, B. R., Hippensteel, R. G., Hoffman, A. J., and Schlueter, S.D., The Air Blast From Simultaneously Detonated Explosive Spheres: Part II - Optimization, BRL Memorandum Report 1384, Department of the Army Project No. 503-04-002, Aberdeen Proving Ground, Maryland, January 1962.
4. Ayvazyan, H.E., Dobbs N., Computer Program Impres, special publication ARLCD-SP-84001, prepared by Ammann and Whitney, New York, New York, for U.S. Army Armament Research and Development Center, Large Caliber Weapon Systems Laboratory, Dover, New Jersey.
5. Baker, W. E., Explosions in Air, University of Texas Press, Austin, Texas 1973.
6. Baker, W. E., Prediction and Scaling of Reflected Impulse From Strong Blast Waves, International Journal of Mechanical Science, 9, 1967, pp. 45-51.
7. Bleakney, W., The Diffraction of Shock Waves Around Obstacles and the Transient Loading of Structures, Princeton University, March 1950, (Published and Distributed by the Armed Forces Special Weapons Project).
8. Coulter, G.A., Air Shock and Flow in Model Rooms, BRL Memorandum Report 1987, Aberdeen Proving Ground, Maryland, June 1969.
9. Coulter, G. A., Air Shock Filling of Model Rooms, BRL Memorandum Report 1916, Aberdeen Proving Ground, Maryland, March 1968.
10. Coulter, G. A. and Peterson, R.L., Blast Fill Time of a One-Room Structure, Operation Prairie Flat Project Officers Report, Project LN 111 POR-2102, Ballistic Research Laboratory, Aberdeen Proving Ground, Maryland, November 1964.
11. Coulter, G. A., Bulmash G., and Kingery C., Feasibility Study of Shock Wave Modification in the BRL 2.44 m Blast Simulator, Memorandum Report ARBRL-MR-0339, prepared by U.S. Army Armament Research and Development Center, Ballistic Research Laboratory, Aberdeen Proving Ground, Maryland, March 1984.
12. Cranz, C., Lehrbuch der Ballistik, Springer-Verlag, Berlin, 1926.
13. Dewey, J.M., Johnson, O.T., and Patterson, J.D. II, Mechanical Impulse Measurements Close to Explosive Charges, BRL Report 1182, Aberdeen Proving Ground, Maryland, November 1962.
14. Dobratz, B.M., LLNL Explosives Handbook, Properties of Chemical Explosives and Explosive Simulants, URCL-52997, Lawrence Livermore National Laboratory, Livermore, California, March 1981.
15. Engineering Design Handbook, Principles of Explosive Behavior, AMCP 706-180, Headquarters, U.S. Army Material Command, Washington, D.C., April 1972.
16. Goodman, H. J., Compiled Free Air Blast Data on Bar Spherical Pentolite, BRL Report 1092, Aberdeen Proving Ground, Maryland, 1960.
17. Granstorm, S. A., Loading Characteristics of Air Blasts From Detonating Charges, Transactions of the Royal Institute of Technology, Stockholm, Sweden, Nr.100, 1956.
18. Hokanson, J.C., Esparza, E. D., and Wenzel, A. B., Blast Effects of Simultaneous Multiple-Charge Detonations, Contractor Report ARLCD-CR-78032, ARRADCOM, Dover, New Jersey, AD E400232, October 1978.

19. Hokanson, J.C., Esparza, E.D., Baker W.E., Sandoval, N.R. and Anderson, C.E., Determination of Blast Loads in the Damaged Weapons Facility, Vol 3, Final Report, Purchase Order F0913400, SwR1-6578, prepared by Southwest Research Institute, San Antonio, Texas, for Mason and Hanger - Silas Mason Company, Inc., Pantex Plant, Amarillo, Texas, July 1982.
20. Hokanson, J. C., Esparza, E. D., and Wenzel, A. B., Reflected Blast Measurements Around Multiple Detonating Charges, Minutes of the Eighteenth Explosives Safety Seminar, Volume I, September 1978, pp. 447-471.
21. Hokanson, J. C., Esparza, E. D., Wenzel, A. B. (Southwest Research Institute). Price, P. D. (ARRADCOM). Blast Effects of Simultaneous Multiple-Charge Detonations, Contractor Report ARLCD-CR-78032, prepared by U.S. Army Armament Research and Development Command, Large Caliber Weapon Systems Laboratory, Dover, New Jersey, October 1978.
22. Hopkinson, B. British Ordnance Board Minutes, 13565, 1915.
23. Iwanski, E. C., et al., Blast Effects on Buildings and Structures Operation of 6-Foot and 2-Foot Shock Tubes: High Pressure Tests on Simple Shapes, Report No. 54, Final Test Report No. 10, ARF Project No. D087, Armour Research Foundation of Illinois Institute of Technology.
24. Jack, W. H., Jr., Measurements of Normally Reflected Shock Waves From Explosive Charges, BRL Memorandum Report 1499, Aberdeen Proving Ground, Maryland, AD 422886, July 1963.
25. Jack, W. H., Jr. and Armendt, B. F., Jr., Measurements of Normally Reflected Shock Parameters Under Simulated High Altitude Conditions, BRL Report 1280, Aberdeen Proving Ground, Maryland, AD 469014, April 1965.
26. Johansson, C. H. and Persson, P.A., Detonics of High Explosives, Academic Press, London, England, and New York, New York, 1970.
27. Johnson, O.T., Patterson, J.D. II, and Olson, W.C., A Simple Mechanical Method for Measuring the Reflected Impulse of Air Blast Waves, BRL Report 1099, Aberdeen Proving Ground, Maryland, July 1957.
28. Kaplan, K., Lewis, K. S., and Morris, P. J., Blast Loading and Response of Military Equipment, Draft Final Report URS 7339-6, URS Research Company, San Mateo, California, Prepared for Ballistic Research Laboratory, December 1973.
29. Kaplan, K. and Price, P.D., Accidental Explosions and Effects of Blast Leakage Into Structures, Contractor Report ARLCD-CR-79009, U.S. Army ARRADCOM, Dover, New Jersey, AD E400320, June 1979.
30. Keenan, W. A., and Tancreto, J. E., Blast Environment From Fully and Partially Vented Explosions in Cubicles, Technical Report R 828, prepared by Civil Engineering Laboratory, Naval Construction Battalion Center, Port Hueneme, California, sponsored by Department of the Army Picatinny Arsenal, November 1975.
31. Keenan, W., Tancreto, J., Meyers, G., Johnson, F., Hopkins, J., Nickerson, H., and Armstrong, W., NCEL Products Supporting DOD Revision of NAVFAC P-397, Program No. Y0995-01-003-201, Technical Memorandum 2591TM, sponsored by Naval Facilities Engineering Command, Alexandria, Virginia, and Naval Civil Engineering Laboratory, Port Hueneme, California, March 1983.
32. Kingery, C.N., and Bulmash G., Airblast Parameters from TNT Spherical Air Burst and Hemispherical Surface Burst, Technical Report ARBRL-TR-02555, prepared by U.S. Army Armament Research and Development Center, Ballistic Research Laboratory, Aberdeen Proving Ground, Maryland, April 1984.
33. Kingery, C. N. and Coulter G. A., Reflected Overpressure Impulse on a Finite Structure, Technical Report ARBRL-TR-02537. prepared by U. S.

- Army Armament Research and Development Center, Ballistic Research Laboratory, Aberdeen Proving Ground Maryland, December 1983.
34. Kingery, C. N. and Coulter G. A., Enhanced Blast as a Function of Multiple Detonations and Shape for Bare Pentolite Charges, Memorandum Report BRL-MR-3539, prepared by U.S. Army Ballistic Research Laboratory, Aberdeen Proving Ground, Maryland, July 1986.
 35. Kingery, C. N., Bulmash G., and Muller P., Blast Loading on Above Ground Barricaded Munition Storage Magazines, Technical Report ARBL-TR-02557, prepared by U.S. Army Armament Research and Development Center, Ballistic Research Laboratory, Aberdeen Proving Ground, Maryland, May 1984.
 36. Kriebel, A.R., Air Blast in Tunnels and Chambers, Final Report DASA 1200-11, Supplement 1, Prepared for Defense Civil Preparedness Agency, URS Research Company, San Mateo, California, September 1972.
 37. Makino, R. The Kirkwood-Brinkley Theory of the Propagation of Spherical Shock Waves and Its Comparison With Experiment, BRL Report 750, Aberdeen Proving Ground, Maryland, April 1951.
 38. McIntyre, F. L., TNT Equivalency Test Results of Selected High Explosives, Propellants, and Pyrotechnics in Surface Burst Configurations, Contractor Report, Prepared by Technical Services Laboratory, National Space Technology Laboratories, NSTL MS 39529, for U.S. Army Research and Development Engineering Center, Dover, New Jersey, Sponsored by U.S. Army - AMCCOM, July 1986.
 39. Melichar, J. F., The Propagation of Blast Waves Into Chambers, BRL Memorandum Report 1920, Aberdeen Proving Ground, Maryland, March 1968.
 40. Olson, W. C., Patterson, J. D. II, and Williams, J. S., The Effect of Atmospheric Pressure on the Reflected Impulse From Blast Waves, BRL Memorandum Report 1241, Aberdeen Proving Ground, Maryland, January 1960.
 41. Reeves H., and Robinson W. T., Hastings Igloo Hazards Tests for Small Explosive Charges, Memorandum Report ARBL-MR-03356, prepared by U. S. Army Armament Research and Development Center, Ballistic Research Laboratory, Aberdeen Proving Ground, Maryland, May 1984.
 42. Reisler, R. E., Kennedy, L. W., and Keefer, J. H., High Explosive Multi-Burst Air Blast Phenomena (Simultaneous and Non-Simultaneous Detonations), BRL Technical Report ARBRL-TR-02142, Aberdeen Proving Ground, Maryland, February 1979.
 43. Sachs, R. G., The Dependence of Blast on Ambient Pressure and Temperature, BRL Report 466, Aberdeen Proving Ground, Maryland, 1944.
 44. Shear, R. E., Incident and Reflected Blast Pressures for Pentolite, BRL Report 1262, Aberdeen Proving Ground, Maryland, September 1964.
 45. Shear, R. E. and McCane, P., Normally Reflected Shock Front Parameters, BRL Memorandum Report 1273, Aberdeen Proving Ground, Maryland, May 1960.
 46. Swisdak, M.M., Jr., Explosion Effects and Properties: Part I - Explosion Effects in Air, NSWC/WOL/TR 75-116, Naval Surface Weapons Center, White Oak, Silver Spring, Maryland, October 1975.
 47. The Effects of Nuclear Weapons, S. Glasstone, Editor, U. S. Atomic Energy Commission, Washington, D. C., (Revised Edition), 1964.
 48. Voltz, R. D., and Kiger, S. A., An Evaluation of the Separated Bay Concept for a Munition Assembly Complex; An Experimental Investigation of the Department of Energy Building 12-64 Complex, Technical Report SL-83-6, prepared by Structures Laboratory, U.S. Army Engineer Waterways Experiment Station, Vicksburg, Mississippi, for Department of Energy, Albuquerque Operations, Amarillo, Texas, September 1983.
 49. Ward, J. M. (DOD Explosives Safety Board), Swisdak, M. M., Jr., Peckham P. J., and Soper W. G. (NSWC), Lorenz R. A. (Boeing Military Aircraft Company), Modeling of Debris and Airblast Effects from Explosions

- inside Scaled Hardened Aircraft Shelters, Final Report NSWC TR 85-470, prepared by Naval Surface Weapons Center, Silver Spring, Maryland, May 1985.
50. Warnecke, C. Data Report: Support Test Evaluation of a Pre-Engineered Building, TECOM Project No. 2-CO-PIC-004, U.S. Army Dugway Proving Ground, Dugway, Utah, June 1977.
 51. Wenzel, A. B. and Esparza, E. D., Measurements of Pressures and Impulses at Close Distances From Explosive Charges Buried and in Air, Final Report on Contract No. DAAK02-71-C-0393 with U.S. Army MERDC, Fort Belvoir, Virginia, 1972.
 52. Wilton, C. and Gabrielsen, B. L., Shock Tunnel Tests of Preloaded and Arched Wall Panels, Final Report URS 7030-10, prepared for Defense Civil Preparedness Agency, URS Research Company, San Mateo, California, June 1973.
 53. Wilton, C. and Gabrielsen, B. L., Shock Tunnel Tests of Wall Panels, Technical Report, Volume I, Test Information and Analysis, URS 7030-7, prepared for Defense Civil Preparedness Agency, URS Research Company, San Mateo, California, January 1972.
 54. Wilton, C., Kaplan, K., and Gabrielsen, B.L., The Shock Tunnel: History and Results, Volume II - Loading Studies, Final Report SSI 7618-1, prepared for Defense Civil Preparedness Agency, Scientific Service, Inc., Redwood City, California, March 1978.
 55. Zaker, T. A., Blast Pressures From Sequential Explosions, Phase Report II, Project J6166, IIT Research Institute, Chicago, Illinois, March 25, 1969.

Primary and Secondary Fragments

56. Amos, C. W., Fragment Resistance of Martensitic Steel Sheets (U), AMRA TR-64-01, (CONFIDENTIAL), U.S. Army Materials Research Agency, Watertown, Massachusetts, January 1964.
57. Apgar, J. W., Reaction of Mild Steel Targets to Exploding Munitions (U), U.S. Army Ballistic Research Laboratories, Aberdeen Proving Ground, Maryland (CONFIDENTIAL), October 1967.
58. Baker, W. E., Non-Nuclear Weapons Effects on Protective Structures (U), AFWL-TR-67-133 (SECRET), Mechanics Research, Inc., Houston, Texas, for U.S. Air Force Weapons Laboratory, January 1969.
59. Beth, R. A., Final Report on Concrete Penetration, Report No A-388, National Defense Research Committee, Office of Scientific Research and Development, March 1946.
60. Bulmash, G., Kingery C.N., and Coulter, G.A., Velocity Measurements of Acceptor Wall Fragments From the Mass Detonation of Neighboring Above-Ground Barricaded Munition Storage Magazine Model. Technical Report BRL-TR-2719, prepared by U.S. Army Ballistic Research Laboratory, Aberdeen Proving Ground, Maryland, March 1986.
61. Cohen, E. and Dobbs N., Design Procedures and Details for Reinforced Concrete Structures Utilized in Explosive Storage and Manufacturing Facilities, Ammann and Whitney, Consulting Engineers, New York, New York, Annals of the New York Academy of Sciences, Conference on Prevention of and Protection Against Accidental Explosion of Munitions, Fuels and Other Hazardous Mixtures, Vol. 152, Art. 1, 1968.
62. Doyle, J.M., Klein, M.J. and Shah, H., Design of Missile Resistant Concrete Panels, Preprints of the 2nd International Conference on Structural Mechanics in Reactor Technology, Vol. 4, Commission of the European Communities, Brussels, 1973, Paper No. J 3/3.

63. Effects of Impact and Explosion, Volume 1, Office of Scientific Research and Development, National Defense Research Committee, Washington, D.C., 1946.
64. Fundamentals of Protective Design for Conventional Weapons, prepared by U.S. Army Engineer Waterways Experiment Station, Vicksburg, Mississippi, for Office, Chief of Engineers, U.S. Army, Washington, D.C., July 1984.
65. Gewaltney, R. C., Missile Generation and Protection in Light-Water-Cooled Power Reactor Plants, Nuclear Safety, 10(4): July-August 1969.
66. Giere, A. C., Calculating Fragment Penetration and Velocity Data for Use in Vulnerability Studies, NAVORD Report 6621, U.S. Naval Nuclear Evaluation Unit, Albuquerque, New Mexico, October 1959.
67. Gurney, R. W., The Initial Velocities of Fragments from Bombs, Shells and Grenades, Report No. 405, Ballistic Research Laboratories, Aberdeen Proving Ground, Maryland, September 1943.
68. Gurney, R. W., The Mass Distribution of Fragments from Bombs, Shells and Grenades, Report No. 448, Ballistic Research Laboratories, Aberdeen Proving Ground, Maryland, February 1944.
69. Healey, J. J., and Weissman, S., Primary Fragment Characteristics and Impact Effects in Protective Design, Minutes of the Sixteenth Explosive Safety Seminar, September 1974.
70. Hoffman, P. R., McMath, R.R., and Migotsky, E., Projectile Penetration Studies, AFWL Technical Report No. WL-TR-64-102, Avco Corporation for the Air Force Weapons Laboratory, Kirtland Air Force Base, December 1964.
71. Industrial Engineering Study to Establish Safety Design Criteria for Use in Engineering of Explosive Facilities and Operations, Ammann and Whitney, Consulting Engineers, New York, New York, Report for Picatinny Arsenal, Dover, New Jersey, April 1963.
72. Johnson, C. and Moseley, J.W., Preliminary Warhead Terminal Ballistic Handbook. Part 1: Terminal Ballistic Effects, NAVWEPS Report No. 7673, U.S. Naval Weapons Laboratory, Dahlgren, Virginia, March 1964.
73. Kolsky, H., Stress Waves in Solids, Dover Publications, New York, New York, 1963.
74. Kymer, J.R., Penetration Performance of Arrow Type Projectiles, Report R-1814, U.S. Army Frankford Arsenal, Philadelphia, Pennsylvania, May 1966.
75. Mott, R.I., A Theoretical Formula for the Distribution of Weights of Fragments, AC-3642 (British). March 1943.
76. Mott, R.I., A Theory of Fragmentation, Army Operational Research Group Memorandum, 113-AC-6427, Great Britain, 1943.
77. Non-Nuclear Weapons Effects on Protective Structures (U), Technical Report No. AFWL-TR-69-57, Air Force Weapons Laboratory, Kirtland Air Force Base, December 1964.
78. Non-Nuclear Weapons Effects on Protective Structures (U), Technical Report No. AFWL-TR-69-57, (SECRET), Mechanics Research, Inc., for the Air Force Weapons Laboratory, Kirtland Air Force Base, September 1969.
79. Recht, R., et al., Application of Ballistic Perforation Mechanics to Target Vulnerability and Weapons Effectiveness Analysis (U), NWC TR 4333 (CONFIDENTIAL), Denver Research Institute for the Naval Weapons Center, China Lake, California, October 1967.
80. Reeves H., and Robinson W. T., Hastings Igloo Hazards Tests for Small Explosive Charges, Memorandum Report ARBL-MR-03356, prepared by U.S. Army Armament Research and Development Center, Ballistic Research Laboratory, Aberdeen Proving Ground, Maryland, May 1984.

81. Rinehart, J. S. and Pearson, J., Behavior of Metals Under Impulsive Loads, The American Society of Metals, Cleveland, Ohio, 1954.
82. Robertson, H. P., Terminal Ballistics, Preliminary Report, Committee on Passive Protection Against Bombing, National Research Council, January 1941.
83. Sterne, T. E., A Note on the Initial Velocities of Fragments from Warheads, Report No. 648, Ballistic Research Laboratories, Aberdeen Proving Ground, Maryland, September 1947.
84. Thomas, L. H., Computing the Effect of Distance on Damage by Fragments, Report No. 468, Ballistic Research Laboratories, Aberdeen Proving Ground, Maryland, May 1944.
85. Voltz, R.D., and Kiger, S. A., An Evaluation of the Separated Bay Concept for a Munition Assembly Complex; an Experimental Investigation of the Department of Energy Building 12-64 Complex, Technical Report SL-83-6, prepared by Structures Laboratory, U. S. Army Engineer Waterways Experiment Station, Vicksburg, Mississippi, for Department of Energy, Albuquerque Operations, Amarillo, Texas .
86. Ward, J. M. (DOD Explosives Safety Board), Swisdak, M. M., Jr., Peckham, P. J., and Soper, W. G. (NSWC), Lorenz, R. A. (Boeing Military Aircraft Company). Modeling of Debris and Airblast Effects from Explosions Inside Scaled Hardened Aircraft Shelters, Final Report NSWC TR 85-470, prepared by Naval Surface Weapons Center, Silver Spring, Maryland, May 1985.

Shock Loads

87. American Society of Civil Engineers (ASCE), A Comparative Study of Structural Response to Explosion-Induced Ground Motions, ASCE, New York, New York, 1975.
88. Auld, H. E., A Study of Air-Blast-Induced Ground Motions, Ph.D. Thesis, University of Illinois, May 1967.
89. Baladi, G. Y., and P. F. Hadala, Ground Shock Calculation Parameter Study Report I Effect of Various Nonlinear Elastic Plastic Model Formulations, Waterways Experiment Station Technical Report S-71-4, April 1971.
90. Ballard, R. F., R. E. Leach, Middle North Series, Mixed Company Event, Strong Motion Seismic Measurements, Defense Nuclear Agency Report POR-6746, July 25, 1973.
91. Barkan, D. D., Dynamics of Bases and Foundations, McGraw Hill Book Co., New York, New York 1962.
92. Baron, M. L., A Summary of Some Analytical Studies on Air Blast Induced Ground Motions, Defense Atomic Support Agency Report 2634, March 1971.
93. Baron, M. L., I. Nelson, and I. Sandler, Investigation of Air Induced Ground Shock Effect Resulting from Various Explosive Sources, Report 2 Influence of Constitutive Models on Ground Motion Predictions, Waterways Experiments Station Contract Report S-71-10, November 1971.
94. Batchelder, F. E., et al., Hardness Program - Non-EMP, Hardness Program Plan for Safeguard Ground Facilities, Vol. 1, Management and Technical Plan, U. S. Army Corps of Engineers, Huntsville Division, HNDDSP-73-153-ED-R, August 16, 1974.
95. Carder, D. S., and W. K. Cloud. Surface Motion from Large Underground Explosions, J. Geophys. Res., 64, 1471-1487, 1959.
96. Carnes, B. L., and J. A. Conway. Mine Throw I: Cratering Effects of a Multiton Near Surface Detonation in Desert Alluvium, Waterways Experiment Station Technical Report N-73-3, May 1973.

97. Christensen, W. J., Air Blast Induced Ground Shock, Navy Bureau of Yards and Decks Technical Study 27, September 1959.
98. Cooper, H. Jr., and J. L. Bratton, Calculation of Vertical Airblast-Induced Ground Motions from Nuclear Explosions in Frenchman Flat, Air Force Weapons Laboratory Report AFWL-TR-73-111, October 1973.
99. Cooper, H. F., Jr., Empirical Studies of Ground Shock and Strong Motions in Rock, Defense Nuclear Agency Report 3245F, October 1973.
100. Crandell, F. J., Ground Vibrations Due to Blasting and Its Effect Upon Structures, Journal Boston Soc., Civil Engineers, Vol. 36, p. 245, 1949.
101. Crandell, F. J., Transmission Coefficient for Ground Vibrations Due to Explosions, J. Boston Soc. Civil Engineering, 47, 152-168, 1960.
102. Crawford, R. E., C. J. Higgins, and E. H. Bultmann. Air Force Manual for Design and Analysis of Hardened Structures, Air Force Weapons Laboratory Report AFWL-TR-74-102, October 1974.
103. Day, J. D., H. J. Stout, and D. W. Murrell, Middle Gust Calibration Shots: Ground Motion Measurements, Waterways Experiment Station Technical Report N-75-1, February 1975.
104. Duvall, Wilbur I. and D. E. Fogelson, Review of Criteria for Estimating Damage to Residences from Blasting Vibrations, Bureau of Mines Report of Investigation 5968, 1962.
105. Dvorak, A., Seismic Effects of Blasting on Brick Houses, Proce Geofyrikeniha Ustance Ceskoslavenski Akademie, Vol. No. 169, Geofyskialni Sbornik, pp. 189-202, 1962.
106. Edwards, A. T. and T. D. Northwood, Experimental Studies of the Effects of Blasting on Structures, The Engineer, V. 210, pp. 538-546, September 30, 1960.
107. Eubanks, R. A. and B. R. Juskie, Shock Hardening of Equipment, Shock and Vibrations Bulletin, No. 32, Part III, December 1963.
108. Galbraith, F. W., Operation Distant Plain Final Report Proj. 3.02b Shock Spectrum Measurements, TRW Systems Group Report 05318-6001-R000, January 1968.
109. Galbraith, F. W., Operation Prairie Flat, Proj. LN-306 Shock Spectrum Measurements, Defense Atomic Support Agency Report POR-2107, February 1970.
110. Grubaugh, R. E., and L. E. Elliot, Scaling of Ground Shock Spectra, Defense Atomic Support Agency Report DASA-1921, February 1967.
111. Habberjam, G. M. and J. T. Whetton, On the Relationship Between Seismic and Amplitude and Charge of Explosive Fired in Routine Blasting Operations, Geophysics 17. 116-128, January 1952.
112. Hendron, A. J. Jr., Correlation of Operation Snowball Ground Motions with Dynamic Properties of Test Site Soils, Waterways Experiment Station Miscellaneous Paper I-745. October 1965.
113. Hoffman, H. V., F. M. Sauer, and B. Barclay, Operation Prairie Flat, Proj. LN-308 Strong Ground Shock Measurements, Defense Atomic Support Agency Report POR-2108, April 1971.
114. Hudson, D. E., J. L. Alford, and W. D. Iwan, Ground Accelerations Caused by Large Quarry Blasts, Bull. Seismic Soc., A, 51, 191-202, 1961.
115. Ichiro, I., On the Relationship Between Seismic Ground Amplitude and the Quantity of Explosives in Blasting, Reprint from Memoirs of the Faculty of Engineering, Kyoto University, 15, 579-587, 1953.
116. Ingram, J. K., Project Officer's Final Report Operation Distant Plain Events 1, 2A, 3, 4, and 5, Proj. 3.02A Earth Motion and Stress Measurements, Waterways Experiment Station Technical Report N-71-3, May 1971.
117. Ingram, L. F., Ground Motions from High Explosive Experiments, Waterways Experiment Station Miscellaneous Paper N-72-10, December 1972.

118. Jaramillo, E. E., and R. E. Pozega, Middle Gust Free-Field Data Analysis, Air Force Weapons Laboratory Report AFWL-TR-73-251, April 1974.
119. Joachim, C. E., Mine Shaft Series, Events Mine Under and Mine Ore; Ground Motion and Stress Measurements, Waterways Experiment Station Technical Report N-72-1, January 1972.
120. Kennedy, T. E., In-Structure Motion Measurements, Proj. LN-315 Operation Prairie Flat, Waterways Experiment Station Technical Report N-70-11, July 1970.
121. Kochly, J. A., and T. F. Stubbs, Mine Shaft Series, Mineral Rock Particle Velocity Measurements from a 100-ton TNT Detonation on Granite, Defense Nuclear Agency Report POR-2162, May 24, 1971.
122. Lamb, H., On the Propagation of Tremors Over the Surface of an Elastic Solid, Philosophical Transactions of Royal Society London, Series A, Volume 203, September 1904.
123. Langefors, Ulf, B. Kihlstron, and H. Westerberg, Ground Vibrations in Blasting, Water Power, pp. 335-338, 390-395, 421-424, February 1958.
124. Lockard, D. M., Crater Parameters and Material Properties, Air Force Weapons Laboratory Report AFWL-TR-74-200, October 1974.
125. Meireis, E. C. and A. R. Wright, Hardness Program - No-EMP, Hardness Program Plan for Safeguard Ground Facilities, Vol. 2, Safeguard Structures and TSE Description, U.S. Army Corps of Engineers, Huntsville Division, HNDDSP-73-153-ED-R, November 1973.
126. Morris, G., The Reduction of Ground Vibrations from Blasting Operations, Engineering, pp. 460-465, April 1957.
127. Morris, W. E., and others, Operation Jangle Blast and Shock Measurements I, Armed Forces Special Weapons Project Report WT 366, June 1952.
128. Murphey, B. F., Particle Motions Near Explosions in Halite, Journal of Geophysical Research, Vo. 66, No. 3, March 1961, pp. 947-958.
129. Murrell, D. W., Operation Mine Shaft, Mineral Rock Event, Far-out Ground Motions From a 100-ton Detonation on Granite, Waterways Experiment Station Technical Report N-72-6, April 1972.
130. Murrell, D. Operation SNOWBALL, Project 3.6 - Earth Motion Measurements, Waterways Experiment Station Technical Report TR 1-759. March 1967.
131. Newmark, N. M., and others, Air Force Design Manual Principles and Practices for Design of Hardened Structures, Air Force Special Weapons Center Report AFSWC-TDR-62-138, December 1962.
132. Nicholls, H. R., C. F. Johnson, and W. I. Duvall, Blasting Vibrations and Their Effects on Structures, Bureau of Mines Bulletin 656, 1971.
133. Odello, R. and P. Price, Ground Shock Effects from Accidental Explosions, Picatinny Arsenal Technical Report 4995, November 1976.
134. Palaniswamy, K., and J. L. Merritt, Evaluation of Middle Gust Data: Acoustic Path Length Scaling of Peak Velocities, Space and Missile Systems Organization Report 72-006-T4, November 1973.
135. Parsons, R. M., and others, Guide for the Design of Shock Isolation Systems for Underground Protective Structures, Air Force Special Weapons Center Report AFSWC-TDR-62-64, October 1962.
136. Phillips, B. R., and G. Y. Baladi, Results of Two Free-Field Code Calculations Versus Field Measurements for the Distant Plain 1A Event, Waterways Experiment Station Miscellaneous Paper S-73-21, April 1973.
137. Proceedings of the Mixed Company/Middle Gust Results Meeting 13-15 March 1973, Vol. II. Edited by General Electric-Tempo, Defense Nuclear Agency Report 3151-P2, May 1973.
138. Rausch, Maschinenfundamente Und Andere Dynamische Bauaufgaben, Vertrieb VDE Verlag G.M.B.H. (Berlin), 1943.

139. Reiher, H. and F. J. Meister, Die Empfindlichkeit der Menschen gegen Erschutterungen, Forsch. Gebiete Ingenieurwesen, Vol. 2, No. 11, pp. 381-386, 1931.
140. Richart, F. E. Jr., J. R. Hall, and R. D. Woods, Vibration of Soils and Foundations, Prentice-Hall, Inc., Englewood Cliffs, New Jersey, 1970.
141. Ricker, N., The Form and Nature of Seismic Waves and the Structure of Seismograms, Geophysics, 5, 348-366, 1940.
142. Sachs, D. C., and C. M. Swift, Small Explosion Tests, Project Mole, Armed Forces Special Weapons Project Report 291, Vols. I and II, December 1955.
143. Sager, R. A., Concrete Arch Studies, Proj. 3.2, Operation Snowball, Waterways Experiment Station Miscellaneous Paper I-736, August 1965.
144. Sandler, I.S., J. P. Wright, and M. L. Baron, Ground Motion Circulations for Events II and III of the Middle Gust Series, Defense Nuclear Agency Report DNA 3290T, April 1974.
145. Steffens, R. J., The Assessment of Vibration Intensity and its Application to the Study of Building Vibrations, National Building Studies Special Report No. 19, Department of Scientific and Industrial Research, Building Research Station, London, England, 1952.
146. Sauer, F. M., and C. T. Vincent, Ferris Wheel Series - Flat Top Event Earth Motion and Pressure Histories, Defense Atomic Support Agency Report Ferris Wheel POR-3002, April 1967.
147. Sauer, F. M., editor, Nuclear Geoplosics, A Sourcebook of Underground Phenomena and Effects of Nuclear Explosions, in 5 parts, Defense Atomic Support Agency Report DASA-1285, May 1964.
148. Sauer, F. M., Summary Report on Distant Plain Events 6 and 1a Ground Motion Experiments, Defense Atomic Support Agency Report DASA-2587, October 1970.
149. Teichmann, G. A. and R. Westwater, Blasting and Associated Vibrations, Engineering, pp. 460-465. April 1957.
150. Thoenen, J. R., and S. L. Windes, Seismic Effects of Quarry Blasting, Bureau of Mines Bulletin, 442, 83, 1942.
151. URS/John A. Blume and Associates, Seismic Hazard and Building Structure Behavior at the Pantex Facility, April 1976.
152. Vincent, C. T., Operation Prairie Flat, Proj. LN-304 Earth Pressure and Ground Shock Profile Measurements, Defense Atomic Support Agency Report POR-2113, May 1969.
153. Weidlinger, P., and A. Matthews, A Method for the Prediction of Ground Shock Phenomena in Soils, Air Force Special Weapons Center Report AFSWC-TDR-61-66, March 1962.
154. Westline, P. S., Esparza, E. D., and Wenzel, A. B., Analysis and Testing of Pipe Response to Buried Explosive Detonations, SwRI Final Report for American Gas Association, July 1978.
155. Willis, D. E. and J. T. Wilson, Maximum Vertical Ground Displacement of Seismic Waves Generated by Explosive Blasts, Bulletin Seismic Safety of America, 50, 455-459, 1960.
156. Zaccor, J. V., Procedures for Prediction of Ground Shock Phenomena Based on One-Dimensional Shock Propagation Considerations: Procedures and Applications, Waterways Experiment Station Contract Report 3-171. April 1967.
157. Zolasko, J. S., and G. Y. Baladi, Free-Field Code Predictions Versus Field Measurements: A Comparative Analysis for the Prairie Flat Event, Waterways Experiment Station Miscellaneous Paper S-71-6, March 1971.

"STRUCTURES TO RESIST THE EFFECTS OF ACCIDENTAL EXPLOSIONS"

CHAPTER 3. PRINCIPLES OF DYNAMIC ANALYSIS

CHAPTER 3

PRINCIPLES OF DYNAMIC ANALYSIS

INTRODUCTION

3-1. Purpose

The purpose of this manual is to present methods of design for protective construction used in facilities for development, testing, production, storage, maintenance, modification, inspection, demilitarization, and disposal of explosive materials.

3-2. Objective

The primary objectives are to establish design procedures and construction techniques whereby propagation of explosion (from one structure or part of a structure to another) or mass detonation can be prevented and to provide protection for personnel and valuable equipment.

The secondary objectives are to:

- (1) Establish the blast load parameters required for design of protective structures.
- (2) Provide methods for calculating the dynamic response of structural elements including reinforced concrete, and structural steel.
- (3) Establish construction details and procedures necessary to afford the required strength to resist the applied blast loads.
- (4) Establish guidelines for siting explosive facilities to obtain maximum cost effectiveness in both the planning and structural arrangements, providing closures, and preventing damage to interior portions of structures because of structural motion, shock, and fragment perforation.

3-3. Background

For the first 60 years of the 20th century, criteria and methods based upon results of catastrophic events were used for the design of explosive facilities. The criteria and methods did not include a detailed or reliable quantitative basis for assessing the degree of protection afforded by the protective facility. In the late 1960's quantitative procedures were set forth in the first edition of the present manual, "Structures to Resist the Effects of Accidental Explosions". This manual was based on extensive research and development programs which permitted a more reliable approach to current and future design requirements. Since the original publication of this manual, more extensive testing and development programs have taken place. This additional research included work with materials other than reinforced concrete which was the principal construction material referenced in the initial version of the manual.

Modern methods for the manufacture and storage of explosive materials, which include many exotic chemicals, fuels, and propellants, require less space for a given quantity of explosive material than was previously needed. Such concentration of explosives increases the possibility of the propagation of accidental explosions. (One accidental explosion causing the detonation of

other explosive materials.) It is evident that a requirement for more accurate design techniques is essential. This manual describes rational design methods to provide the required structural protection.

These design methods account for the close-in effects of a detonation including the high pressures and the nonuniformity of blast loading on protective structures or barriers. These methods also account for intermediate and far-range effects for the design of structures located away from the explosion. The dynamic response of structures, constructed of various materials, or combination of materials, can be calculated, and details are given to provide the strength and ductility required by the design. The design approach is directed primarily toward protective structures subjected to the effects of a high explosive detonation. However, this approach is general, and it is applicable to the design of other explosive environments as well as other explosive materials as mentioned above.

The design techniques set forth in this manual are based upon the results of numerous full- and small-scale structural response and explosive effects tests of various materials conducted in conjunction with the development of this manual and/or related projects.

3-4. Scope

It is not the intent of this manual to establish safety criteria. Applicable documents should be consulted for this purpose. Response predictions for personnel and equipment are included for information.

In this manual an effort is made to cover the more probable design situations. However, sufficient general information on protective design techniques has been included in order that application of the basic theory can be made to situations other than those which were fully considered.

This manual is applicable to the design of protective structures subjected to the effects associated with high explosive detonations. For these design situations, the manual will apply for explosive quantities less than 25,000 pounds for close-in effects. However, this manual is also applicable to other situations such as far- or intermediate-range effects. For these latter cases the design procedures are applicable for explosive quantities in the order of 500,000 pounds which is the maximum quantity of high explosive approved for aboveground storage facilities in the Department of Defense manual, "Ammunition and Explosives Safety Standards", DOD 6055.9-STD. Since tests were primarily directed toward the response of structural steel and reinforced concrete elements to blast overpressures, this manual concentrates on design procedures and techniques for these materials. However, this does not imply that concrete and steel are the only useful materials for protective construction. Tests to establish the response of wood, brick blocks, and plastics, as well as the blast attenuating and mass effects of soil are contemplated. The results of these tests may require, at a later date, the supplementation of these design methods for these and other materials.

Other manuals are available to design protective structures against the effects of high explosive or nuclear detonations. The procedures in these manuals will quite often complement this manual and should be consulted for specific applications.

Computer programs, which are consistent with procedures and techniques contained in the manual, have been approved by the appropriate representative of the US Army, the US Navy, the US Air Force and the Department of Defense Explosives Safety Board (DDESB). These programs are available through the following repositories:

- (1) Department of the Army
 Commander and Director
 U.S. Army Engineer
 Waterways Experiment Station
 Post Office Box 631
 Vicksburg, Mississippi 39180-0631
 Attn: WESKA

- (2) Department of the Navy
 Commanding Officer
 Naval Civil Engineering Laboratory
 Port Hueneme, California 93043
 Attn: Code L51

- (3) Department of the Air Force
 Aerospace Structures
 Information and Analysis Center
 Wright Patterson Air Force Base
 Ohio 45433
 Attn: AFFDL/FBR

If any modifications to these programs are required, they will be submitted for review by DDESB and the above services. Upon concurrence of the revisions, the necessary changes will be made and notification of the changes will be made by the individual repositories.

3-5. Format

This manual is subdivided into six specific chapters dealing with various aspects of design. The titles of these chapters are as follows:

Chapter 1	Introduction
Chapter 2	Blast, Fragment, and Shock Loads
Chapter 3	Principles of Dynamic Analysis
Chapter 4	Reinforced Concrete Design
Chapter 5	Structural Steel Design
Chapter 6	Special Considerations in Explosive Facility Design

When applicable, illustrative examples are included in the Appendices.

Commonly accepted symbols are used as much as possible. However, protective design involves many different scientific and engineering fields, and, therefore, no attempt is made to standardize completely all the symbols used. Each symbol is defined where it is first used, and in the list of symbols at the end of each chapter.

CHAPTER CONTENTS

3-6. General

This chapter contains the procedures for analyzing structural elements subject to blast overpressures. These procedures are contained in the next eleven sections; Section 3-7 deals with a simplified discussion of the basic principles of dynamics as well as the procedures for calculating the various components used to perform the dynamic analyses. Presented in Sections 3-8 through 3-15 are resistance-deflection functions for various elements including both one- and two-way panels as well as beam elements. These functions include the elastic, elasto-plastic, and plastic ranges of response. In addition, a discussion of dynamic equivalent systems is presented in Sections 3-16 and 3-17. These include single- and multi-degree-of-freedom systems. Presented in this Section also are methods for calculating load and mass factors required to perform the dynamic analyses.

Sections 3-18 through 3-20 include both a step-by-step numerical integration of an element's motion under dynamic loads utilizing the Acceleration-Impulse-Extrapolation Method or the Average Acceleration Method and design charts for idealized loads. Presented also in these Sections are methods for analyzing elements subjected to impulse type loadings; that is, loadings whose durations are short in comparison to the time to reach maximum response of the elements.

BASIC PRINCIPLES

3-7. General

The principles used in the analysis of structures under static load will be reviewed briefly, since the same principles are used in the analysis and design of structures subjected to dynamic loads. Two different methods are used either separately or concurrently in static analysis: one is based on the principle of equilibrium, and the other on work done and internal energy stored.

Under the application of external loads, a given structure is deformed and internal forces developed in its members. In order to satisfy static equilibrium, the vector sum of all the external and internal forces acting on any free body portion of the structure must be equal to zero. For the equilibrium of the structure as a whole, the vector sum of the external forces and the reactions of the foundation must be equal to zero.

The method based on work done and energy considerations is sometimes used when it is necessary to determine the deformation of a structure. In this method, use is made of the fact that the deformation of the structure causes the point of application of the external load to be displaced. The force then does work on the structure. Meanwhile, because of the structural deformations, potential energy is stored in the structure in the form of strain energy. By the principle of energy conservation, the work done by the external force and the energy stored in the members must be equal. In static analysis, simplified methods such as the method of virtual work and the method of the unit load are derived from the general principle of energy conservation.

In the analysis of statically indeterminate structures, in addition to satisfying the equations of equilibrium, it is necessary to include a calculation of the deformation of the structure in order to arrive at a complete solution of the internal forces in the structure. The methods based on energy considerations such as the method of least work and the method based on Castigliano's theorems are generally used.

For the analysis of structures under dynamic loading, the same two methods are basically used; but the load changes rapidly with time and the acceleration velocity and, hence, the inertia force and kinetic energy are of magnitudes requiring consideration. Thus, in addition to the internal and external forces, the equation of equilibrium includes the inertia force and the equation of dynamic equilibrium takes the form of Newton's equation of motion:

$$F - R = Ma \qquad 3-1$$

where

- F = total external force as a function of time
- R = total internal force as a function of time
- M = total mass
- a = acceleration of the mass

As for the principle of conservation of energy, the work done must be equal to the sum of the kinetic energy and the strain energy:

$$WD = KE + SE \qquad 3-2$$

where WD = work done

KE = kinetic energy

SE = strain energy

and the strain energy includes both reversible elastic strain energy and the irreversible plastic strain energy. Thus, the difference between structures under static and dynamic loads is the presence of inertial force (Ma) in the equation of dynamic equilibrium, and of kinetic energy in the equation of energy conservation. Both terms are related to the mass of the structure; hence, the mass of the structure becomes an important consideration in dynamic analysis.

In the dynamic analysis of structures, both the energy balance equation and the force balance equation are applied with explicit description of the external forcing function F , and the internal resisting forcing function R . The difference between these forcing functions is the inertia force as described above. The following is a discussion of the details of how these forces are utilized in the design of structures which respond in the ductile mode.

In the design of a structure to resist the blast from an HE explosion, the total external force acting on the structure can be obtained by the principles discussed Chapter 2. The design method also consists of the determination of the total internal force, i.e. the resistance of the structure required to limit calculated deflections of the individual members and the structure as a whole under the external force (blast loading), to within prescribed maximum values. The determination of the resistance of the individual members of the structure is presented in Sections 3-8 through 3-17. Subsequent sections of this manual present the principles and methods of dynamic analysis and equations, charts, and procedures for design.

RESISTANCE - DEFLECTION FUNCTIONS

3-8. Introduction

Under the action of external loads, a structural element is deformed and internal forces set up. The sum of these internal forces tending to restore the element to its unloaded static position is defined as the resistance. The resistance of a structural element is a reactive force associated with the deflection of the element produced by the applied load. It is convenient to consider the resistance as an equivalent load in the same manner as the applied load, but opposite in direction. The variation of the resistance vs. displacement is expressed by a resistance-deflection function and may be represented graphically. An idealized resistance-deflection function for an element spanning in two directions and covering in the complete flexural range to incipient failure is shown in Figure 3-1.

As load is applied to a structural element, the element deflects and, at any instant, exerts a resistance to further deformation, which is a function of its units stiffness K , until the ultimate unit resistance r_u (total resistance is $r_u A$ where A is the element area) of the element is reached at deflection X_p . The initial portion of the resistance-deflection diagram is composed of the elastic and elasto-plastic ranges, each with its corresponding stiffness, the transition from one range to another occurring as plastic hinges are formed at points of maximum stress (yield lines). The number of elasto-plastic ranges required before the ultimate resistance of a particular element is reached depends upon the type and number of supports, and the placement of reinforcing steel (in the case of reinforced concrete elements). For example a beam with simple supports subjected to uniformly distributed loads needs only one plastic hinge to develop the ultimate resistance (or full plastic strength) of the element; whereas for the same beam fixed at both ends, more than one plastic hinge is required.

In subsequent paragraphs, various procedures, equations and illustrations are presented to enable the designer to determine the resistances of both one- and two-way elements. The procedures outlined apply mainly to reinforced concrete elements and so do the equations appearing in the text, unless the equations are given as part of an illustrative example. However, they can also be used for structural steel elements as well as other structural elements such as aluminum, plastics, etc. Equations have been derived for specific cases most often encountered in practice. These are applicable for structural steel and reinforced concrete elements of uniform thickness in both the horizontal and vertical directions. Before the equations and figures can be used for reinforced concrete element, however, the reinforcing steel across any yield line must have a uniform distribution in both the vertical and horizontal directions; however, the reinforcement across the positive yield lines can be different from that across the negative yield lines and the reinforcing pattern in the vertical direction different from that in the horizontal direction.

Regardless of whether it is reinforced concrete or structural steel element, any opening in the element must be compact in shape and small in area, compared to the total area of the element.

3-9. Ultimate Resistance

3-9.1. General

The ultimate resistance of an element depends upon:

- (1) The distribution of the applied loads.
- (2) The geometry of the element (length and width).
- (3) The number and type of supports.
- (4) The distribution of the moment capacity or reinforcement in the case of reinforced concrete elements.

The distribution of the loads depends upon the design range of the element; i.e., high, intermediate or low pressure. For intermediate and low pressure ranges, it can be assumed that the pressure is uniform across the surface of the element although it varies with time. At high pressure ranges, however, the blast loads are variable across the surface of the element. However, for structural steel elements and concrete elements utilizing laced reinforcement, or for concrete elements with standard shear reinforcement which sustain relatively small deflections, a good estimate of the resulting deflections can be made using the resistance functions conforming to those of uniformly loaded elements.

The other factors that affect the ultimate resistance of an element are predetermined by the requirements of the protective structure (where the element is used) and the magnitude of the blast output.

3-9.2. One-Way Elements

The ultimate resistance of a one-way reinforced concrete element with an elastic distribution of its reinforcing steel is based on the moment capacity at first yield since all critical sections yield simultaneously. For one-way reinforced concrete elements (such as beams or slabs) with non-elastic distribution of reinforcing steel and for structural steel elements, the ultimate resistance is a function of the moment capacity at the first yield plus the added moment capacity due to subsequent yielding at other critical sections.

Values of the ultimate resistance for one-way elements are shown in Table 3-1 where the following symbols are used:

- M_N - ultimate negative unit moment capacity at the support.
- M_p - ultimate positive unit moment capacity at midspan.
- L - length
- r_u - ultimate unit resistance
- R_u - total ultimate resistance

Table 3-1 applies to both beams and slabs. However, special attention must be paid to the units used for the respective element. The moment capacity of a slab is expressed for a unit strip of the slab (inch-pounds per inch) whereas the total moment capacity (inch-pounds) is considered for a beam. Consequently, the resistance of a slab is expressed in load per unit area (psi) where the resistance of a beam is expressed in load per length along the beam (pounds per inch).

3-9.3. Two-Way Elements

The amount of data available on the limit analysis of rectangular steel plates is very limited. However, an elementary approach imagines a mechanism formed of straight yield lines, as is customary in reinforced concrete. This approach for reinforced concrete elements will be considered appropriate for structural steel elements.

In the design of two-way reinforced concrete elements, it is not necessary to define accurately the stress distribution during the initial and intermediate stages of loading since the ultimate load capacity can be readily determined by the use of yield line procedures. The yield line method assumes that after initial cracking of the concrete at points of maximum moment, yielding spreads until the full moment capacity is developed along the length of the cracks on which failure will take place. Several illustrative examples of the simplified yield or crack lines for two-way elements are illustrated in Figure 3-2.

In using the yield line solution, the initial step is to assume a yield line pattern (as shown in Figure 3-2) applying the following rules:

- (1) To act as plastic hinges of a collapse mechanism made up of plane segments, yield lines must be straight lines forming axes of rotation for the movements of the segments.
- (2) The supports of the slabs will act as axes of rotation. A yield line may form along a fixed support and an axis of rotation will pass over a column.
- (3) For compatibility of deformations, a yield line must pass through the intersection of the axes of rotation of the adjacent slab segments.

Tests indicate that the actual location and extent of these lines on reinforced concrete elements differ only slightly at failure from the theoretical ones. Use of the idealized yield lines results in little error in the determination of the ultimate resistance and the error is on the side of safety.

The corner sections of two-way elements are stiff in comparison to the remainder of the member; therefore, straining of the reinforcement which is associated with the reduced rotations at these sections will be less. To account for the corner effects, the design of any one particular section of a two-way element should consider a variation of the moment capacity along the yield lines rather than a uniform distribution.

This variation is approximated by taking the full moment capacity along the yield lines, except in the corners where two-thirds of the moment capacity over the lengths described in Figure 3-3 are used. The variation applies to both the negative moments along the supports and the positive moments at the interior. The ultimate unit resistance can be determined from the yield line pattern using either the principle of virtual work or the equations of equilibrium. Each approach has its advantages; in general, the virtual work method is easier in principle but difficult to manipulate algebraically since it involves differentiating a usually complex mathematical expression for a minimum value of resistance. The equilibrium method, which is used in this

manual, also has its disadvantages. Since equilibrium requires that the shear forces acting on each side of a yield line have to be equal and opposite, correction forces (also known as nodal forces) have to be introduced around openings in two-way members and at free edges, and these correction forces may not be available from simple analysis. However, in three of the six cases shown in Figure 3-2, (cases c, e, f), nodal forces exist; but their effects are negligible.

In order to calculate the ultimate unit resistance r_u of a two-way element, the equation of equilibrium of each sector formed by the yield lines is expressed in terms of the moments produced by the internal and external forces. The sum of the resisting moments acting along the yield lines (both positive and negative) of each sector is equated to the moment produced by the applied load about the axis of rotation (support of the sector), assuming that the shear forces are zero along the positive yield lines.

$$\Sigma M_N + \Sigma M_p = Rc = r_u A c \quad 3-3$$

where

- M_N = sum of the ultimate unit resisting moments acting along the support (negative yield lines)
- M_p = sum of the ultimate unit resisting moments acting along the interior failure lines (positive yield lines)
- R = total ultimate resistance of the sector
- c = distance from the centroid of the load to the line of rotation of the sector
- r_u = ultimate unit resistance of the sector
- m = area of the sector

Once the equations of equilibrium are known for all sectors, the ultimate resistance is obtained either by solving the equations simultaneously or by a trial and error procedure noting that the unit resistance of all sectors must be equal.

To illustrate the above procedure (Equation 3-3), consider the two-way concrete element shown in Figure 3-3 which is fixed on three edges and free on the fourth, and where the nomenclature is as follows:

- L = length of element
- H = height of element
- x = yield line location in horizontal direction
- y = yield line location in vertical direction
- M_{VN} = ultimate unit negative moment capacity in the vertical direction
- M_{VP} = ultimate unit positive moment capacity in the vertical direction
- M_{HN} = ultimate unit negative moment capacity in the horizontal direction
- M_{HP} = ultimate unit positive moment capacity in the horizontal direction

The nomenclature as stated in the paragraph above is strictly applicable to two-way elements which are used as walls. However, when roof slabs or other horizontal elements are under consideration, the preceding nomenclature will

also be applicable if the element is treated as being rotated into a vertical position.

The first step in the solution is to assume the location of the yield lines as defined by the coordinates x and y . It should be noted that in some cases, because of geometry, the value of x and y will be known and therefore need not be evaluated. In this example, the negative reinforcement in the horizontal direction at opposite supports is assumed to be equal; therefore, the vertical yield line is located at the center of the span and the value of x is numerically equal to $L/2$ (a, Figure 3-3). However, in other cases, neither the location of x nor y will be known, and the solution will require the determination of both coordinates.

Once the yield lines have been assumed, the distribution of the resisting moments along the yield lines is determined. In the case at hand, the reduced moments, as a result of the increased stiffness at the corners, act over lengths equal to $x/2$ and $y/2$ in the horizontal and vertical directions, respectively (a, Figure 3-3). The equations of equilibrium are then written for each sector with the use of the free body diagrams (b, Figure 3-3). For the triangular sector I:

$$\begin{aligned} M_{VN} &= (2/3)M_{VN} (L/4 + L/4) + M_{VN} (L/2) \\ &= (5/6)M_{VN} L \end{aligned} \tag{3-4}$$

$$\begin{aligned} M_{VP} &= (2/3)M_{VP} (L/4 + L/4) + M_{VP} (L/2) \\ &= (5/6)M_{VP} L \end{aligned} \tag{3-5}$$

$$C_I = y/3 \tag{3-6}$$

$$\begin{aligned} R_I &= (M_{VN} + M_{VP})/C_I \\ &= [5L(M_{VN} + M_{VP})]/2y \end{aligned} \tag{3-7}$$

$$A_I = Ly/2 \tag{3-8}$$

$$\begin{aligned} r_u(\text{Sector 1}) &= R_I/A_I \\ &= [5(M_{VN} + M_{VP})]/y^2 \end{aligned} \tag{3-9}$$

For the trapezoidal sector II, a similar procedure gives

$$\begin{aligned} M_{HN} &= (2/3)M_{HN} (y/2) + M_{HN} (H - y/2) \\ &= M_{HN} (H - y/6) \end{aligned} \tag{3-10}$$

$$\begin{aligned} M_{HP} &= (2/3)M_{HP} (y/2) + M_{HP} (H - y/2) \\ &= M_{HP} (H - y/6) \end{aligned} \tag{3-11}$$

$$\begin{aligned} C_{II} &= (1/3)(L/2)[2(H-y) + H]/(H + H - y) \\ &= [L(3H - 2y)]/6(2H - y) \end{aligned} \tag{3-12}$$

$$R_{II} = (M_{HN} + M_{HP})/C_{II}$$

$$= [(6H - y)(2H - y)(M_{HN} + M_{HP})]/L(3H - 2y) \quad 3-13$$

$$A_{II} = (1/2)(L/2)(H + H - y)$$

$$= [L(2H - y)]/4 \quad 3-14$$

$$r_u(\text{Sector II}) = R_{II}/A_{II}$$

$$= [4(M_{HN} + M_{HP})(6H - y)]/L^2(3H - 2y) \quad 3-15$$

Equations 3-9 and 3-15 are the equations of equilibrium for the triangular (I) and the trapezoidal (II) sectors, respectively. As mentioned previously, these equations can be solved simultaneously or by a trial and error procedure. In the latter method, values of y are substituted into both equations until r_u (sector I) is equal to r_u (sector II).

If a numerical solution based on the above procedure (Equation 3-3)-yields negative values for either x , y or r then the assumed yield line location is wrong. In this example, the only other possible yield line pattern ($x \leq L/2$) would be as shown in Figure 3-2c.

The solution of Equation 3-3 is universally applicable for any two-way element. If the negative reinforcement in the horizontal direction had been unequal at the opposing supports, the value of $x = L/2$ would have changed, and all three sectors would have had to be considered to determine x , y and hence, r_u .

Simultaneous solution of Equations 3-9 and 3-15 reveals that the locations of the yield lines are a function of the ratio of the spans L/H and the ratio of the sum of the unit vertical to horizontal moment capacities as follows:

$$r_u(\text{Sector I}) = r_u(\text{Sector II}) \quad 3-16$$

$$5(M_{VN} + M_{VP})/y^2 = [4(M_{HN} + M_{HP})(6H - y)]/L^2(3H - 2y) \quad 3-17a$$

$$L^2(M_{VN} + M_{VP})/H^2(M_{HN} + M_{HP}) =$$

$$[4y^2(6 - y/H)]/[5H^2(3 - 2y/H)] \quad 3-17b$$

$$(L/H)[(M_{VN} + M_{VP})/(M_{HN} + M_{HP})]^{1/2} =$$

$$(y/H)[(4(6 - y/H)/5(3 - 2y/H))]^{1/2} \quad 3-17c$$

Equation 3-17c, which relates the location of the yield lines to the moment capacity of the element, is used to plot Figure 3-6. Knowing the location of the yield lines, the resistance of the two-way element can be obtained from either Equation 3-9 or 3-15 which are also presented in Table 3-2.

Using the procedure outlined above, the values of the ultimate unit resistances for several two-way elements with various support conditions are given in Tables 3-2 and 3-3, the nomenclature confirming to that previously listed. Table 3-2 covers the special cases where opposite supports provide the same

degree of restraint thus resulting in symmetrical yield line patterns. Table 3-3 deals with the general cases when the yield line patterns are not symmetrical (that is, when opposite supports provide different restraints). Yield line location ratios x/L and y/H for the same elements are depicted in Figures 3-4 through 3-20.

Figures 3-4 and 3-5 show the location of the yield lines for two-way elements with two adjacent edges supported and the other two free. In each of these figures eight curves are shown which represent different ratios of the positive to the negative moment capacities in both the vertical and horizontal directions. Figures 3-6 through 3-16 illustrate the yield line location for two-way elements with three edges supported and one edge free. Figures 3-6 and 3-11 covers the case when the yield line pattern is symmetrical opposite supports provide the same degree of restraint). Figures 3-17 through 3-20 show the yield line location for two-way elements with four sides supported.

Figure 3-17 covers the special case when opposite supports provide the same degree of restraint thus resulting in a symmetrical yield pattern. An example illustrating the use of some of these figures is provided in Appendix A.

3-9.4. Openings in Two-Way Elements

The use of openings in two-way elements, whether for access as a door opening or for visual communication as in the case of observation ports, is permissible with certain reservations. It is difficult to state exact rules concerning openings, but their effect on the design is generally a function of location, size and shape.

Small compact openings with approximate areas of less than 5 percent of the panel area and located away from regions of high stress can usually be ignored in the design. However, as in the case of conventional design, reinforcement at least equal to the amount interrupted should be placed adjacent to the opening. For example, in Figure 3-21, the openings shown in (a) and (b) can be disregarded. If the opening in (b) were made more rectangular as in (c), then the design must be modified to account for the change in the yield lines and, hence, the change in the resistance. This change in resistance is a function of both the shape and the location of the opening.

Door openings invariably require special analysis because of their size. As depicted in (d), (e) and (f), Figure 3-21, the presence of door openings causes gross relocations of the yield lines which generally propagate from the corners of the openings. Since the door also sustains the blast loading, concentrated line loads are present around the periphery of such openings. These concentrated loads must be included in the analysis since they change the resistance. As previously outlined for solid elements and for this case also, the yield line locations are assumed and each sector is individually analyzed. The presence of line loads modifies Equation 3-3 to

$$\Sigma M_N + \Sigma M_P = r_u A_c + M_c \quad 3-18$$

where M_c is the moment of the concentrated loads about the line of rotation of the sector being considered. Solution of elements with openings is most easily accomplished through a trial and error procedure by setting up the simultaneous equations for each sector and assuming various values of x and y until the several values of r_u agree to within a few percent.

3-10. Post-Ultimate Resistance

In general, the two-way elements described in this manual exhibit a post-ultimate resistance after initial failure occurs as indicated in Figure 3-1. Prior to this partial failure, the element is spanning in two directions with a resistance equal to the ultimate resistance r_u . At a particular deflection, denoted as X_1 , failure occurs along one side or two opposite sides, and the element then spans in one direction with the reduced post-ultimate unit resistance r_{up} until complete failure occurs at deflection X_u . One-way elements do not exhibit this behavior.

The location of the yield lines determines the presence or absence of this range. If the yield lines emanating from the corners of the elements bisect the 90-degree corner angle, then all supports fail simultaneously and there is no post-ultimate range. As previously shown, the location of the yield lines for a particular element is a function of L/H and the ratio of the unit vertical to horizontal moment capacities. Post-ultimate resistances for two-way elements are shown in Table 3-4.

3-11. Partial Failure and Ultimate Deflection

Partial failure deflection X_1 , for two-way elements and ultimate deflections X_u for both one-way and two-way elements are a function of the angle of rotation of the element at its supports and the geometry of the sectors formed by the position yield lines.

Once the ultimate resistance r_u is reached (full moment capacity developed along the yield lines), the structural element becomes a mechanism which rotates with no further increase in either the moment or curvature between the hinges. For one-way elements, the rotation continues and the deflection increases until either the maximum deflection X_m is reached or failure occurs at θ_{max} . The equations for the maximum deflection X_m in the range $0 \leq X < X_u$ for several one-way elements as a function of the rotation angle θ and the ultimate deflection X_u are given in Table 3-5, when the values for X_u are based on the development of a maximum support rotation, θ_{max} , prior to failure.

Actually, the maximum support rotation will vary with the material type and geometry of the element. The criteria for partial and incipient failure for concrete and structural steel elements can be found in Chapters 4 and 5 respectively.

For two-way elements, the rotations of all the sectors must be considered in order to define the deflections of partial and incipient failure. Prior to partial failure ($0 \leq X_m \leq X_1$), the maximum deflection is a function of the larger angle of rotation formed along either the vertical or horizontal supports. At deflection X_1 , this larger angle equals θ_{max} , and failure occurs along this support. Beyond this point, the element spans in one direction until the angle of rotation at the adjacent supports (in the direction opposite to that at which failure has already occurred) reaches θ at which time total collapse occurs ($X_m = X_u$).

To illustrate the above, consider a two-way element (Figure 3-22) which is fully restrained on four edges and whose positive yield lines are defined by $H/2 < x < L/2$ and $y = H/2$. Denoting θ_H as the angle of rotation in the

horizontal direction (along vertical supports) and Θ_V as the vertical angle of rotation (along horizontal supports), the maximum deflection X_m at the center of the element prior to reaching the deflection X_1 is

$$X_m = (H \tan \Theta_V)/2 \quad 3-19$$

and at the partial failure deflection X_1 where Θ_V max

$$X_1 = (H \tan \Theta_{\max})/2 \quad 3-20$$

Referring to Figure 3-22, the deflected shape at deflection X_1 is indicated by the solid line and Θ_H has value β which is defined as

$$\beta = \tan^{-1}(X_1/x) = \tan^{-1}(H \tan \Theta_{\max}/2x) \quad 3-21$$

As the element continues to deflect the angle of rotation Θ_H increases, its magnitude becoming equal to

$$\Theta_H = \lambda + \beta \quad 3-22$$

where λ is the angular rotation in excess of β . For a two-way element which undergoes partial failure but does reach incipient failure, the maximum deflection in the range $X_1 \leq X_m \leq X_u$ becomes

$$X_m = x \tan \Theta_H + [(L/2) - x] \tan (\Theta_H - \beta) \quad 3-23$$

When Θ_H equal Θ_{\max} , the ultimate deflection X_u at incipient failure is

$$X_u = x \tan \Theta_{\max} + [(L/2) - x] \tan [\Theta_{\max} - \tan^{-1} (H \tan \Theta_{\max}/2x)] \quad 3-24$$

Equations 3-19 through 3-24 are specifically for two-way elements described in Figure 3-2 and will vary for other two-way elements with different material properties and geometry.

The maximum deflection X_m for several two-way elements in the ranges $0 \leq X_m \leq X_1$, and $X_1 < X_m \leq X_u$ as a function of the rotation angles Θ_H and Θ_V are given in Table 3-6 along with the values of partial failure (X_1) and ultimate (X_u) deflections. The support which fails at partial deflection X_1 is also indicated.

3-12. Elasto-Plastic Resistance

As stated in Section 3-8, the initial portion of the resistance function (Figure 3-1) generally is composed of an elastic and one or more elasto-plastic ranges. The elastic unit resistance r_e is defined as the resistance at which first yield occurs; similarly, the elasto-plastic unit resistance r_{ep} is the resistance at which second yields subsequently occur. Where all hinges form in a member at one time, r_e will be equal to the ultimate unit resistance r_u ; where two or more hinges are formed at separate times, the maximum value of r_{ep} will be equal to r_u (depending upon the hinges formed, one or more values of r_{ep} may exist).

These resistances for one-way elements are listed in Table 3-7. In those cases where the elasto-plastic resistance is equal to the ultimate resistance, the value can be determined from Table 3-1.

The determination of the elasto-plastic resistances of two-way elements is more complicated than that for one-way elements, since the resistance varies with the span ratio and, in the case of reinforced concrete elements, with the placement of the reinforcement. Data for calculating the resistances of two-way elements during the elasto-plastic ranges (graphically summarized in Figure 3-23) are presented in Figures 3-24 through 3-38.

Figures 3-24 through 3-26 are for a two-way element supported on two adjacent sides and free at the others. Figures 3-27 through 3-32 are for a two-way element supported on three sides and free on the fourth, while Figures 3-33 through 3-38 are for elements fixed on four sides. The resistances in each range can readily be determined using the coefficients β , the subscript referring to the points listed in the accompanying illustration.

For example, in Figure 3-27, for an element fixed on three sides and free on the fourth, if the ultimate unit resisting moments M_u are known for points 1, 2 and 3, a resistance r for each point can be calculated from

$$r = M_u / \beta H^2 \quad 3-25$$

where the values of β are found in Figure 3-27. The smallest value of resistance r , (say at point 2) corresponds to the first yield and is equal to r_e . Next, the moments at the remaining two points are computed for this value of r_e , and the differences between these and the ultimate values are determined. These differences represent the remaining moment capacities available for additional load. At r_e , the elements supports become free, fixed, and simply-supported on opposite sides. Using the moment differences and entering Figure 3-29 two values of the change in resistance can be calculated as above, the smaller being Δr and therefore:

$$r_{ep} = r_e + \Delta r \quad 3-26$$

In similar fashion, the resistance at the end of each range can be determined until the ultimate unit resistance r_u is reached.

3-13. Elasto-Plastic Stiffnesses and Deflections

The slopes of the elastic and elasto-plastic ranges of the resistance function are defined by the stiffness K of the element:

$$K = r/X \quad 3-27$$

where r is the unit resistance and X is the deflection corresponding to the value of r . The elastic range stiffness is denoted as K_e , the elasto-plastic range as K_{ep} , while in the plastic range the stiffness is zero.

Typical resistance-deflection functions used for design are shown in Figure 3-39. One- and two-step systems are generally used for one-way elements while two- and three-step systems are used for two-way elements. Two way elements fixed on all four sides will exhibit a four step system. As can be seen from the figure, the elastic range stiffness

$$K_e = r_e / X_e \quad 3-28$$

the elasto-plastic stiffness for a two-step system

$$K_{ep} = (r_u - r_e) / (X_p - X_e) \quad 3-29$$

and for a three-step system, the elasto-plastic stiffnesses

$$K_{ep} = (r_{ep} - r_e) / (X_{ep} - X_e) \quad 3-30$$

and

$$K'_{ep} = (r_u - r_{ep}) / (X_p - X_{ep}) \quad 3-31$$

The elastic and elasto-plastic stiffnesses of one-way elements are given in Table 3-8 as a function of the modulus of elasticity E, moment of inertia I, and span length. Knowing the resistances and stiffnesses, the corresponding elastic and elasto-plastic deflections can be computed from the above equations.

The determination of the elasto-plastic stiffnesses and deflections of two-way elements is more complicated than for one-way elements since another variable, namely, the aspect ratio L/H, must be considered. For two-way elements, the deflections at the end of each range of behavior is obtained from the γ coefficients presented in Figures 3-24 through 3-38. The deflection for each range of behavior is obtained from

$$XD = \gamma r H^4 \quad 3-32$$

where D, the flexural rigidity of the element is defined as

$$D = EI / (1 - \nu^2) \quad 3-33$$

E is the modulus of elasticity, I is the moment of inertia, and ν is Poisson's ratio. It must be realized that except for the elastic range, the values of X (the displacement) and r in Equation 3-32 represent change in deflection and resistance from one range of behavior to another. Therefore, for two-way members the change in deflection and resistance (as previously explained) is obtained from Figures 3-24 through 3-38 and the stiffnesses are computed from Equations 3-28 through 3-33.

3-14. Resistance-Deflection Functions for Design

3-14.1. General

The resistance-deflection function used for design depends upon the maximum permitted deflection according to the design criteria of the element being considered. This maximum deflection X_m can be categorized as either limited or large. In the limited deflection range, the maximum deflection of the system is limited to the elastic, elasto-plastic and plastic ranges. When the maximum deflection falls in the large deflection range, the response of the system is mainly within the plastic range and the elastic and elasto-plastic ranges need not be considered. The error resulting from the omission of the elastic and elasto-plastic portions in this analysis is negligible.

The support rotation that corresponds to limited deflection varies for the different materials used in protection design. The response criteria for each material is obtained from the chapter that describes the design procedures for that material.

3-14.2. Limited Deflections

When designing for limited deflections, the maximum deflection X_m of the element is kept within the elastic, elasto-plastic, and limited plastic ranges, and the resistance-deflection function for design takes the form shown in Figure 3-39 a, b, and c for a one-step system, a two-step system, and a three-step system, respectively. The design charts presented in Section 3-19.3 were established for a one-step system; for two- and three-step systems, these charts can be used if the resistance-deflection functions are replaced with equivalent elastic resistance-deflection functions defined by K_E and X_E as indicated by the dotted lines in Figure 3-39. The equivalent elastic stiffness K_E and the equivalent maximum elastic deflection X_E are calculated such that the area under the dotted curve is equal to the area under the solid curve, thereby producing the same potential energy in each system. The equivalent maximum elastic deflection X_E for the two-step and three-step systems shown is expressed by Equations 3-34 and 3-35, respectively.

$$X_E = X_e + X_p(1 - r_e/r_u) \tag{3-34}$$

$$X_E = x_e (r_{ep}/r_u) + X_{ep}(1 - r_e/r_u) + X_p(1 - r_{ep}/r_u) \tag{3-35}$$

The equivalent elastic stiffness K_E in each case is equal to

$$K_E = r_u/X_E \tag{3-36}$$

One-way elements exhibit one- and two-step resistance deflection curves depending on the type of supports. Consequently, the equivalent elastic stiffness K_E is given for one-way elements in Table 3-8. The equivalent elastic deflection can then be calculated from Equation 3-36. Two-way elements generally exhibit two- and three-step resistance-deflection curves which are a function of not only the type of supports but also of the aspect ratio L/H of the element. The equivalent elastic deflection X_E of the element under consideration must be calculated from Equations 3-34 and 3-35 for two- and three-step systems, respectively. The value of K_E for the system can then be obtained from Equation 3-36.

3-14.3. Large Deflections

When designing for a large deflection, it can be assumed without significant error that the resistance rises instantaneously from zero to its ultimate value r_u at the onset of the blast loading thus neglecting the elastic and elasto-plastic ranges. The design resistance function for one-way elements is approximated by a constant plastic range resistance as shown in Figure 3-40a, while for two-way elements, the resistance function becomes that shown in Figure 3-40b, where the maximum deflection X_m can be either smaller or larger than the partial failure deflection X_1 .

3-15. Support Shears or Reactions

Support shears or reactions are a function the applied load and the maximum resistance attained by an element, its geometry and yield line location. However, for short duration blast loads, the support shears can be reasonably estimated by neglecting the applied load. Therefore, the ultimate support shear can be assumed to be developed when the resistance reaches the ultimate value, r_u .

Equations for the ultimate support shears V_s for one-way elements are given in Table 3-9. For those cases where an element does not reach its ultimate resistance, the support shears are obtained based upon elastic theory for the actual resistance r attained by the element.

For two-way elements, the ultimate shears acting at each section are calculated by use of the "yield line procedure" previously outlined for the determination of the ultimate resistance r_u . The shear along the support is assumed to vary in the same manner as the moment varies ($2/3 V$ at the corners and V elsewhere) to account for the higher stiffness of the corners (Figure 3-41). Since the shear is assumed to be zero along the interior (usually positive) yield lines, the total shear at any section of a sector is equal to the resistance r_u times the area between the section being considered and the positive yield lines. Referring to Figure 3-41, the support shear V_{sV} for the triangular sector I is

$$(2/3)V_{sV}(L/4 + L/4) + V_{sV}(L/2) = r_u(Ly/2) \quad 3-37$$

$$V_{sV} = 3r_u y/5 \quad 3-38$$

and for the trapezoidal sector II

$$(2/3)V_{sH}(y/2) + V_{sH}(H - y/2) = r_u(L/2)[(H - y + H)/2] \quad 3-39$$

$$V_{sH} = [3r_u L(2-y/H)]/2(6 - y/H) \quad 3-40$$

Values of the ultimate support shears V_{sH} and V_{sV} for several two-way elements derived as above are presented in Tables 3-10 and 3-11. Table 3-10 gives the ultimate support shears for the case where opposite supports provide the same degree of restraint resulting in symmetrical yield line patterns. Table 3-11 is for completely general situations where opposing supports provide different degrees of restraint and result in the formation of unsymmetrical yield lines. In these cases, the ultimate support shears are not equal at opposing supports. For the situations where the ultimate resistance of an element is not attained, the support shears are less than the ultimate value. The proportion of the total load along each support as well as the distribution of the shears along the support is assumed to be the same as previously cited for the ultimate support shear. Therefore, the support shears corresponding to the resistance r of the element is obtained from the equations presented in Tables 3-10 and 3-11 by replacing r_u with the actual resistance attained (r_e , r_{ep} , etc.).

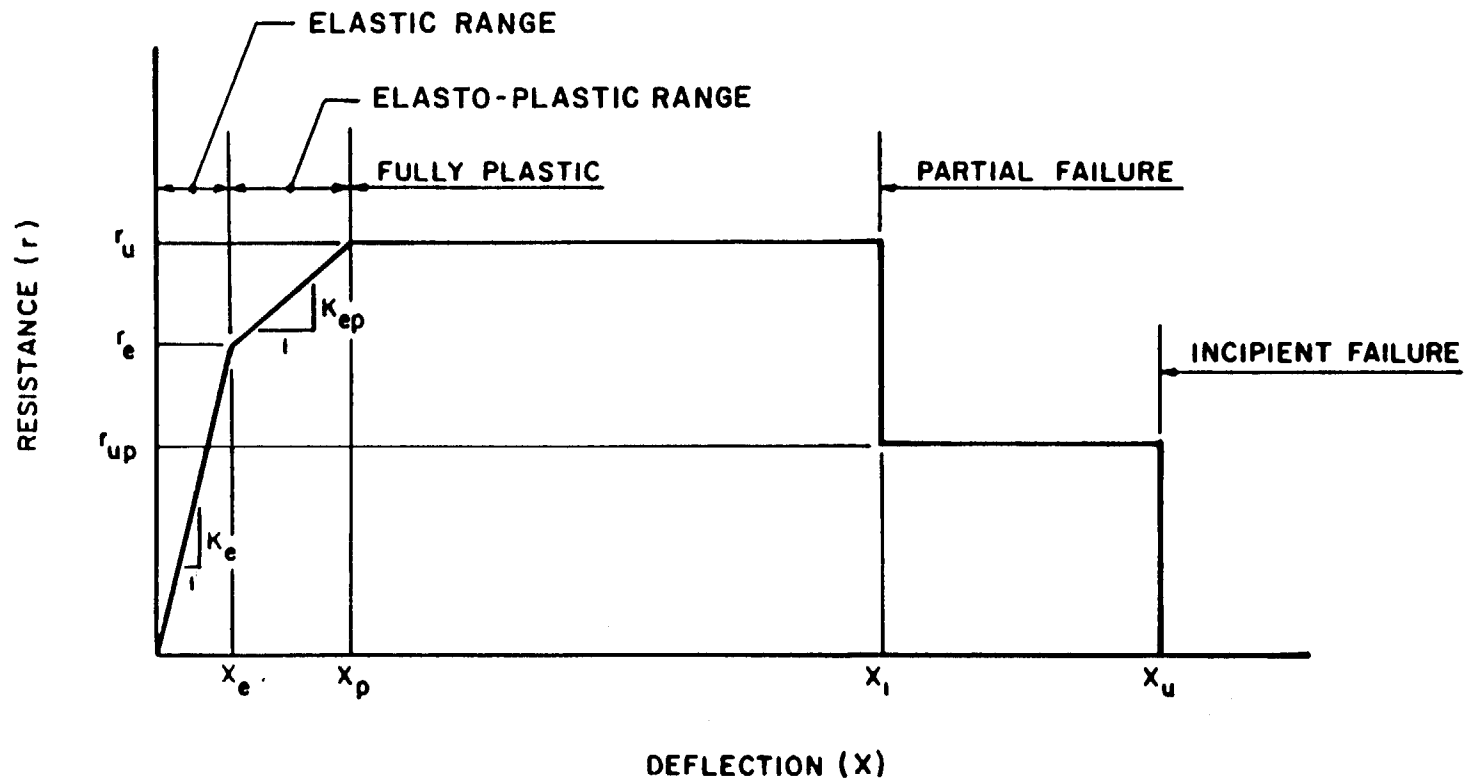


Figure 3-1 Typical resistance-deflection function for two-way element

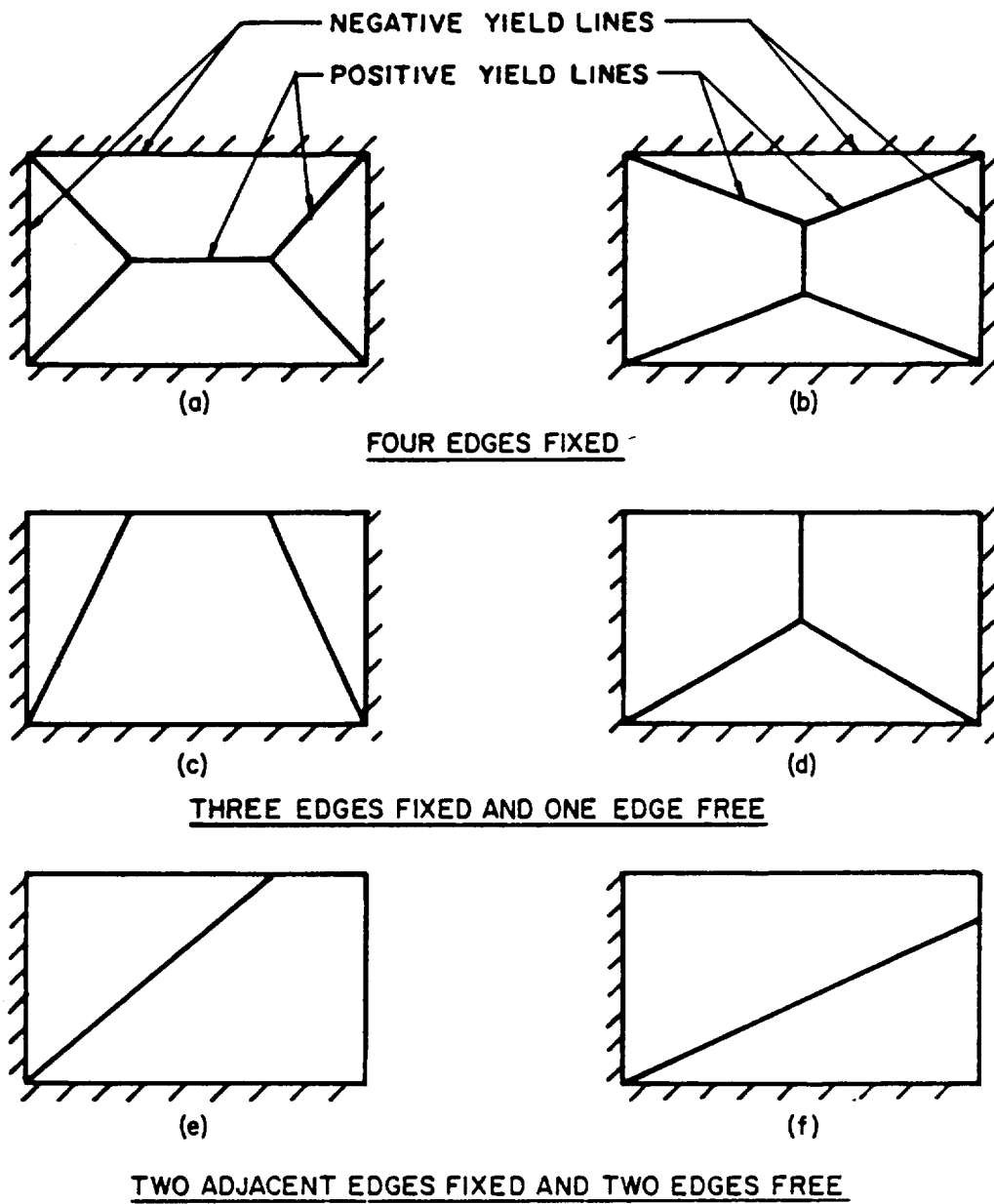
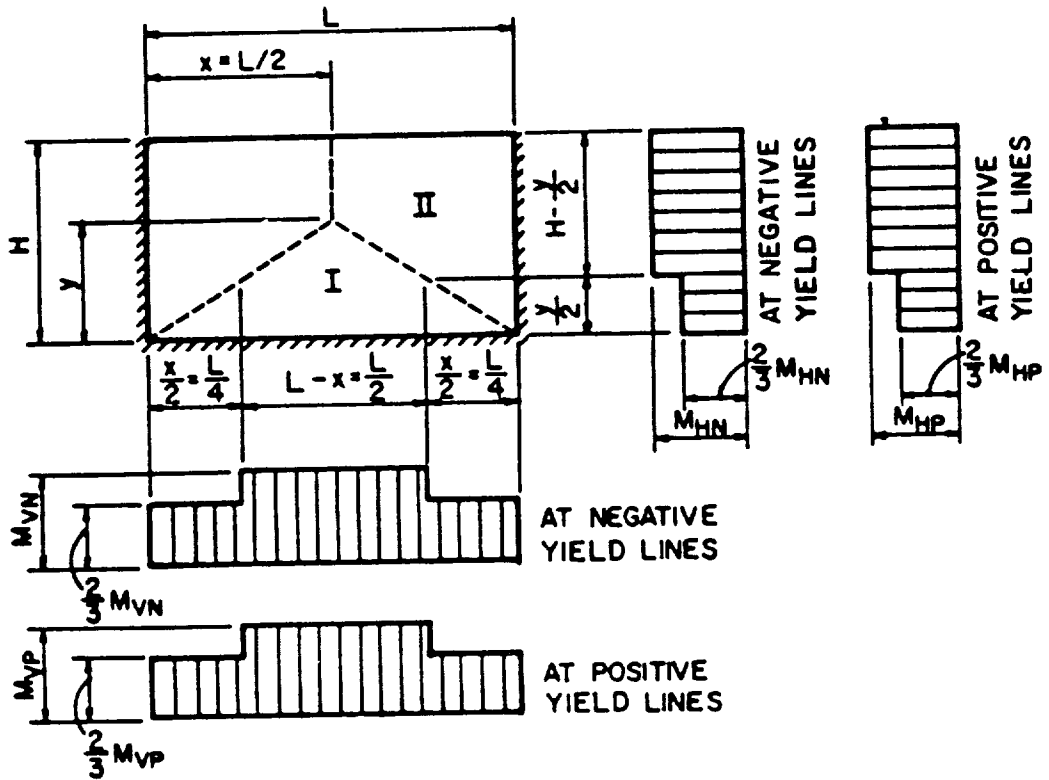
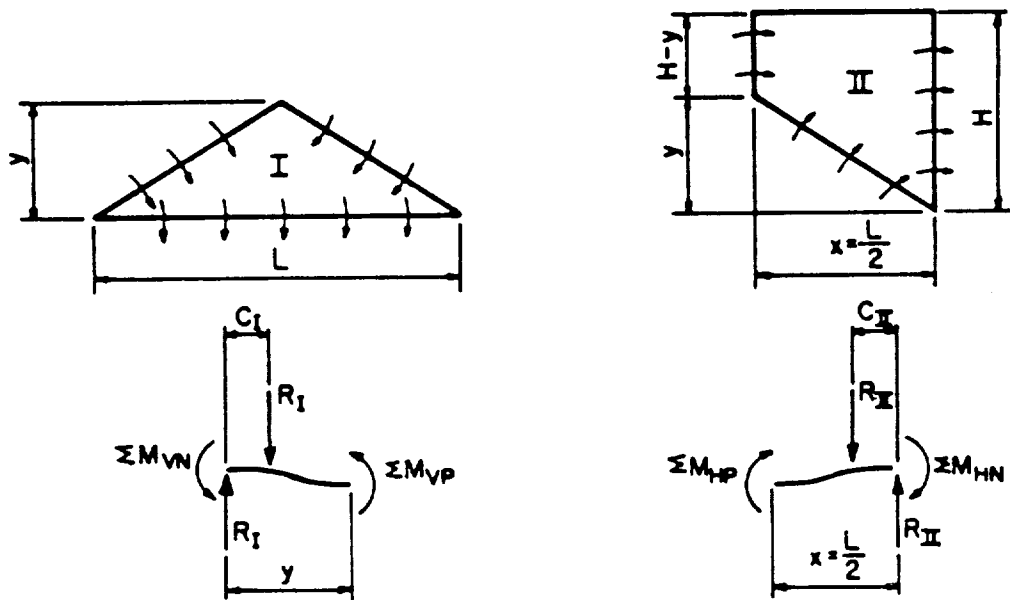


Figure 3-2 Idealized yield line locations for several two-way elements



a) YIELD LINES AND DISTRIBUTION OF MOMENTS



b) FREE - BODY DIAGRAMS FOR INDIVIDUAL SECTORS

Figure 3-3 Determination of ultimate unit resistance

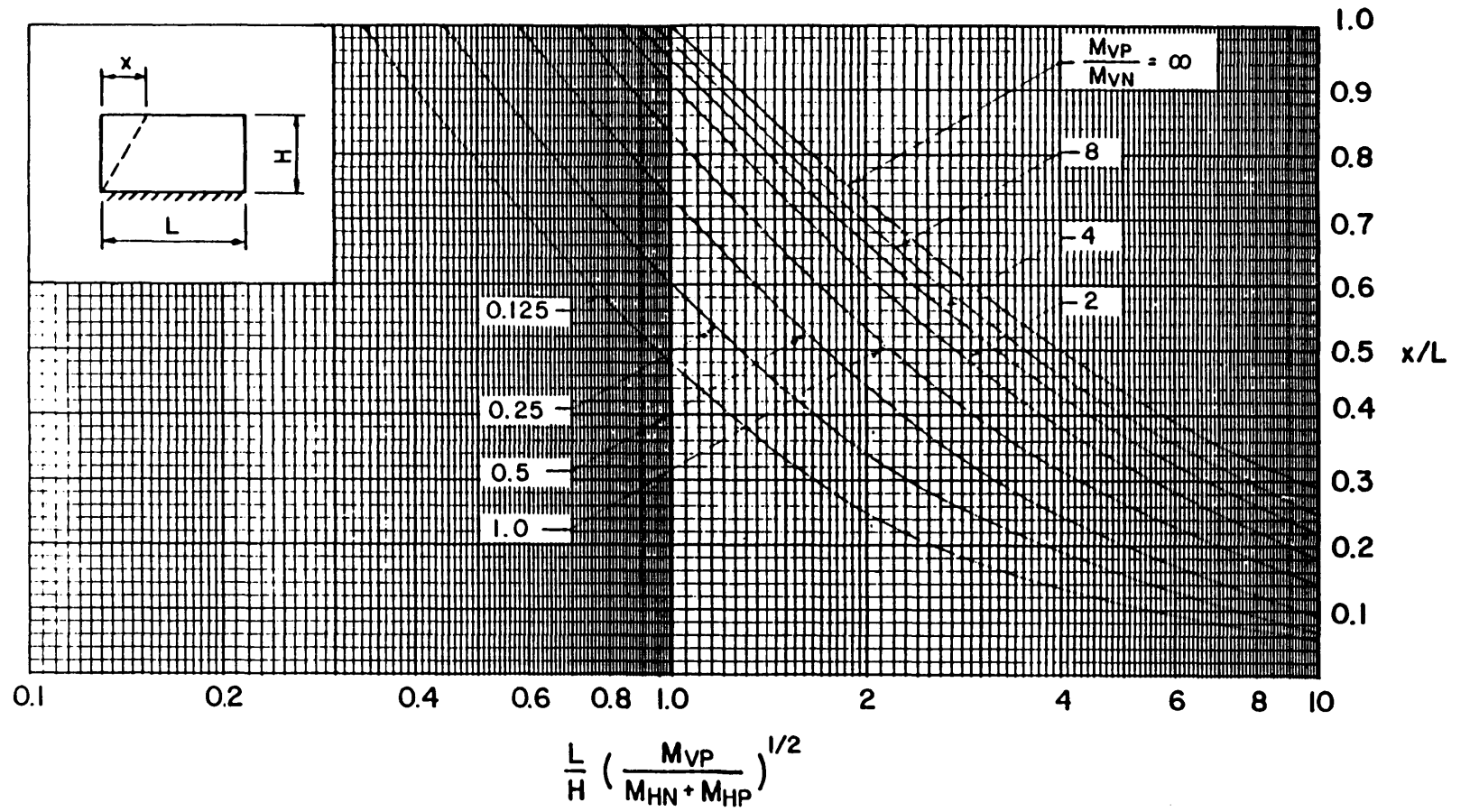


Figure 3-4 Location of yield lines for two-way element with two adjacent edges supported and two edges free (values of x)

3-24

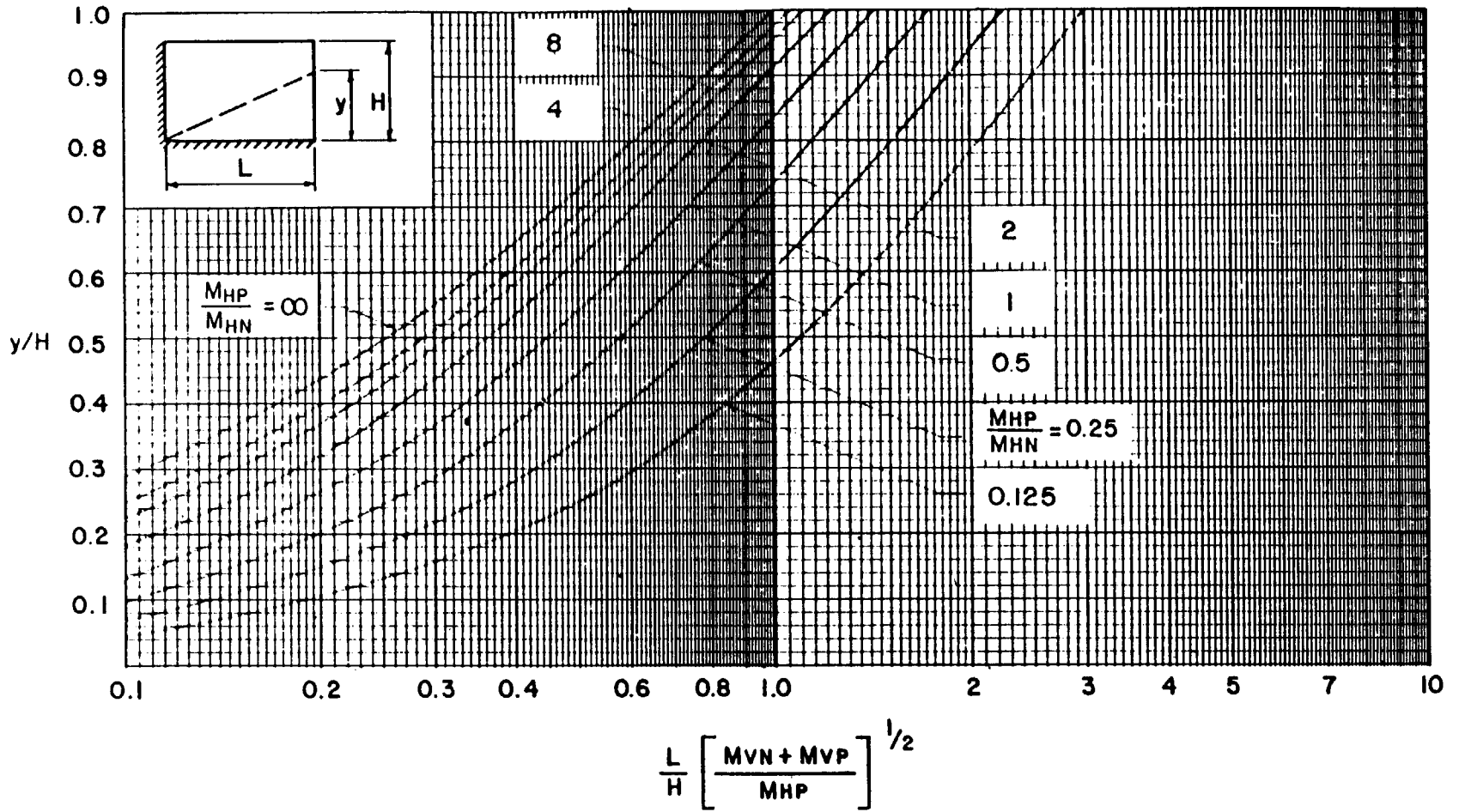


Figure 3-5 Location of yield lines for two-way element with two adjacent edges supported and two edges free (values of y)

3-25

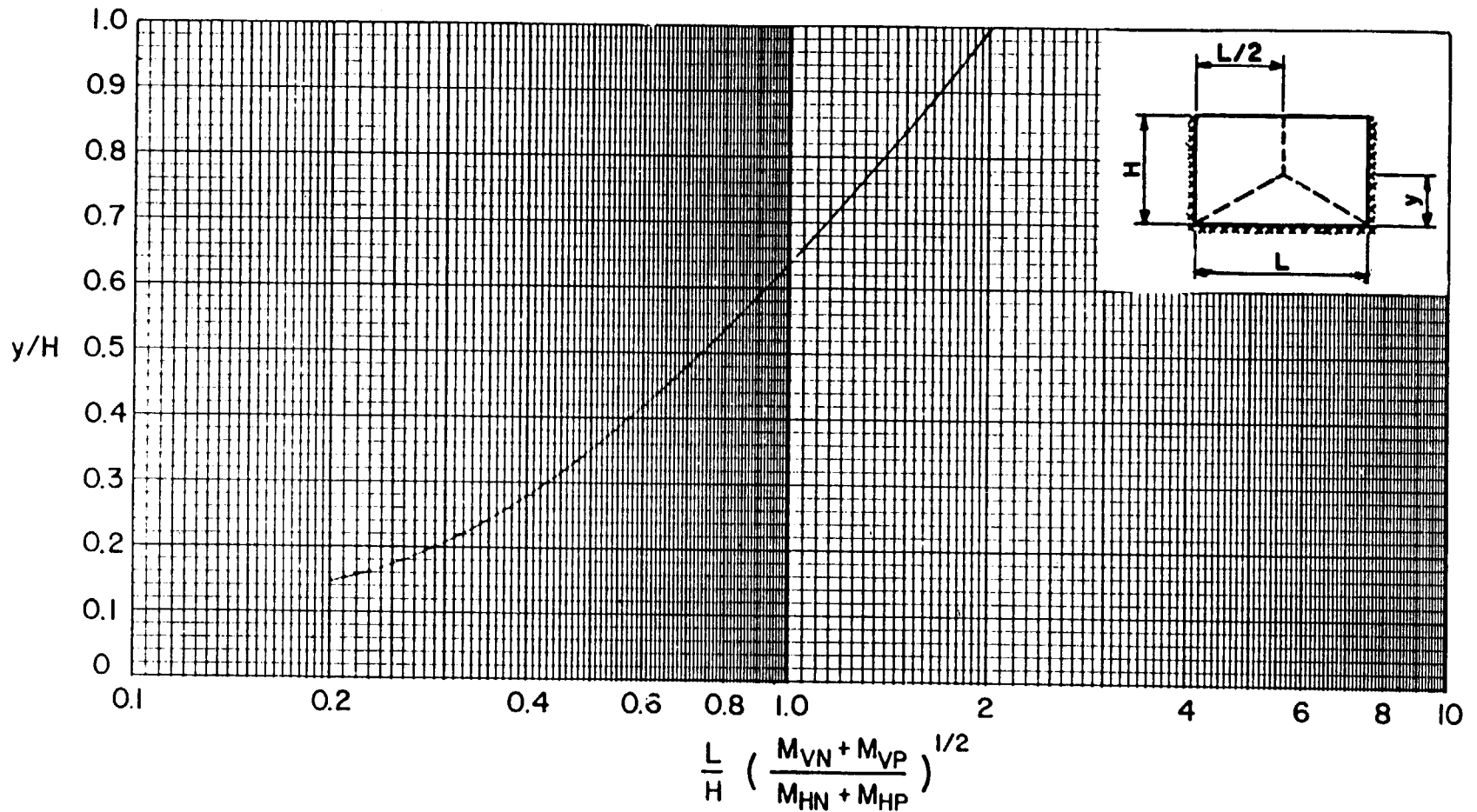


Figure 3-6 Location of symmetrical yield lines for two-way element with three edges supported and one edge free (values of y)

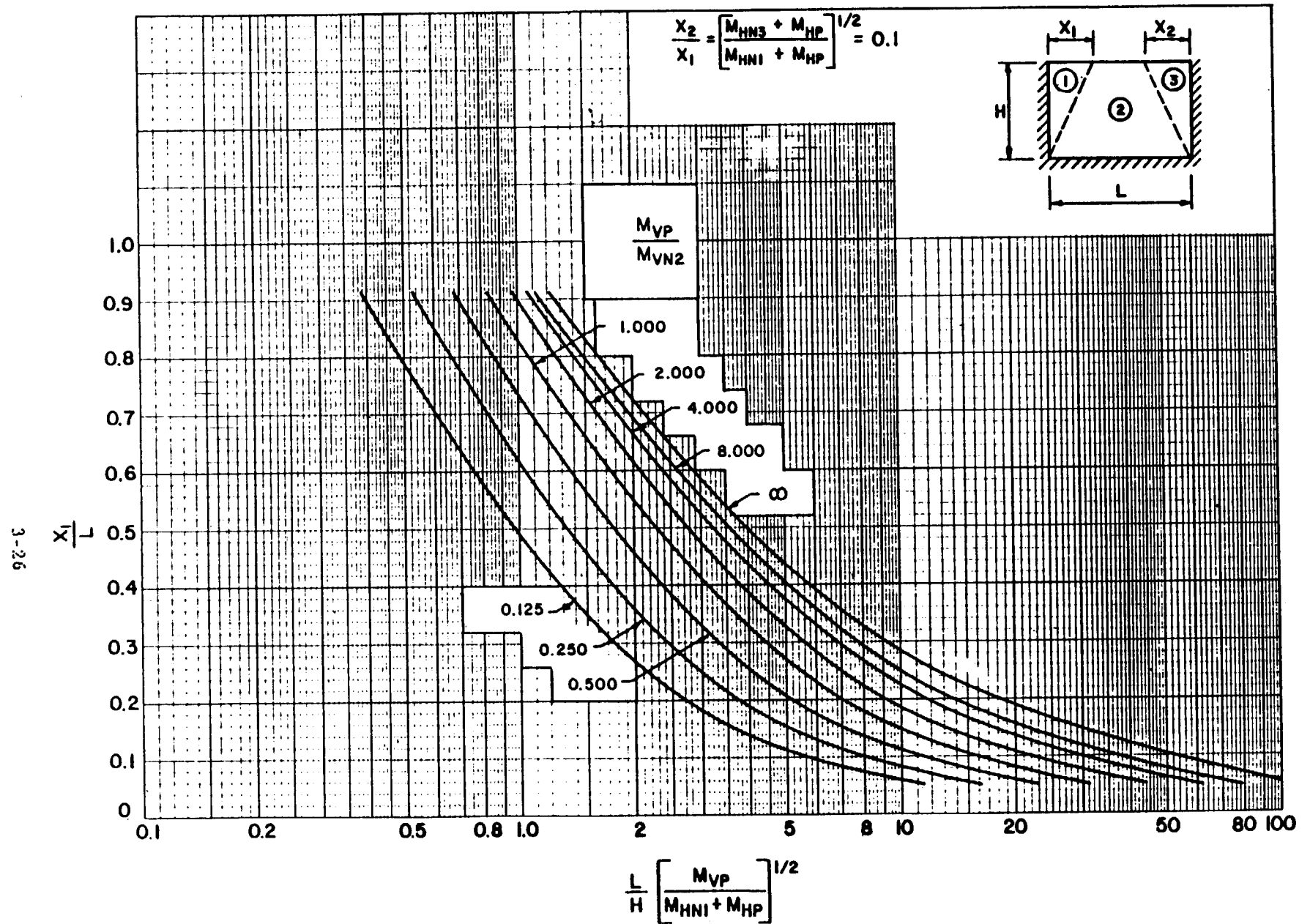


Figure 3-7 Location of unsymmetrical yield lines for two-way element with three edges supported and one edge free ($x_2/x_1=0.1$)

3-27

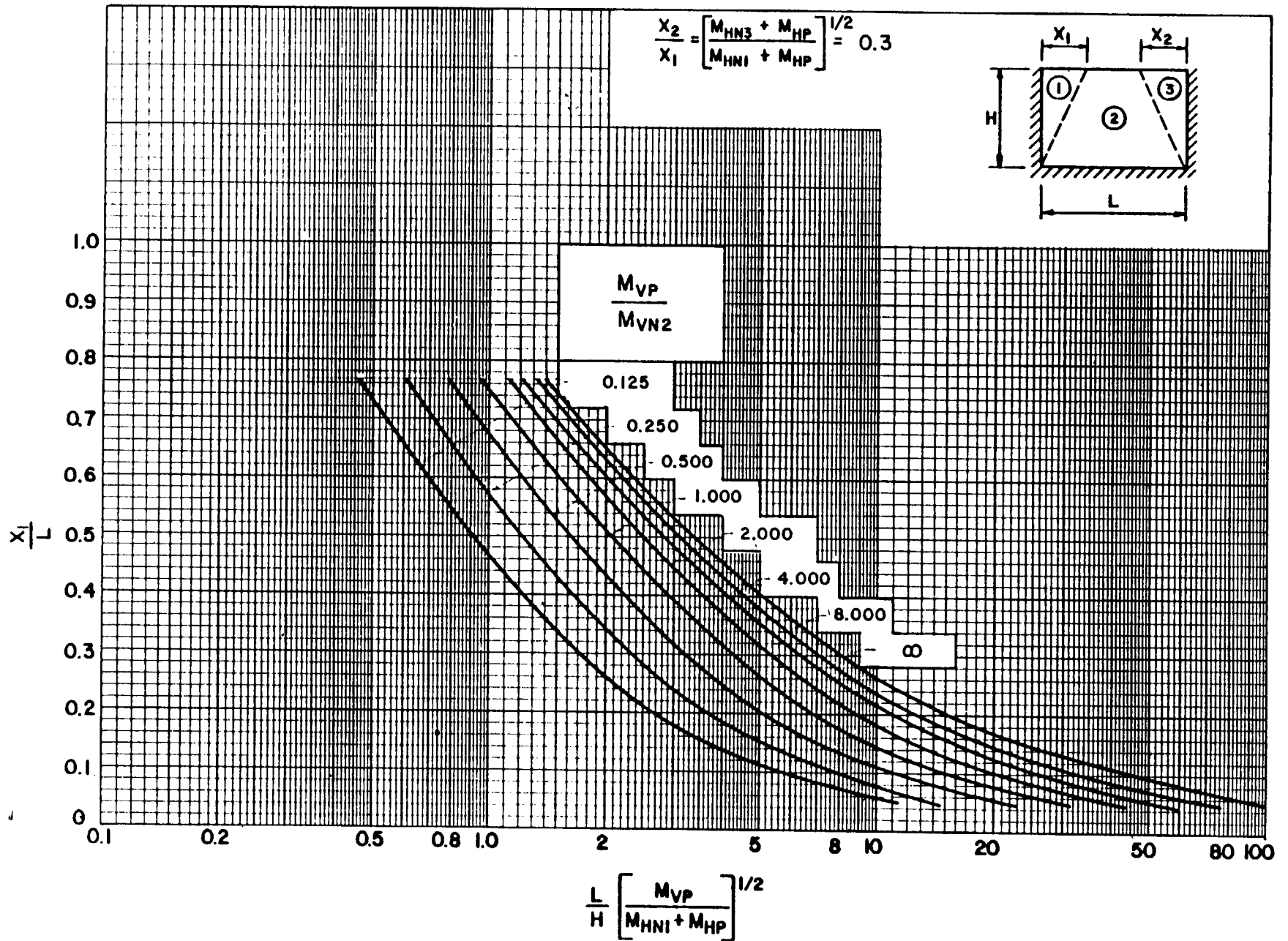


Figure 3-8 Location of unsymmetrical yield lines for two-way element with three edges supported and one edge free ($x_2/x_1=0.3$)

3-28

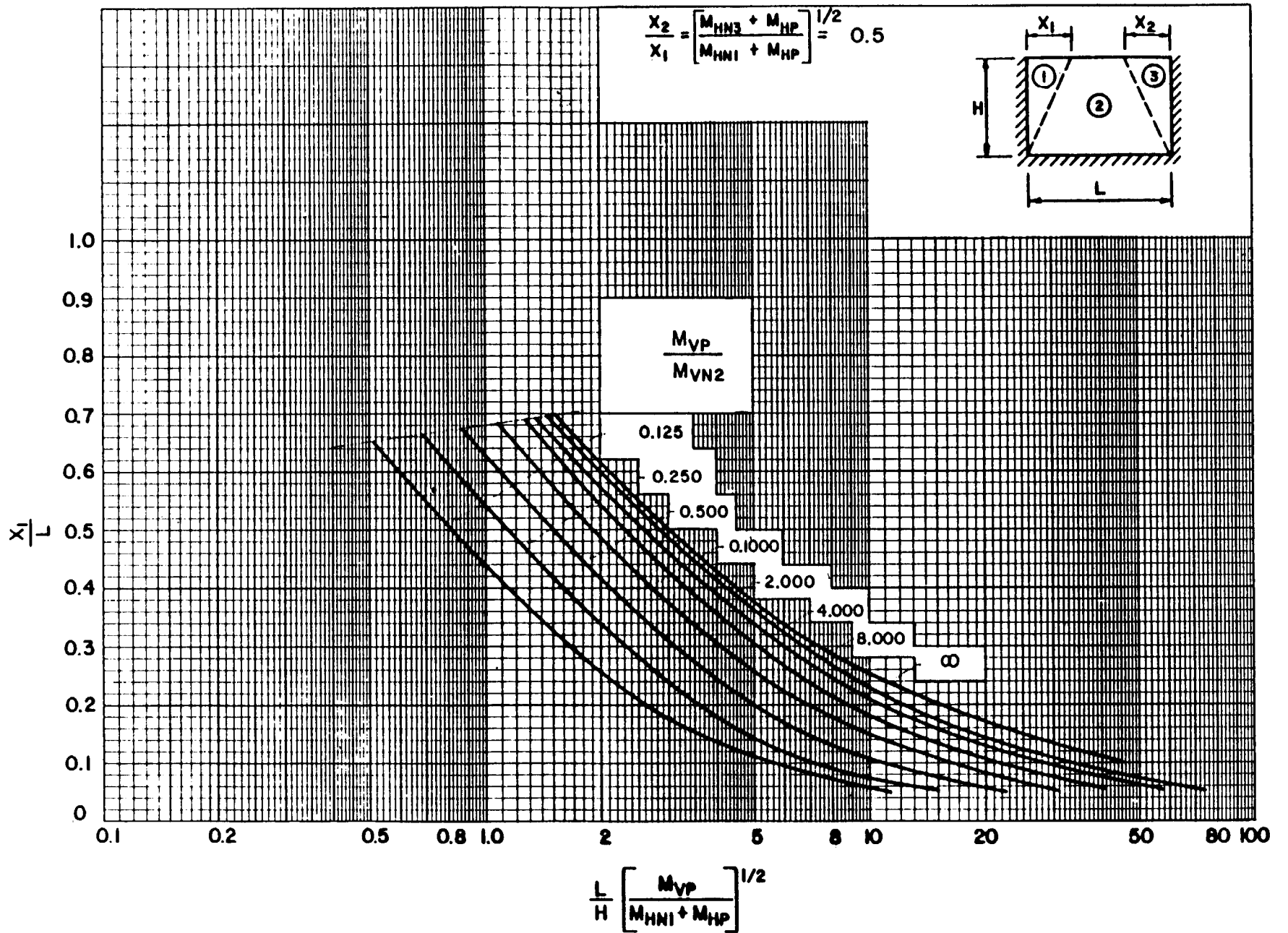


Figure 3-9 Location of unsymmetrical yield lines for two-way element with three edges supported and one edge free ($X_2/X_1=0.5$)

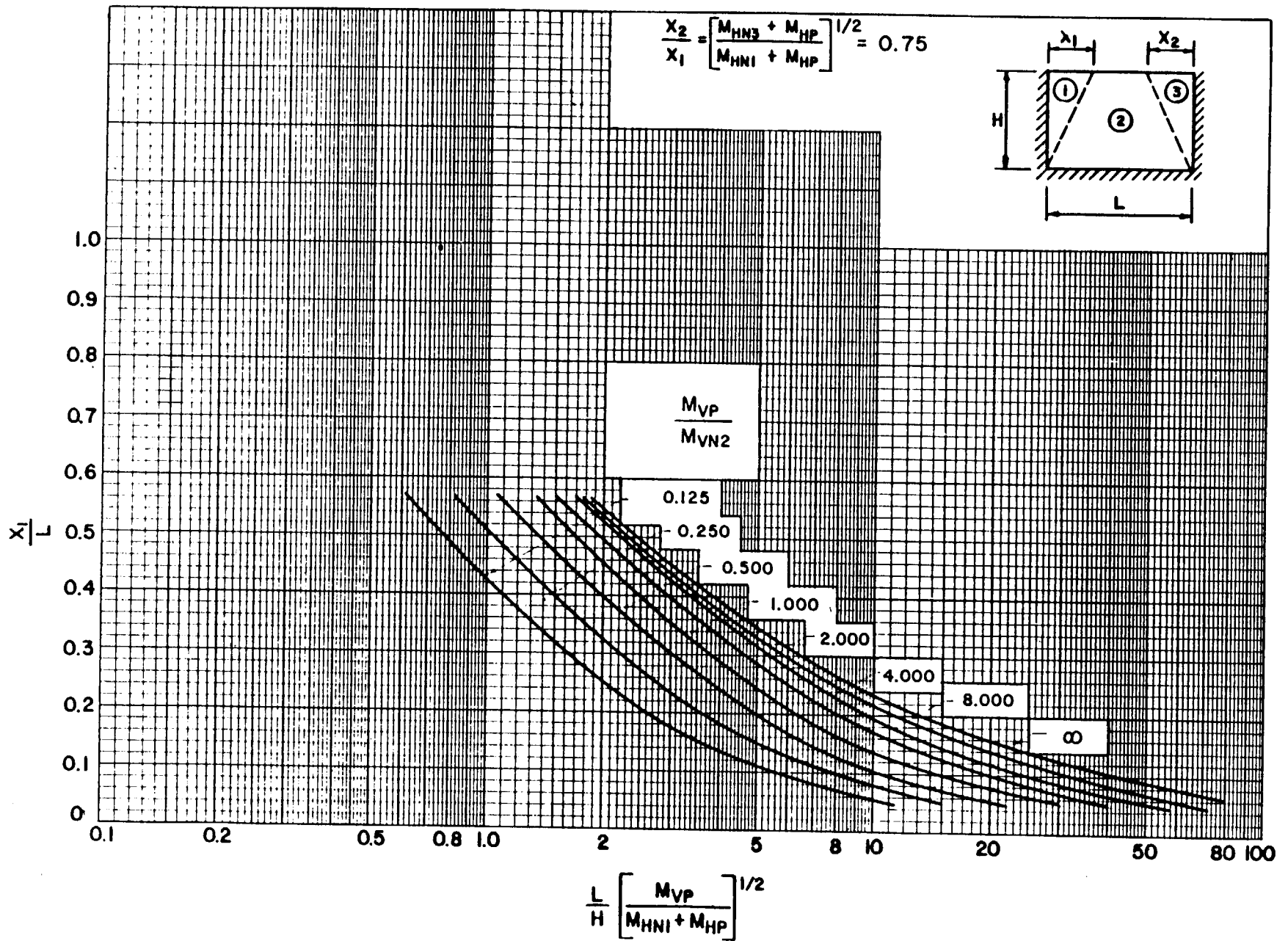


Figure 3-10 Location of unsymmetrical yield lines for two-way element with three edges supported and one edge free ($x_2/x_1=0.75$)

3-30

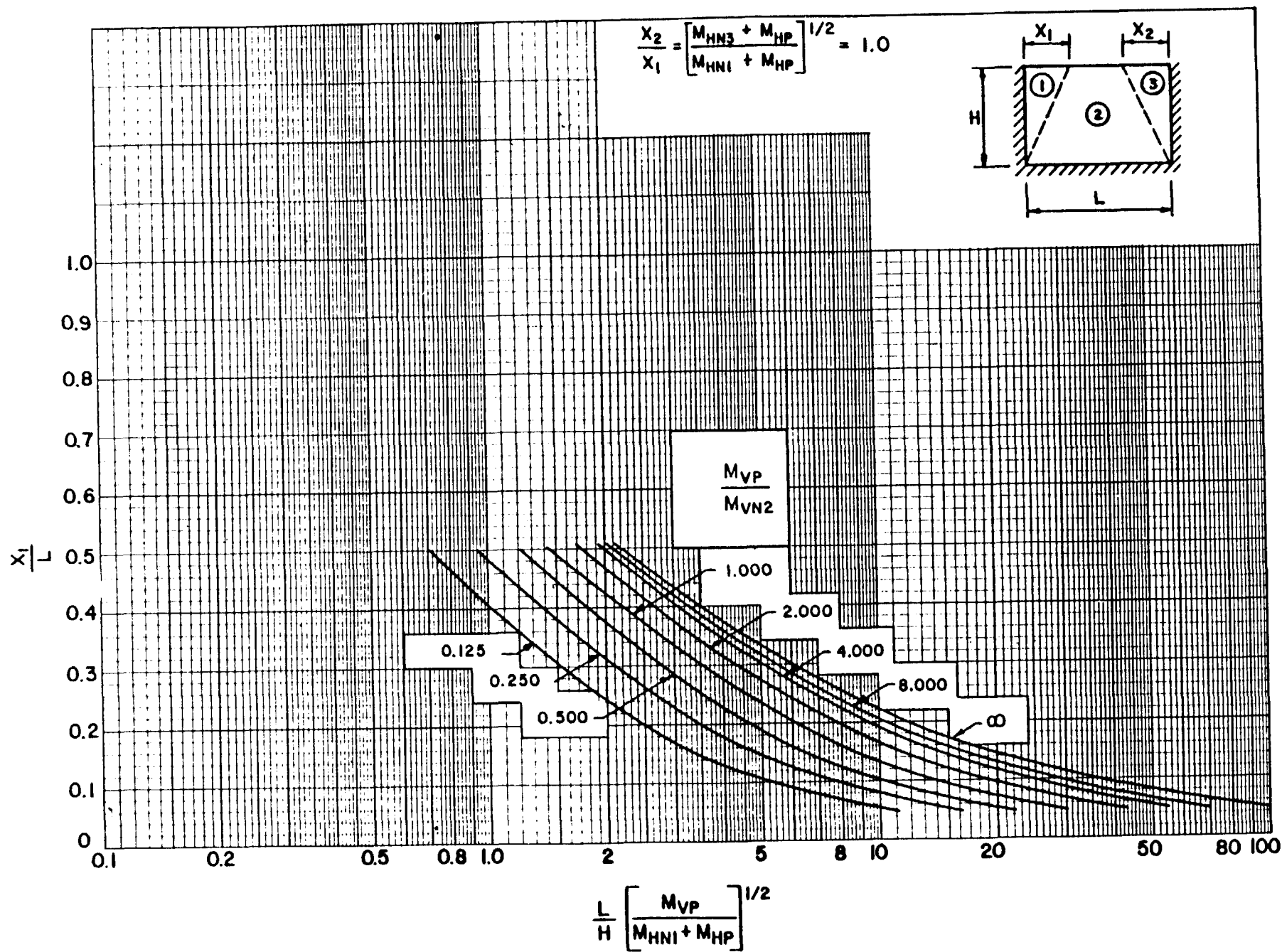


Figure 3-11 Location of unsymmetrical yield lines for two-way element with three edges supported and one edge free ($X_2/X_1=1.0$)

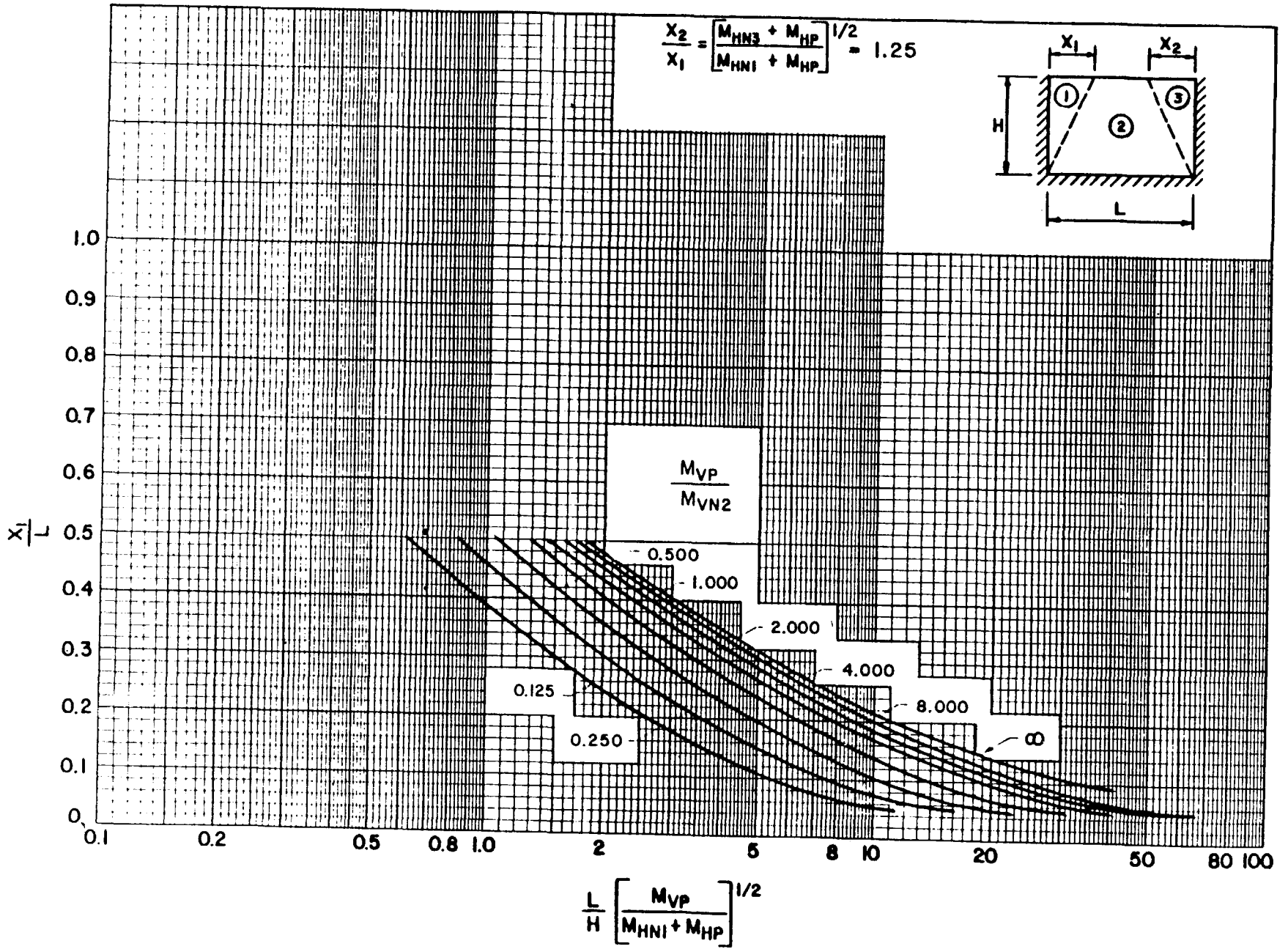


Figure 3-12 Location of unsymmetrical yield lines for two-way element with three edges supported and one edge free ($x_2/x_1=1.25$)

3-32

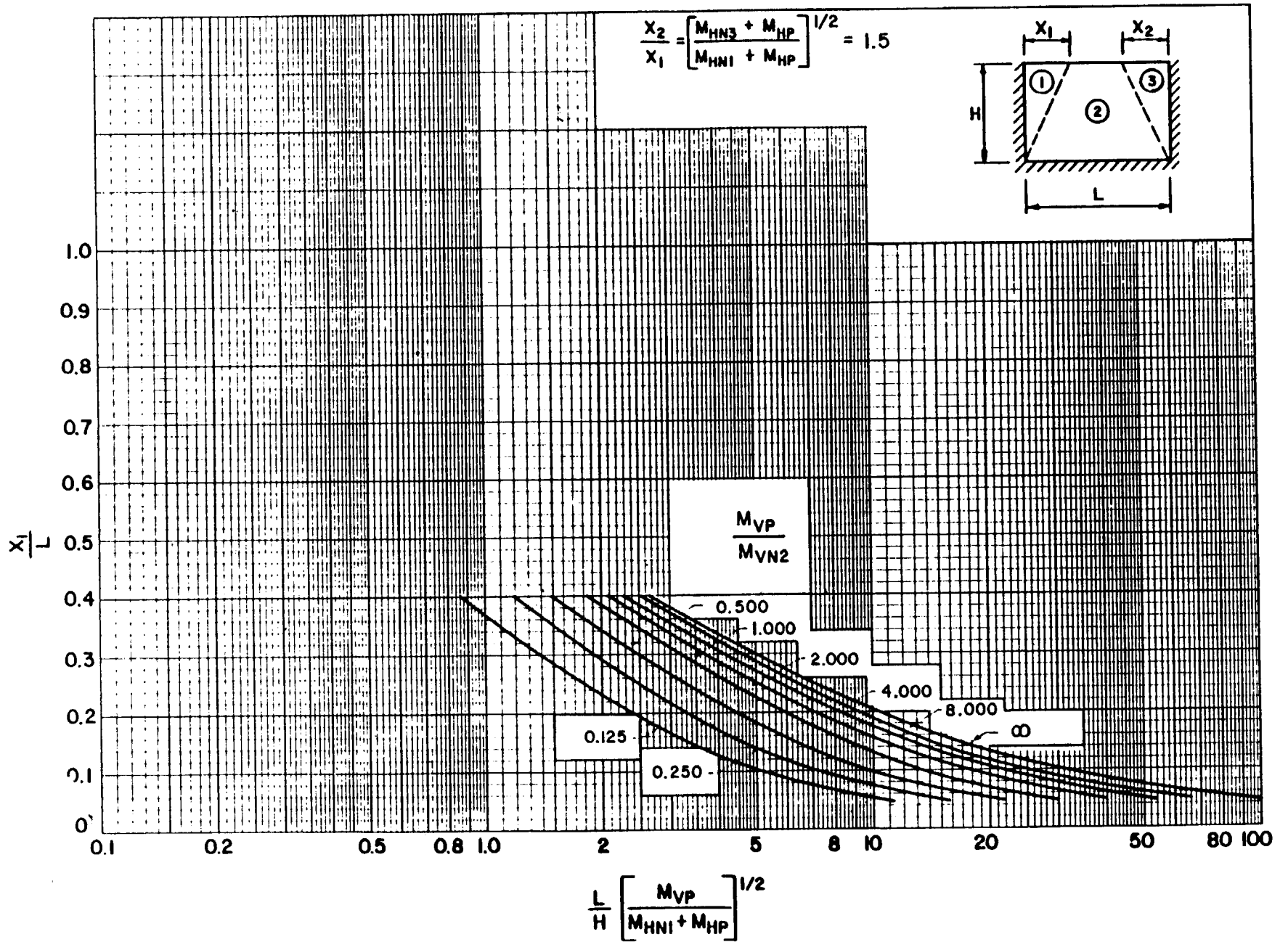


Figure 3-13 Location of unsymmetrical yield lines for two-way element with three edges supported and one edge free ($x_2/x_1=1.5$)

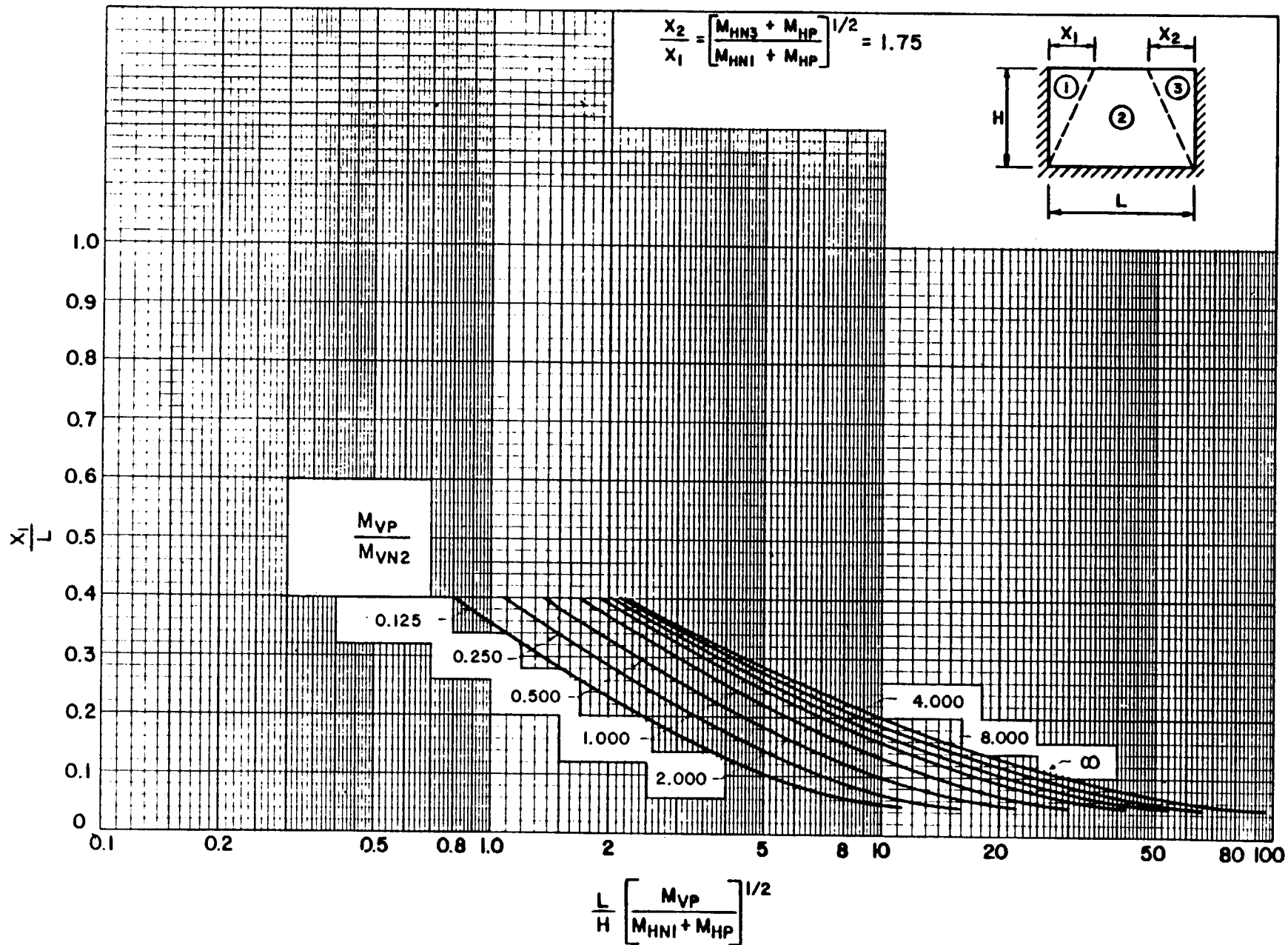


Figure 3-14 Location of unsymmetrical yield lines, for two-way element with three edges supported and one edge free ($X_2/X_1 = 1.75$)

3-34

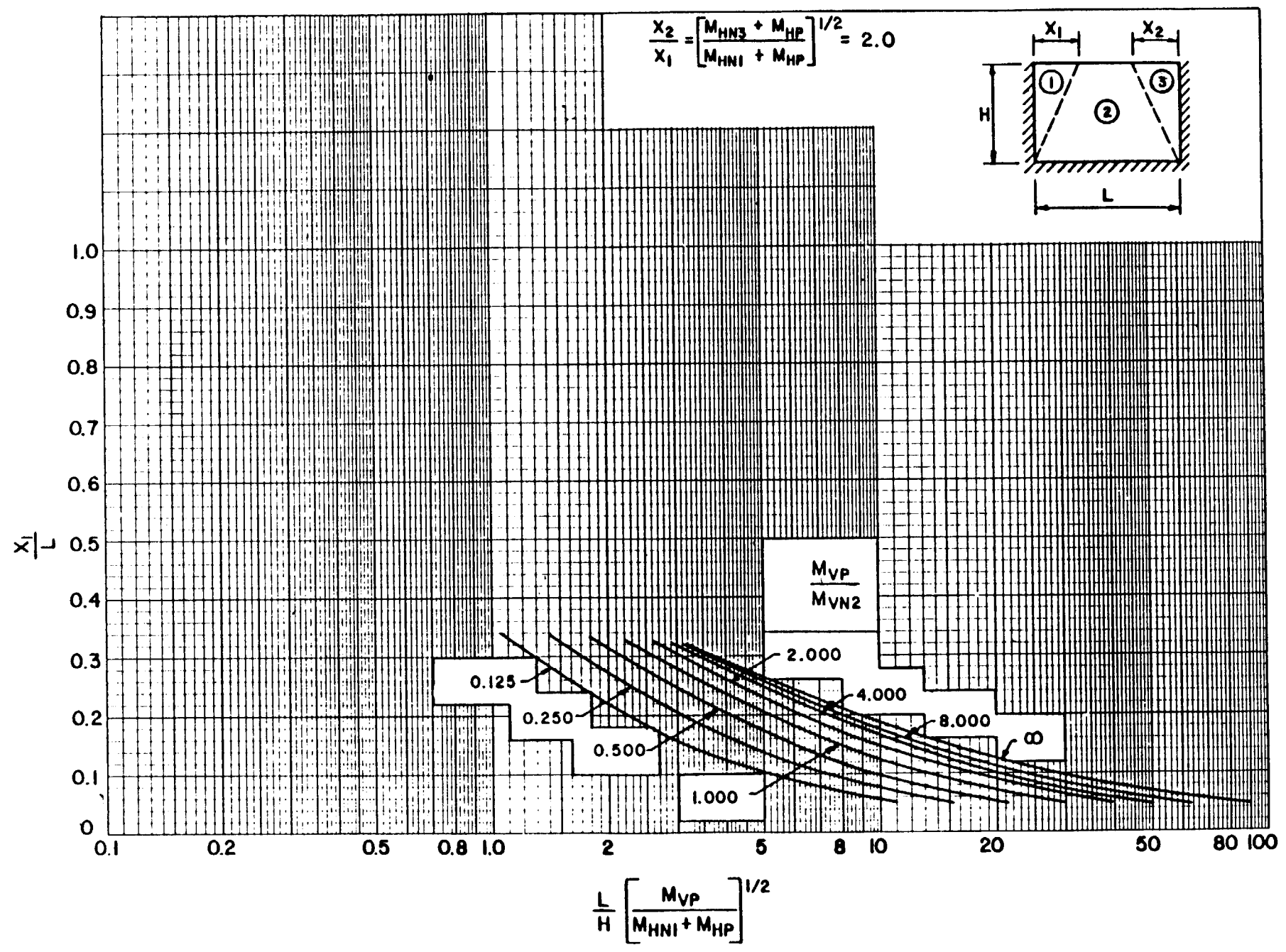


Figure 3-15 Location of unsymmetrical yield lines for two-way element with three edges supported and one edge free ($X_2/X_1 = 2.0$)

3-35

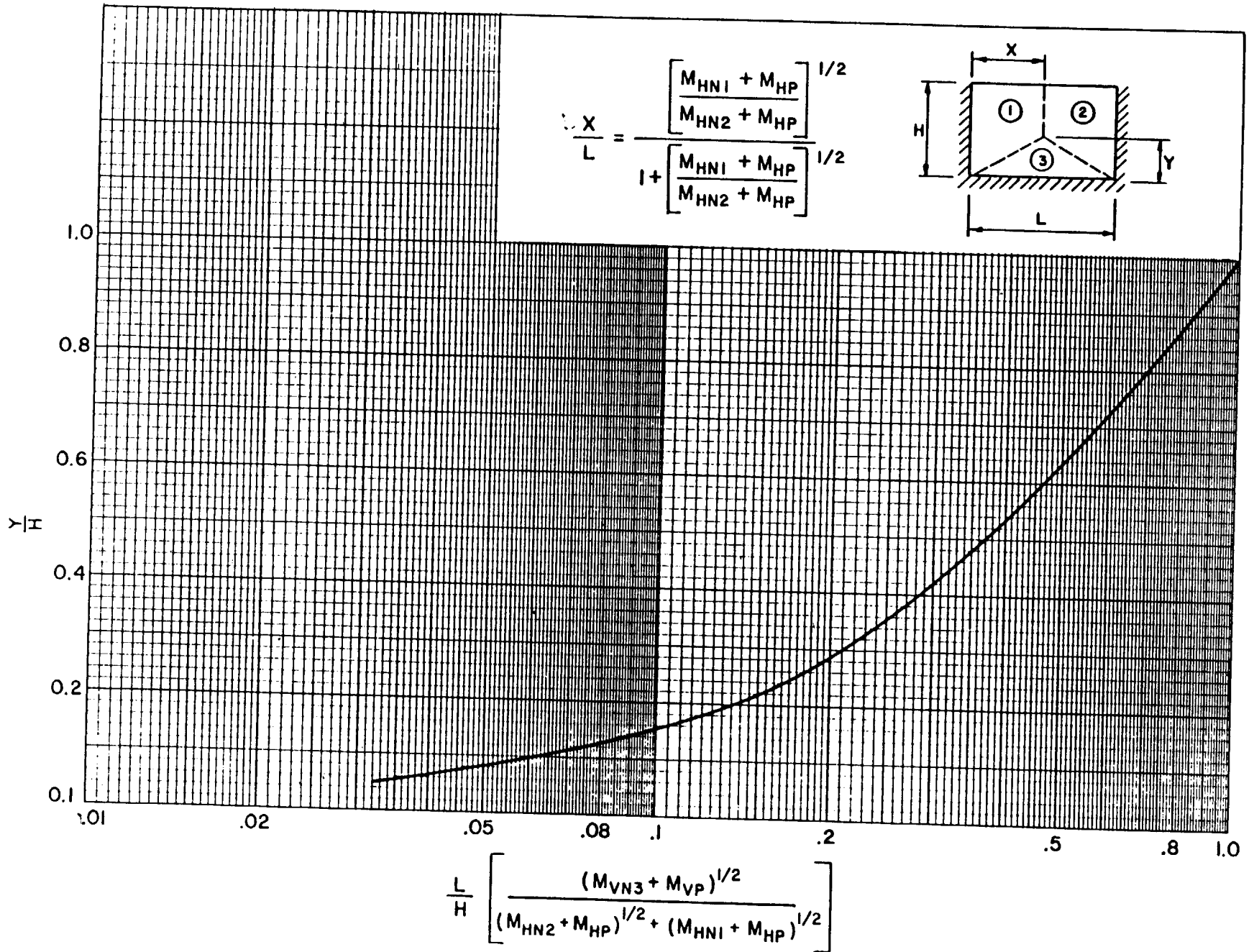


Figure 3-16 Location of unsymmetrical yield lines for two-way element with three edges supported and one edge free (values of y)

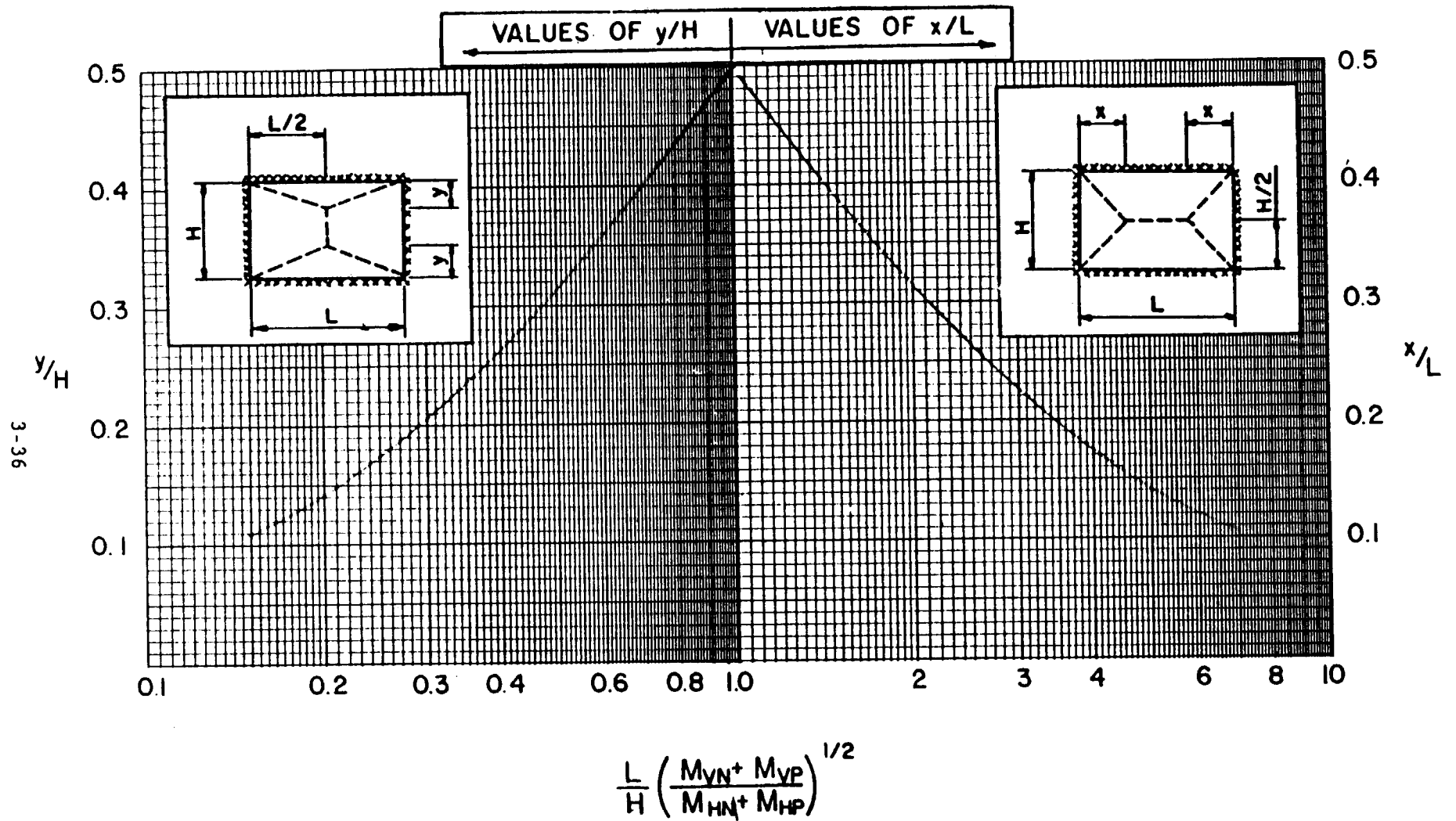


Figure 3-17 Location of symmetrical yield lines for two-way element with four edges supported

3-37

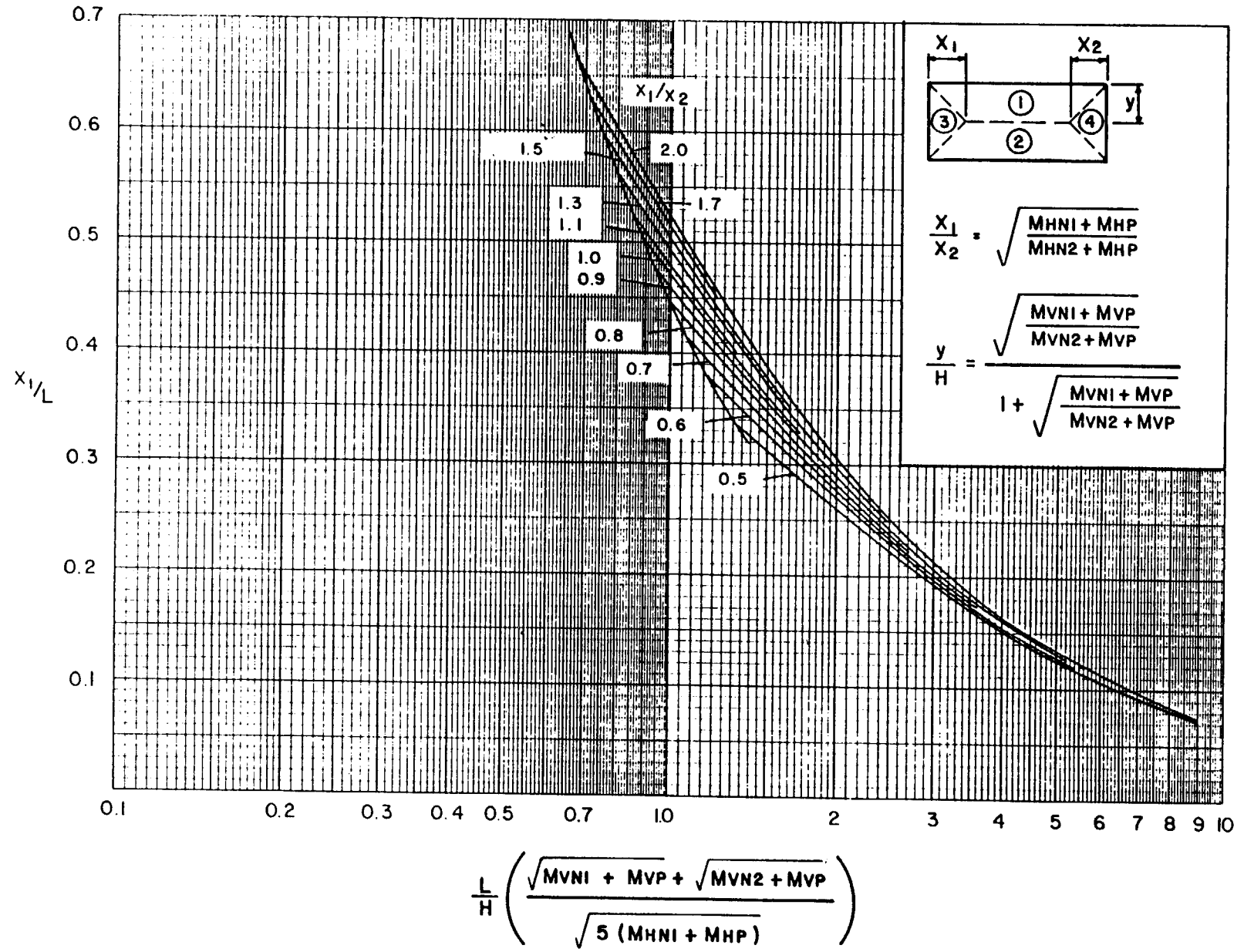


Figure 3-18 . Location of unsymmetrical yield lines for two-way element with four edges supported (values of x_1)

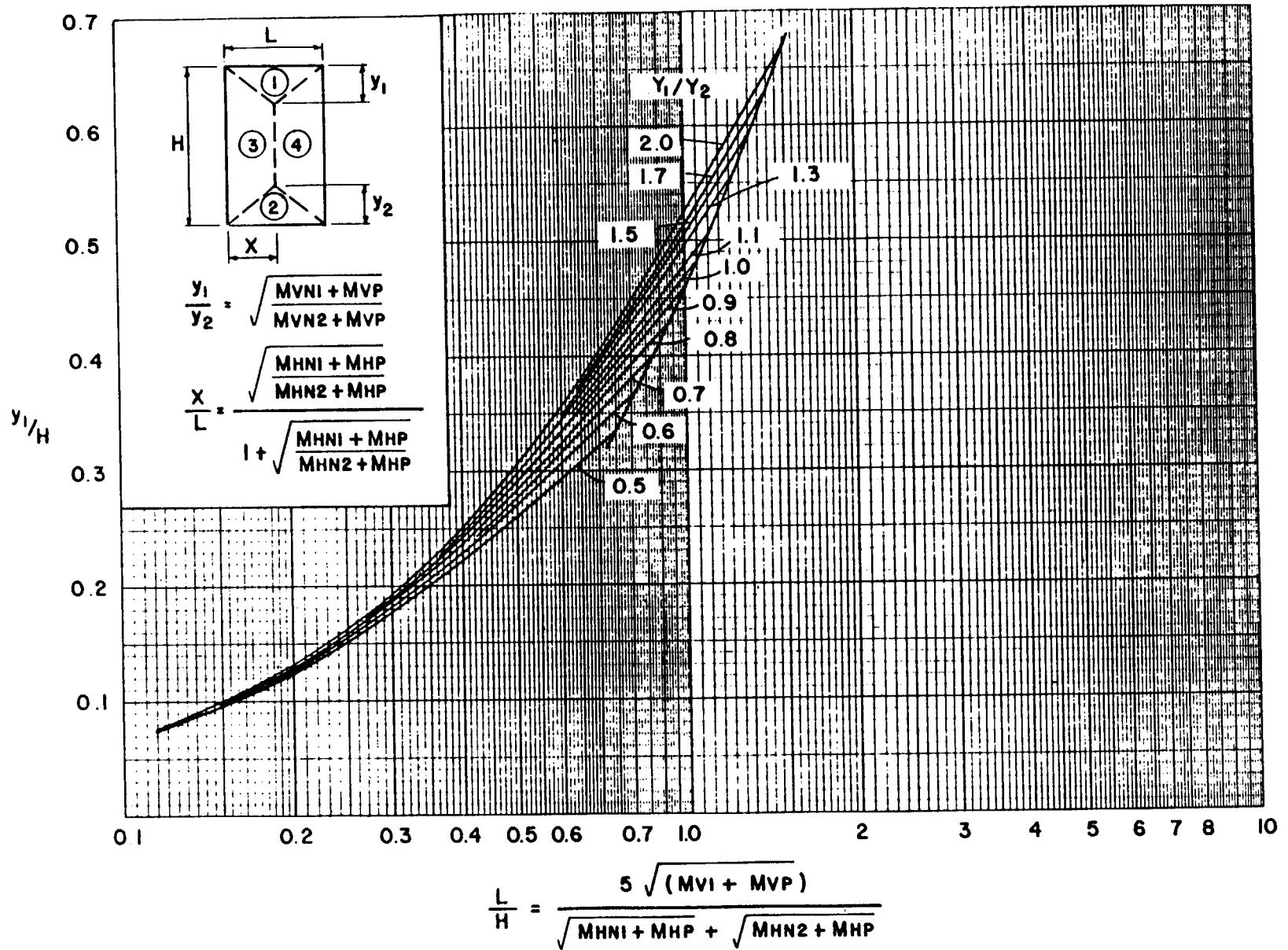


Figure 3-19 Location of unsymmetrical yield lines for two-way element with four edges supported (values of Y_1)

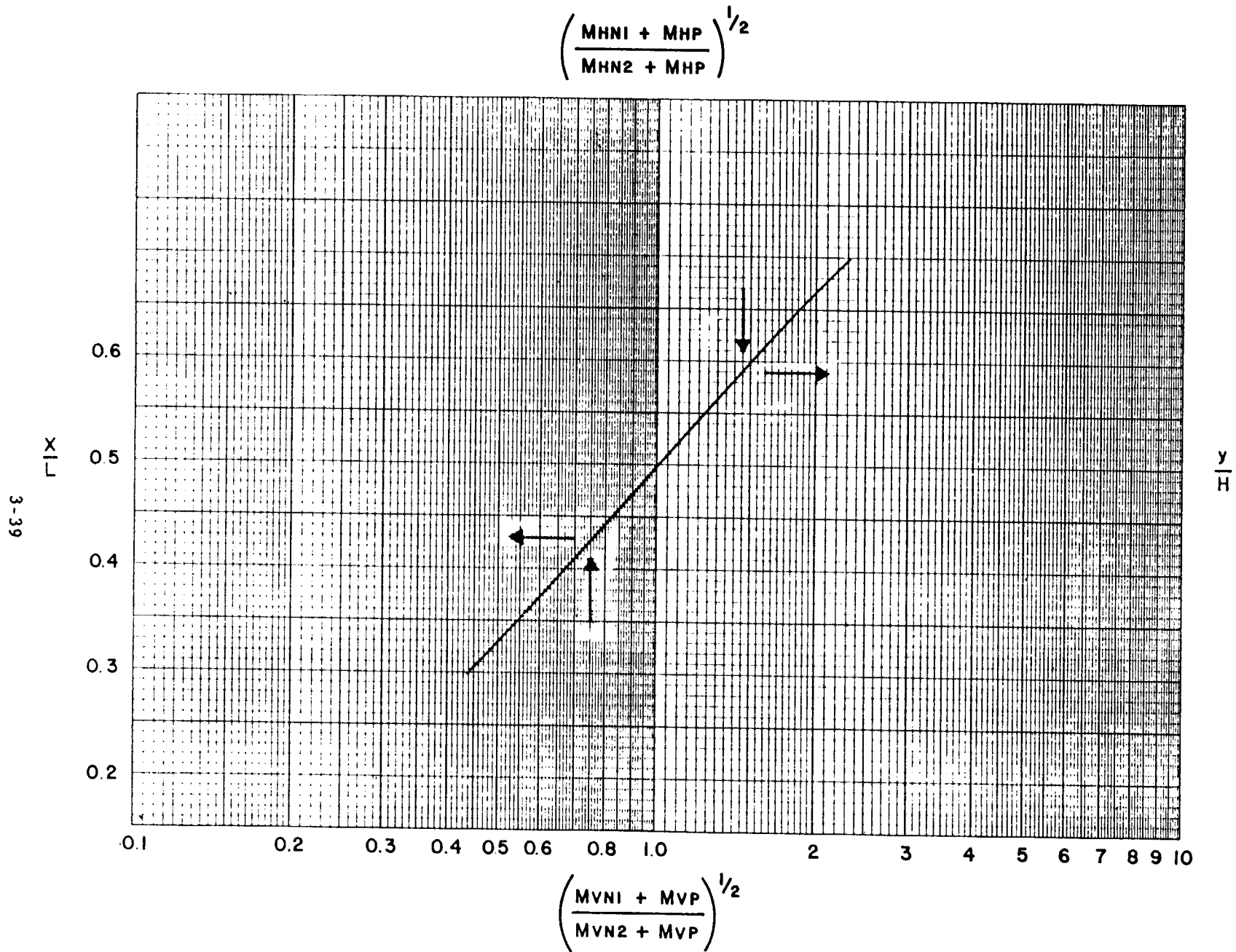
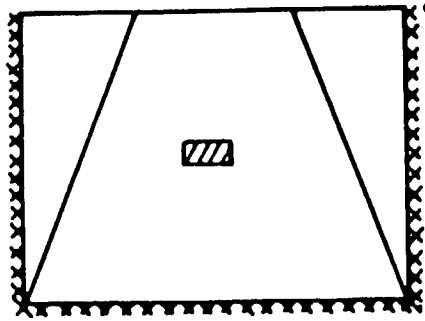
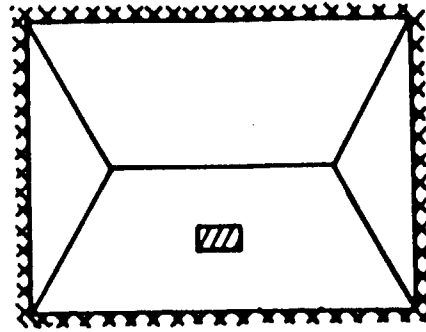


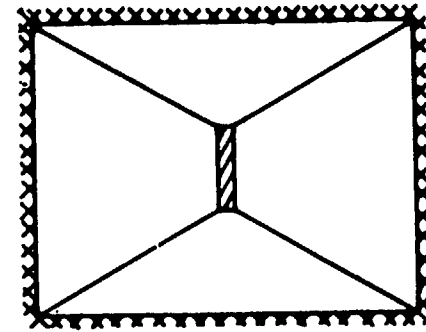
Figure 3-20 Location of unsymmetrical yield lines for two-way element with four edges supported (values of X/L and y/H)



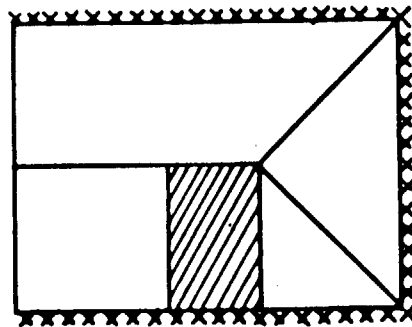
(a)



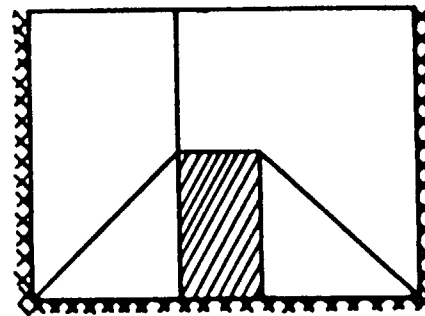
(b)



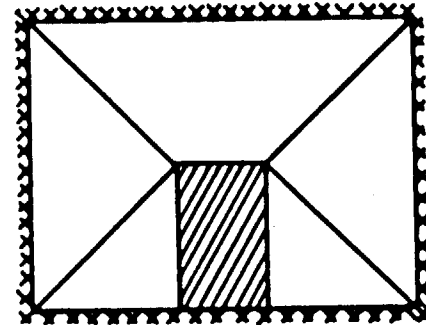
(c)



(d)

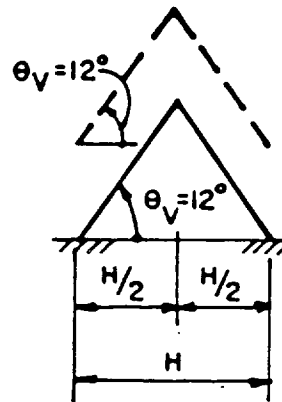
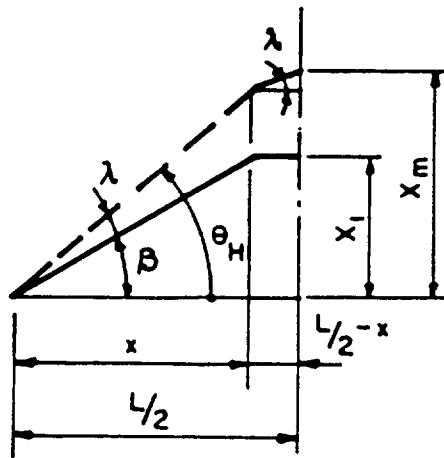
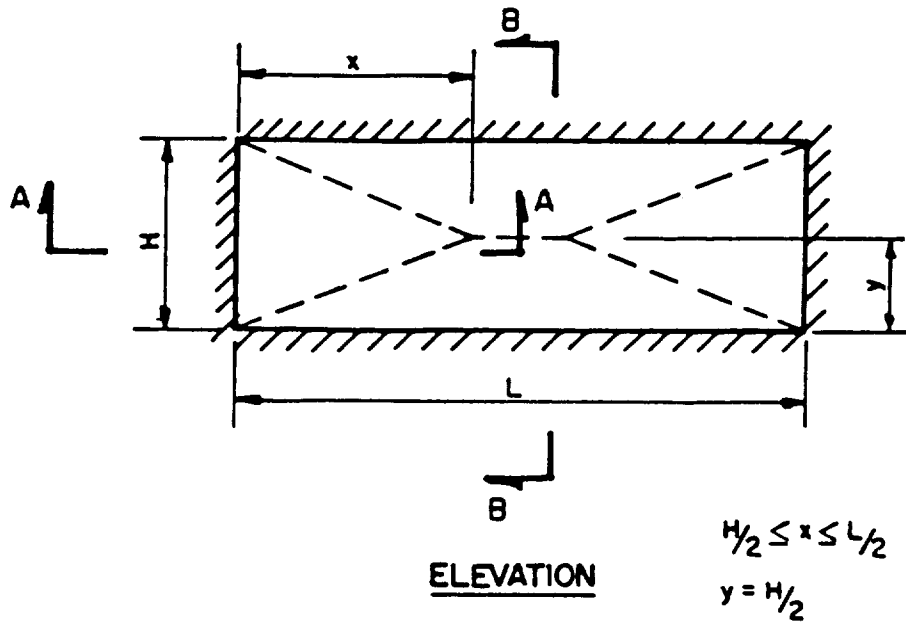


(e)



(f)

Figure 3-21 Effects of openings on yield lines locations



— PARTIAL FAILURE
 --- INCIPIENT FAILURE

Figure 3-22 Deflection of two-way element

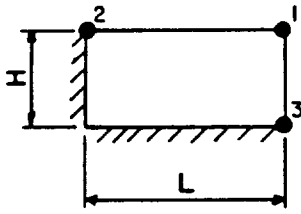


FIG. 3-24

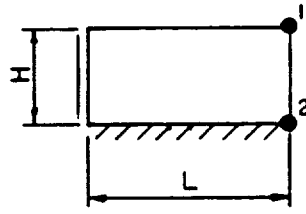


FIG. 3-25

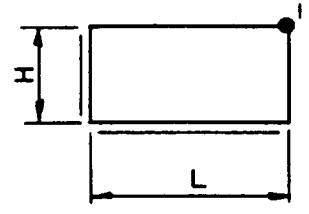


FIG. 3-26

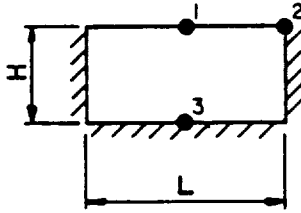


FIG. 3-27

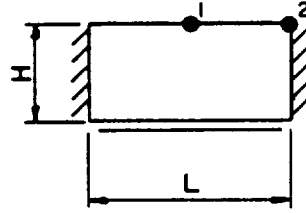


FIG. 3-28

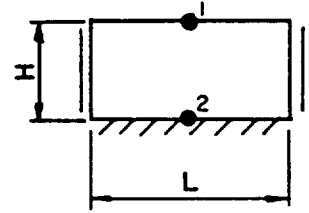


FIG. 3-29

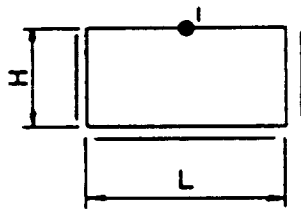


FIG. 3-30

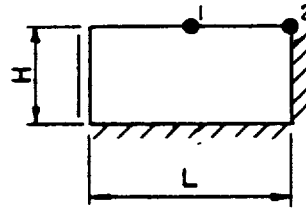


FIG. 3-31

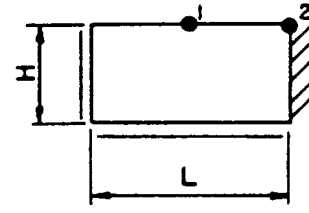


FIG. 3-32

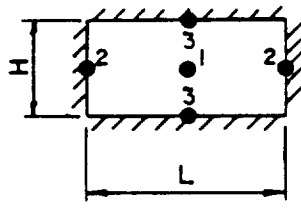


FIG. 3-33

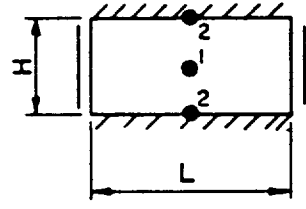


FIG. 3-34

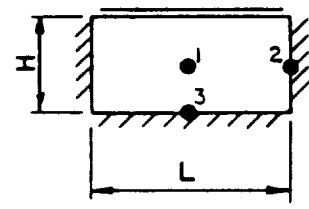


FIG. 3-35

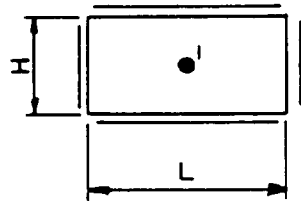


FIG. 3-36

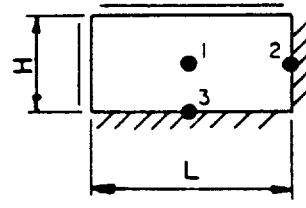


FIG. 3-37

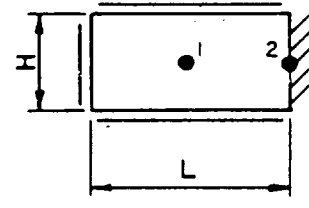


FIG. 3-38

LEGEND: EDGE CONDITIONS

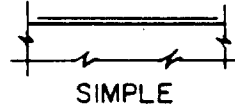
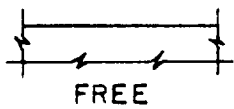


Figure 3-23 Graphical summary of two-way elements

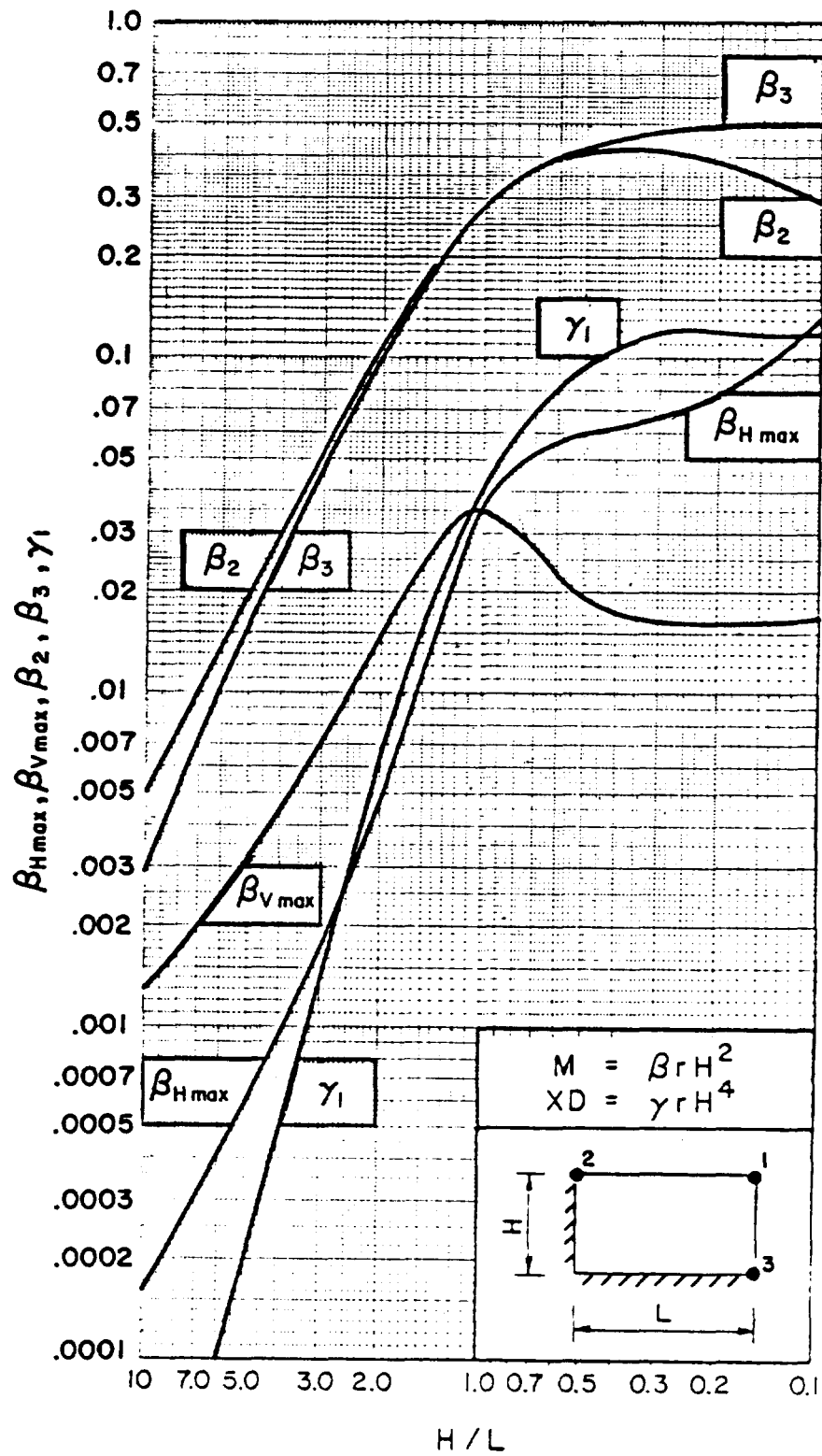


Figure 3-24 Moment and deflection coefficients for uniformly-loaded, two-way element with two adjacent edges fixed and two edges free

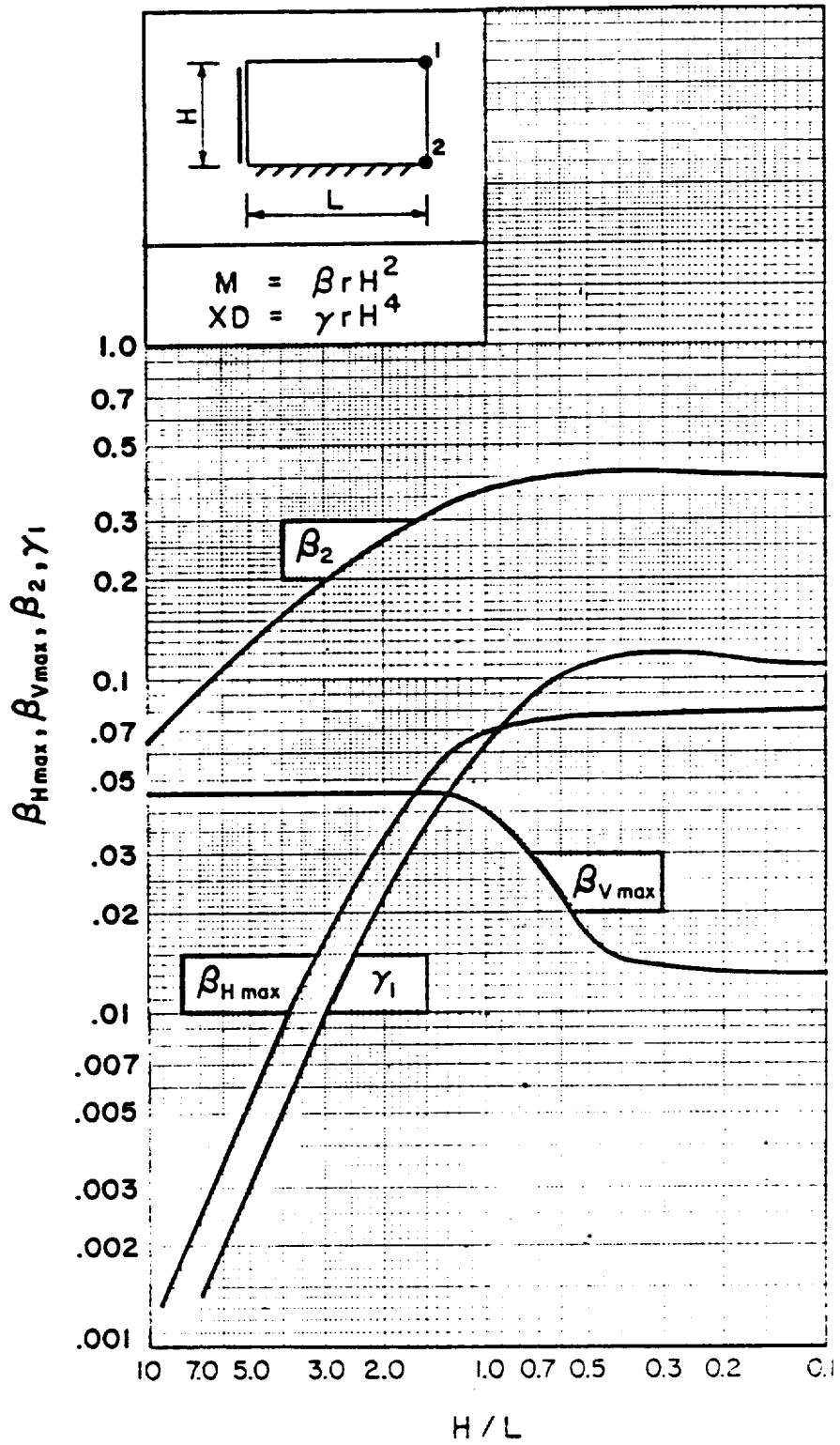


Figure 3-25 Moment and deflection coefficients for uniformly-loaded, two-way element with one edge fixed, an adjacent edge simply-supported and two edges free

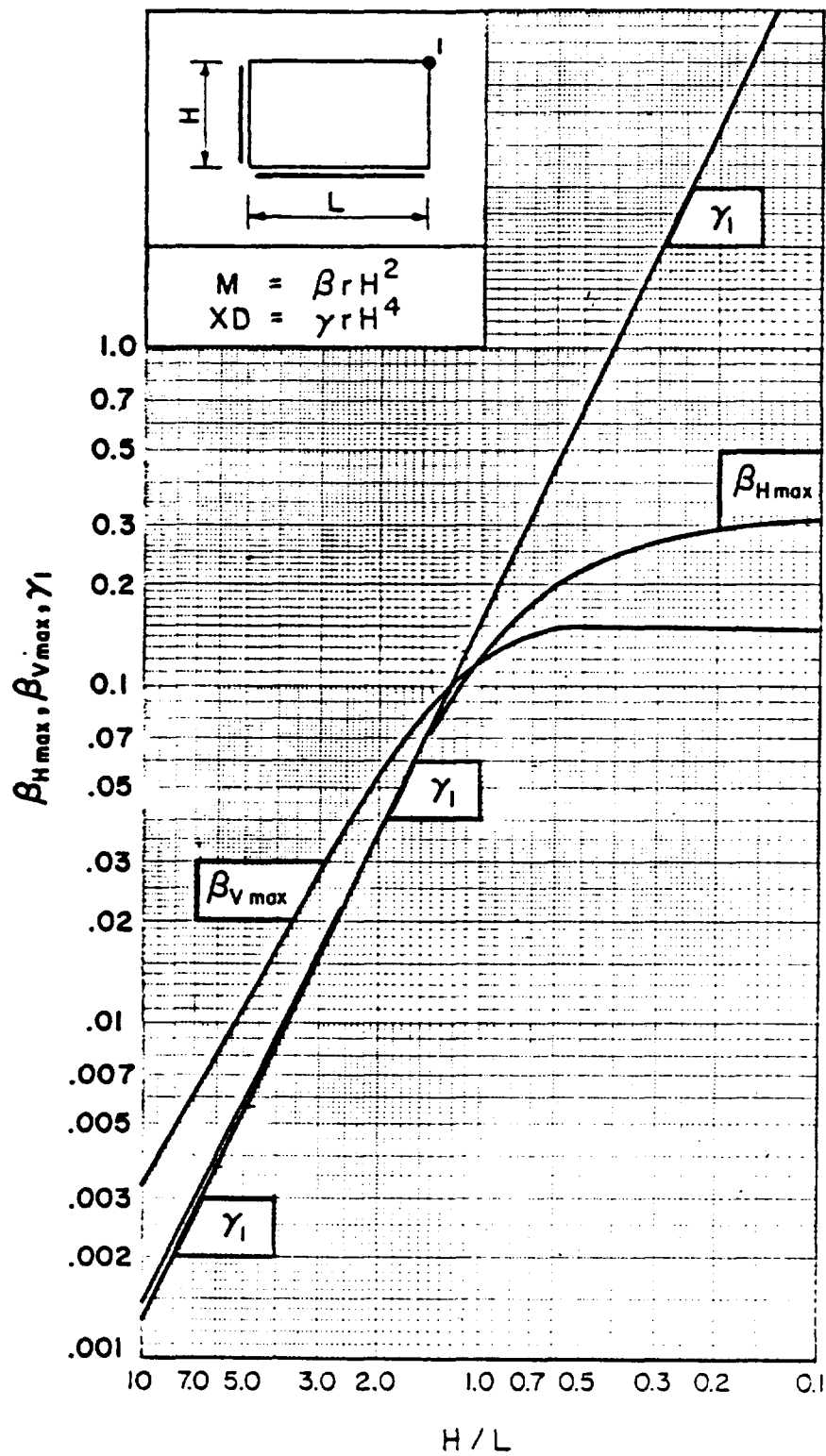


Figure 3-26 Moment and deflection coefficients for uniformly-loaded, two-way element with two adjacent edges simply-supported and two edges free

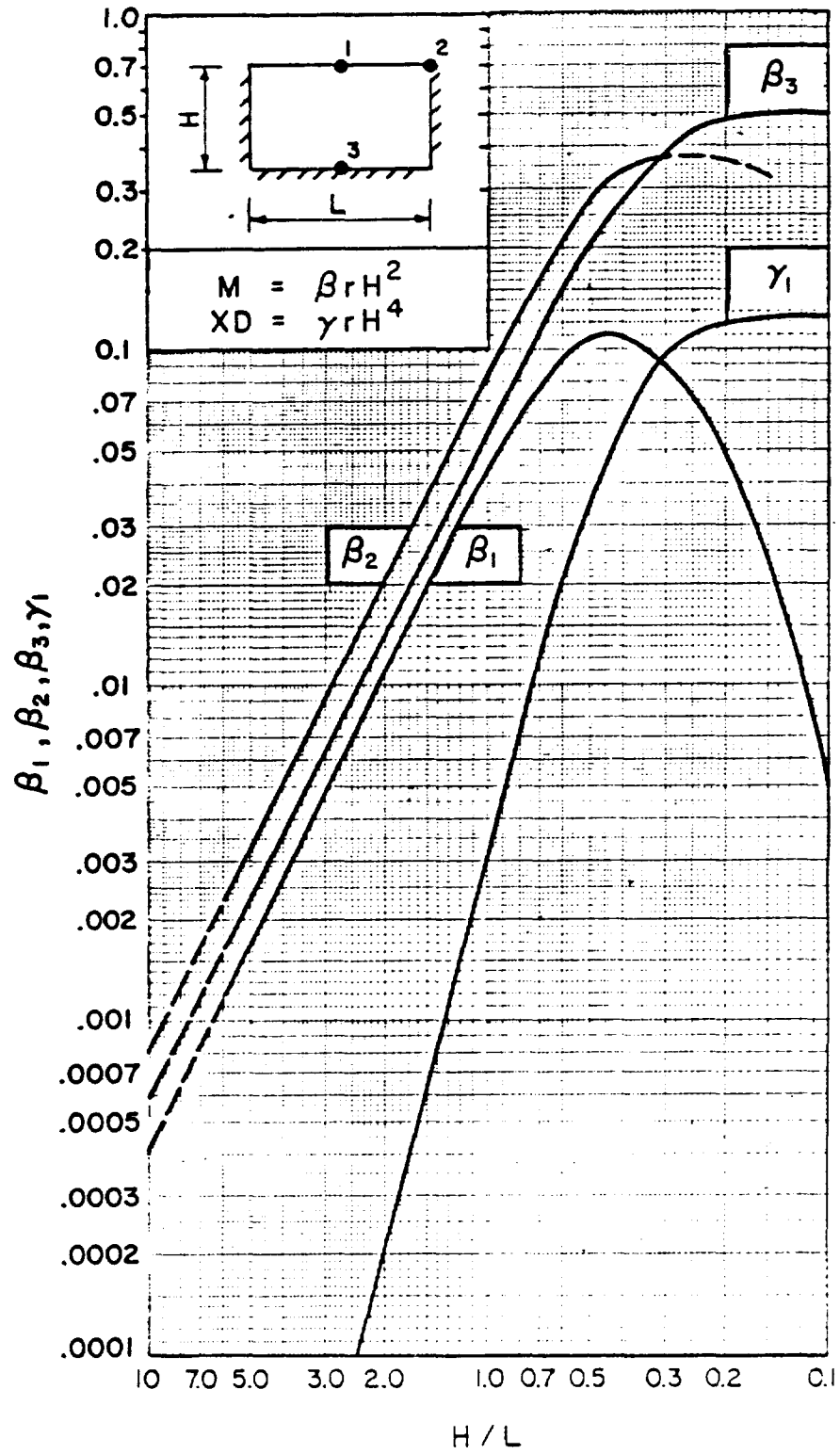


Figure 3-27 Moment and deflection coefficients for uniformly-loaded, two-way element with three edges fixed and one edge free

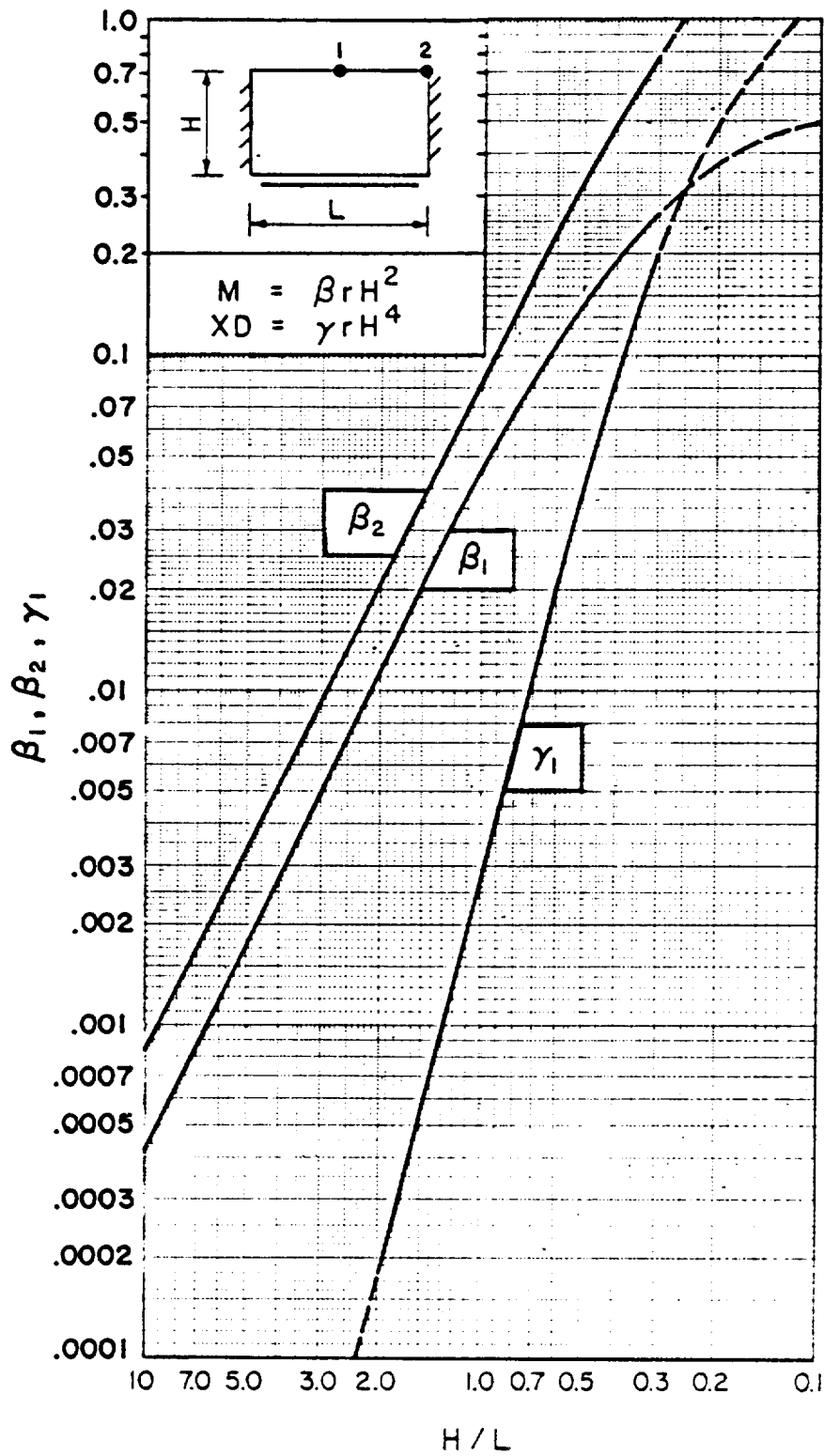


Figure 3-28 Moment and deflection coefficients for uniformly-loaded, two-way element with two opposite edges fixed, one edge simply-supported and one edge free

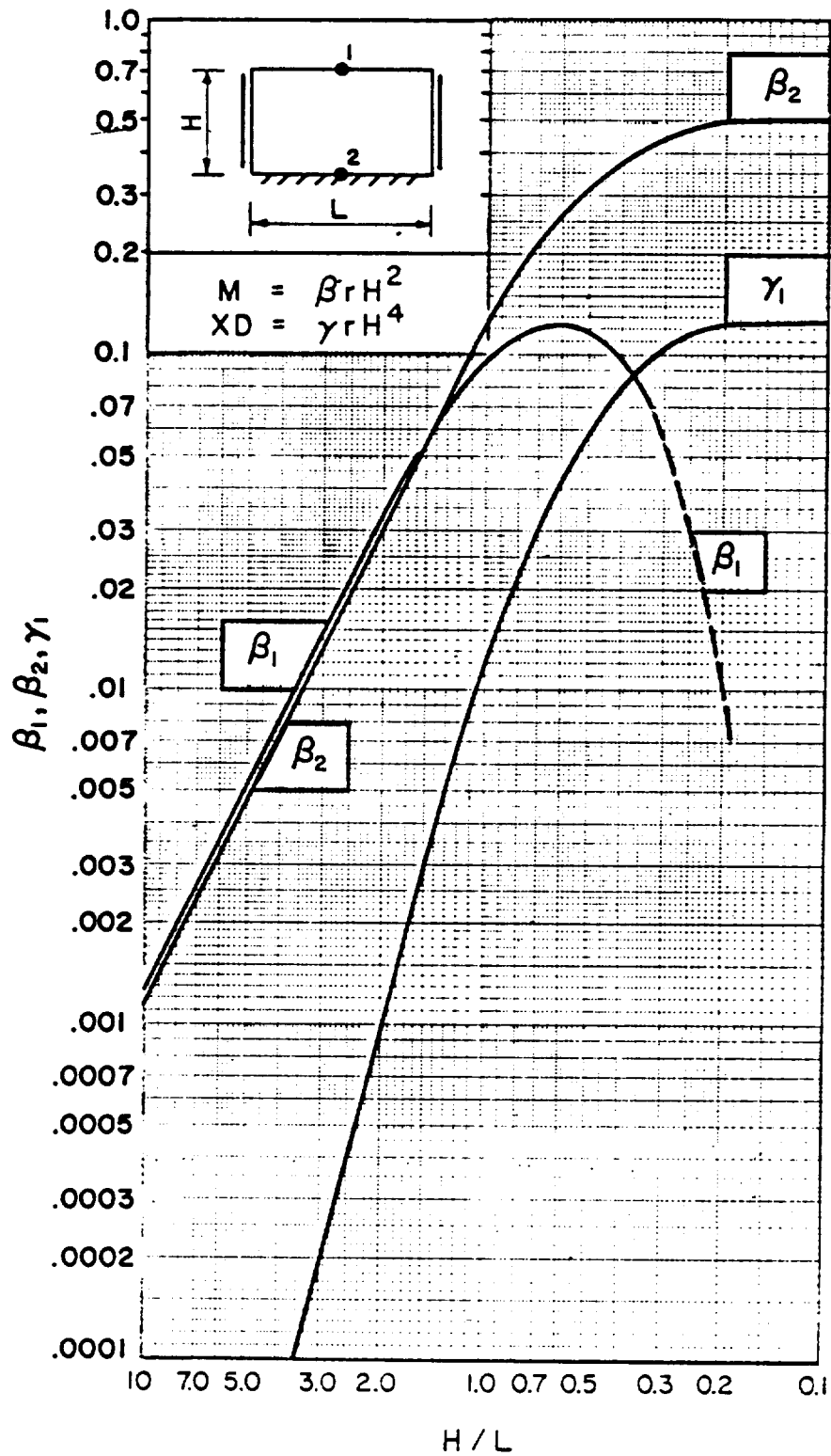


Figure 3-29 Moment and deflection coefficients for uniformly-loaded, two-way element with two opposite edges simply-supported, one edge fixed, and one edge free

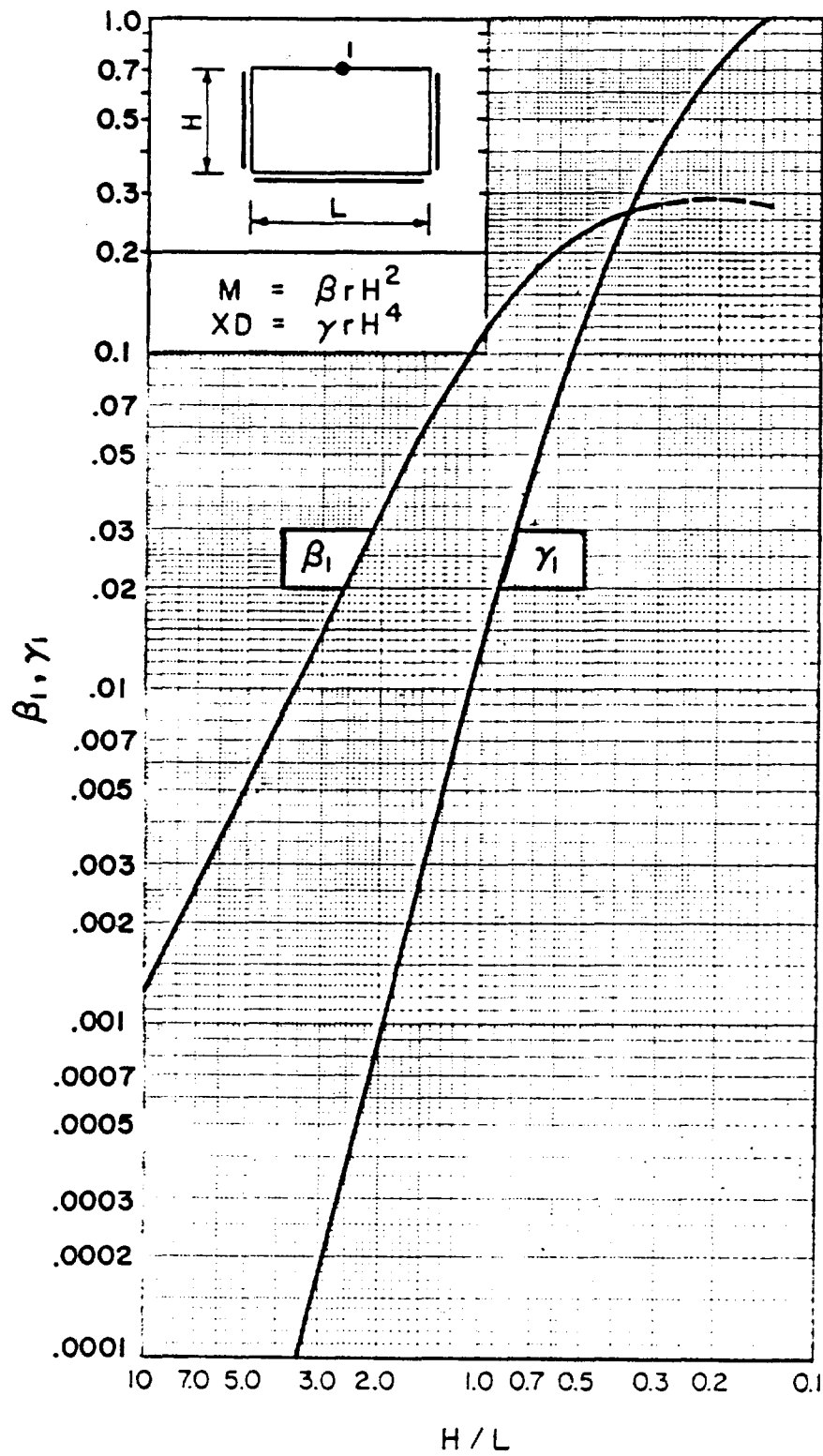


Figure 3-30 Moment and deflection coefficients for uniformly-loaded, two-way element with three edges simply-supported and one edge free

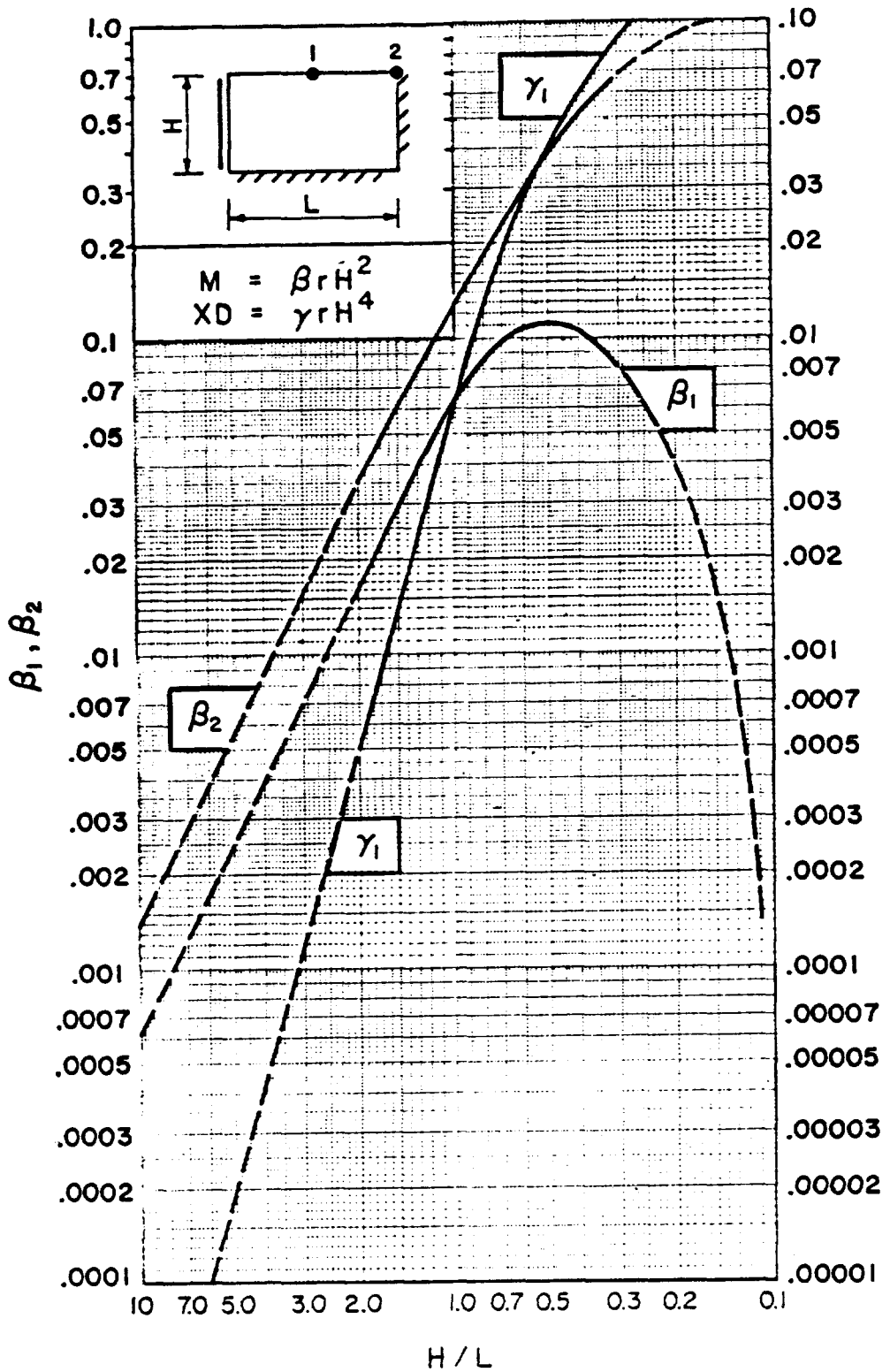


Figure 3-31 Moment and deflection coefficients for uniformly-loaded, two-way element with two adjacent edges fixed, one edge simply-supported, and one edge free

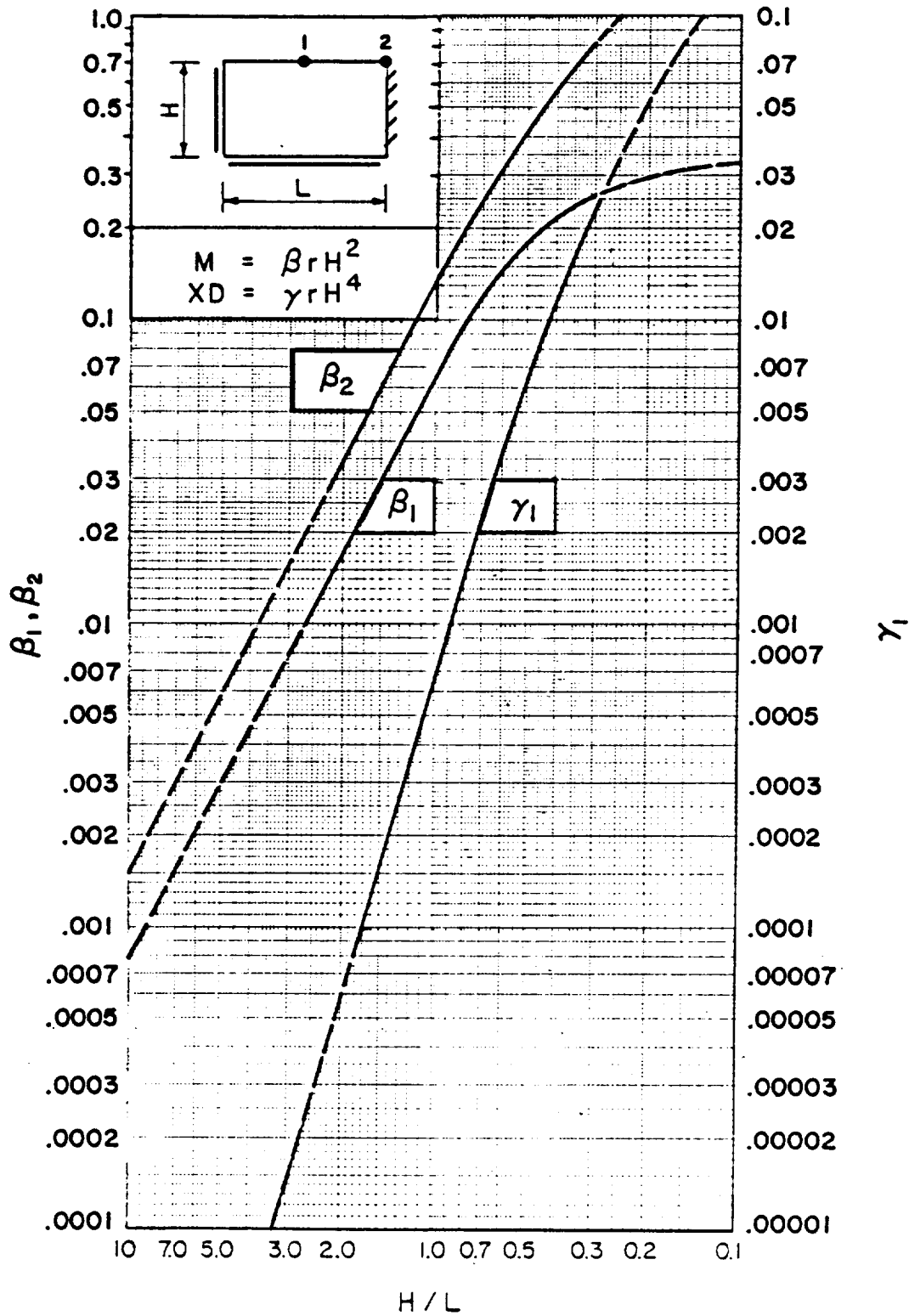


Figure 3-32 Moment and deflection coefficients for uniformly-loaded, two-way element with two adjacent edges simply-supported, one edge fixed, and one edge free

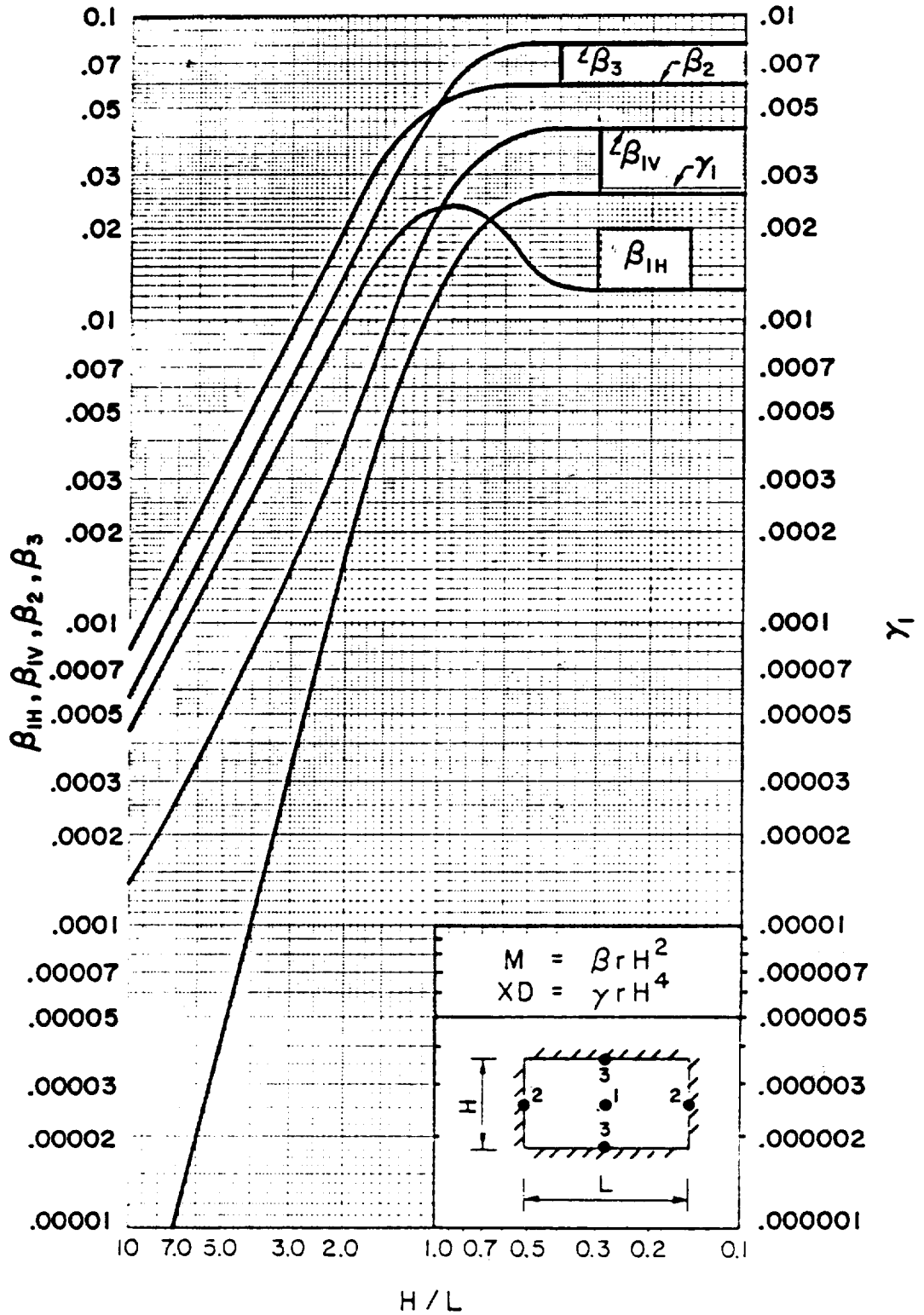


Figure 3-33 Moment and deflection coefficients for uniformly-loaded, two-way element with all edges fixed

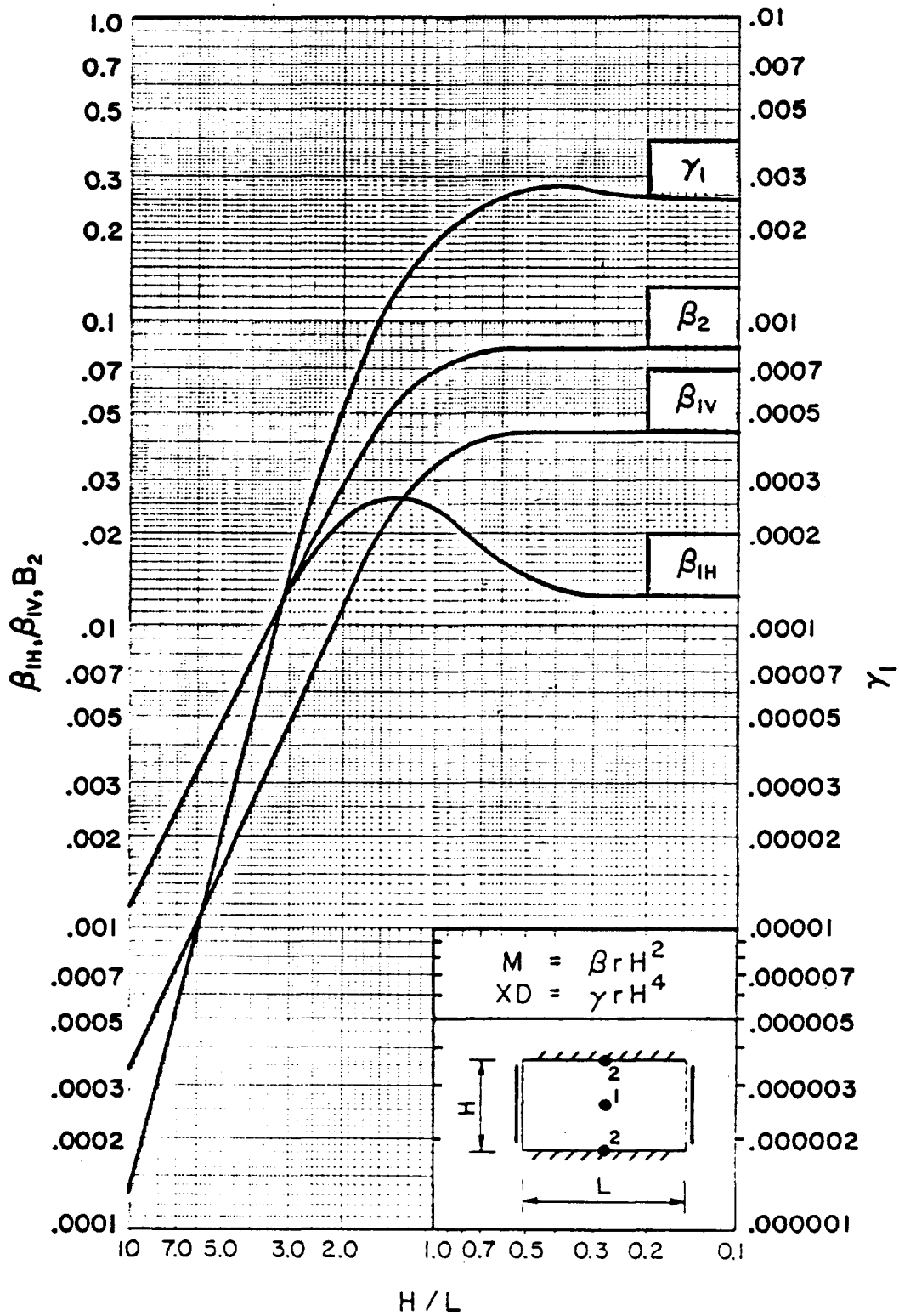


Figure 3-34 Moment and deflection coefficients for uniformly-loaded, two-way element with two opposite edges fixed and two edges simply-supported

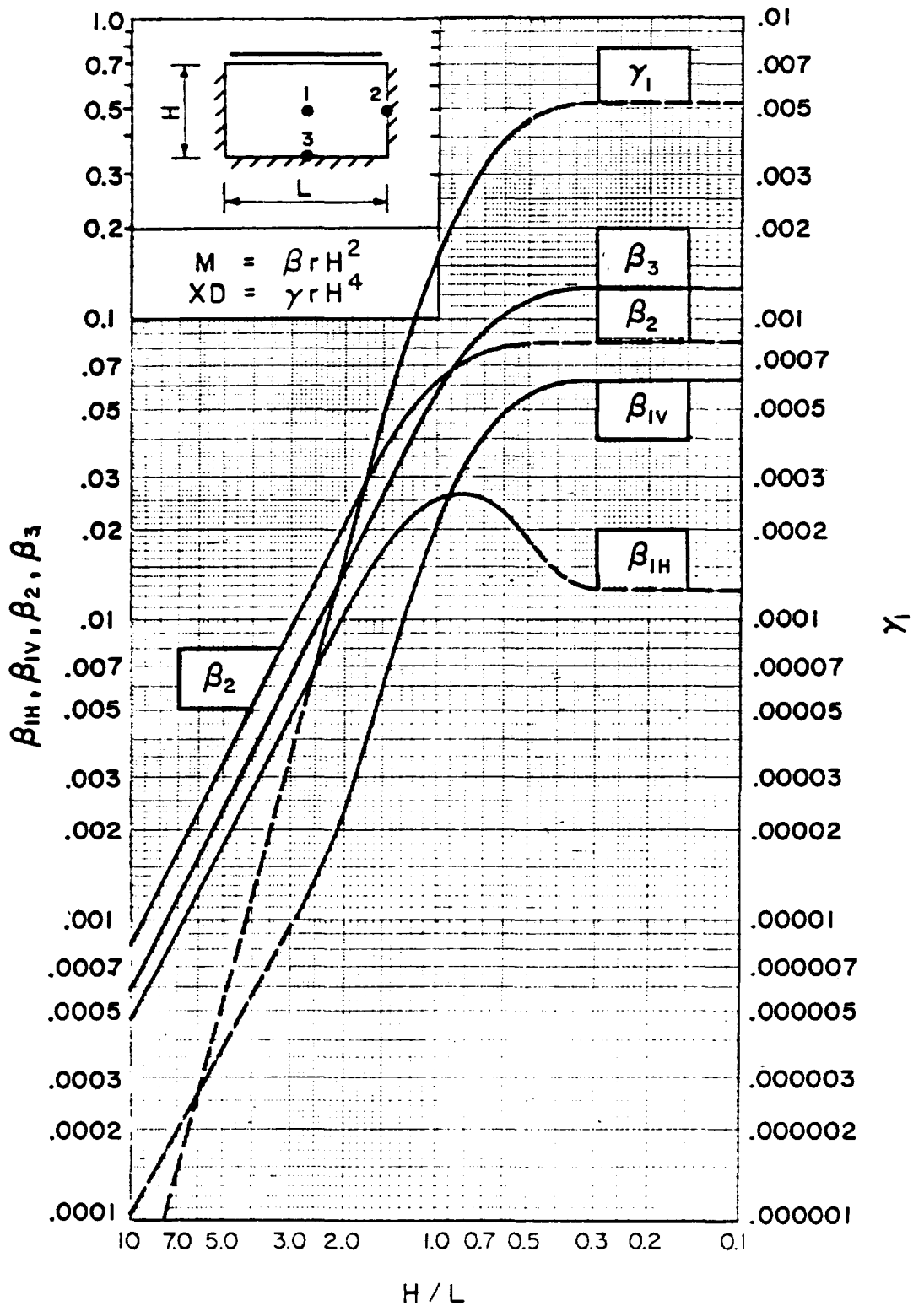


Figure 3-35 Moment and deflection coefficients for uniformly-loaded, two-way element with three edges fixed and one edge simply-supported

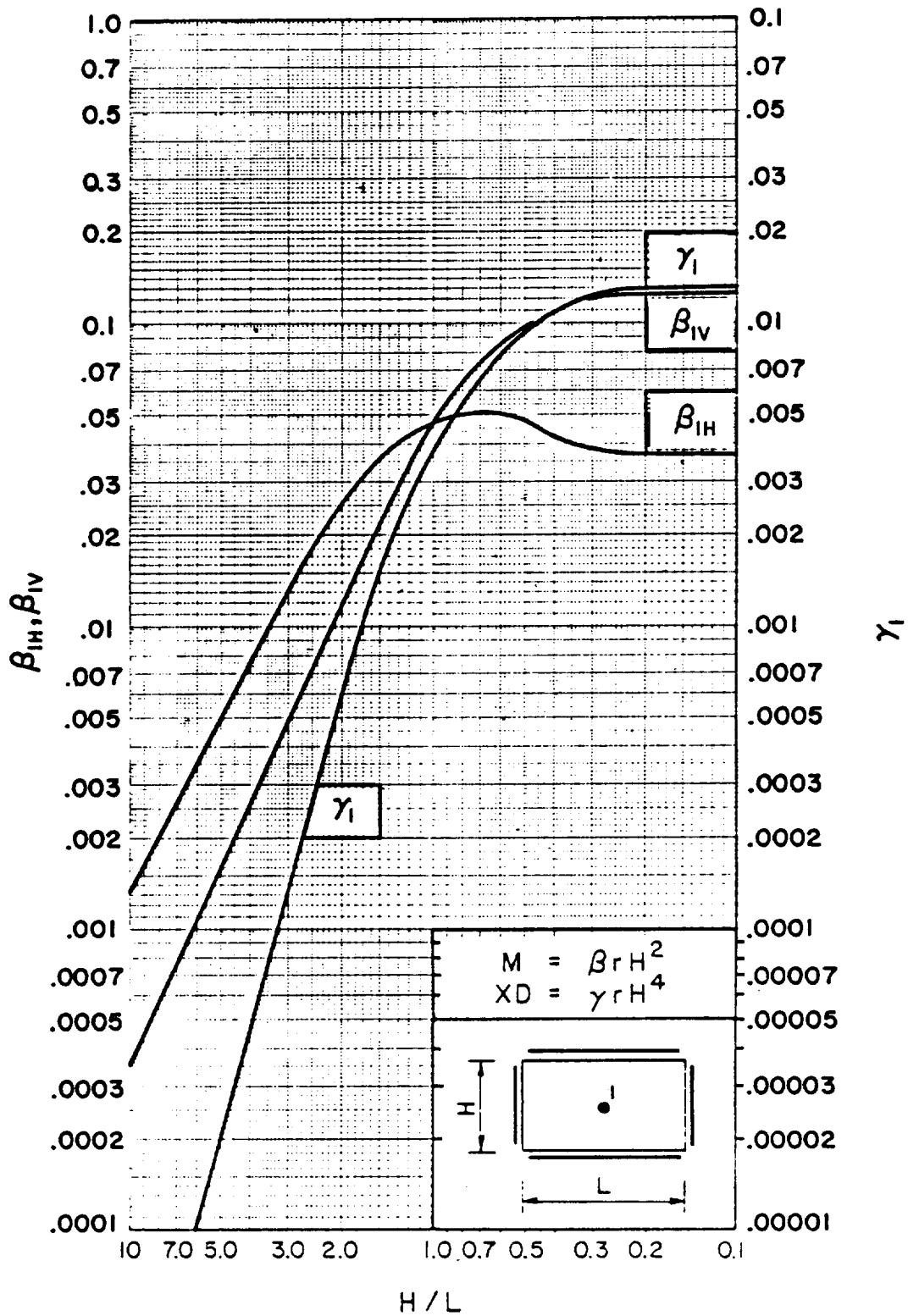


Figure 3-36 Moment and deflection coefficients for uniformly-loaded, two-way element with all edges simply-supported

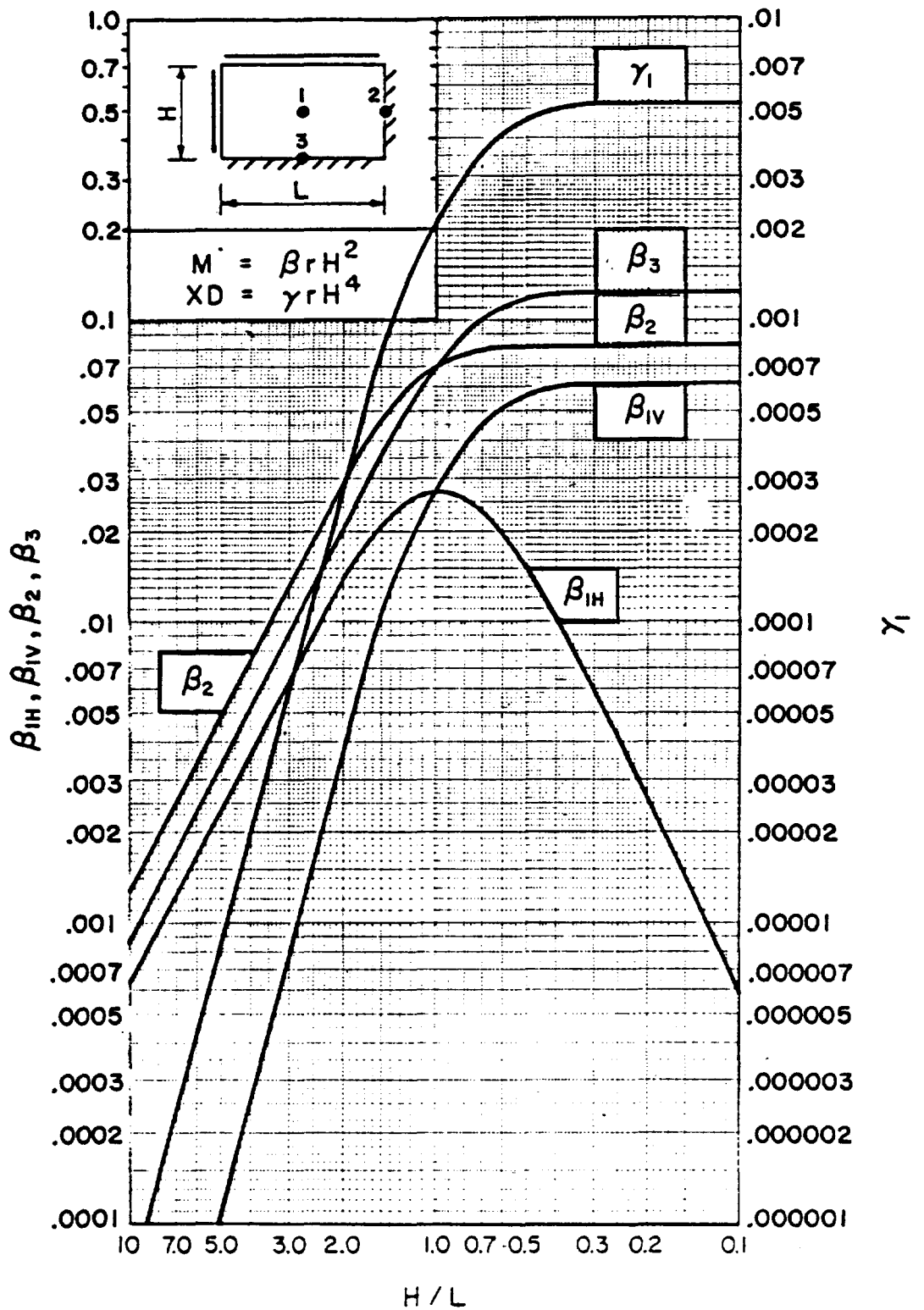


Figure 3-37 Moment and deflection coefficients for uniformly-loaded, two-way element with two adjacent edges fixed, and two edges simply-supported

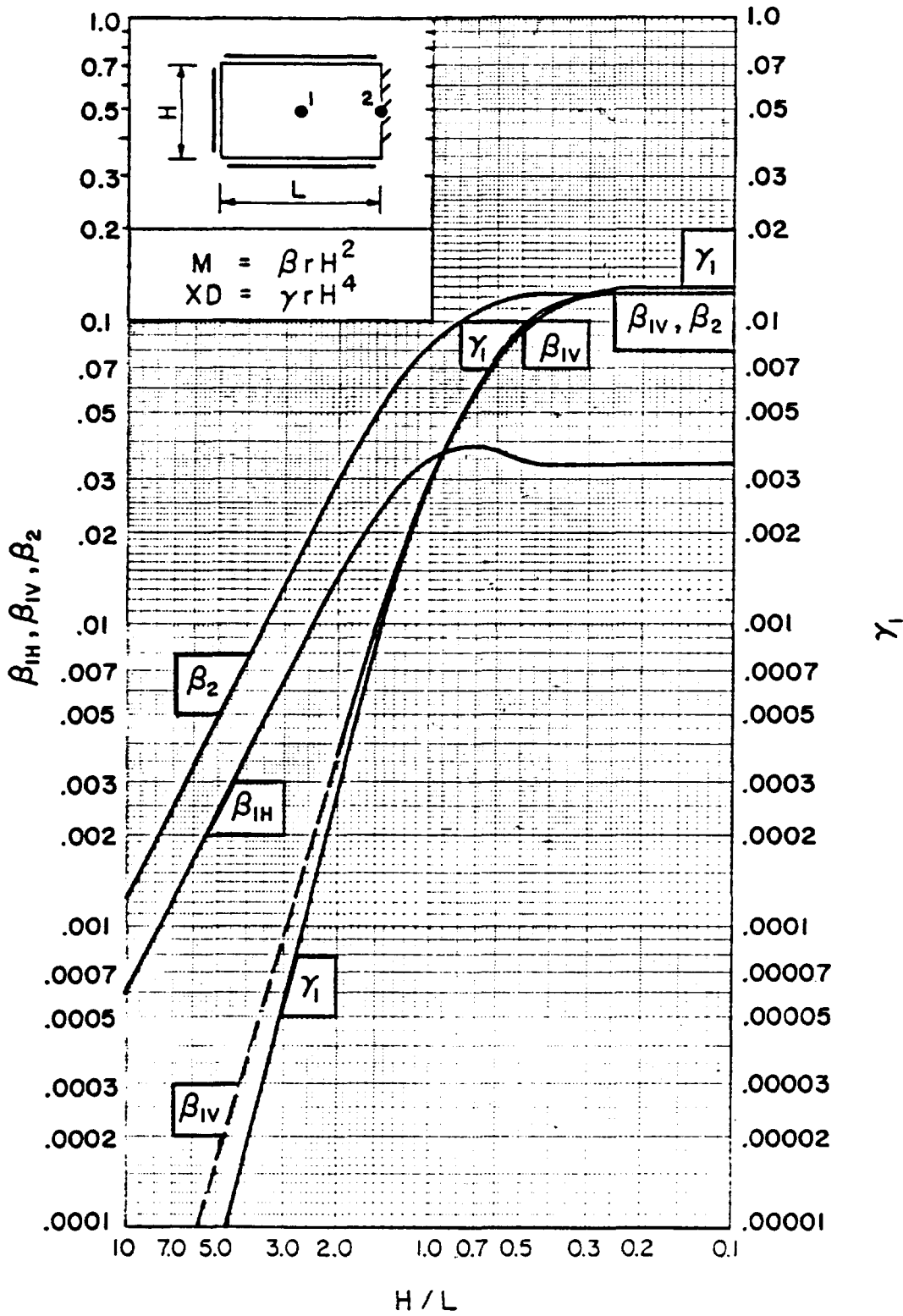
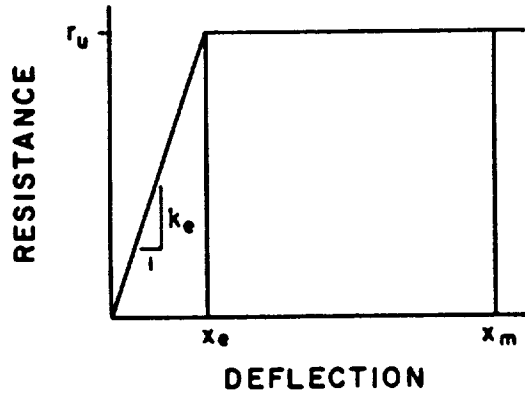
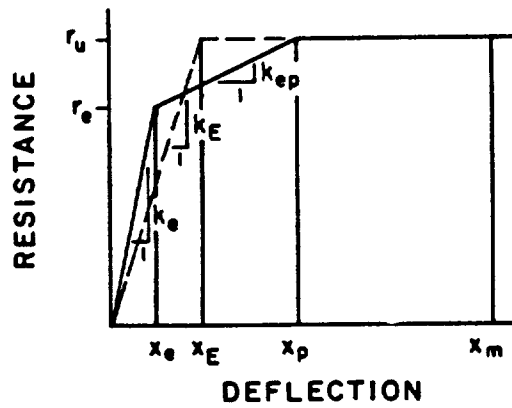


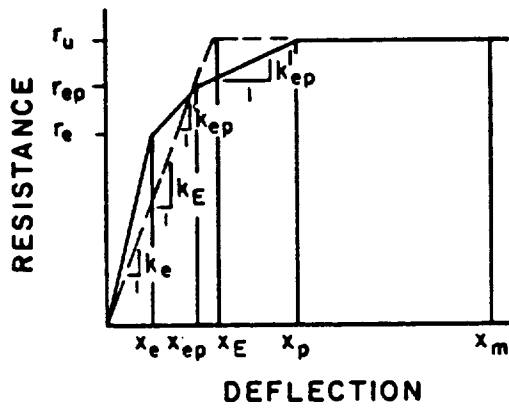
Figure 3-38 Moment and deflection coefficients for uniformly-loaded, two-way element with three edges simply-supported and one edge fixed



(a) ONE STEP ELASTO-PLASTIC SYSTEM

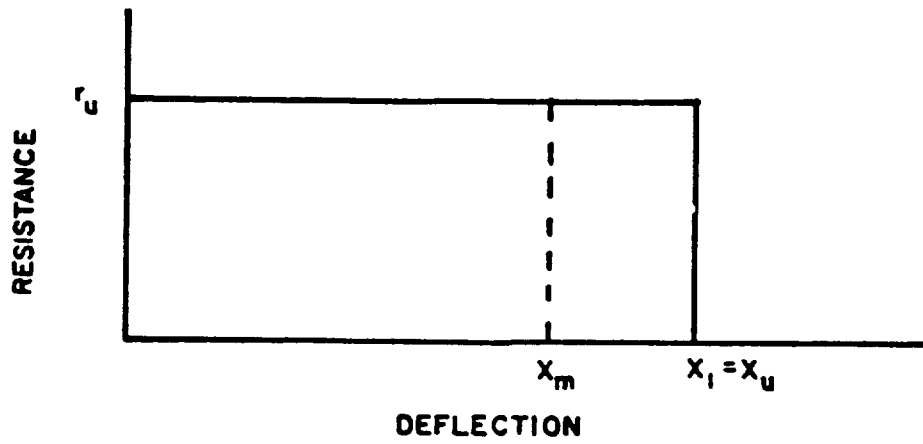


(b) TWO STEP ELASTO-PLASTIC SYSTEM

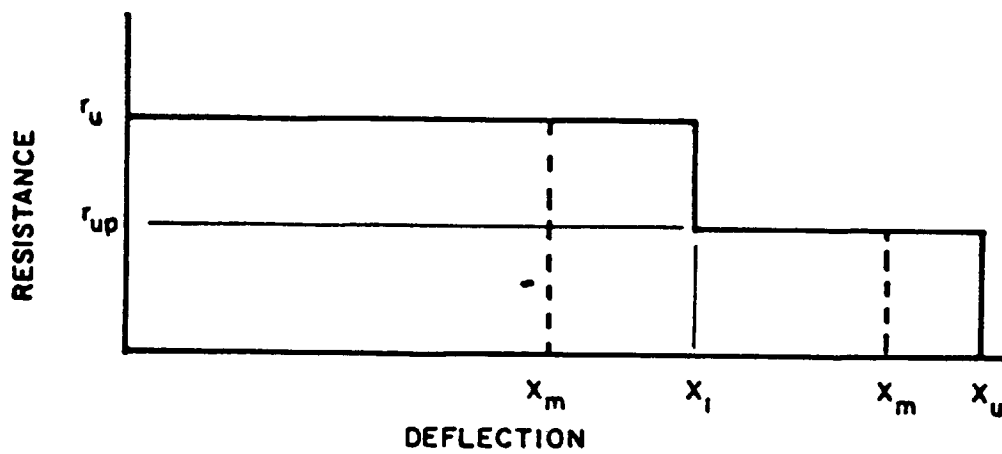


(c) THREE STEP ELASTO-PLASTIC SYSTEM

Figure 3-39 Resistance-deflection functions for limited deflections



a) ONE-WAY ELEMENT



b) TWO-WAY ELEMENT

Figure 3-40 Resistance-deflection functions for large deflections

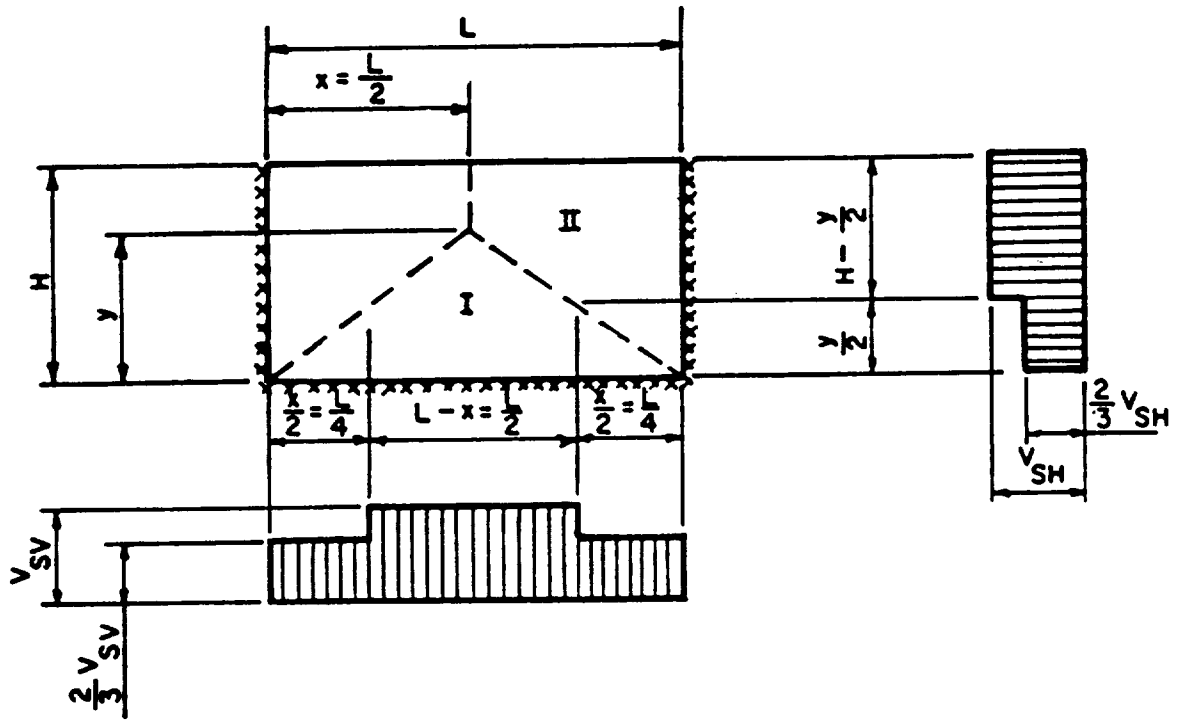


Figure 3-41 Determination of ultimate support shear

Table 3-1 Ultimate Unit Resistances for One-Way Elements

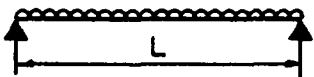
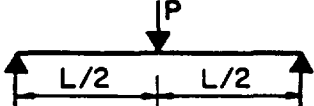
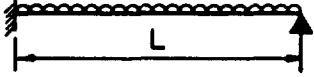
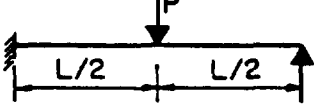
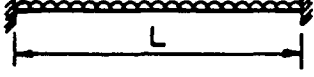
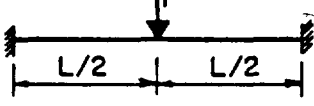
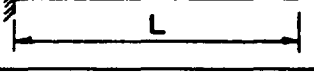
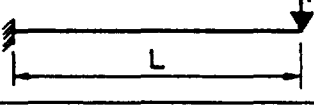
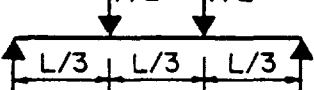
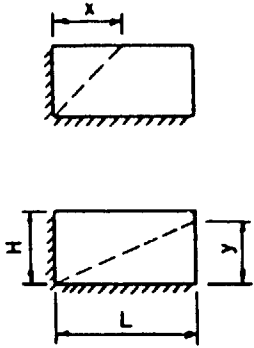
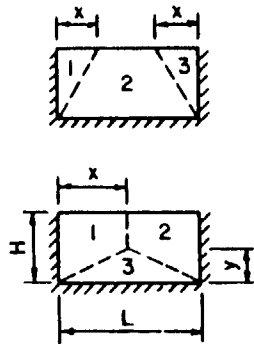
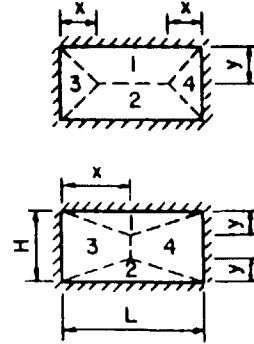
Edge Conditions and Loading Diagrams	Ultimate Resistance
	$r_u = \frac{8 M_p}{L^2}$
	$R_u = \frac{4 M_p}{L}$
	$r_u = \frac{4 (M_N + 2 M_p)}{L^2}$
	$R_u = \frac{2 (M_N + 2 M_p)}{L}$
	$r_u = \frac{8 (M_N + M_p)}{L^2}$
	$R_u = \frac{4 (M_N + M_p)}{L}$
	$r_u = \frac{2 M_N}{L^2}$
	$R_u = \frac{M_N}{L}$
	$R_u = \frac{6 M_p}{L}$

Table 3-2

Ultimate Unit Resistances for Two-Way Elements
(Symmetrical Yield Lines)

Edge Conditions	Yield Line Locations	Limits	Ultimate Unit Resistance
Two adjacent edges supported and two edges free		$x \leq L$ $y \leq H$	$\frac{5(M_{HN} + M_{HP})}{x^2} \quad \text{OR} \quad \frac{6L M_{VN} + (5M_{VP} - M_{VN})x}{H^2(3L - 2x)}$ $\frac{5(M_{VN} + M_{VP})}{y^2} \quad \text{OR} \quad \frac{6H M_{HN} + (5M_{HP} - M_{HN})y}{L^2(3H - 2y)}$
Three edges supported and one edge free		$x \leq \frac{L}{2}$ $y \leq H$	$\frac{5(M_{HN} + M_{HP})}{x^2} \quad \text{OR} \quad \frac{2M_{VN}(3L - x) + 10x M_{VP}}{H^2(3L - 4x)}$ $\frac{5(M_{VN} + M_{VP})}{y^2} \quad \text{OR} \quad \frac{4(M_{HN} + M_{HP})(6H - y)}{L^2(3H - 2y)}$
Four edges supported		$x \leq \frac{L}{2}$ $y \leq \frac{H}{2}$	$\frac{5(M_{HN} + M_{HP})}{x^2} \quad \text{OR} \quad \frac{8(M_{VN} + M_{VP})(3L - x)}{H^2(3L - 4x)}$ $\frac{5(M_{VN} + M_{VP})}{y^2} \quad \text{OR} \quad \frac{8(M_{HN} + M_{HP})(3H - y)}{L^2(3H - 4y)}$

3-62

Table 3-3

Ultimate Unit Resistances for Two-Way Elements
(Unsymmetrical Yield Lines)

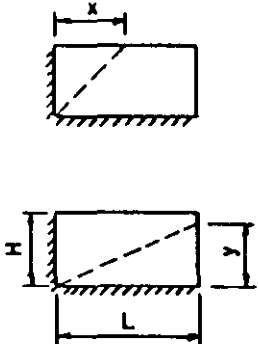
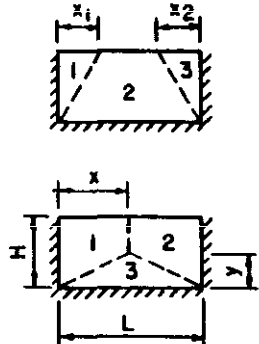
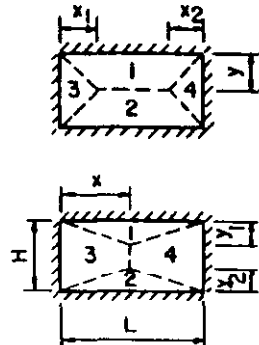
Edge Conditions	Yield Line Locations	Limits	Ultimate Unit Resistance
Two adjacent edges supported and two edges free		$x \leq L$ $y \leq H$	Same as in Table 3-2
Three edges supported and one edge free		$x_1 \leq \frac{L}{2}$ $y \leq H$	$\frac{5(M_{HN1} + M_{HP1})}{X_1^2} \text{ OR } \frac{5(M_{HN3} + M_{HP})}{X_2^2}$ $\text{OR } \frac{(5M_{VP} - M_{VN2})(X_1 + X_2) + 6M_{VN2}L}{H^2(3L - 2X_1 - 2X_2)}$ $\frac{(M_{HN1} + M_{HP})(6H - Y)}{X^2(3H - 2Y)} \text{ OR } \frac{(M_{HN2} + M_{HP})(6H - Y)}{(L - X)^2(3H - 2Y)}$ $\text{OR } \frac{5(M_{VN3} + M_{VP})}{Y^2}$
Four edges supported		$x_1 \leq \frac{L}{2}$ $y_1 \leq \frac{H}{2}$	$\frac{(M_{VN1} + M_{VP})(6L - X_1 - X_2)}{Y^2(3L - 2X_1 - 2X_2)} \text{ OR } \frac{(M_{VN2} + M_{VP})(6L - X_1 - X_2)}{(H - Y)^2(3L - 2X_1 - 2X_2)}$ $\frac{5(M_{HN1} + M_{HP})}{X_1^2} \text{ OR } \frac{5(M_{HN2} + M_{HP})}{X_2^2}$ $\frac{5(M_{VN1} + M_{VP})}{Y_1^2} \text{ OR } \frac{5(M_{VN2} + M_{VP})}{Y_2^2}$ $\frac{(M_{HN1} + M_{HP})(6H - Y_1 - Y_2)}{X^2(3H - 2Y_1 - 2Y_2)} \text{ OR } \frac{(M_{HN2} + M_{HP})(6H - Y_1 - Y_2)}{(L - X)^2(3H - 2Y_1 - 2Y_2)}$

Table 3-4 Post-Ultimate Unit Resistances for Two-Way Elements

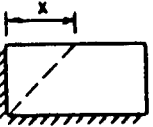
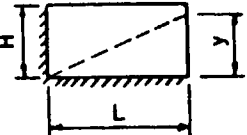
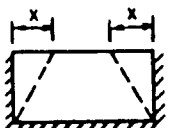
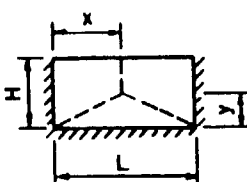
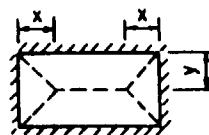
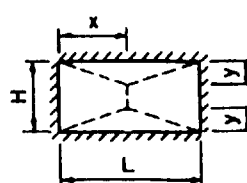
Edge Conditions	Yield Line Locations	Limits	Post - Ultimate Unit Resistance
Two adjacent edges supported and two edges free		$x < H$ $x > H$	$2 M_{VN} / H^2$ $2 M_{HN} / L^2$
		$y < H$ $y > L$	$2 M_{HN} / L^2$ $2 M_{VN} / H^2$
Three edges supported and one edge free		$x < H$ $x > H$	$2 M_{VN} / H^2$ $8 (M_{HN} + M_{HP}) / L^2$
		$y < L/2$ $y > L/2$	$8 (M_{HN} + M_{HP}) / L^2$ $2 M_{VN} / H^2$
Four edges supported		$x < H/2$ $x > H/2$	$8 (M_{VN} + M_{VP}) / H^2$ $8 (M_{HN} + M_{HP}) / L^2$
		$y < L/2$ $y > L/2$	$8 (M_{VN} + M_{VP}) / L^2$ $8 (M_{HN} + M_{HP}) / H^2$

Table 3-5 General and Ultimate Deflections for One-Way Elements


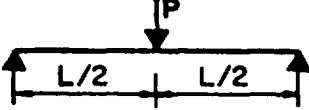
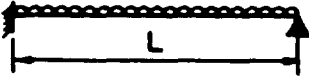
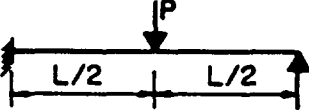
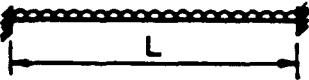
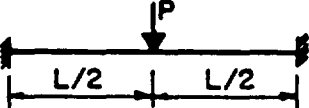
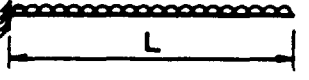
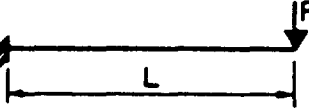
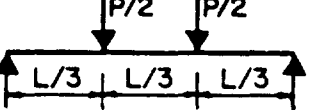
Edge Conditions and Loading Diagrams	Maximum Deflection, X_m	Ultimate Deflection, X_u
	$\frac{L}{2} \tan \theta$	$\frac{L}{2} \tan \theta \text{ max}$
	$(L/2) \tan \theta$	$(L/2) \tan \theta \text{ max}$
	$\frac{L}{2} \tan \theta$	$\frac{L}{2} \tan \theta \text{ max}$
	$(L/2) \tan \theta$	$(L/2) \tan \theta \text{ max}$
	$\frac{L}{2} \tan \theta$	$\frac{L}{2} \tan \theta \text{ max}$
	$(L/2) \tan \theta$	$(L/2) \tan \theta \text{ max}$
	$L \tan \theta$	$L \tan \theta \text{ max}$
	$L \tan \theta$	$L \tan \theta \text{ max}$
	$(L/3) \tan \theta$	$(L/3) \tan \theta \text{ max}$

Table 3-6 General, Partial Failure, and Ultimate Deflections for Two-Way Elements

Edge Conditions	Yield Line Location	Limits	Maximum Deflection, X_m		Partial Failure Deflection X_i	Ultimate Deflection, X_u	Support Failing Deflection X_l
			$(0 < X_m < X_l)$	$(X_l < X_m < X_u)$			
Two adjacent edges supported and two edges free		$x \leq H$	$x \tan \theta_H$	$H \tan \theta_V$	$x \tan \theta_{max}$	$H \tan \theta_{max}$	H
		$x \geq H$	$H \tan \theta_V$	$x \tan \theta_H + (L-x) \tan \left[\theta_H - \tan^{-1} \left(\frac{\tan \theta_V}{x/H} \right) \right]$	$H \tan \theta_{max}$	$x \tan \theta_{max} + (L-x) \tan \left[\theta_{max} - \tan^{-1} \left(\frac{\tan \theta_{max}}{x/H} \right) \right]$	L
		$y \leq L$	$y \tan \theta_V$	$L \tan \theta_H$	$y \tan \theta_{max}$	$L \tan \theta_{max}$	L
		$y \geq L$	$L \tan \theta_H$	$y \tan \theta_V + (H-y) \tan \left[\theta_V - \tan^{-1} \left(\frac{\tan \theta_H}{y/L} \right) \right]$	$L \tan \theta_{max}$	$y \tan \theta_{max} + (H-y) \tan \left[\theta_{max} - \tan^{-1} \left(\frac{\tan \theta_{max}}{y/L} \right) \right]$	H
Three edges supported and one edge free		$x \leq H$	$x \tan \theta_V$	$H \tan \theta_V$	$x \tan \theta_{max}$	$H \tan \theta_{max}$	H
		$x \geq H$	$H \tan \theta_V$	$x \tan \theta_H + \left(\frac{L}{2} - x \right) \tan \left[\theta_H - \tan^{-1} \left(\frac{\tan \theta_V}{x/H} \right) \right]$	$H \tan \theta_{max}$	$x \tan \theta_{max} + \left(\frac{L}{2} - x \right) \tan \left[\theta_{max} - \tan^{-1} \left(\frac{\tan \theta_{max}}{x/H} \right) \right]$	L
		$y \leq \frac{L}{2}$	$y \tan \theta_V$	$\frac{L \tan \theta_H}{2}$	$y \tan \theta_{max}$	$\frac{L \tan \theta_{max}}{2}$	L
		$y \geq \frac{L}{2}$	$\frac{L \tan \theta_H}{2}$	$y \tan \theta_V + (H-y) \tan \left[\theta_V - \tan^{-1} \left(\frac{\tan \theta_H}{2y/L} \right) \right]$	$\frac{L \tan \theta_{max}}{2}$	$y \tan \theta_{max} + (H-y) \tan \left[\theta_{max} - \tan^{-1} \left(\frac{\tan \theta_{max}}{2y/L} \right) \right]$	H
Four edges supported		$x \leq \frac{H}{2}$	$x \tan \theta_H$	$\frac{H \tan \theta_V}{2}$	$x \tan \theta_{max}$	$\frac{H \tan \theta_{max}}{2}$	H
		$x \geq \frac{H}{2}$	$\frac{H \tan \theta_V}{2}$	$x \tan \theta_H + \left(\frac{L}{2} - x \right) \tan \left[\theta_H - \tan^{-1} \left(\frac{\tan \theta_V}{2x/H} \right) \right]$	$\frac{H \tan \theta_{max}}{2}$	$x \tan \theta_{max} + \left(\frac{L}{2} - x \right) \tan \left[\theta_{max} - \tan^{-1} \left(\frac{\tan \theta_{max}}{2x/H} \right) \right]$	L
		$y \leq \frac{L}{2}$	$y \tan \theta_V$	$\frac{L \tan \theta_H}{2}$	$y \tan \theta_{max}$	$\frac{L \tan \theta_{max}}{2}$	L
		$y \geq \frac{L}{2}$	$\frac{L \tan \theta_H}{2}$	$y \tan \theta_V + \left(\frac{H}{2} - y \right) \tan \left[\theta_V - \tan^{-1} \left(\frac{\tan \theta_H}{2y/L} \right) \right]$	$\frac{L \tan \theta_{max}}{2}$	$y \tan \theta_{max} + \left(\frac{H}{2} - y \right) \tan \left[\theta_{max} - \tan^{-1} \left(\frac{\tan \theta_{max}}{2y/L} \right) \right]$	H

3-66

Table 3-7 Elastic and Elasto-Plastic Unit Resistances for One-Way Elements.

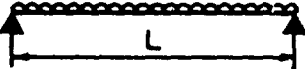
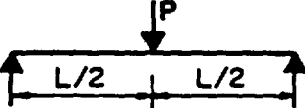
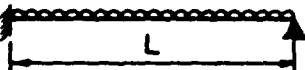
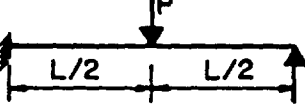
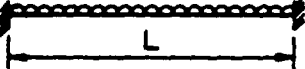
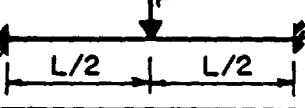

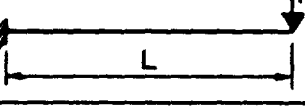
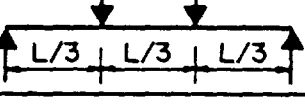
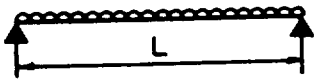
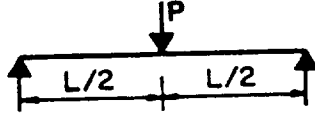
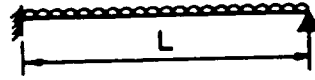
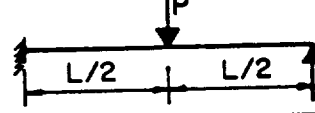
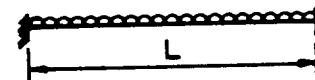
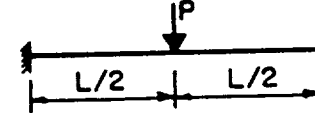
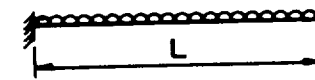
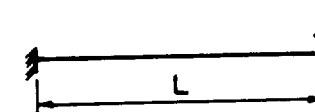
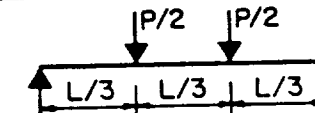
Edge Conditions and Loading Diagrams	Elastic Resistance, r_e	Elasto - Plastic Resistance, r_{ep}
	r_u	—
	R_u	—
	$\frac{8M_N}{L^2}$	r_u
	$\frac{16M_N}{3L}$	R_u
	$\frac{12M_N}{L^2}$	r_u
	$\frac{8M_N}{L}$	R_u
	r_u	—
	R_u	—
	R_u	—

Table 3-8 Elastic, Elasto-Plastic and Equivalent Elastic Stiffnesses
for One-Way Elements

Edge Conditions and Loading Diagrams	Elastic Stiffness, K_e	Elasto-Plastic Stiffness, K_{ep}	Equiv. Elastic Stiffness, K_E
	$\frac{384EI}{5L^4}$	—	$\frac{384EI}{5L^4}$
	$\frac{48EI}{L^3}$	—	$\frac{48EI}{L^3}$
	$\frac{185EI}{L^4}$	$\frac{384EI}{5L^4}$	$\frac{160EI^*}{L^4}$
	$\frac{107EI}{L^3}$	$\frac{48EI}{L^3}$	$\frac{106EI^*}{L^3}$
	$\frac{384EI}{L^4}$	$\frac{384EI}{5L^4}$	$\frac{307EI^*}{L^4}$
	$\frac{192EI}{L^3}$	$\frac{48EI^{**}}{L^3}$	$\frac{192EI^*}{L^3}$
	$\frac{8EI}{L^4}$	—	$\frac{8EI}{L^4}$
	$\frac{3EI}{L^3}$	—	$\frac{3EI}{L^3}$
	$\frac{56.4EI}{L^3}$	—	$\frac{56.4EI}{L^3}$

* Valid only if $M_N = M_p$

** Valid only if $M_N < M_p$

Table 3-9 Support Shears for One-Way Elements

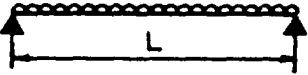
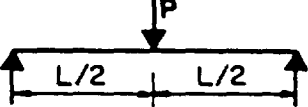
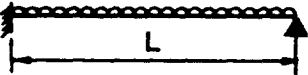
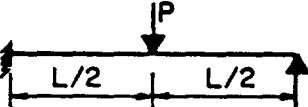
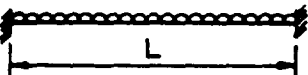
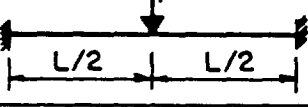
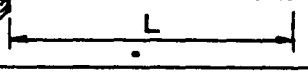
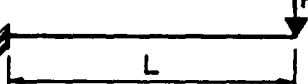
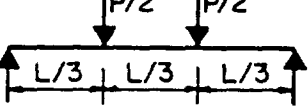
Edge Conditions and Loading Diagrams	Support Reactions, V_s
	$\frac{r_u L}{2}$
	$\frac{R_u}{2}$
	L. Reaction $\frac{5r_u L}{8}$ R. Reaction $\frac{3r_u L}{8}$
	L. Reaction $\frac{11R_u}{16}$ R. Reaction $\frac{5R_u}{16}$
	$\frac{r_u L}{2}$
	$\frac{R_u}{2}$
	$r_u L$
	R_u
	$\frac{R_u}{2}$

Table 3-10 Ultimate Support Shears for Two-Way Elements (Symmetrical Yield Lines)

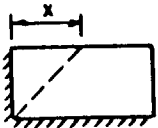
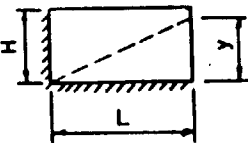
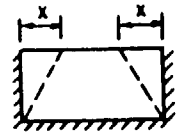
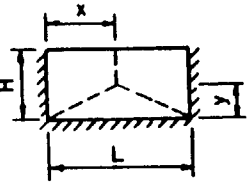
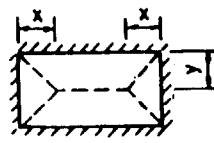
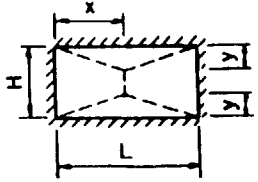
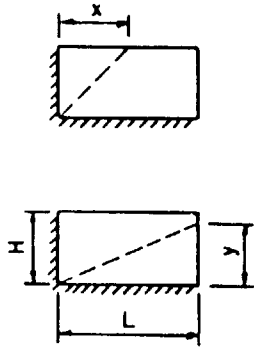
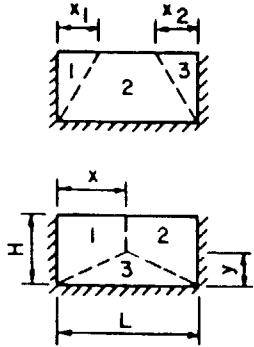
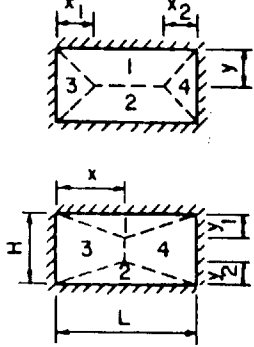
Edge Conditions	Yield Line Locations	Limits	Horizontal shear, V_{sH}	Vertical shear, V_{sV}
Two adjacent edges supported and two edges free		$x \leq L$	$\frac{3r_u x}{5}$	$\frac{3r_u H (2 - \frac{x}{L})}{(6 - \frac{x}{L})}$
		$y \leq H$	$\frac{3r_u L (2 - \frac{y}{H})}{(6 - \frac{y}{H})}$	$\frac{3r_u y}{5}$
Three edges supported and one edge free		$x \leq \frac{L}{2}$	$\frac{3r_u x}{5}$	$\frac{3r_u H (1 - \frac{x}{L})}{(3 - \frac{x}{L})}$
		$y \leq H$	$\frac{3r_u L (2 - \frac{y}{H})}{2(6 - \frac{y}{H})}$	$\frac{3r_u y}{5}$
Four edges supported		$x \leq \frac{L}{2}$	$\frac{3r_u x}{5}$	$\frac{3r_u H (1 - \frac{x}{L})}{2(3 - \frac{x}{L})}$
		$y \leq \frac{H}{2}$	$\frac{3r_u L (1 - \frac{y}{H})}{2(3 - \frac{y}{H})}$	$\frac{3r_u y}{5}$

Table 3-11 Ultimate Support Shears for Two-Way Elements
(Unsymmetrical Yield Lines)

Edge Conditions	Yield Line Locations	Limits	Horizontal shear, V_{sH}	Vertical shear, V_{sV}
Two adjacent edges supported and two edges free		$x \leq L$ $y \leq H$	Same as in Table 3-10	Same as in Table 3-10
Three edges supported and one edge free		$x_1 \leq \frac{L}{2}$ $x_2 \leq \frac{L}{2}$ $y \leq H$	$\frac{3x_1 r_u}{5}$ $\frac{3x_2 r_u}{5}$ $\frac{3r_u x (2H-y)}{6H-y}$ $\frac{3r_u x (L-x)(2H-y)}{6H-y}$	$\frac{3r_u H (2L-x_1-x_2)}{6L-x_1-x_2}$ $\frac{3r_u y}{5}$
Four edges supported		$x_1 \leq \frac{L}{2}$ $x_2 \leq \frac{L}{2}$ $y_1 \leq \frac{H}{2}$ $y_2 \leq \frac{H}{2}$	$\frac{3r_u x_1}{5}$ $\frac{3r_u x_2}{5}$ $\frac{3r_u x (2H-y_1-y_2)}{6H-y_1-y_2}$ $\frac{3r_u (L-x)(2H-y_1-y_2)}{6H-y_1-y_2}$	$\frac{3r_u y (2L-x_1-x_2)}{6L-x_1-x_2}$ $\frac{3r_u (H-y)(2L-x_1-x_2)}{6L-x_1-x_2}$ $\frac{3r_u y_1}{5}$ $\frac{3r_u y_2}{5}$

DYNAMICALLY EQUIVALENT SYSTEMS

3-16. Introduction

In dynamic analysis, there are only three quantities to be considered: (1) the work done, (2) the strain energy, and (3) the kinetic energy. To evaluate the work done, the displacement at any point on the structure under externally distributed or concentrated loads must be known. The strain energy is equal to the summation of the strain energies in all the structural elements which may be in bending, tension, compression, shear or torsion. The kinetic energy involves the energy of translation and rotation of all the masses of the structure. The actual evaluation of these quantities for a given structure under dynamic load would be complicated. However, for practical problems, this can be avoided by using appropriate assumptions.

In most cases, a structure can be replaced by an idealized (or dynamically equivalent) system which behaves timewise in nearly the same manner as the actual structure. The distributed masses of the given structure are lumped together into a number of concentrated masses. The strain energy is assumed to be stored in several weightless springs which do not have to behave elastically; similarly, the distributed load is replaced by a number of concentrated loads acting on the concentrated masses. Therefore, the equivalent system consists merely of a number of concentrated masses joined together by weightless springs and subjected to concentrated loads which vary with time. This concentrated mass-spring-load system is defined as an equivalent dynamic system.

Although all structures possess many degrees of freedom, one mode usually predominates in the response to short duration loads; thus, for all practical purposes, this one mode may be considered to define the behavior of the structure and the problem can be simplified by considering a single-degree-of-freedom system whose properties are those of the fundamental mode of the structures. A single-degree-of-freedom system is defined as one in which only one type of motion is possible or, in other words, only one coordinate is required to define its motion. Such a system is shown in Figure 3-42 which consists of a concentrated mass on a frictionless surface attached to a weightless spring and subjected to a concentrated load. A single displacement variable x is sufficient to describe its motion. The material presented herein will be limited to single-degree-of-freedom systems only.

Many structures, however, exist which can not be adequately described by the first vibration, particularly when consideration of dynamic strain is necessary. For these situations, a two-(or more)-degree-of-freedom analysis may be required. Procedures are presented in section 3-19.2 for performing these analyses.

Two fundamental methods are available for treating simple systems subjected to dynamic forces. The first of these methods is concerned with solving the differential equations of the system by either classical, numerical or graphical means. The second method of analysis and chart solutions depend on solutions which have been determined by the use of the first method and are approximate solutions to the problems in hand. There is a third method which may also be very useful in vibrational problems; this involves the energy equation.

In the following paragraphs the design factors used to determine the equivalent dynamic system that is used to analyze structural elements are defined and the methods used to obtain these factors are discussed.

3-17. Dynamic Design Factors

3-17.1. Introduction

The values of the mass and external force used in the equation of motion (Equation 3-1) are the actual values only if all the elements of the mass of the structure experience the same force and, consequently, move as a unit, in which case, the entire mass may be assumed to be concentrated at its center of gravity. In other cases, the assumption of uniform motion of the entire mass cannot be made without introducing serious error. This is true for members with uniformly distributed mass which bend or rotate under load. In such cases, the motion of the particles of mass varies along the length of the member. Beams, slabs, etc., with such distributed mass actually have an infinite number of degrees of freedom; however, such structural elements can be represented by an equivalent single-degree-of-freedom system.

In order to define an equivalent one-degree system, it is necessary to evaluate the parameters of that system; namely, the equivalent mass M_E , the equivalent spring constant K_E and the equivalent load F_E . The equivalent system is selected usually so that the deflection of the concentrated mass is the same as that for a significant point of the structure. The single-degree-of-freedom approximation of the dynamic behavior of the structural element may be achieved by assuming a deflected shape for the element which is usually taken as the shape resulting from the static application of the dynamic loads. The assumption of a deflected shape establishes an equation relating the relative deflection of all points of the element.

The accuracy of the computed deformation of the single-degree-of-freedom system is dependent on the assumed deflected shape and the loading region. For example, in the impulsive loading realm, if the assumed deformed shape for a simply supported beam is taken to be a parabola, then the exact solution will be obtained for the deflection of the beam. In the quasi-static loading realm, however, the static deformed shape gives the exact answer. For blast resistance design, however, the differences in either a static deformed shape or a first mode approximation is negligible and thus either way is permissible. Usually, though, the static deformed shape is easier to use as it covers both symmetric and asymmetric deformation.

To permit rapid design of structural elements subjected to dynamic loads, it is convenient to introduce design or transformation factors. These factors are used to convert the real system to the equivalent system. To obtain them, it is necessary to equate the relations expressing the kinetic energy, strain and work done on the actual structural element deflecting according to the assumed deflected shape, with the corresponding relations for the equivalent mass and spring system.

3-17.2. Load, Mass, and Resistance Factors

3-17.2.1. Load Factor

The load factor is the design or transformation factor by which the total load applied on the structural element is multiplied to obtain the equivalent concentrated load for the equivalent single-degree-of-freedom system. If the actual total load on the structure is F and the equivalent load is F_E , the load factor K_L is defined by the equation

$$K_L = F_E / F \quad 3-41$$

The load factor is derived by setting the external work done by the equivalent load F_E on the equivalent system equal to the external work done by the actual load F on the actual element deflecting to the assumed deflected shape.

For a structure with distributed loads;

$$WD = F_E \delta_{max} = \int_0^L p(x) \delta(x) dx \quad 3-42a$$

- where δ_{max} = maximum deflection of actual structure
- $p(x)$ = distributed load per unit length
- $\delta(x)$ = deflection at any point of actual structure
- L = length of structure

rearranging terms

$$F_E = \int_0^L p(x) \phi(x) dx \quad 3-42b$$

where $\phi(x) = \delta(x) / \delta_{max} \quad 3-43$

and is called the shape function.

NOTE. The shape function, $\phi(x)$ is different for the elastic range and the plastic range and therefore the load factor, K_L , will be different.

For example; the shape factor for a simply supported beam with a uniformly distributed load, in the elastic range is defined as

$$\phi(x) = (16/5L^4)(L^3x - 2Lx^3 + x^4) \quad 3-44a$$

while for the plastic range

$$\phi(x) = 2x/L \quad x < L/2 \quad 3-44b$$

For a structure with concentrated loads

$$WD = F_e \delta_{\max} = \sum_{r=1}^i F_r \delta_r \quad 3-45a$$

where F_r = r^{th} concentrated load
 δ_r = deflection at load r
 i = number of concentrated loads

rearranging terms

$$F_E = \sum_{r=1}^i F_r \phi_r \quad 3-45b$$

where the shape factor is defined as

$$\phi_r = \sum_{r=1}^i \delta_r / \delta_{\max} \quad 3-46$$

Again there is a K_L for the elastic range and a K_L for the plastic range. However, for a single concentrated load located at the point of maximum deflection (i.e. the center of a simply supported or fixed-fixed beam, or the end of a cantilever beam) ϕ_r is equal to one for both the elastic and plastic ranges and therefore K_L is equal to one for both ranges.

Values for K_L for one-way elements are presented in Table 3-12. Equation 3-41 through 3-46 were used to calculate these values. An example calculating K_L is shown in Appendix A.

3-17.2.2. Mass Factor

The mass factor is the design or transformation factor by which the total distributed mass of an element is multiplied to obtain the equivalent lumped mass of the equivalent single-degree-of-freedom system. If the total mass of the actual element is M and the mass of the equivalent system is M_E , the mass factor K_M is defined by the equation

$$K_M = M_E / M \quad 3-47$$

K_M can be obtained by setting the kinetic energy of the equivalent system equal to the kinetic energy of the actual structure as determined from its deflected shape.

For a structure with continuous mass

$$K_E = 1/2 M_E (\omega \delta_{\max})^2 = 1/2 \int_0^L m(x) [\omega \delta(x)]^2 dx \quad 3-48a$$

where ω = natural circular frequency

$m(x)$ = distributed mass per unit length

rearranging terms

$$M_E = \int_0^L m(x)\phi^2(x) dx \quad 3-48b$$

where the shape function $\phi(x)$ is based on the deflected shape of the element due to the applied loading and not to the distribution of the mass. Since the deflected shape of the element is different for the elastic and plastic ranges, $\phi(x)$, and therefore K_M , will also be different.

Using Equations 3-47 and 3-48, values for K_M were calculated for one-way elements with constant mass. These values are shown in Table 3-12.

For a concentrated mass system,

$$K_E = 1/2 M_E (\omega \delta_{max})^2 = 1/2 \sum_{r=1}^i M_r (\omega \delta_r)^2 \quad 3-49a$$

where

M_r = r^{th} mass

δ_r = deflection of mass r

i = number of lumped masses

rearranging terms

$$M_E = \sum_{r=1}^i M_r \phi_r^2 \quad 3-49b$$

An example of calculations for finding K_M can be found in Appendix A.

3-17.2.3. Resistance Function

Resistance factor is the design factor by which the resistance of the actual structural element must be multiplied to obtain the resistance of the equivalent single-degree-of-freedom system. To obtain the resistance factor, it is necessary to equate the strain energy of the structural element, as computed from the assumed deflection shape, and the strain energy of the equivalent single-degree-of-freedom system. If the computed total resistance of the structural element is R and the equivalent total resistance of the equivalent system is R_E , then the resistance factor is defined by the equation

$$K_R = R_E / R \quad 3-50$$

Since the resistance of an element is the internal force tending to restore the element to its unloaded static position, it can be shown that the resistance factor K_R must always equal the load factor K_L .

3-17.3. Load-Mass Factor

The load-mass factor is a factor formed by combining the two basic transformation factors, K_L and K_M . It is merely the ratio of the mass factor to the load factor, and it is convenient since the equation of motion may be written in terms of that factor alone. The equation of motion of the actual system is given as

$$F - R = Ma \tag{3-51}$$

and for the equivalent system

$$K_L F - K_L R = K_M Ma \tag{3-52a}$$

which can be re-written as

$$F - R = (K_M / K_L) Ma \tag{3-52b}$$

or $F - R = K_{LM} Ma = M_e a \tag{3-52c}$

where K_{LM} = load-mass factor

$$= K_M / K_L \tag{3-53}$$

and M_e = effective total mass of the equivalent system

when expressed in terms of the unit area of the element, Equation 3-52c can be written as

$$f - r = K_{LM} ma = m_e a \tag{3-54}$$

Values of load, mass and load-mass factors are presented in Table 3-12. Equation 3-53 was used to calculate the load mass factor.

Instead of computing the several factors above, the load-mass factors in the elastic and elasto-plastic ranges can be determined by relating the primary mode of vibration of the member to that of an equivalent single-degree-of-freedom system. In the plastic range, it can be assumed that neither the moment nor the curvature changes between the plastic hinges under increasing deflection. This behavior results in a linkage action, consideration of which can be used to evaluate the effective plastic mass as follows:

In Figure 3-43, a portion of a two-way element bounded by the support and the yield line is shown. The equation of angular motion for this section is

$$\Sigma M = I_m \Theta'' \tag{3-55}$$

where ΣM = summation of moments

I_m = mass moment of inertia about the axis of rotation

Θ'' = angular acceleration

Substituting in equation

$$Fc - (\Sigma M_N + \Sigma M_p) = (I_m / L_1)a \quad 3-56a$$

where a is the acceleration. Dividing through by c

$$F - (\Sigma M_N + \Sigma M_p)/c = (I_m / cL_1)a \quad 3-56b$$

Since the second term is the resistance R

$$F - R = (I_m / cL_1)a = M_e a \quad 3-56c$$

and the load-mass factor K_{LM} for the sector shown is

$$K_{LM} = I_m / cL_1 M \quad 3-57$$

where c is the distance from the resultant applied load to the axis of rotation, L_1 is the total length of the sector normal to the axis of rotation and M is the total mass of the sector.

When the element is composed of several sectors, each sector must be considered separately and the contributions then summed to determine the load-mass factor for the entire element.

$$K_{LM} = \Sigma(I_m / cL_1) / M \quad 3-58$$

For elements of constant depth and, therefore, of constant unit mass, the above equation can be written in terms of the area moment of inertia I and the areas A of the individual sectors.

$$K_{LM} = \Sigma(I/cL_1) / A \quad 3-59$$

Table 3-13 gives the load-mass factors for the elastic and elasto-plastic response ranges for various two-way elements. The values given in the table apply for two-way elements of uniform thickness and supported as indicated. Also if there are openings in the element, they must be compact in shape and small in area compared to the total area of the element.

Figure 3-44 gives the load-mass factors for the plastic response of various two-way elements. The load-mass factors are a junction of support condition and yield line location. These two-way elements must conform to the following limitations:

- (1) Element must be of constant thickness.
- (2) Opposite support must provide the same restraint so that a symmetrical yield line pattern occurs.
- (3) Any openings must be compact in shape and small in area compared to the total area of the element.

3-17.4. Natural Period of Vibration

To determine the maximum response of a system either by numerical methods or design charts (both methods are described in Section 3-19), the effective natural period of vibration is required. This effective natural period of vibration, when related to the duration of a blast loading of given intensity and a given structural resistance, determines the maximum transient deflection X_m of the structural element.

The effective natural period of vibration is

$$T_n = 2\pi(m_e/K_E)^{1/2} = 2\pi(K_{LM}m/K_E)^{1/2} \quad 3-60$$

where m_e - the effective unit mass

K_E - the equivalent unit stiffness of system

The values used for the effective mass and stiffness for a particular element depends on the allowable maximum deflection. When designing for completely elastic behavior, the elastic stiffness is used. In all other cases the equivalent elasto-plastic stiffness, K_E , is used. The elastic value of the effective mass is used for the elastic range, while in the elasto-plastic range the effective mass is the average of the elastic and elasto-plastic values. For small plastic deflections ($\theta \leq 2^\circ$), the value of the effective mass is equal to the average of the plastic value and the equivalent elastic value. The plastic effective mass is used for large plastic deflections.

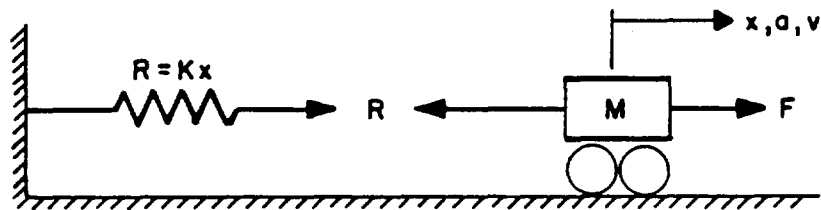
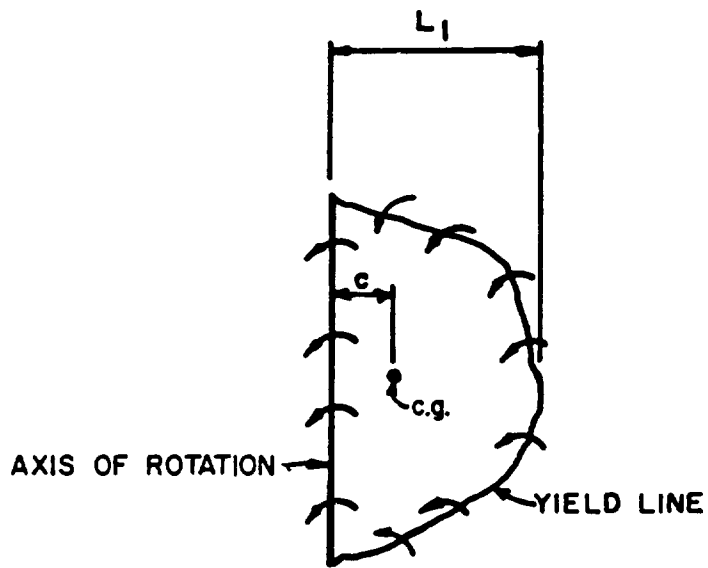
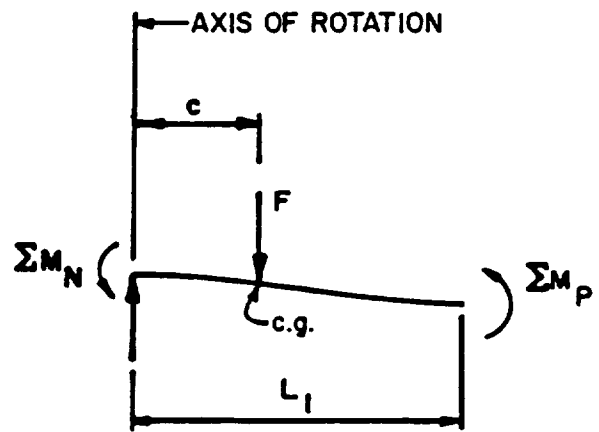


Figure 3-42 Typical single-degree-of-freedom system



a) PLAN



b) SECTION

Figure 3-43 Determination of load-mass factor in the plastic range

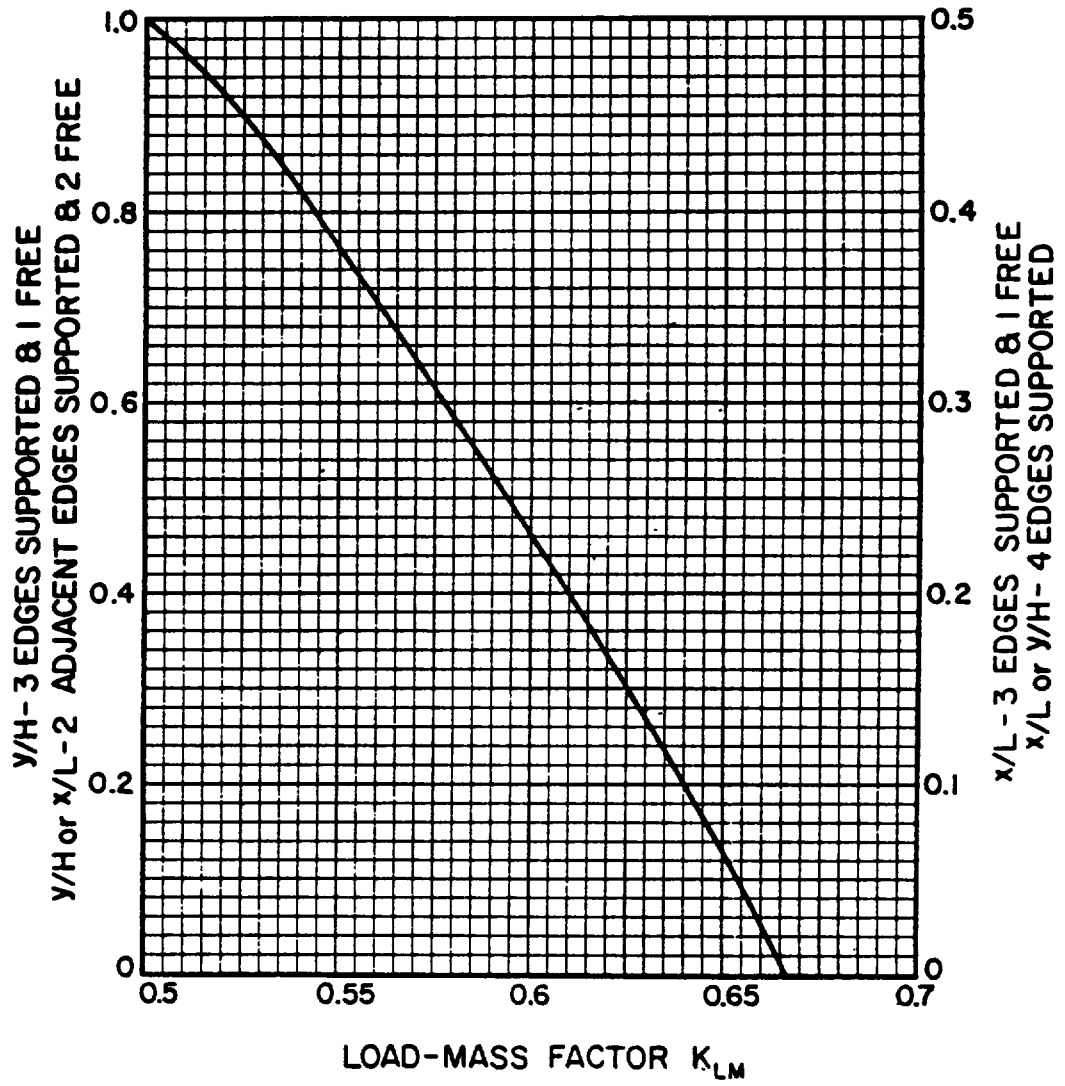


Figure 3-44 Load-mass factors in plastic range for two-way elements

Table 3-12 Transformation Factors for One-Way Elements

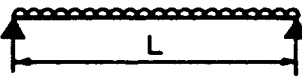
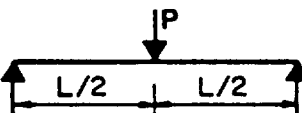
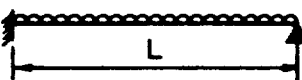
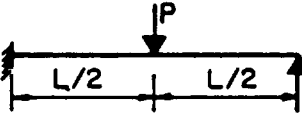
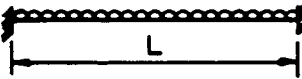
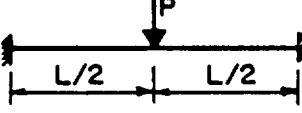
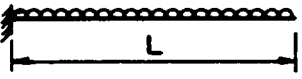
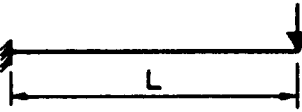
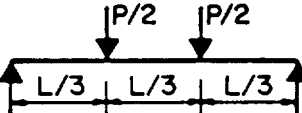
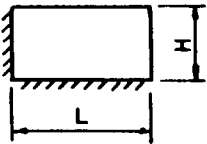
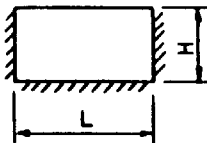
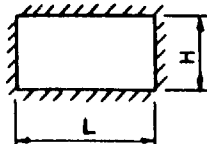
Edge Conditions and Loading Diagrams	Range of Behavior	Load Factor K_L	Mass Factor K_M	Load-Mass Factor K_{LM}
	Elastic Plastic	0.64 0.50	0.50 0.33	0.78 0.66
	Elastic Plastic	1.0 1.0	0.49 0.33	0.49 0.33
	Elastic Elasto-Plastic Plastic	0.58 0.64 0.50	0.45 0.50 0.33	0.78 0.78 0.66
	Elastic Elasto-Plastic Plastic	1.0 1.0 1.0	0.43 0.49 0.33	0.43 0.49 0.33
	Elastic Elasto-Plastic Plastic	0.53 0.64 0.50	0.41 0.50 0.33	0.77 0.78 0.66
	Elastic Plastic	1.0 1.0	0.37 0.33	0.37 0.33
	Elastic Plastic	0.40 0.50	0.26 0.33	0.65 0.66
	Elastic Plastic	1.0 1.0	0.24 0.33	0.24 0.33
	Elastic Plastic	0.87 1.0	0.52 0.56	0.60 0.56

Table 3-13 Load-Mass Factors in the Elastic and Elasto-Plastic Ranges for Two-Way Elements

Support Conditions		Value of L/H	Elastic and Elasto-Plastic Ranges (Support Conditions)				
			All Supports Fixed	One Support Simple Other Supports Fixed	Two Supports Simple Other Supports Fixed	Three Supports Simple Other Supports Fixed	All Supports Simple
Two adjacent edges supported and two edges free		ALL	0.65	0.66	—	—	0.66
Three edges supported and one edge free		L/H < 0.5	0.77	0.77	0.79	—	0.79
		$0.5 \leq L/H \leq 2$	$0.65 - 0.16 \left(\frac{L}{2H} - 1 \right)$	$0.66 - 0.144 \left(\frac{L}{2H} - 1 \right)$	$0.65 - 0.186 \left(\frac{L}{2H} - 1 \right)$	—	$0.66 - 0.175 \left(\frac{L}{H} - 1 \right)$
		L/H ≥ 2	0.65	0.66	0.65	—	0.66
Four edges supported		L/H = 1	0.61	0.61	0.62	0.63	0.63
		$1 \leq L/H \leq 2$	$0.61 + 0.16 \left(\frac{L}{H} - 1 \right)$	$0.61 + 0.16 \left(\frac{L}{H} - 1 \right)$	$0.62 + 0.16 \left(\frac{L}{H} - 1 \right)$	$0.63 + 0.16 \left(\frac{L}{H} - 1 \right)$	$0.63 + 0.16 \left(\frac{L}{H} - 1 \right)$
		L/H ≥ 2	0.77	0.77	0.78	0.79	0.79

3-84

DYNAMIC ANALYSIS

3-18. Introduction

Structural elements must develop an internal resistance sufficient to maintain all motion within the limits of deflection prescribed for the particular design. The load capacity of the member depends on the peak strength developed by the specific member (see Chapters 4 and 5) and on the ability of the member to sustain its resistance for a specific though relatively short period of time. This section describes the methods used for the analysis of structural elements subjected to dynamic loads, and these elements are divided into three groups, namely: (1) elements which respond to the pressure only (low pressure range), (2) elements which respond to pressure-time relationship (intermediate-pressure design range) and (3) elements which respond to the impulse which corresponds to the high pressure design range.

The method of analysis is different for the groups of elements. Those elements that respond to pressure only (this is still a pressure-time relationship) and those that respond to pressure-time relationship may be analyzed using either numerical methods or design charts, while elements that respond to the impulse are analyzed using either design charts for large deflection or an impulse method for designs with limited deflections.

The method of analysis employing numerical techniques provides a solution that is obtained by a step-by-step integration, and is generally applicable for any type of load and resistance function. This method of analysis is presented in this section. Also presented is the result of a systematic analysis of single-degree dynamic systems for several idealized loadings plotted in non-dimensional design charts.

3-19. Elements Which Respond to Pressure Only and Pressure-Time Relationship.

3-19.1. General

To analyze these elements, the true magnitudes for the pressure-time relationship of the applied blast loads must be known. The determination of the dynamic response of these systems is accomplished using numerical techniques or design charts which relate the dynamic properties of the element (natural period of vibration, resistance, and deflection) to those of the blast overpressures.

3-19.2. Analysis by Numerical Methods

The numerical method of analysis involves a step-by-step integration procedure, starting at zero time, when displacement and the velocity of the system are presumably known. The time scale is divided into several discrete intervals, and one progresses by successively extrapolating the displacement from one time station to the next. As the time interval in the sequence of time is reduced, i.e., as the number of discrete intervals is increased, the accuracy of the numerical method is improved.

3-19.2.1. Single-Degree-Of-Freedom Systems

As stated previously, a single degree of freedom system is one in which only one coordinate is essential to define its motion. The equation of motion for the single-degree-of-freedom system shown in Figure 3-42 can be expressed as:

$$F - kx - cv = Ma \tag{3-61}$$

when c = damping constant

There are several methods that can be used to numerically integrate Equation 3-61, but the two procedures applied to this problem will be the average acceleration, and the acceleration-impulse extrapolation methods.

3-19.2.1.1. Average Acceleration Method

In the average acceleration method, the velocity and displacement at any time t are expressed as

$$v_t = v_{t-1} + 1/2 (a_t + a_{t-1})\Delta t \tag{3-62}$$

$$x = x_{t-1} + 1/2 (v_t + v_{t-1}) \Delta t \tag{3-63}$$

Substituting Equation 3-62 into Equation 3-63,

$$x = x_{t-1} + v_{t-1} \Delta t + 1/4 (a_t + a_{t-1}) \Delta t^2 \tag{3-64}$$

Substituting Equations 3-62 and 3-63 into Equation 3-61, we have

$$F - k [x_{t-1} + 1/2(v_t + v_{t-1})\Delta t] - c[v_{t-1} + 1/2 (a_t + a_{t-1})\Delta t] = Ma \tag{3-65}$$

Equation 3-65 can be simplified to

$$a = \frac{1}{m + (1/2)c \Delta t + (1/4)k \Delta t^2} [F - k (x_{t-1} + v_{t-1} \Delta t + 1/4a_{t-1} \Delta t^2) - c (v_{t-1} + 1/2 a_{t-1} \Delta t)] \tag{3-66}$$

The integrating procedure can be summarized as follows:

- Step 1. At $t = 0$: Compute: a_0 using Equation 3-61 and specified values for $x_0(t = 0)$, $v_0(t = 0)$, and $F(t = 0)$.
- Step 2. Increment time: $t = t + \Delta t$
- Step 3. At $t = t + \Delta t$: Compute $a(t = t + \Delta t)$ using Equation 3-66, $v(t = t + \Delta t)$ using Equation 3-62 and $x(t = t + \Delta t)$ using Equation 3-63.
- Step 4. Repeat steps 2 and 3 until some specified time or until the maximum displacement is reached.

It should be noted that if $x(t = 0)$ and $v(t = 0)$ are zero, then the system will not move as long as $F(t = 0)$ is zero; however, if $F(t = 0)$ is not zero, Equation 3-66 will give an acceleration and motion will start. Thus the system of equation is self-starting and requires no special starting provisions.

The procedure outlined above for an elastic single-degree-of-freedom system can be easily extended to accommodate elastic-plastic behavior. To do so, Equation 3-61 is re-written to include the restoring force R which replaces the spring restoring force kx , Equation 3-61 becomes

$$F - R - cv = ma \tag{3-67}$$

Substituting Equations 3-62 and 3-63 into Equation 3-67, the following equation for acceleration is obtained:

$$a_t = \frac{1}{m + (c\Delta t)/2} \left[F - R - c \left[v_{t-1} + \Delta t a_{t-1} / 2 \right] \right] \tag{3-68}$$

Unlike Equation 3-66, Equation 3-68 has a non-linear term R , and it depends on the displacement x at time t . Therefore, instead of using the direct integration approach as in the previous case, a predictor-corrector method is utilized. Briefly, the displacement x at time t is estimated (predicted) and then corrected and convergence of this procedure can be obtained in a single iteration if the value of Δt is small enough. The step-by-step procedure is outlined as follows:

- Step 1. At $t = 0$: Compute a_t ($t = t_0$) from Equation 3-67 and the initial conditions.
- Step 2. Increment time: $t = t + \Delta t$
- Step 3. At $t = t + \Delta t$: Set $a_t = a_{t-1}$ ($t - 1 = 0$, initially)
- Step 4. Compute v_t and x_t from Equations 3-62 and 3-63
- Step 5. Compute R
- Step 6. Compute a_t from Equation 3-68
- Step 7. If you are in the predicting pass, return to Step 4, if in the correcting pass, set $x_{t-1} = x_t$, $v_{t-1} = v_t$, $a_t = a_{t-1}$ and go to Step 2.

3-19.2.1.2. Acceleration Impulse Extrapolation Method

Suppose the acceleration of the system is defined by Figure 3-45a. The acceleration-impulse extrapolation method assumes that the actual acceleration curve can be replaced by a series of equally spaced impulses occurring at $t_0, t_1, t_2, \dots, t_n$, as shown in Figure 3-45b.

The magnitude of the acceleration impulse at t_n is given by

$$I(t_n) = a_n(\Delta t)$$

3-69

where $t - t_1 - t_0 = t_2 - t_1 = \dots = t_n - t_{n-1}$. This is shown in Figure 3-45b. Since an impulse is applied at t_n , there is a discontinuity in the value of velocity at t_n . In the time interval from t to t_{n-1} , the velocity is constant and the displacement varies linearly with time. The velocity and displacement thus obtained are shown in Figures 3-45c and 3-45d.

Suppose t_n^- and t_n^+ indicate the time immediately before and after the application of the impulse at t_n , and let v_n^- and v_n^+ indicate respectively the velocity at t_n^- and t_n^+ ; these two velocities are related by the following equation:

$$v_n^+ = v_n^- + a_n(\Delta t)$$

3-70

The relationship between x_{n-1} and x_n , and between x_n and x_{n+1} are given by:

$$x_n - x_{n-1} = v_n^-(\Delta t)$$

3-71a

$$x_{n+1} - x_n = v_n^+(\Delta t)$$

3-71b

Combining Equations 3-70 and 3-71, the three successive displacements are related by:

$$x_{n+1} = 2x_n - x_{n-1} + a_n(\Delta t)^2$$

3-72

This is the basic recurrence formula for the acceleration impulse extrapolation method. Once the values of x at t_{n-1} and t_n are known, the value at t_{n+1} can be directly computed without resorting to a trial and error procedure.

It is necessary, however, to use a special procedure in the first time interval because, at $t = 0$, no value of x_{n-1} is available. Two different procedures may be used. The first assumes the acceleration varies linearly up to the first time station, in which case, the displacement of the system at that time can be expressed as:

$$x_1 = (1/6)(2a_0 + a_1)(\Delta t)^2$$

3-73

The second procedure assumes that the acceleration is constant during the first time interval and is equal to the initial value. This assumption results in the following expression for x_1 :

$$x_1 = (1/2)a_0(\Delta t)^2$$

3-74

It should be noted that Equation 3-73 has to be solved by trial and error since a_1 depends on x_1 . This trial-and-error procedure can be avoided by taking the value of a_1 to be $f(t)/m$ instead of the exact value of $[f(t_1) - R(t_1)]/m$. In Figure 3-46a if $a_0' = 0$, a_0 is equal to $a_0'/6$ and in Figure 3-46b if a_0 and a_1 are approximately equal to each other, the value $a_0'/2$ may be used for a_0 . The recurrence formula is directly applicable for the evaluation of x_2, x_3, \dots, x_{n+1} whenever the acceleration is a continuous function. When there is a discontinuity in the acceleration, this equation can still be used but not before some modifications are made to reflect this discontinuity. In Figure 3-46a there is a discontinuity at t_4 which occurs at the end of the time interval Δt . Under this condition, the value of a_n used in the numerical

procedure is the average value at discontinuity, namely $1/2 (a_4' + a_4'')$ for a_4 . In Figure 3-46b the discontinuity occurs within time interval, t . The correct value for a_3 in this procedure is:

$$a_3 = (1/2)[a_3 + a_3'' + (a_3' - a_3'') (\Delta t'/\Delta t)^2] \quad 3-75$$

When there are more than two discontinuities, this procedure becomes cumbersome and it is more convenient to replace the given acceleration by a smooth curve. Equation 3-73 must be used if there is zero force (and hence zero acceleration) at zero time, for in no other way can x_1 be determined. If acceleration at $t = 0$ is not zero, Equation 3-74 may be used without appreciable error, provided the force does not change greatly in the first interval.

The tedious method of numerical analysis is made somewhat easier if the computation procedure is set up as shown in Table 3-14. In the first time interval, the value used for the acceleration, a_0 , depends on the forcing function. If the value of the forcing function is zero at time zero, then a_0 is taken as one-sixth of a_1 , where a_1 is the ratio of the value of the forcing function at t , to the mass of the system [$a_0 = f(t_1)/6m$]. When the value of the forcing function is not zero at time zero, and if the values of the forcing function at times $t=0$ and $t=t_1$ are approximately equal, then a_0 may be taken as $(P_0 - R_0)/2$. The recurrence formula (Equation 3-72) is used in the other intervals.

It may be necessary during the computational procedure, to increase the value of t so as to reduce the number of time intervals. In Figure 3-47, for example, the forcing function varies linearly after time j . For the next time station $(j + 1)$ st, the value of Δt , can be increased ($\Delta t_2 = 2\Delta t_1$ for example) without introducing any errors in the computations. In such cases, caution has to be exercised when using the recurrence formula. In Table 3-14, the value of Δt changes after the j th step, to $\Delta t_2 = 2\Delta t_1$. In the $(j + 1)$ st step, x_{n-1} should be the value of x for the $(j-1)$ nd step and x_n will be the value of x_{n+1} for the $(j-1)$ st step.

3-19.2.2. A Two-Degree-of-Freedom-System

A two-degree-of-freedom system is shown in Figure 3-48 where the coordinates defining the configuration of the system are X_1 and X_2 . The equation of motion for each of the two masses can be expressed as follows:

$$F_1 + R_2 - R_1 = M_1 a_1 \quad 3-76a$$

$$F_2 - R_2 = M_2 a_2 \quad 3-76b$$

Equation 3-76 can be rewritten as:

$$a_1 = F_1/M_1 + R_2/M_1 - R_1/M_1 \quad 3-77a$$

$$a_2 = F_2/M_2 - R_2/M_2 \quad 3-77b$$

The integration procedures described for a single-degree-of-freedom system can also be applied to two-degrees-of-freedom systems. In the average acceleration procedure, if the equations are placed in the same form as Equation 3-61, i.e., if the acceleration at time t are written in terms of displacements and velocities at time $t - \Delta t$, then two equations are obtained which must be

solved simultaneously for a_1 and a_2 . In the other numerical integration procedure, the recurrence formula (Equation 3-72) applies to each of the two displacements independently.

3-19.2.3. Damping

The effects of damping are hardly ever considered in blast design because of the following reasons:

- (1) Damping has very little effect on the first peak of response which is usually the only cycle of response that is of interest.
- (2) The energy dissipated through plastic deformation is much greater than that dissipated by normal structural damping.
- (3) Ignoring damping is a conservative approach.

If damping has to be considered in an analysis, however, it should be expressed as some percentage of critical damping. For free vibration, this is the amount of damping that would remove all vibration from the system and allow it to return to its neutral position. Critical damping is expressed as

$$C_{cr} = 2 \sqrt{kM} \qquad 3-78$$

where k = stiffness of the system

M = mass of system

The damping coefficient, c , in Equations 3-61 and 3-67 is expressed as a percentage of critical damping, C_{cr} . For steel structures, c should be taken as $0.05C_{cr}$ and $0.01 C_{cr}$ for reinforced concrete structures.

3-19.3. Design Charts for Idealized Loadings

3-19.3.1. General

The response of single-degree-of-freedom systems subjected to idealized blast loadings is presented in the form of non-dimensional curves. In order to utilize these response charts, both the blast loads (pressure - time history) and the resistance-deflection curve of the structural system are idealized to linear or bilinear functions. Methods for computing these idealized blast loads are given in Chapter 2 while the methods for computing the resistance-deflection functions as well as converting the actual system to an elastic or elasto-plastic single-degree-of-freedom system have been presented in previous sections of this chapter.

The response of a structural system subjected to a dynamic load is defined in terms of its maximum deflection X_m and the time t_m to reach this maximum deflection. The dynamic load is defined by its peak value P and duration T while the single-degree-of-freedom system is defined in terms of its ultimate resistance r_u , elastic deflection X_E and natural period T_N . Response charts relate the dynamic properties of the blast load (P and T) to those of the element (r_u , X_E , T_N), that is, X_m/X_E and t_m/T are plotted as a function of r_u/P and T/T_N .

Response charts have been prepared for simplified loads as well as for the more complex bilinear loadings. The simplified loadings include triangular,

rectangular, step load with finite rise time, triangular with rise time and sinusoidal pulse. The idealized triangular loading is utilized in the analyses of acceptor structures. These structures are subjected to the effects of unconfined explosions, such as free-air or surface bursts or partially confined explosions in donor structures which are fully vented. On the other hand, idealized instantaneously applied or gradually applied flat top loads are usually encountered in the design of roof elements of acceptor structures. These structures are subjected to very long duration loads produced by very large explosive quantities. The triangular loading with a rise time is similar to the previously mentioned triangular load except that it is an equivalent loading produced by the blast traversing an element. The sinusoidal loadings is usually associated with the vibrational type of load rather than blast induced input. The bilinear loading is utilized in the analysis of containment structures which allow partial venting of an explosion and in the analysis of acceptor structures where reflected pressures clear rapidly around the structure.

The effects of damping have not been included in the preparation of the response charts. In the design of the blast resistant structures, the first peak of response is usually the only cycle of response that is of interest since the maximum resistance and deflection is attained in that cycle. Damping has very little effect on this first peak and consequently, neglecting damping has negligible effects on maximum response calculations.

3-19.3.2. Maximum Response Of Linear Elastic System To Simplified Loads

To obtain the response of a linear elastic system, it is convenient to consider the concept of the dynamic load factor. This factor is defined as the ratio of the maximum dynamic deflection to the deflection which would have resulted from the static application of the peak load P , which is used in specifying the load-time variation. Thus the dynamic load factor (DLF) is given by:

$$DLF = X_m / X_s \quad 3-79a$$

where X_s - static deflection or, in other words, the displacement produced in the system when the peak load is applied statically.

X_m - maximum dynamic deflection

Since deflections, spring forces, and stresses in an elastic system are all proportional, the dynamic load factor may be applied to any of these to determine the ratio of dynamic to static effects. Therefore, the dynamic load factor may be considered as the ratio of the maximum resistance attained to the peak load or:

$$DLF = r/p \quad 3-79b$$

where r - maximum dynamic resistance
 p - peak load used in specifying the load-time variation.

For a linear elastic system subjected to a simplified dynamic load, the maximum response is defined by the dynamic load factor, DLF and maximum response time, t_m . The dynamic load factor and time ratio t_m/T are plotted

versus the time ratio T/T_N for a triangular load, rectangular load, step load with finite rise time (T_r), triangular load with rise time, and sinusoidal pulse in Figures 3-49 through 3-53.

In many structural problems only the maximum value of the DLF is of interest. For the most prevalent load case, namely, the triangular load as well as the rectangular and step load with rise time, the maximum value of the DLF is 2. This immediately indicates that all maximum displacements, forces, and stresses due to the dynamic load are twice the value that would be obtained from a static analysis for the maximum load P .

The above response charts apply for elastic systems. However, the charts can be applied to the entire elasto-plastic range if the actual resistance-deflection curve (two step system, three step system, etc.) is replaced by the equivalent elastic system where the equivalent elastic stiffness K_E and the equivalent elastic deflection X_E are obtained according to previously explained procedures.

In a typical design example, the pressure-time loading is calculated and idealized to one of the simplified loads defined by P and T or T_r . A structural member is assumed and its corresponding dynamic properties are calculated. For a completely elastic response, the values of r_e and T_N are calculated while for a response in the elasto-plastic range, r_u , X_E and T_N are obtained. It should be noted that for a response in the elasto-plastic range, the value of T_N is calculated using the effective mass which is an average of the elastic and elasto-plastic values. Knowing the ratio of T/T_N the dynamic load factor (DLF) and the time ratio can be read from the appropriate figures. The maximum resistance r attained by the structural member is calculated from the DLF and the response time is obtained from the time ratio. If the resistance r is greater than r_e for a completely elastic response in the elasto-plastic range, then the analysis is not valid and the procedure is repeated. The maximum deflection is obtained from the resistance r and the stiffness K_e or K_E .

3-19.3.3. Maximum Plastic Response Of An Elasto-Plastic System To Simplified Loads

An elasto-plastic system may have an elastic or plastic response depending upon the magnitude of the blast load. If the response is elastic, that is, the member attains a resistance r which is less than its ultimate resistance r_u , then the charts of the preceding section are used. The response charts presented in this section are only for the plastic response of members where the ultimate resistance r_u is attained.

The maximum plastic response of an elasto-plastic system subjected to a blast load is defined by the maximum deflection, X_m it attains and the time, t_m it takes to reach this deflection. The blast load is defined by its peak value P and duration T while the single-degree-of-freedom system is defined by its ultimate resistance r_u , elastic deflection X_E and natural period T_N . A non-dimensional response chart is constructed by plotting the ductility ratio X_m/X_E and the time ratio t_m/T as a function of r_u/P and T/T_N . Response charts are given for a triangular load, rectangular load, step load with finite rise time T_r and triangular load with rise time in Figures 3-54 through 3-61. It should be noted that for the step load with finite rise time, the load is

defined by the rise time T_r and, consequently, the response curves are plotted using T_r rather than T .

In a typical example, the pressure-time loading is calculated and idealized to one of the simplified loads defined by either P and T or P and T_r . A structural member is assumed and its corresponding dynamic properties (r_u , X_E , T_N) are calculated. Knowing the ratios of r_u/P and T/T_N (or T_r/T_N), the ductility ratio X_m/X_E and the time ratio t_m/T can be read from the appropriate figures. The maximum deflection X_m and response time t_m can readily be calculated. If the ductility ratio X_m/X_E or the maximum deflection X_m and corresponding response time t_m are unsatisfactory, the procedure is repeated.

It should be noted that the value of the natural period of vibration T_N used in conjunction with the response charts varies according to the magnitude of the ductility ratio X_m/X_E . For small plastic deformations (X_m/X_E less than 5), the calculations of T_N is based on an average of the equivalent elastic and plastic masses. Whereas, for larger plastic deformations (X_m/X_E greater than 5), the equivalent plastic mass is used to obtain T_N .

3-19.3.4. Maximum Plastic Response Of An Elasto-Plastic System to Idealized Bilinear Loads

Response charts have been prepared for bilinear loads in much the same manner as for simplified loads. However, four parameters are required to define the bilinear loading rather than two parameters which are required for the simplified loads. These additional parameters greatly increase the number of charts required for the rapid prediction of the dynamic response of an elasto-plastic system. However, the computational procedures remain comparatively simple.

A bilinear load is illustrated in Figure 3-62c. Four parameters are required to define this load shape, namely:

- P - peak pressure of shock load (primary pulse)
- C_1P = peak pressure of gas load (secondary pulse)
- T - duration of shock load
- C_2T - duration of gas load

It can be seen from Figure 3-62c that the value of C_1 will always be less than 1 while the value of C_2 will always be greater than 1.

Response charts for the bilinear load are prepared in the same way as the simplified loads except that each chart is prepared for a given value of C_1 and C_2 . The ductility ratio X_m/X_E versus T/T_N is plotted on each chart for various values of P/r_u , t_m/T_N and t_E/T (where t_E is the time to reach the maximum elastic deflection x_E). Therefore, each chart contains three families of curves. In addition, each chart contains one, two or three boundaries which are formed by symbols. These boundaries delineate regions of each chart where certain approximations are preferable to chart interpolation. These approximations involve modification of the bilinear load for the various regions. The loads considered for each of the regions are given in Figure 3-62 while the boundary for the various regions are defined in Figure 3-63.

Numerous response charts are required for bilinear loads. Table 3-15 lists the figure numbers of the response charts prepared for the selected values of C_1 and C_2 . These response charts are presented in Figures 3-64 through 3-266.

To use the response charts, the first step is to enter Table 3-15 with the required values of C_1 and C_2 . Locate the points in the table with coordinates C_1 and C_2 . The number in the box containing the point is the appropriate figure number to use to solve the problem. If the point is not located in a box having a number, the two or, more frequently, four numbers bracketing the point are the appropriate figure numbers to use. Interpolation for the required values of C_1 and C_2 must be performed. A graphical and mathematical interpolation procedure is presented in subsequent sections.

In a typical design, a structural member is assumed and the idealized resistance function defined by r_u , X_E and K_E can be determined along with the natural period. As previously explained for simplified loads; the equivalent mass used to calculate T_N varies according to the amount of plastic deformation. Knowing the ratio of P/r_u and T/T_N , note if the intersection point corresponding to these parameters, is located in region A, B, C or D on the response chart(s) for the required values of C_1 and C_2 . The boundaries for these regions are represented by a line of asterisks, solid circles, and solid squares, as illustrated in Figure 3-63.

The final step in obtaining the solution depends on which region of the response chart(s) is applicable. These regions were established to reduce the amount of calculations required for a solution by eliminating, where possible, interpolation between charts. Except for one of the four regions, the actual bilinear blast load is replaced by a simplified load. Solution of the response for these simplified loads will predict a solution which is within 10 percent of the exact solution. Of course, the exact solution of the response for the structural member in these three regions can be obtained by using the required response charts and interpolating, where required, between charts.

3-19.3.4.1. Region A

This region is defined as the area to the left of the solid circles on the response charts. If a chart does not have a line of solid circles, then region A does not exist. Figures 3-221, 3-222 and 3-223 illustrate this case.

In region A the maximum dynamic response depends primarily upon the total impulse in the blast loading (area under the pressure-time curve). The actual pressure-time distribution does not significantly affect the maximum dynamic response because in these regions the durations T and C_2T are small in comparison to the response time, t_m of the structural member. In this region the response charts are not used and a solution is obtained by considering the modified loading shown in Figure 3-62a. This load shape yields the following equations:

$$\frac{X_m}{X_E} = \frac{1}{2} + \frac{\pi^2}{2} \left[\left[\frac{P}{r_u} \right] \left[\frac{T}{T_n} \right] F \right]^2 \quad 3-80$$

and

$$\frac{t_m}{T_n} = \left[\frac{1}{2} \right] F \left[\frac{P}{r_u} \right] \left[\frac{T}{T_n} \right] \quad 3-81$$

where

$$F = C_2 + \frac{C_2 [1-C_1][1-C_2]}{C_2 - C_1} \quad 3-82$$

3-19.3.4.2. Region B

This region is defined as the area in the chart to the left of the asterisks. If a chart has no line of asterisks, then region B does not exist. Figure 3-65 illustrates the case where region B does not exist.

In region B the maximum dynamic response depends primarily upon the gas load which is described by C_1P and C_2T . The shock load described by P and T is neglected. This load condition is shown in Figure 3-62b. Therefore the solution is obtained from consideration of a single triangular load. The dynamic response is obtained from Figure 3-64 which like Figures 3-54 and 3-55 is for a triangular load and will yield the same results. When using Figure 3-64 it must be realized that the P and T used in the chart are actually C_1P and C_2T , respectively. In a typical design, enter Figure 3-64 with the normalized parameters, C_1P/r_u and C_2T/T_n , and read the solution, X_m/X_E , t_m/T_n , and t_E/C_2T .

Figure 3-63 depicts region B as the area between the line of solid circles and the line of asterisks. It should be understood that the solution technique associated with region B (i.e., neglect the shock load and use Figure 3-64) applies everywhere to the left of the line of asterisks, including region A. In other words, two solution techniques are available in region A.

3-19.3.4.3. Region D

This region is defined as the area in the charts to the right of the line of solid squares. If a chart has no line of solid squares, then region D does not exist. Figure 3-69 illustrates the case where region D does not exist.

In region D the maximum dynamic response depends primarily upon the shock load which is described by P and T . The gas load described by C_1P and C_2T is neglected. This load condition is shown in Figure 3-62d. Therefore, the solution is obtained from consideration of a single triangular load. Similar to region B, the dynamic response is obtained from Figure 3-64 which is for a triangular load. Unlike region B, the parameters, P and T which describe the load are used in the figure. Therefore, in a typical design, enter Figure 3-64 with the normalized parameters P/r_u and T/T_n , and read the solution, X_m/X_E , t_m/T_n and t_E/T .

3-19.3.4.4. Region C

This is the region in the charts which do not meet the definitions of regions A, B and D. In most charts, region C is the area to the left of the line of

solid squares and to the right of the line of asterisks, as illustrated in Figure 3-63. Region C does not exist in some charts, such as Figure 3-97 which have overlapping regions A and D.

In region C, both the shock and gas load must be considered. Replacement of the actual bilinear load with a simplified load, as done for the other regions, will yield an incorrect solution. Therefore, in this region the response charts must be used. If the required values of C_1 and/or C_2 do not correspond to the response chart values, interpolation between response charts will be required to obtain a solution. In a few cases one or two response charts are needed, however, in general four response charts are required for a solution.

3-19.3.4.5. Response Chart Interpolation

Interpolation between four response charts will usually be required for region C. For regions A, B, or D, if conditions warrant an exact solution rather than the approximate solution usually used in these regions, interpolation between charts may be required. Either a graphical or mathematical interpolation procedure may be employed. The method selected depends upon personal choice. A brief description of each procedure is presented below and an example of each is given in Appendix A.

Graphical interpolation requires a sheet of log-log graph paper. A convenient size is 2 x 1 cycle with the single-cycle axis representing C_1 and C_2 , and the two-cycle axis representing the desired parameter (X_m/X_E , t_m/T_N or t_E/T), called Y for ease of presentation. The appropriate figures to be used for a solution are obtained from Table 3-15 for the required values of C_1 and C_2 . The procedure will illustrate the interpolation between four figures since this is by far the usual case. For the values of P/r_u and T/T_N corresponding to the structural system selected, determine the desired parameter Y for each of the four figures. Organize a table in the same format as Table 3-16 and enter each figure number and corresponding value of C_1 , C_2 and Y.

In the table, C_{11} and C_{21} are the values of C_1 and C_2 , respectively, from Figure 1. Likewise, C_{12} and C_{22} are the values of C_1 and C_2 , respectively from Figure 2, etc. The symbol Y_1 , is the desired parameter, such as X_m/X_E , which is read from Figure 1. The symbol Y_2 is the value read from Figure 2, etc. The interpolation is first performed for the required value of C_1 and then for the required value of C_2 . That is, with C_{21} constant, graphically interpolate on the log-log paper between points (Y_1, C_{11}) and (Y_2, C_{12}) to find Y_a corresponding to C_1 and C_{21} , as shown on Figure 3-267. Similarly, with C_{23} constant, graphically interpolate between (Y_3, C_{13}) and (Y_4, C_{14}) to find Y_b corresponding to C_1 and C_{23} , also shown in Figure 3-267. The values of Y_a and Y_b are recorded in Table 3-16. Finally, with C_1 constant, graphically interpolate on the log-log paper between (Y_a, C_{21}) and (Y_b, C_{23}) to find Y corresponding to the required C_1 and C_2 , as shown on Figure 3-267. The values of Y is the solution. Since there are three parameters to define the response of a structural, namely, X_m/X_E , t_m/T_N and t_E/T , the interpolation procedure is repeated three times, once for each parameter.

Mathematical interpolation requires the same initial steps as graphical interpolation. That is, the appropriate figures to be used for a solution are obtained from Table 3-15 and the required parameters are determined and

entered into Table 3-16. Logarithmic equations are used to obtain the values of Y_a , Y_b and Y . The value of $\ln Y_a$ is obtained from:

$$\ln Y_a = \ln Y_1 + \frac{\ln(Y_2 / Y_1) \ln(C_1 / C_{11})}{\ln(C_{12} / C_{11})} \quad 3-83$$

and the value of $\ln Y_b$ is obtained from:

$$\ln Y_b = \ln Y_3 + \frac{\ln(Y_4 / Y_3) \ln(C_1 / C_{13})}{\ln(C_{14} / C_{13})} \quad 3-84$$

Using the values of $\ln Y_a$ and $\ln Y_b$; the value of $\ln Y$ is obtained from:

$$\ln Y = \ln Y_a + \frac{(\ln Y_b - \ln Y_a) \ln(C_2 / C_{21})}{\ln(C_{23} / C_{21})} \quad 3-85$$

The desired parameter Y is then obtained from:

$$Y = e^{\ln Y} \quad 3-86a$$

The above equations use natural logarithms. Common logarithms can be used to solve the above equations and then solve for Y using:

$$Y = 10^{\log Y} \quad 3-86b$$

It should be noted that if C_2 is represented by a response chart, then only two charts will be involved, and only Equation 3-83 will apply.

3-19.3.4.6. Accuracy

The prediction error is less than 10 percent for the approximate solutions obtained in regions A, B and D. This is true provided the recommended procedures are employed, that is, the actual load is replaced by the approximate loads as shown on Figure 3-62 and the solution is obtained using the equations provided for region A and using Figure 3-64 for regions B and D.

Exact solutions are obtained from the response charts if the required values of C_1 and C_2 correspond to those given in the charts. This is true for all four regions. Errors result from interpolation between the response charts. The prediction error in X_m/X_E for region C, where interpolation between charts is required, is less than 10 percent provided response charts bounded by the dashed or solid lines on Table 3-15 are not used. The prediction error in X_m/X_E will range from 55 to 100 percent for solutions in region C, if the point (C_1, C_2) lies in the area bounded by the solid line in Table 3-15, and will

range from 10 to 55 percent for the area bounded by the dashed line. If the solution involves charts from both sides of either the dashed or solid lines, the prediction error will range from 10 to 55 percent. The large interpolation error for these charts result from the big change in X_m/X_E for a small change in P/r_u which is peculiar to this chart.

It should be noted that the large errors described above will always be on the high side, that is, the predicted value of X_m/X_E will always be greater than the exact value. Hence, a conservative design will always result. In addition, it should be noted that the prediction error in t_m/T_N is about half the error in X_m/X_E .

While the errors produced from interpolation between the charts in Table 3-15 bounded by the dashed and solid lines is large, the area in which they apply is small. As can be seen, region C is rather small on these charts. It is for points in this small area where interpolation must be performed. For the remaining areas (A, B and D), the approximate solutions may be used rather than interpolation. These approximate solutions will result in a error of less than 10 percent.

Solutions involving $0.920 < C_1 < 1.00$ and $C_2 \geq 100$ can result in very large errors if interpolating procedures are employed. In this region, the dynamic response is primarily due to the gas load. Therefore, Figure 3-64 is used to obtain X_m/X_E for the gas load. However, this value is too low and should be increased by 20 percent. The value of t_m/T_N corresponding to the increased value of X_m/X_E is then obtained from Figure 3-64.

3-19.3.5. Determination of Rebound

In the design of elements which respond to the pressure only and pressure-time relationship, the element must be designed to resist the negative deflection or rebound which can occur after maximum positive deflection has been reached. The ratio of the required unit rebound resistance to the ultimate unit resistance r/r_u , such that the element will remain elastic during rebound is presented in Figure 3-268 for a single-degree-of-freedom system subjected to a triangular loading function. Entering with ratios X_m/X_E and t/T_N previously determined for design, the required unit rebound resistance r can be read in terms of the originally designed ultimate unit resistance r_u . To obtain the rebound resistance for an element subjected to another form of load other than the triangular loading function, a time-history analysis such as the one described in Section 3-19 has to be performed.

It may be noted that if the loading is applied in a relatively short time compared to the natural period of vibration of the system, the required rebound resistance can be equal to the resistance in the initial design direction. When the loading is applied for a relatively long time, the maximum deflection is reached when the positive forces are still large and the rebound resistance is reduced.

3-20. Elements Which Respond to Impulse

3-20.1. General

When an element responds to the impulse, the maximum response depends upon the area under the pressure time curve (impulse of blast loading). The magnitude and time variation of the pressure are not important. The response charts presented in Section 3-19, which are based on pressure-time relationship are therefore not required for these problems. Instead, the element resistance required to limit the maximum deflection to a specific value is obtained through the use of a semigraphical method of analysis.

Consider the pressure-time and resistance-time functions shown in Figure 3-269. The resistance curve depicted is for a two-way element with a resistance-deflection function having a post-ultimate range. From Newton's equation of motion it can be shown that the summation of the areas (considering area A as positive and area B as negative) under the load-time curves up to any time t_a divided by the corresponding effective masses is equal to the instantaneous velocity of that time:

$$v_a = \int_0^{t_a} \frac{(f-r) dt}{m_e} \quad 3-87$$

The displacement at time t_a is found by multiplying each differential area divided by the appropriate effective mass by its distance to t_a and summing the values algebraically:

$$X_a = \int_0^{t_a} \frac{(f-r)}{m_e} [t_a - t] dt \quad 3-88$$

In each range the mass is the effective plastic mass:

Time Interval	Resistance	Effective Mass
$0 \leq t \leq t_1$	r_u	$m_u = [K_{LM}] m_u$
$t_1 \leq t \leq t_m$	r_{up}	$m_{up} = [K_{LM}] m_{up}$

Time t_1 is the time at which the partial failure deflection X_1 occurs, and time t_m is the time at which maximum deflection X_m is reached ($X_m < X_u$).

For an element to be in equilibrium at its maximum deflection, its impulse capacity must be numerically equal to the impulse of the applied blast load. With the use of the foregoing equations, the expressions which define the motion and capacity of elements subjected to impulse type loads, can be defined. These expressions are presented for both large and limited deflection criteria. This criteria varies for the different materials used in protective design. The criteria for each material is obtained from the chapter that describes the design procedures for that material.

Case 1 - large deflections. Utilizing Equation 3-88 and by taking moments of the areas under the pressure-time and resistance-time curves (Figure 3-269) about time t_m , assuming that the unit blast impulse i_b is applied instantaneously at time $t=0$, and that time to reach yield t_y is also close to zero the expression for the maximum deflection is

$$X_m = \frac{i_b t_m}{m_u} - \frac{r_u t_1 [t_m - t_1 / 2]}{m_u} - \frac{r_{up} [t_m - t_1]}{2m_{up}} [t_m - t_1] \quad 3-89$$

If moments of the areas are taken about t_1 , then the deflection at partial failure X_1 , is

$$X_1 = \frac{i_b t_1}{m_u} - \frac{r_u t_1^2}{2m_u} \quad 3-90$$

Using Equation 3-87 and summing the areas of t_m and recognizing that the instantaneous velocity at t_m equals zero.

$$\frac{i_b}{m_u} - \frac{r_u t_1}{m_u} - \frac{r_{up} [t_m - t_1]}{m_{up}} = 0 \quad 3-91$$

Solution of the above three simultaneous equations is accomplished by solving Equation 3-91 for t_m and substituting this expression into Equation 3-89, and solving Equation 3-90 for t_1 and substituting this expression into the modified Equation 3-89. After continuing and rearranging terms, the general response equation becomes

$$\frac{i_b^2}{2m_u} = r_u X_1 + \frac{m_u}{m_{up}} r_{up} (x_m - x_1) \quad 3-92$$

The left side of this equation is simply the initial kinetic energy resulting from the applied blast impulse and the right side is the modified potential energy of the element. The modification is required since the above analysis requires the use of two equivalent dynamic systems (before and after time t_1). The modification factor m_u/m_{up} equates the two dynamic systems. If the effective mass in each range was the same, m_u/m_{up} would equal one and the right side of the expression would be $r_u X_m$ which is the potential energy.

For one-way elements which do not exhibit the post-ultimate resistance range, or for two-way panels where the maximum deflection X_m is less than X_1 , Equation 3-92 becomes

$$\frac{i_b^2}{2m_u} = r_u X_m \quad 3-93$$

The above solutions are valid only for what is considered large deflection design since the variation of resistance with deflection in the elasto-plastic range has been ignored. This limitation is based on the assumption that the time to reach yield t_y and the duration of the impulse t_o are small in comparison to t_m .

Case 2 - limited deflections. For elements which respond to the impulse with limited deflections where the time to reach maximum deflection t_m is greater than three times the duration t_o of the load, but where the support rotations are equal to or less than the established criteria, the elasto-plastic range behavior of the element must be accounted for in determining the overall

response of the element to the applied blast load. For this case, Equation 3-92 becomes

$$\frac{i_b^2}{2m_a} = \frac{r_u X_E}{2} + \frac{m_a}{m_u} r_u [X_m - X_E] \quad 3-94$$

where m_a is the average of the effective elastic and plastic masses and X_E the equivalent deflection.

When the response time t_m of an element is less than three times the load duration t_0 , the element will respond to the pressure pulse rather than to the impulse alone. In this case the response of the element may be obtained through the use of a response chart considering a fictitious pressure pulse as outlined in Chapter 2. However, if the element's maximum deflection is greater than given in the response charts (ductility ratio X_m/X_E greater than 100), the response of the element may be obtained through use of the semi-graphical method of analysis as outlined in this paragraph considering the fictitious pressure pulse. It should be noted that the resistance time relationship used in the analysis to express the element's response should include the elasto-plastic region.

3-20.2. Determination of Time to Reach Maximum Deflection

The time t_m for each of the cases covered previously can be determined by applying Equations 3-87 and 3-88 to the particular problem. The resulting equations are as follows:

Case 1 - large deflections.

A. $X_1 < X_m \leq X_u$

$$t_m = \frac{i_b}{r_u} + \left[\frac{m_{up}}{m_u r_{up}} - \frac{1}{r_u} \right] \left[i_b^2 - 2m_u r_u X_1 \right]^{1/2} \quad 3-95$$

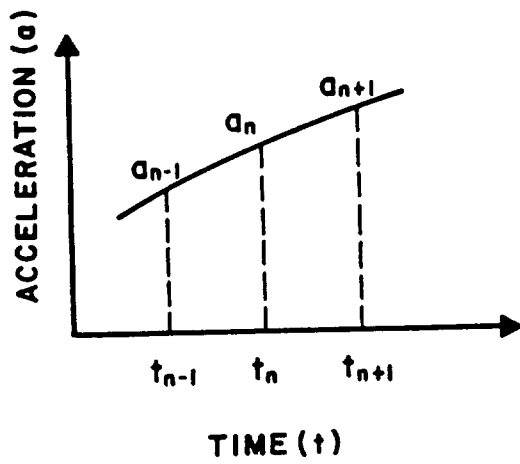
B. $X_m \leq X_1$

$$t_m = i_b / r_u$$

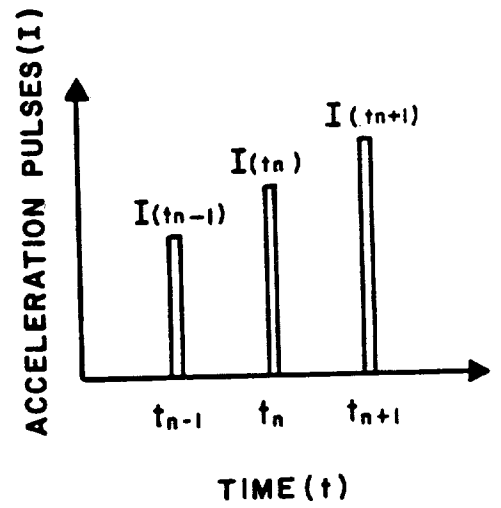
Case 2 - limited deflections.

Since the variation of resistance with time is not known in the elasto-plastic range, t_m can only be determined approximately by assuming a linear variation of resistance with time.

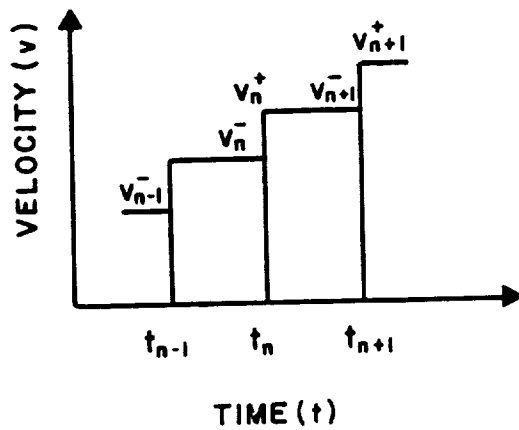
$$t_m(\text{approx}) = \frac{i_b}{r_u} \left[3 - \frac{m_u}{2m_a} \right] + \frac{1}{r_u} \left[\frac{m_u}{2m_a} - 1 \right] \left[9i_b^2 - 6m_a r_u X_E \right]^{1/2} \quad 3-97$$



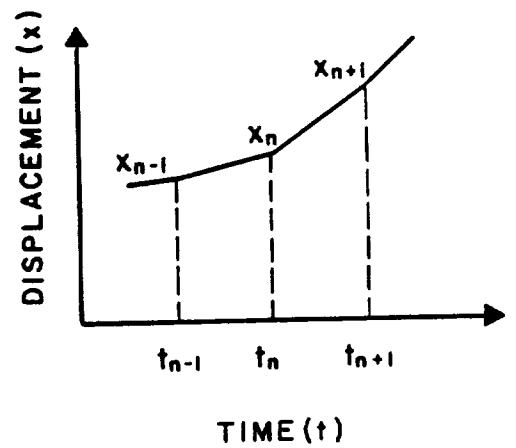
(a) GIVEN ACCELERATION CURVE



(b) ACCELERATION PULSES TO REPLACE THE GIVEN ACCELERATION CURVE



(c) VELOCITY



(d) DISPLACEMENT

Figure 3-45 Acceleration-impulse extrapolation method

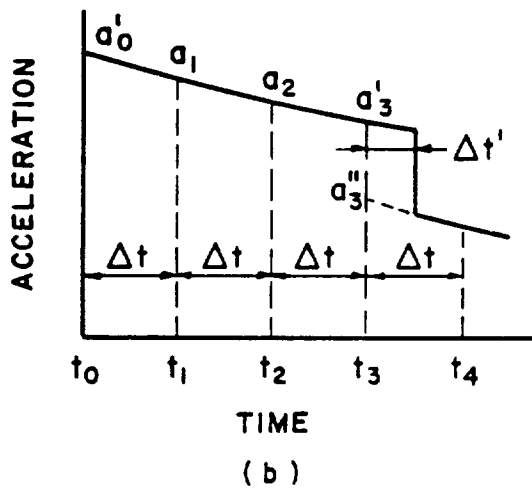
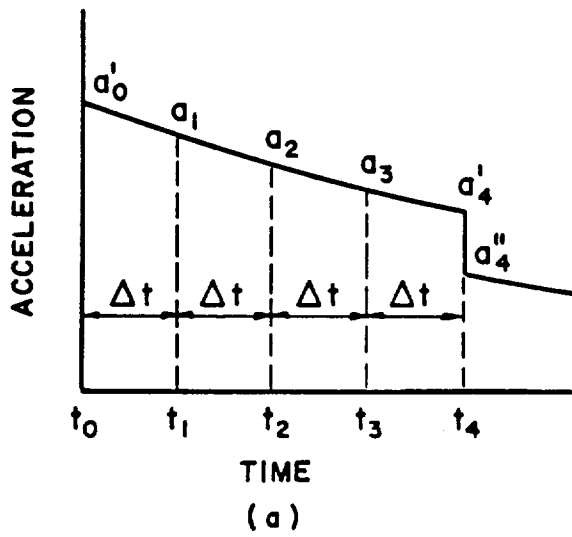


Figure 3-46 Discontinuities in the acceleration curve

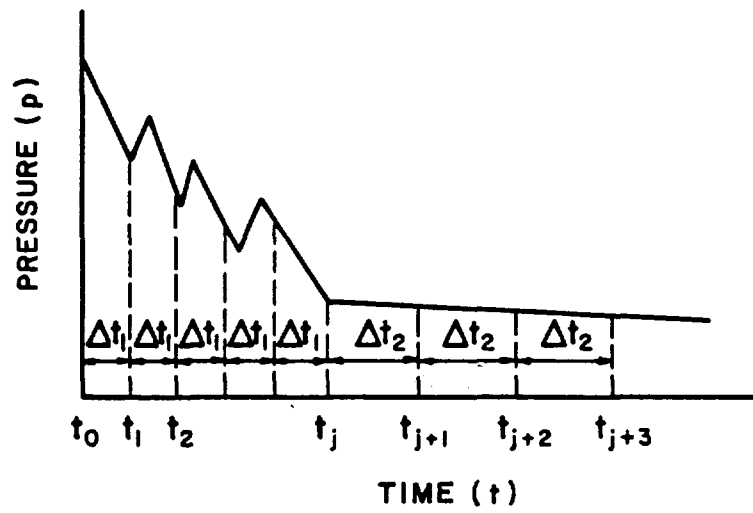


Figure 3-47 Pressure-time function with two different time intervals

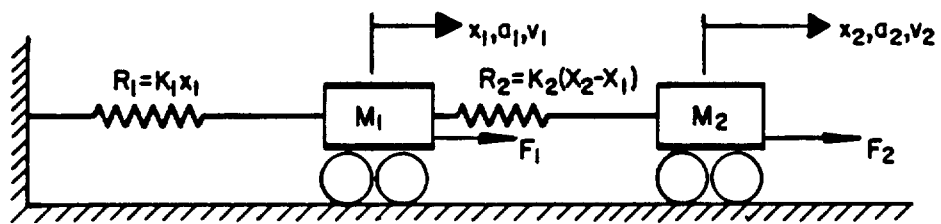


Figure 3-48 A two-degrees-of-freedom system

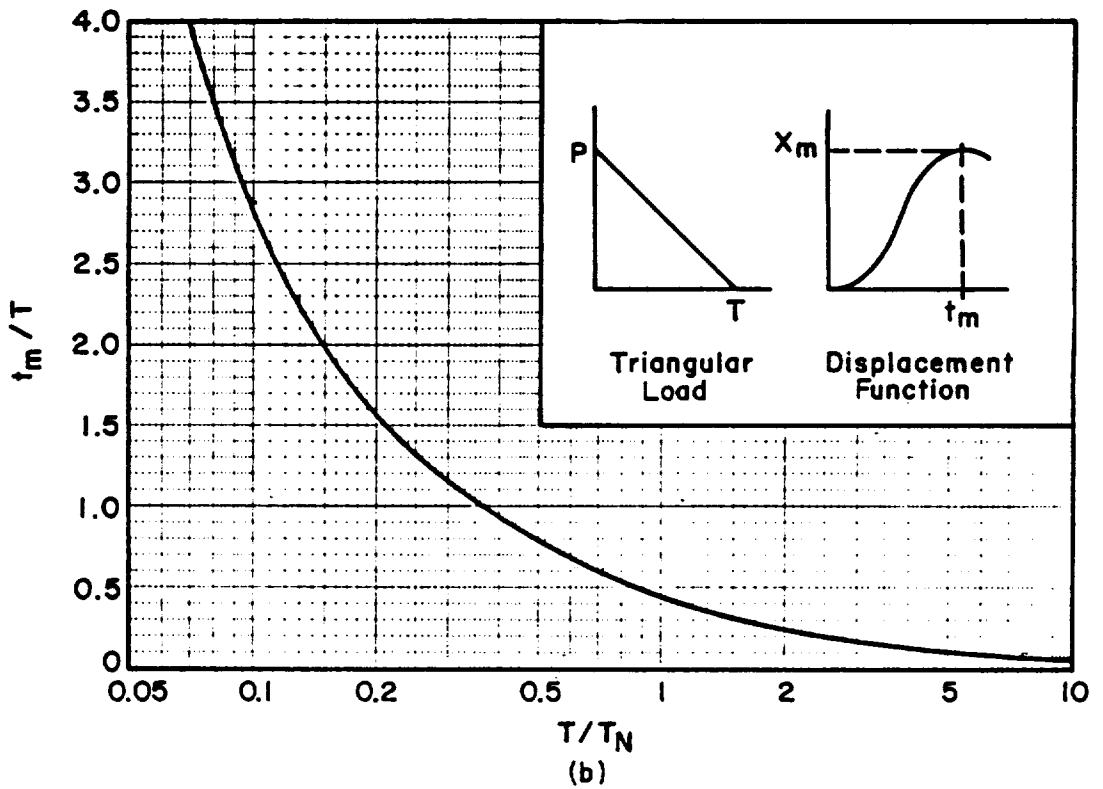
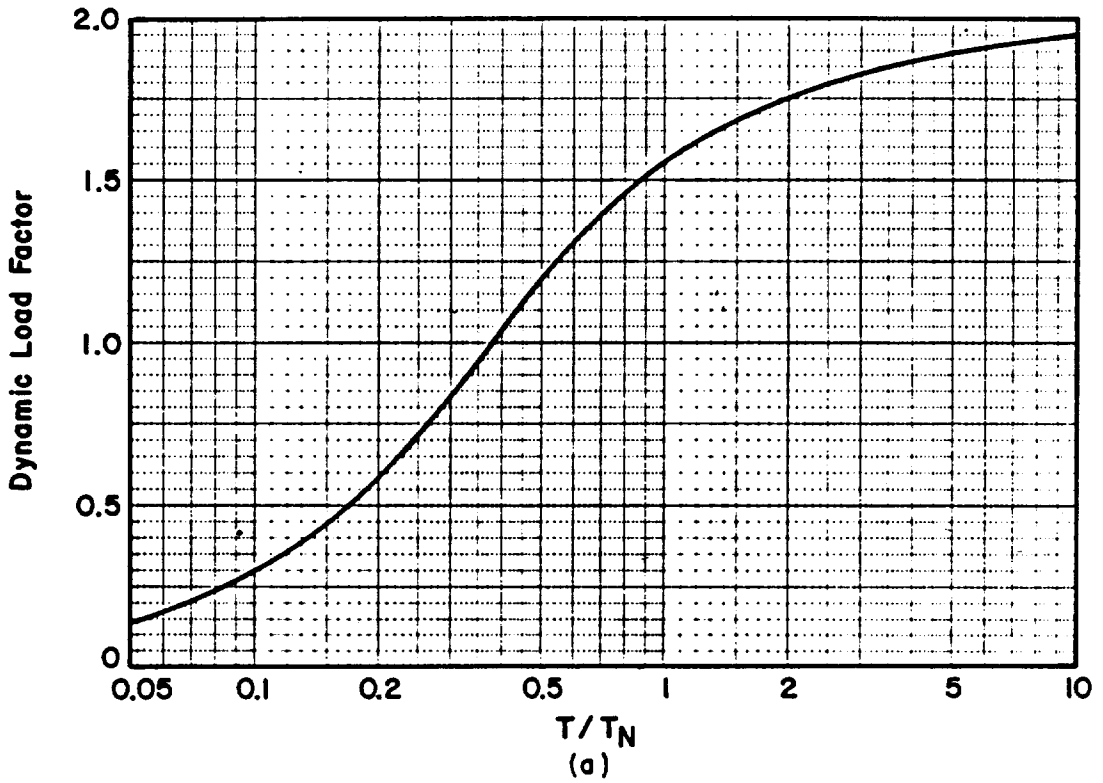


Figure 3-49 Maximum response of elastic one-degree-of-freedom system for triangular load

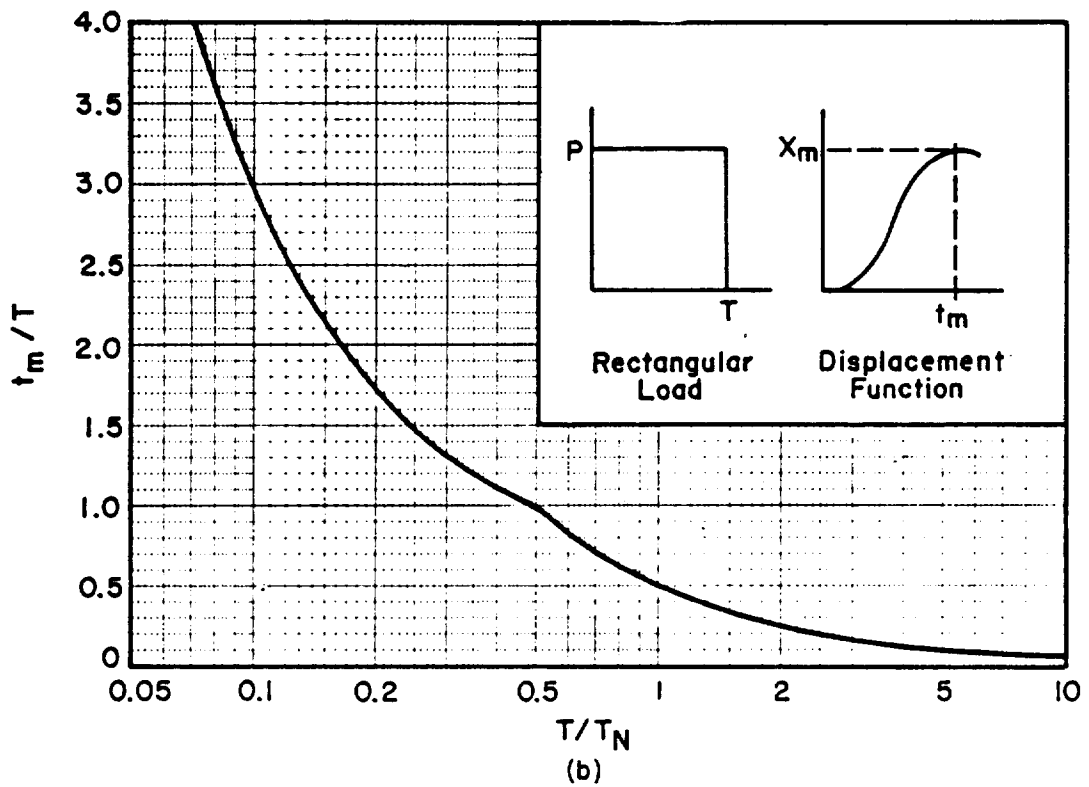
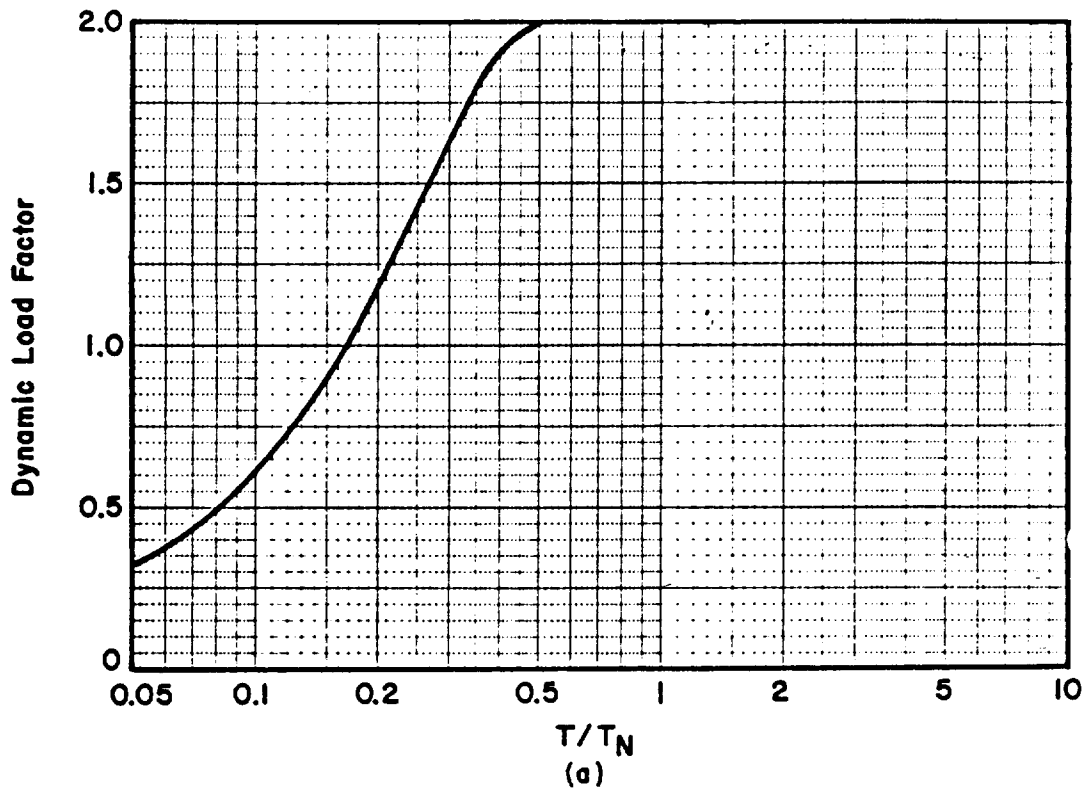


Figure 3-50 Maximum response of elastic, one-degree-of-freedom system for rectangular load

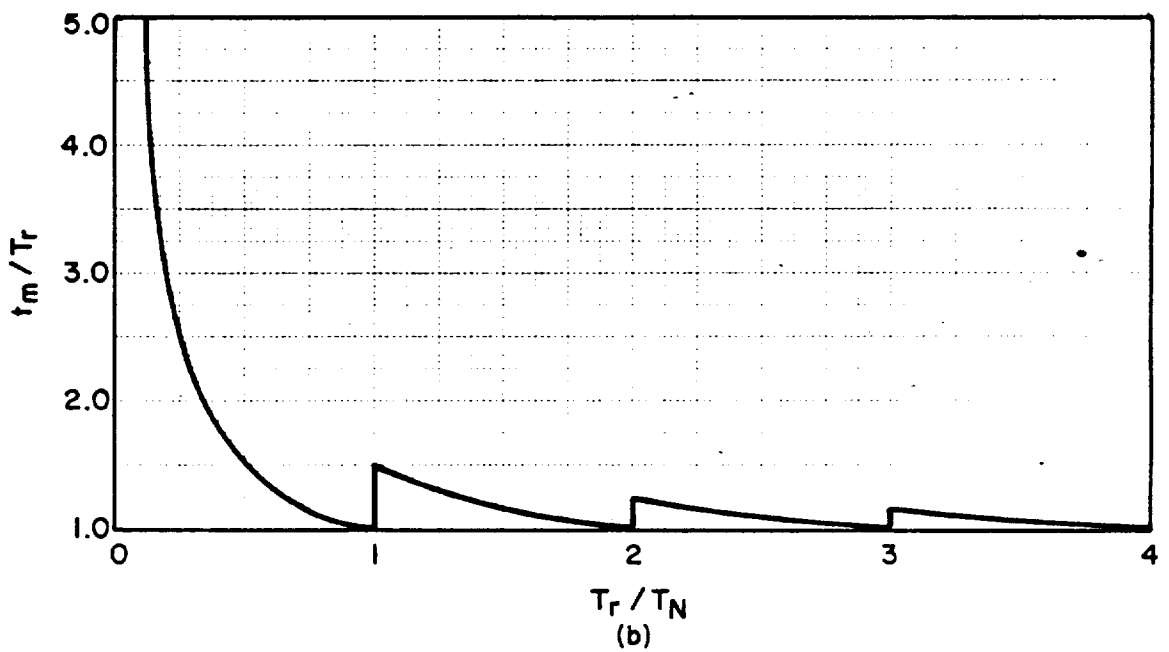
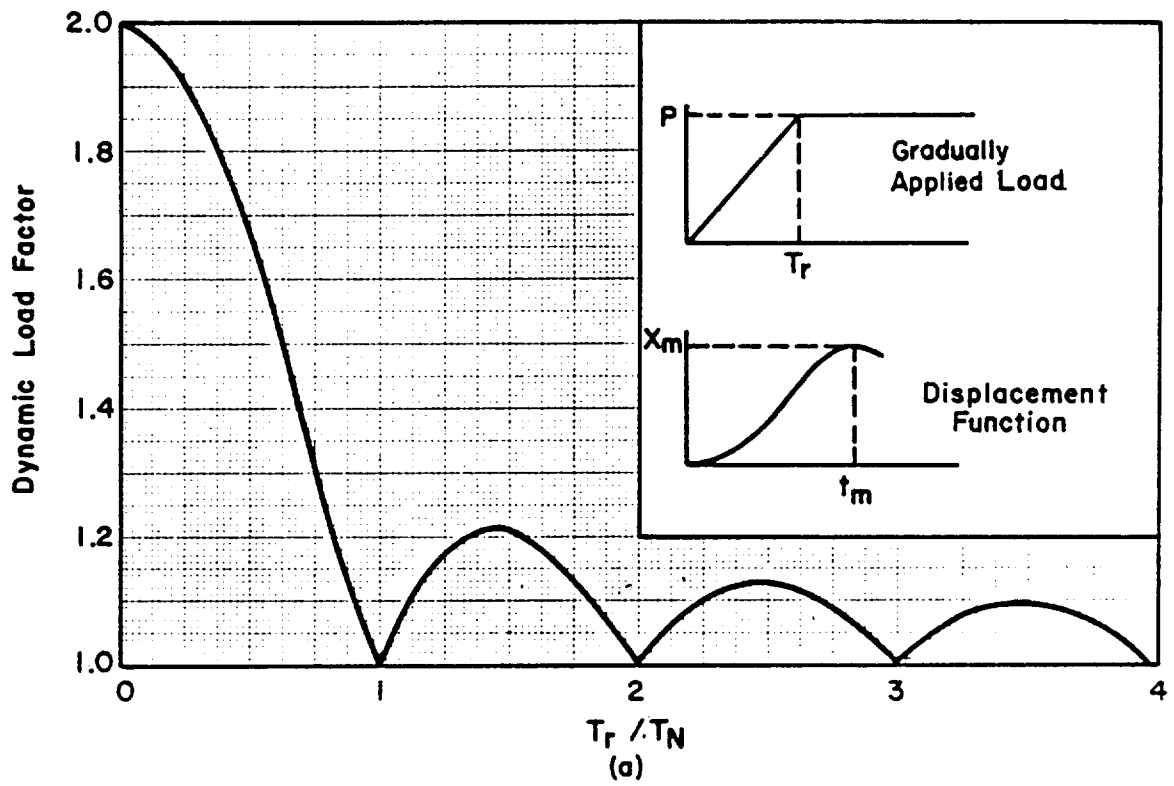


Figure 3-51 Maximum response of elastic, one-degree-of-freedom system for gradually applied load

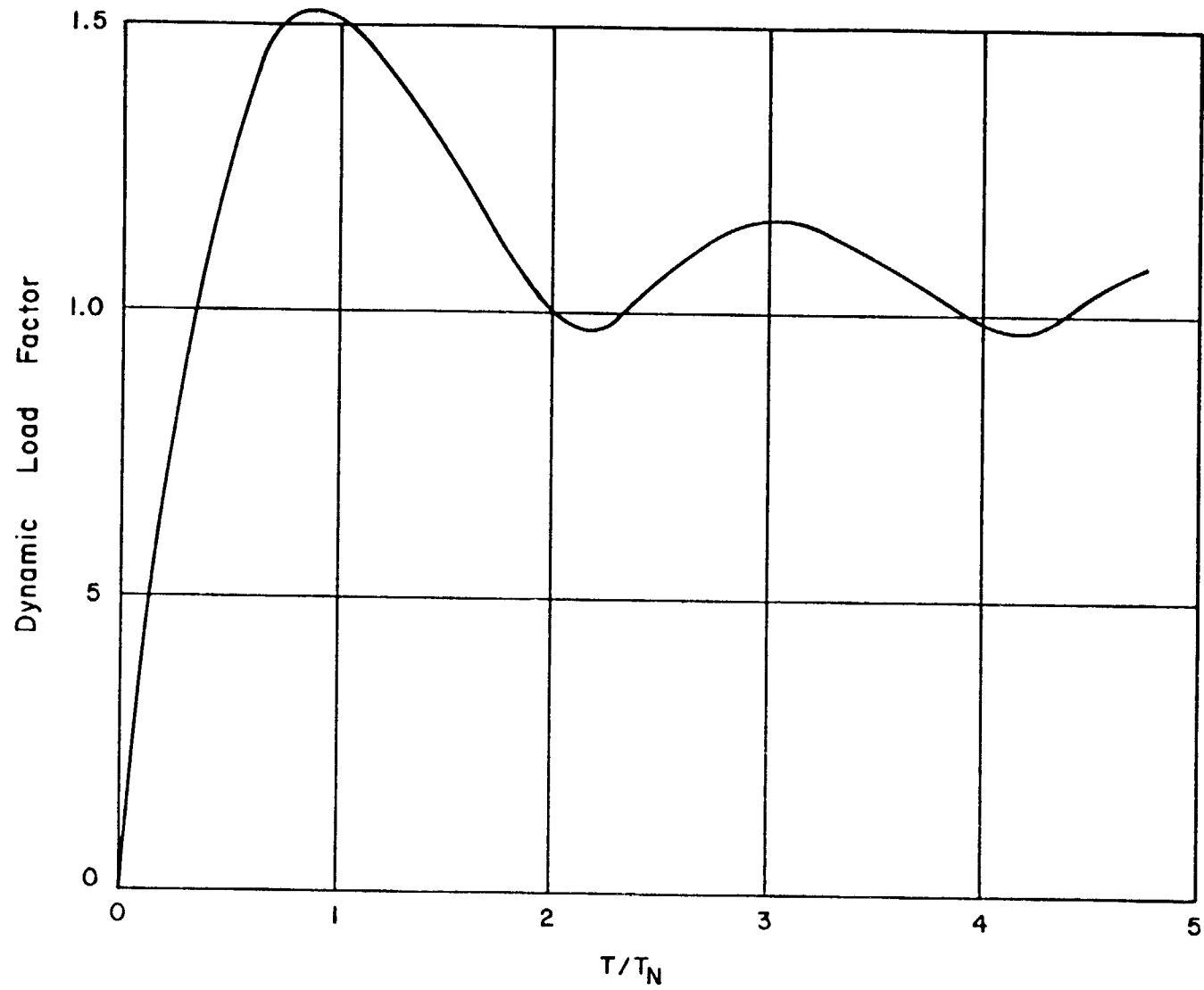


Figure 3-52 Maximum response of elastic one-degree-of-freedom system for triangular pulse load

3-110

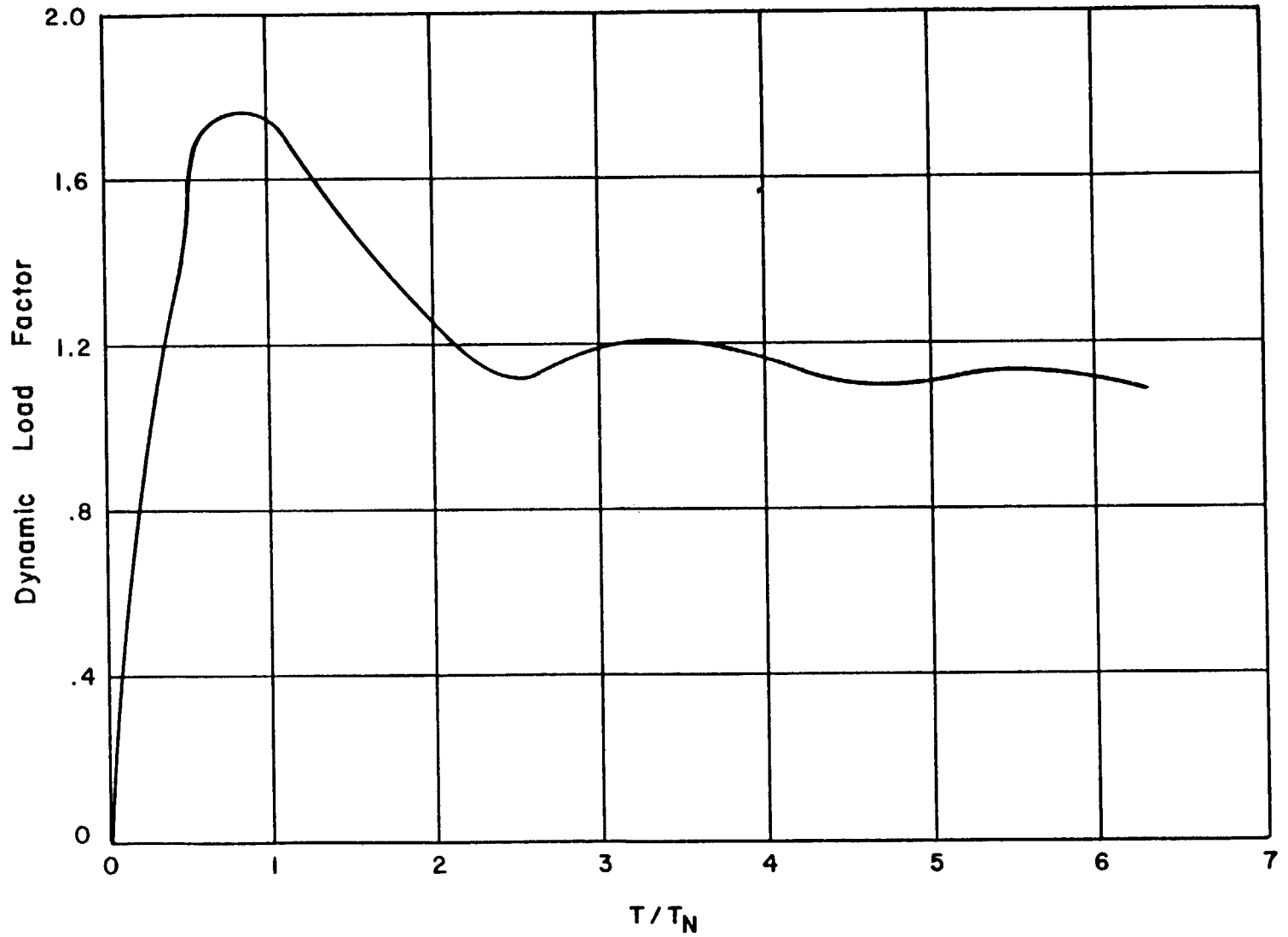


Figure 3-53 Maximum response of elastic one-degree-of-freedom system for sinusoidal pulse load

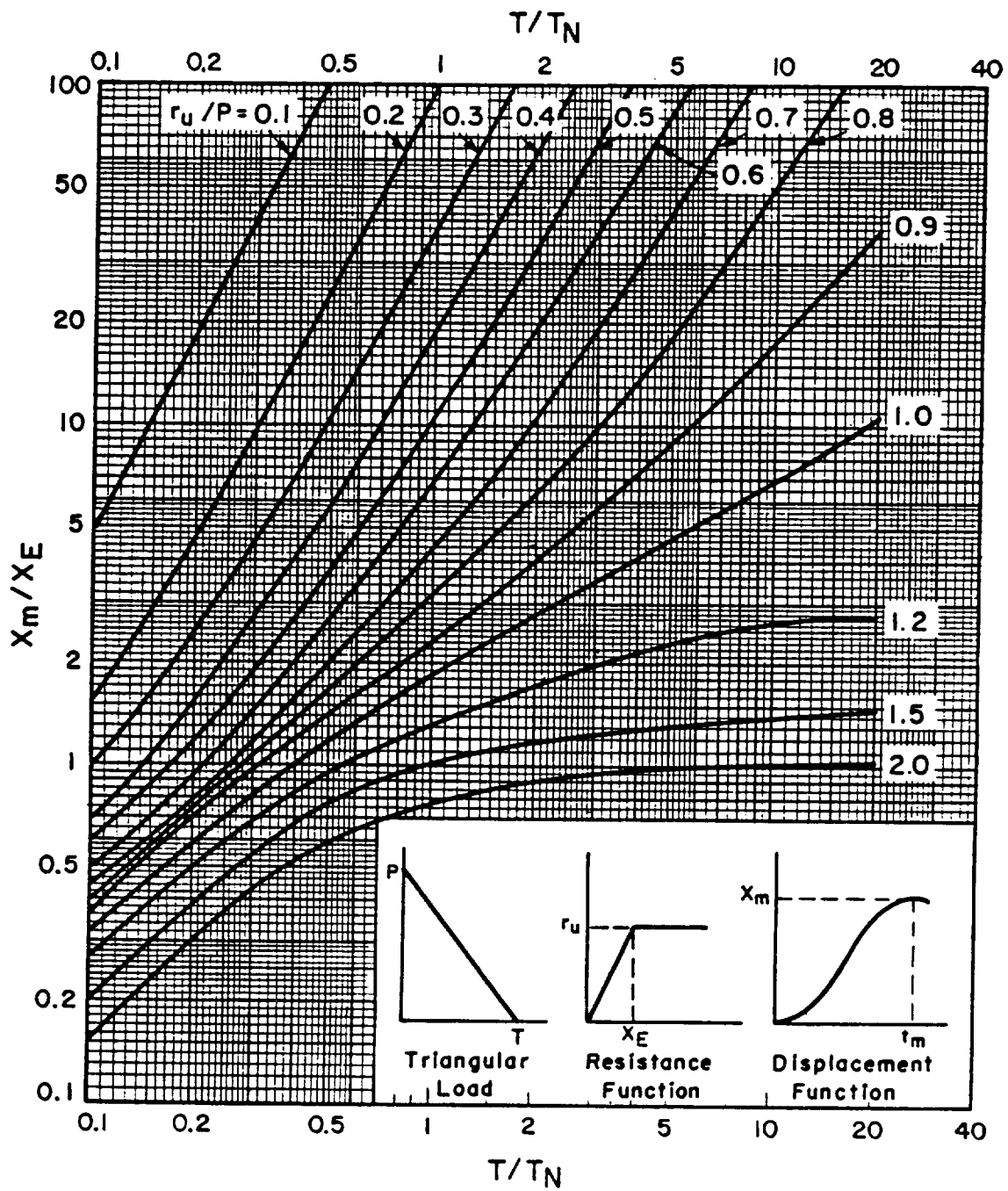


Figure 3-54 Maximum deflection of elasto-plastic, one-degree-of-freedom system for triangular load

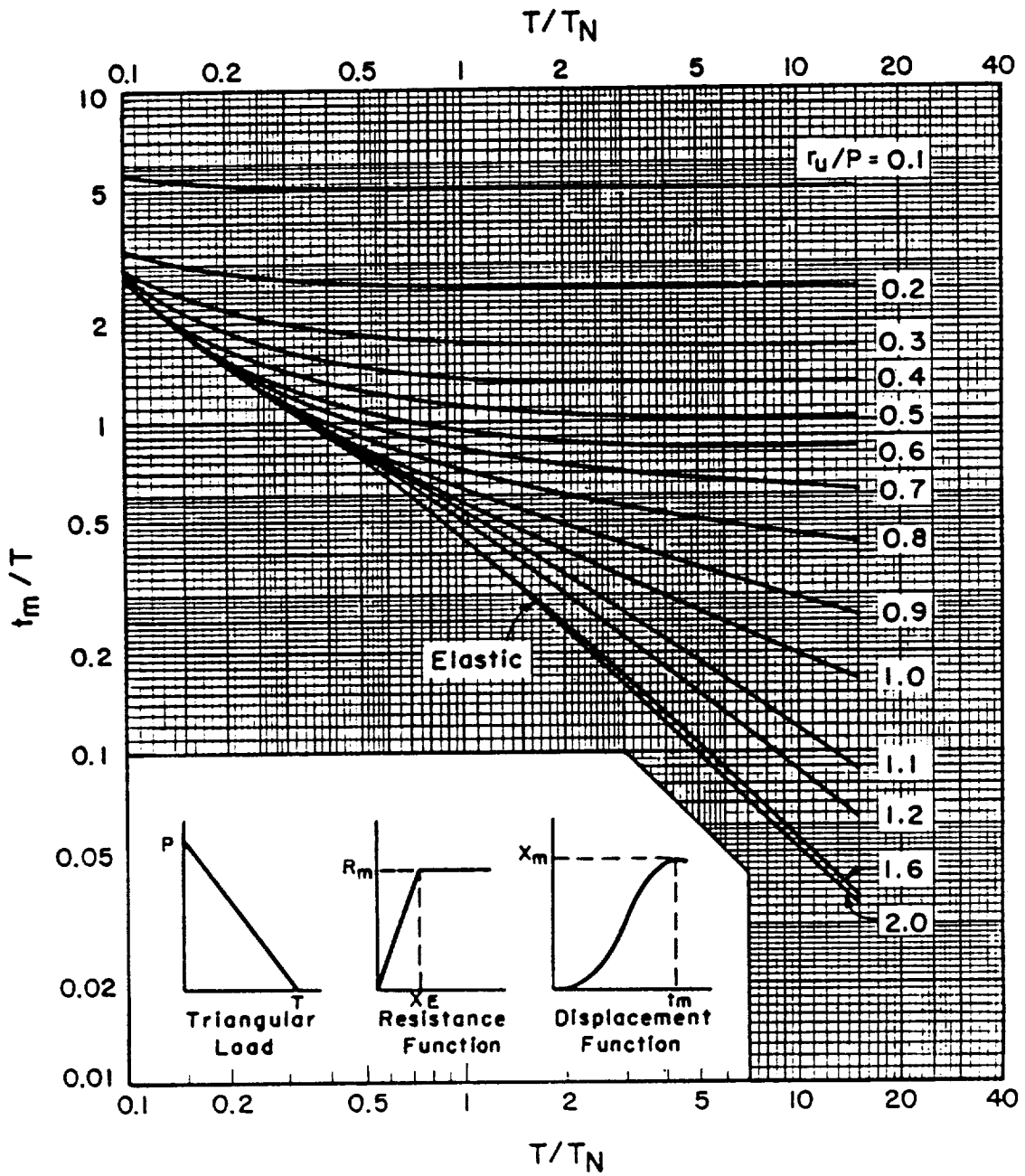


Figure 3-55 Maximum response time of elasto-plastic, one-degree-of-freedom system for triangular load

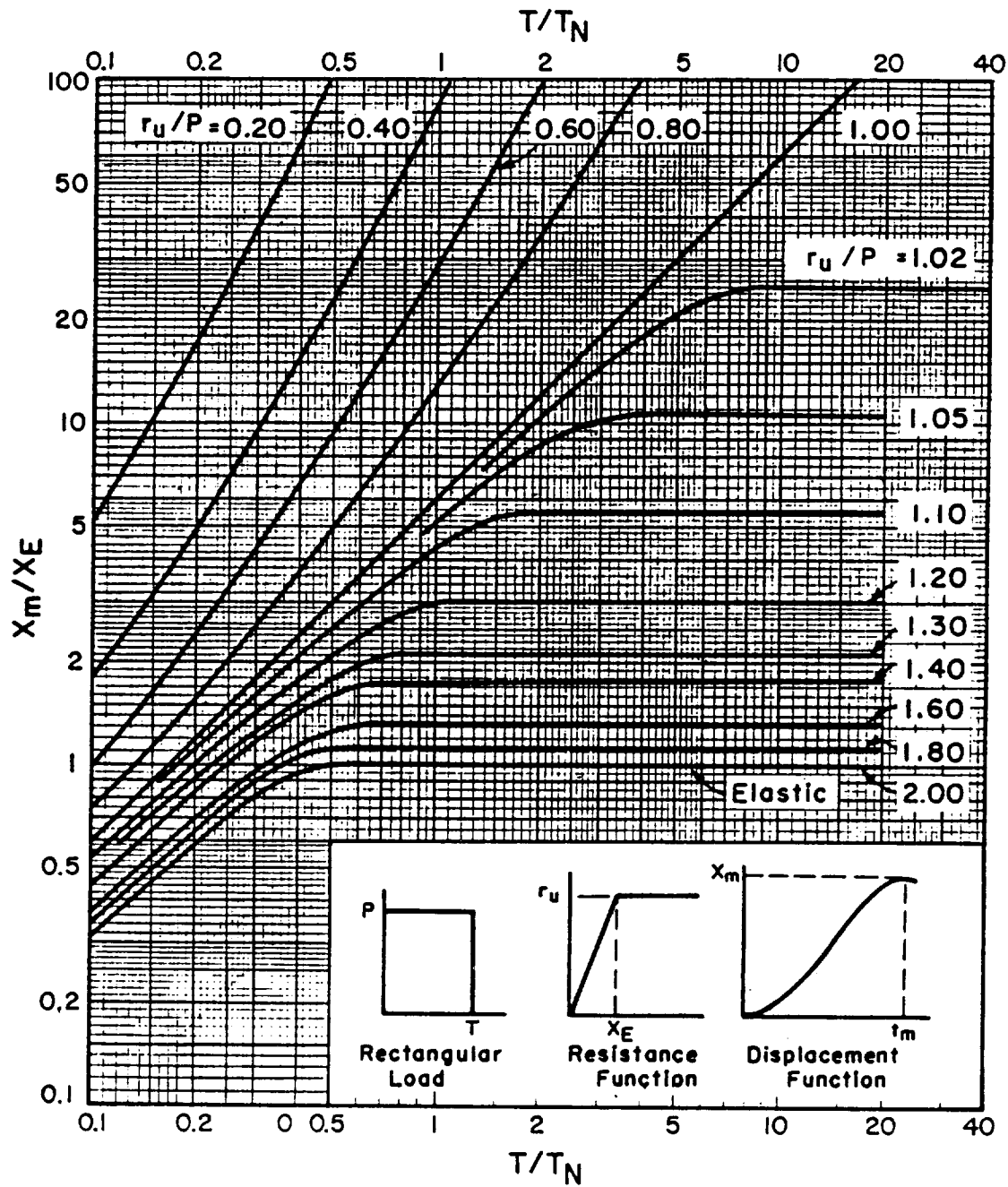


Figure 3-56 Maximum deflection of elasto-plastic, one-degree-of-freedom system for rectangular load

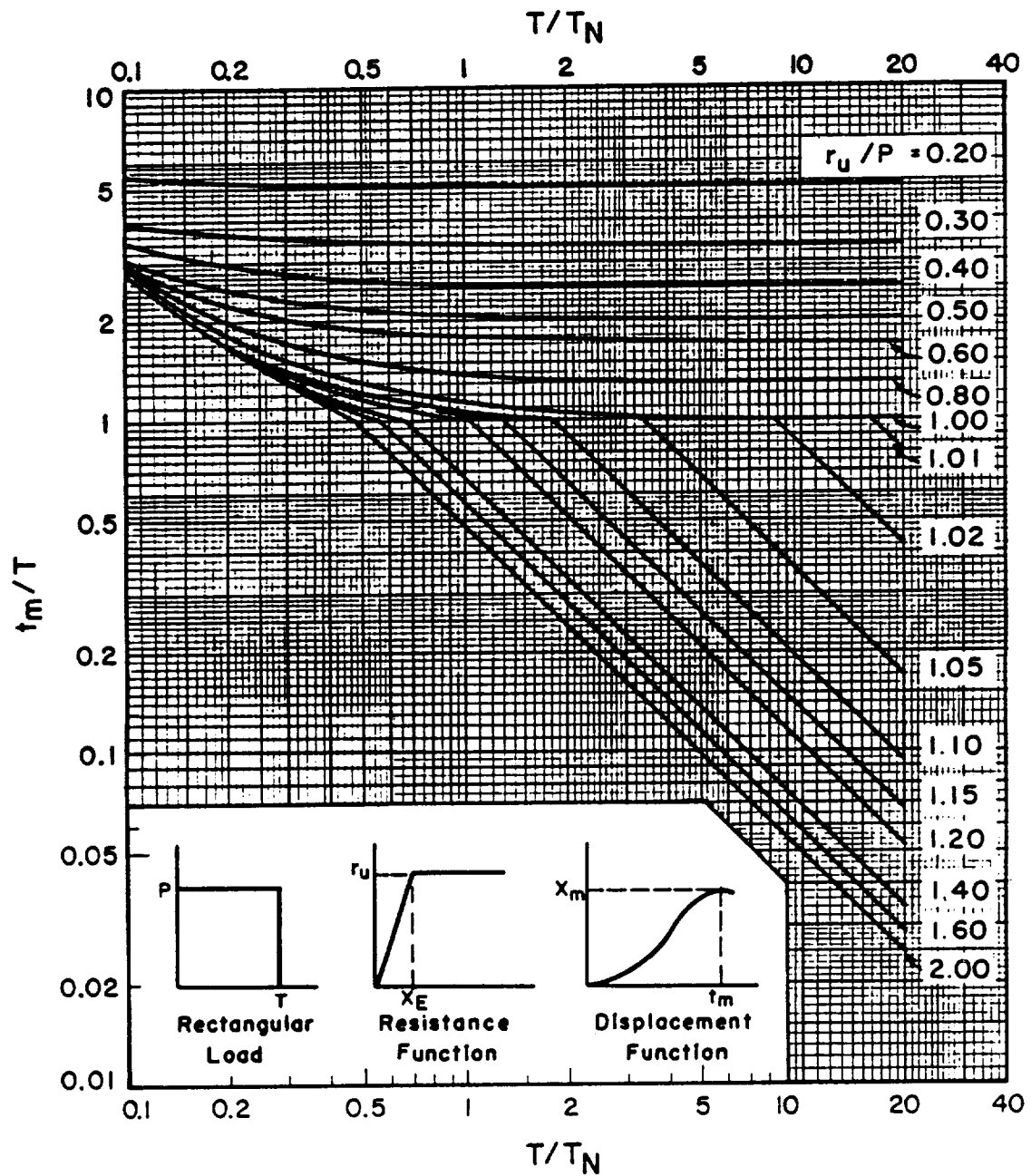


Figure 3-57 Maximum response time of elasto-plastic, one-degree-of-freedom for rectangular load

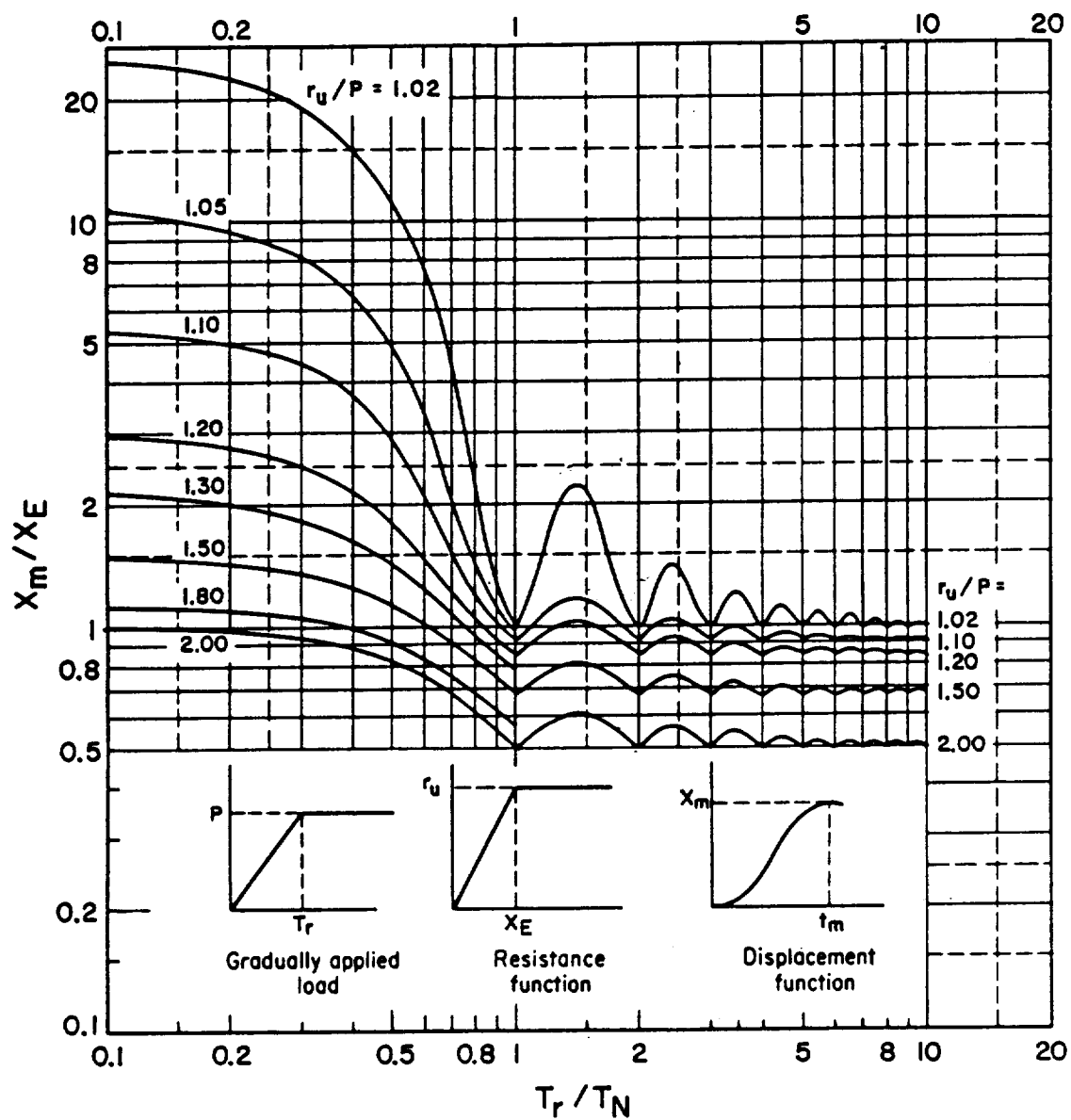


Figure 3-58 Maximum deflection of elasto-plastic, one-degree-of-freedom system for gradually applied load

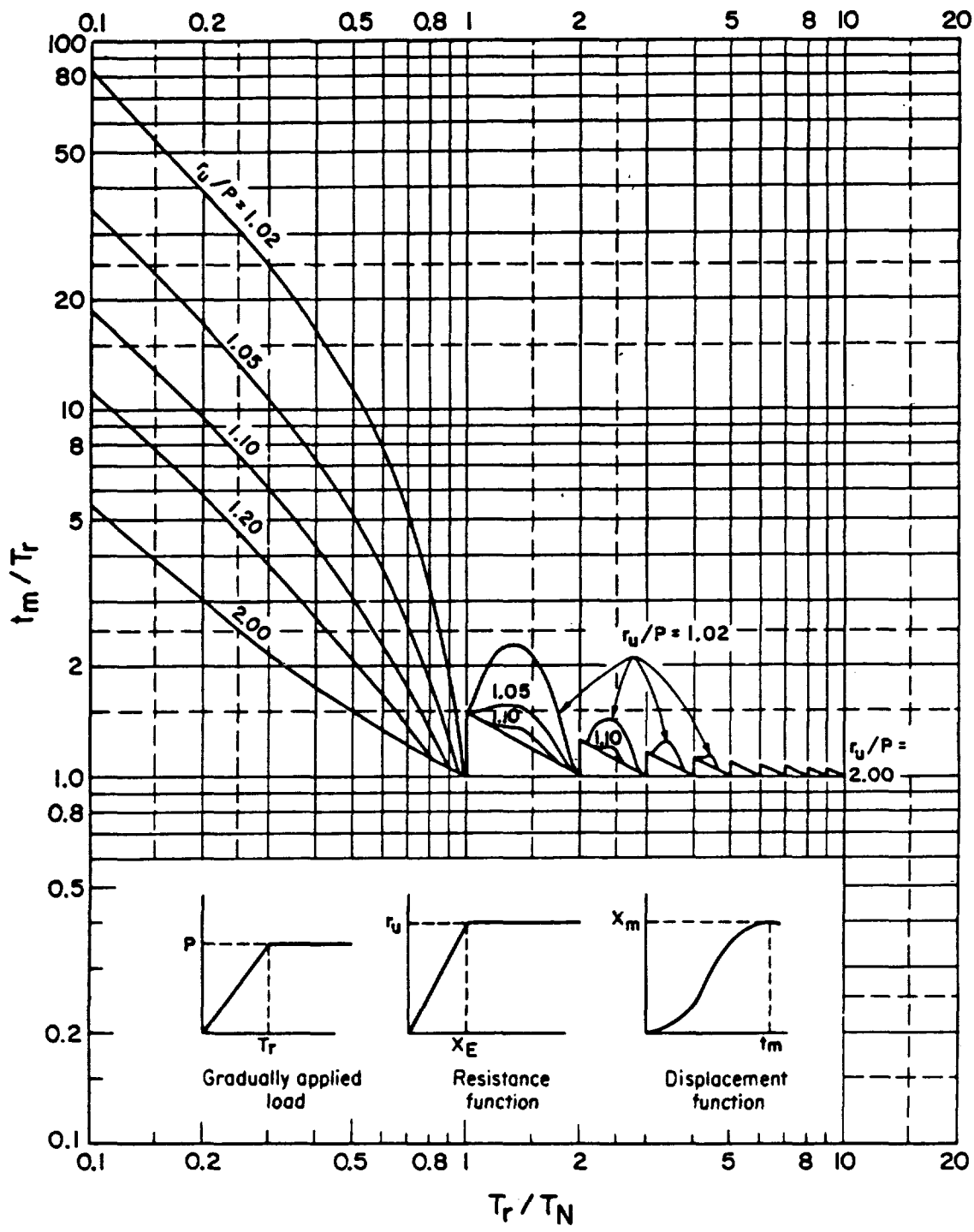


Figure 3-59 Maximum response time of elasto-plastic, one-degree-of-freedom system for gradually applied load

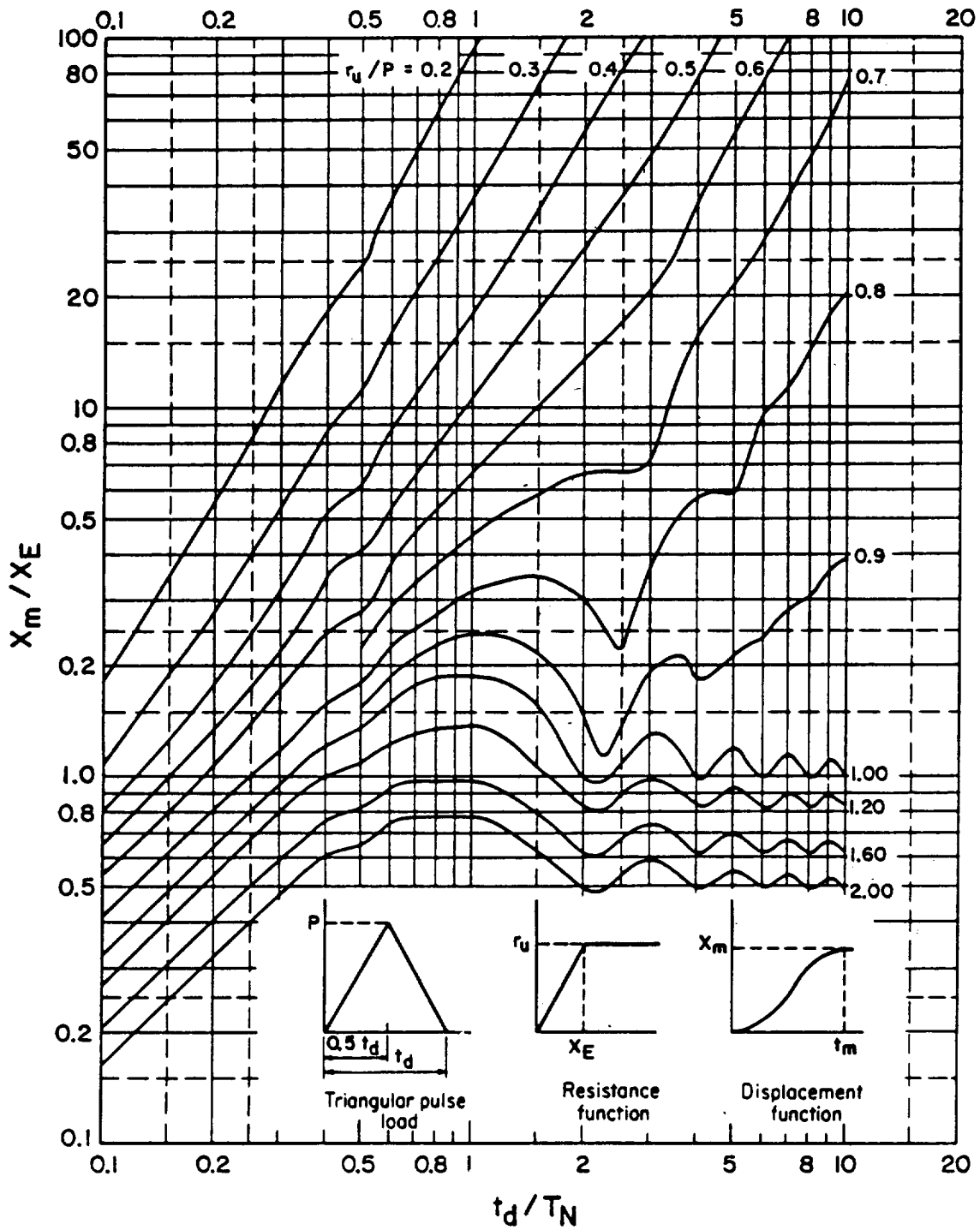


Figure 3-60 Maximum deflection of elasto-plastic, one-degree-of-freedom system for triangular pulse load

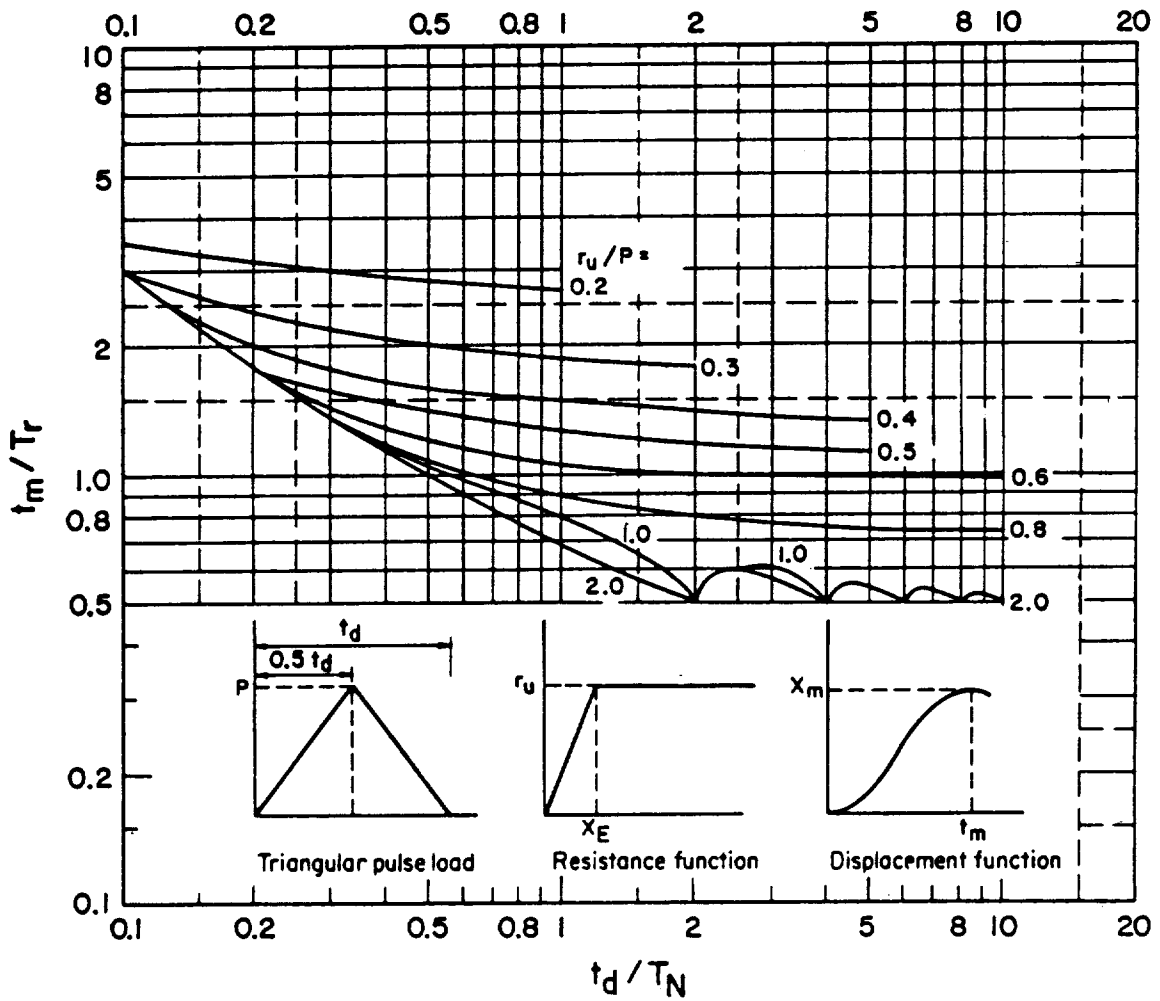
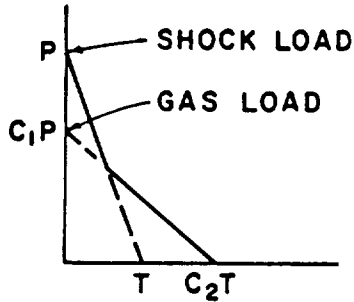
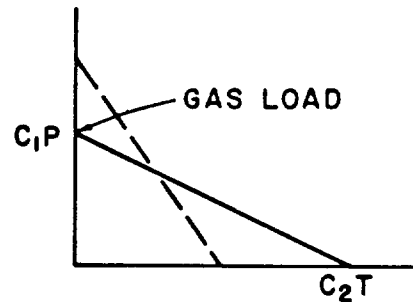


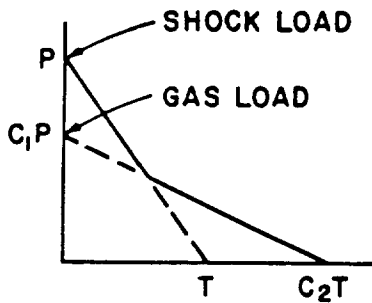
Figure 3-61 Maximum response time of elasto-plastic, one-degree-of-freedom system for triangular pulse load



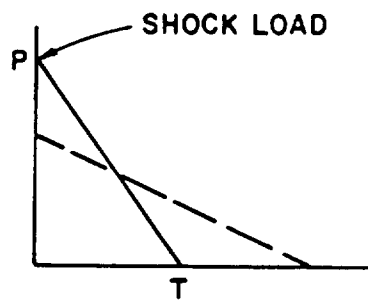
REGION A: NEGLECT CHARTS
 USE EQUATIONS 3-80 AND 3-81



REGION B: NEGLECT SHOCK LOAD
 USE FIGURE 3-64



REGION C: BOTH SHOCK AND GAS
LOADS ARE SIGNIFICANT USE
APPROPRIATE FIGURES AND
INTERPOLATE.



REGION D: NEGLECT GAS LOAD
 USE FIGURE 3-64

Figure 3-62 Various bilinear triangular loads

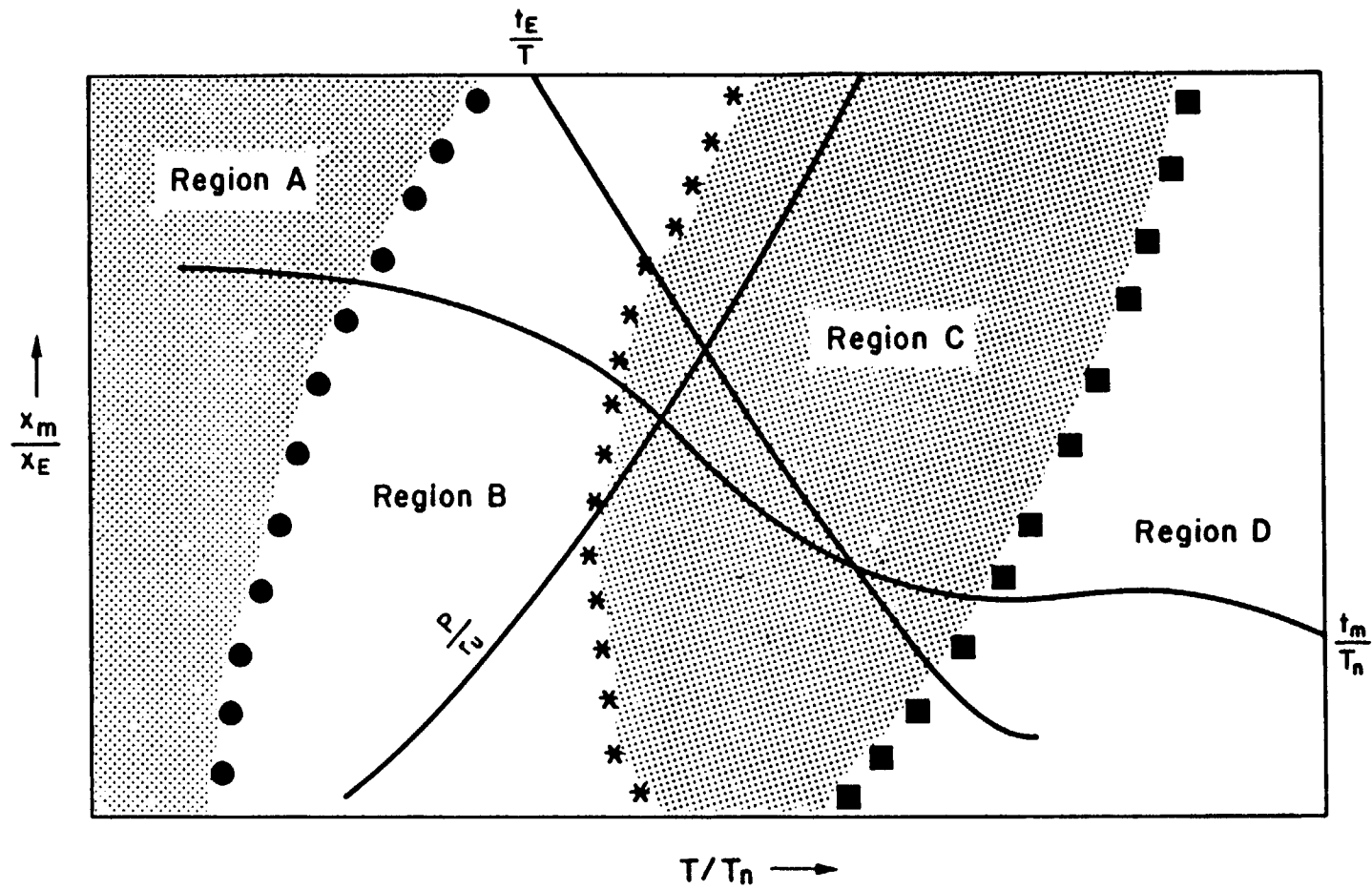


Figure 3-63 Regions of figures 3-64 through 3-266, labeling of axis and curves.

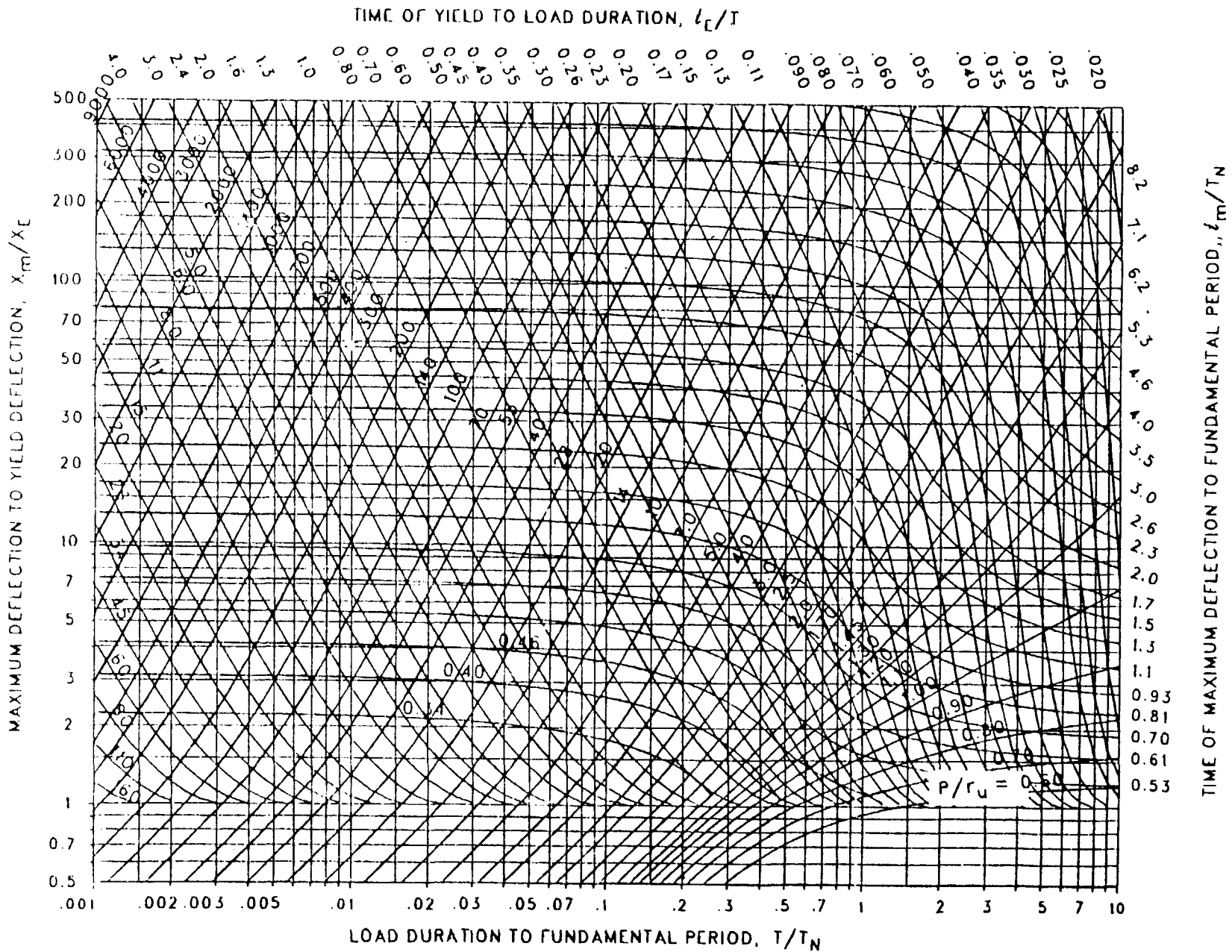


Figure 3-64a Maximum response of elasto-plastic, one-degree-of-freedom system for bilinear-triangular pulse ($C_1 = 1.000$, $C_2 = 1.0$)

3-122

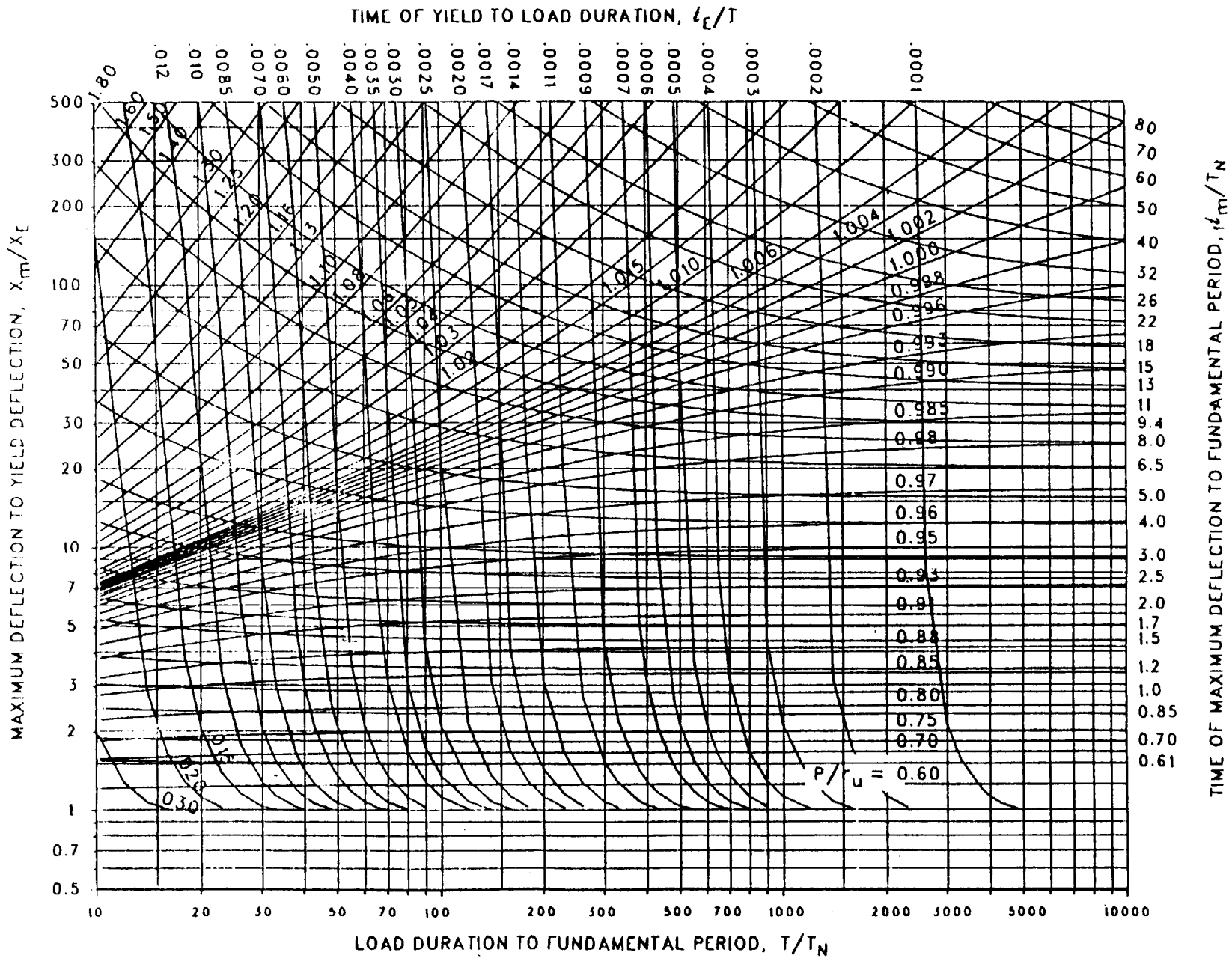


Figure 3-64b Maximum response of elasto-plastic, one-degree-of-freedom system for bilinear-triangular pulse ($C_1 = 1.000$, $C_2 = 1.0$) (cont.)

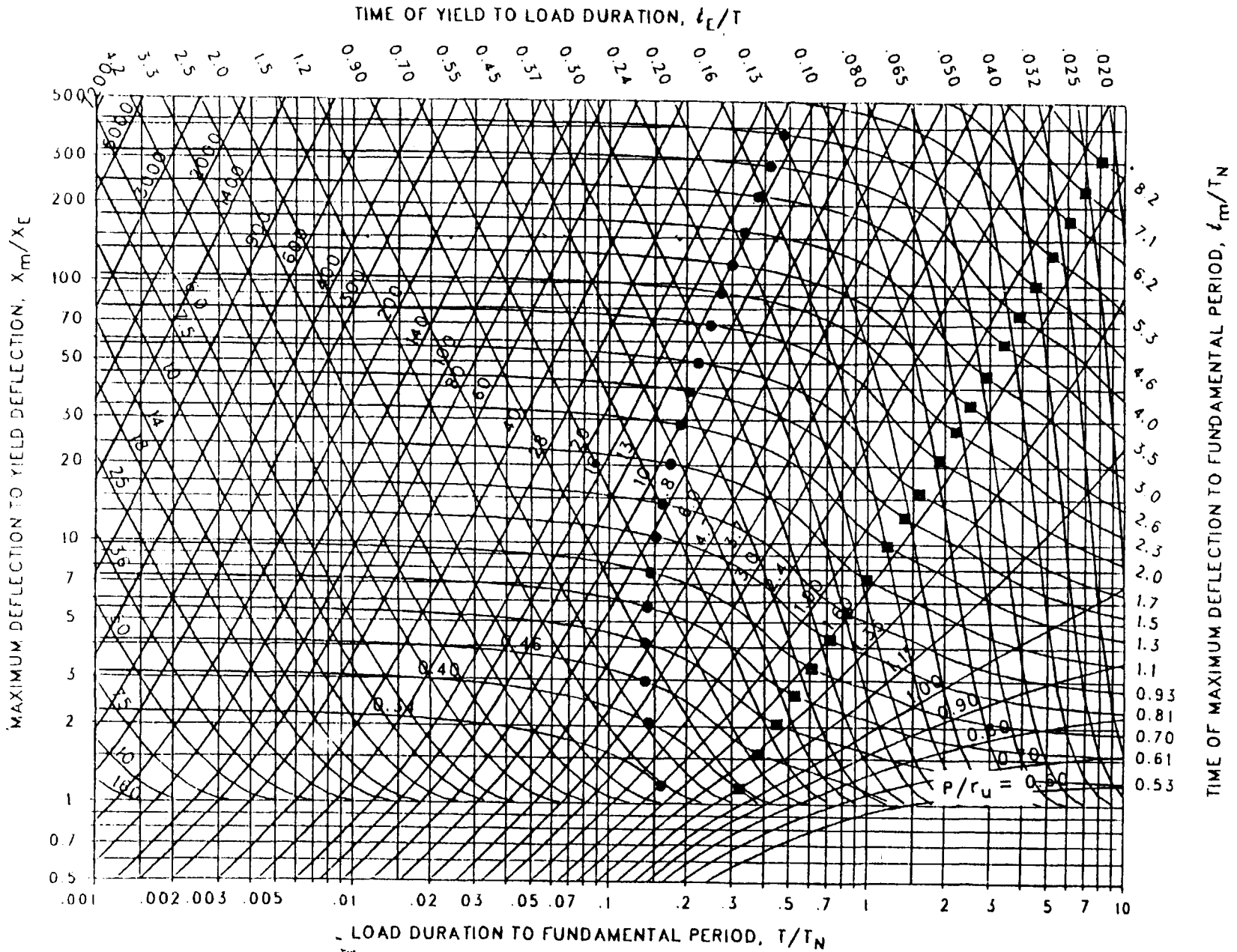


Figure 3-65 Maximum response of elasto-plastic, one-degree-of-freedom system for bilinear-triangular pulse ($C_1 = 0.681$, $C_2 = 1.7$)

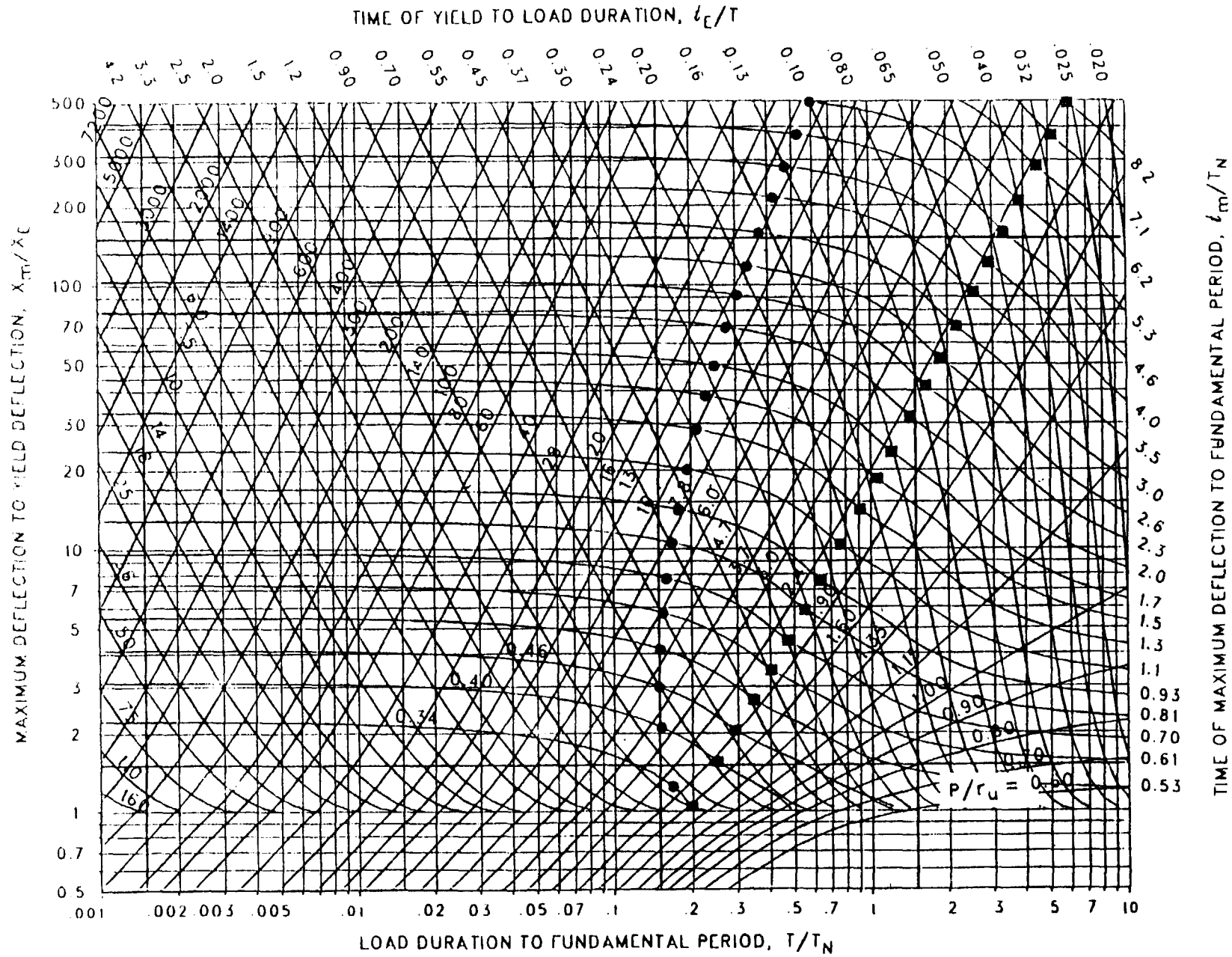


Figure 3-66 Maximum response of elasto-plastic, one-degree-of-freedom system for bilinear-triangular pulse ($C_1 = 0.464$, $C_2 = 1.7$)

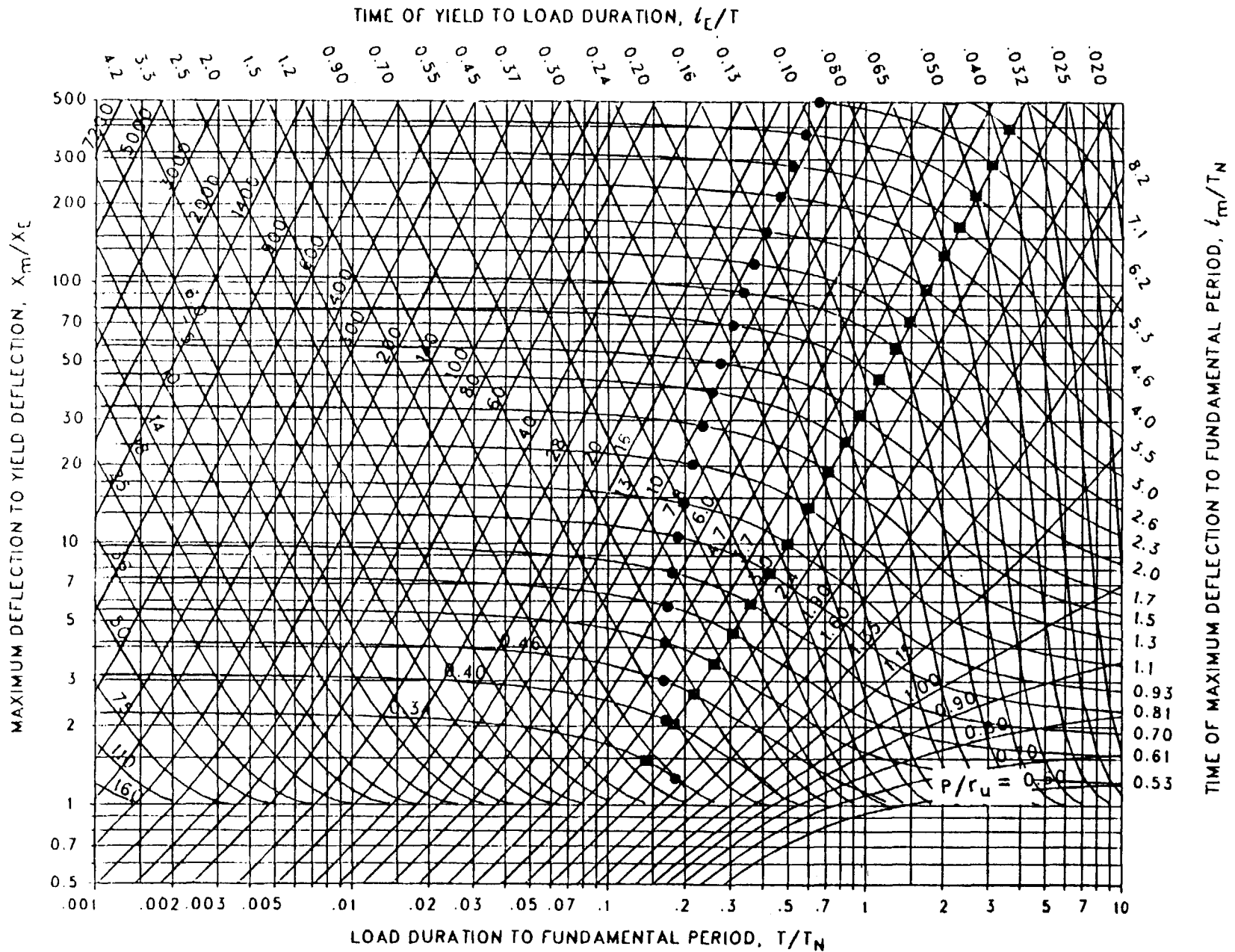


Figure 3-67 Maximum response of elasto-plastic, one-degree-of-freedom system for bilinear-triangular pulse ($C_1 = 0.316$, $C_2 = 1.7$)

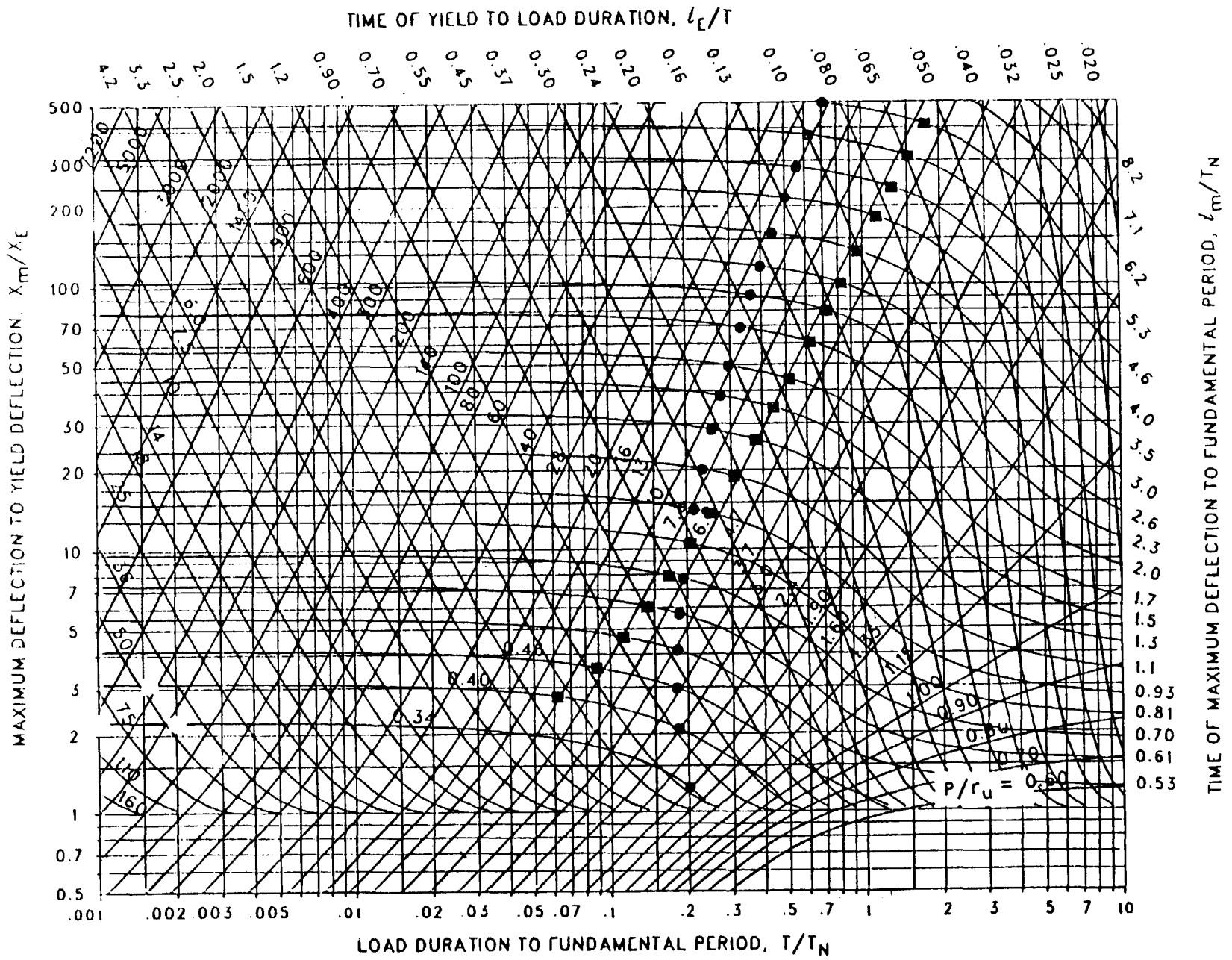


Figure 3-68 Maximum response of elasto-plastic, one-degree-of-freedom system for bilinear-triangular pulse ($C_1 = 1.215$, $C_2 = 1.7$)

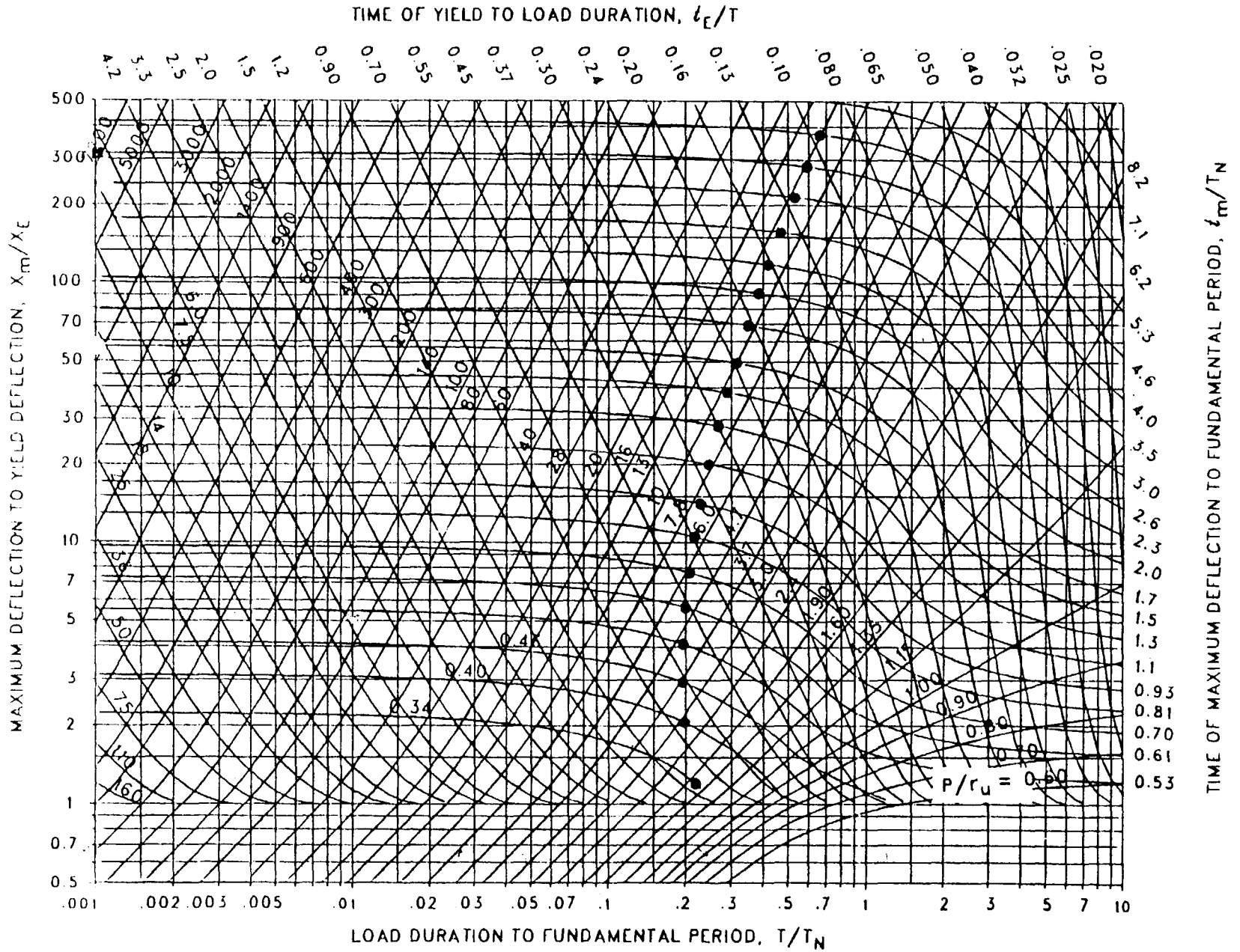


Figure 3-69 Maximum response of elasto-plastic, one-degree-of-freedom system for bilinear-triangular pulse ($C_1 = 0.147$, $C_2 = 1.7$)

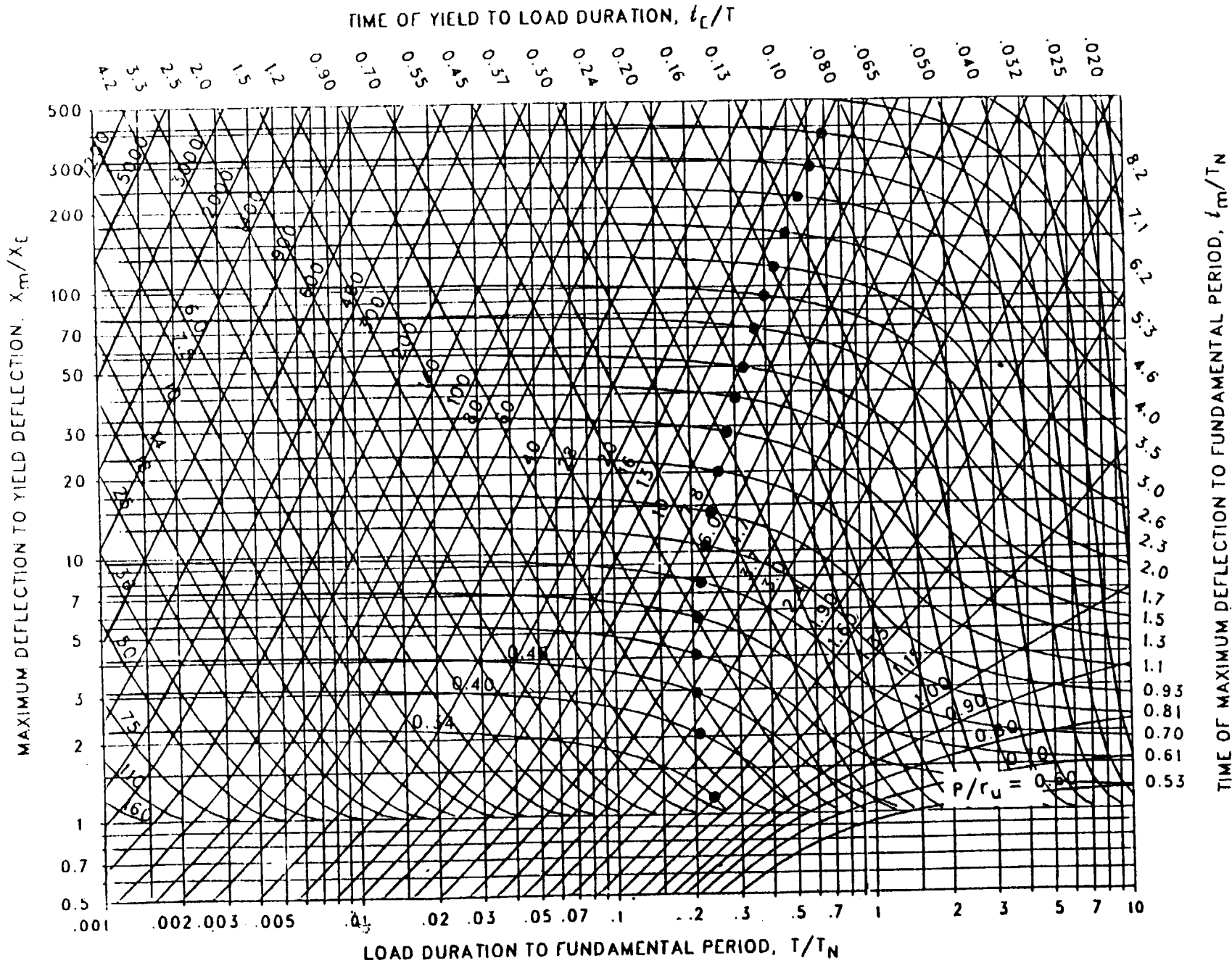
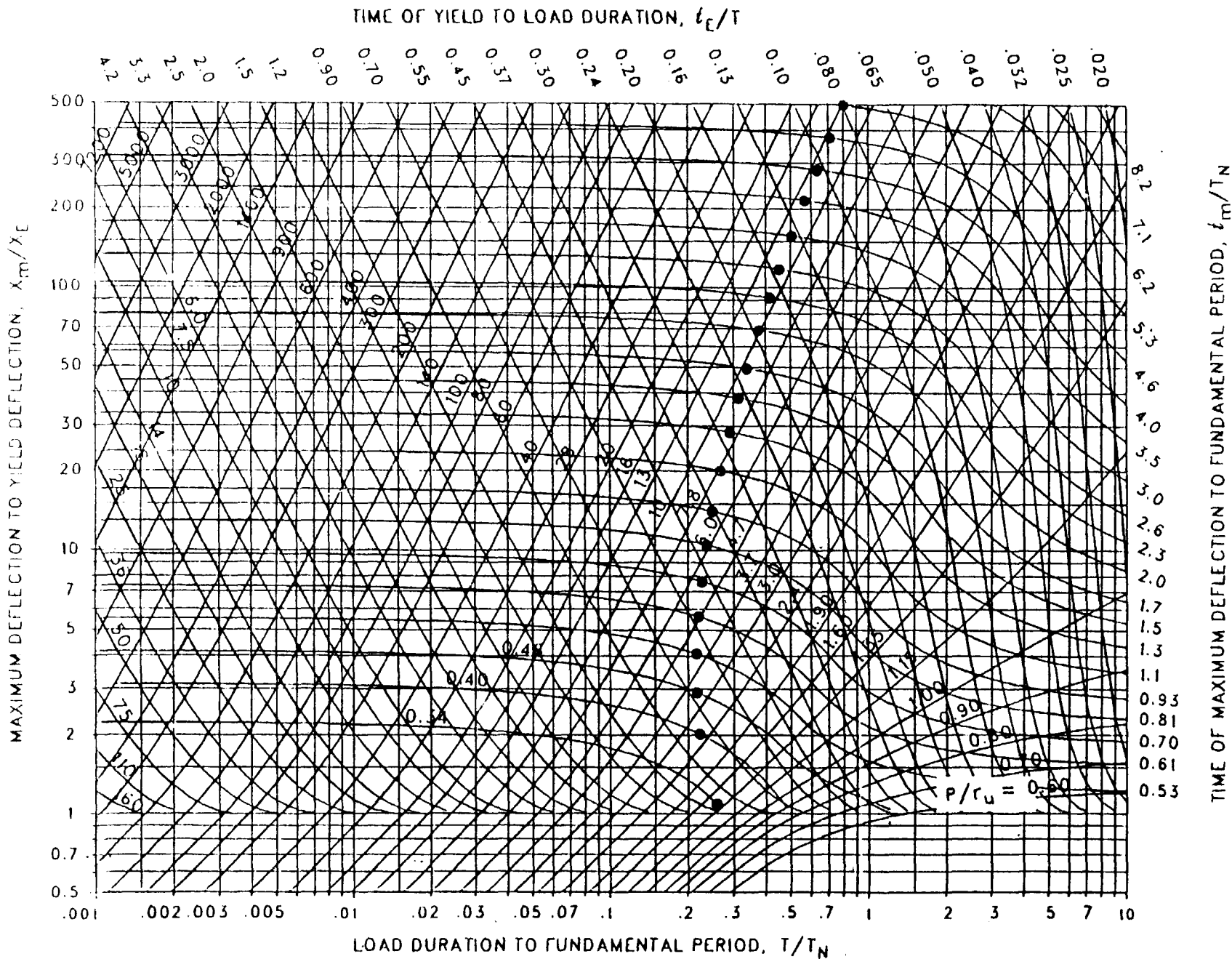


Figure 3-70 Maximum response of elasto-plastic, one-degree-of-freedom system for bilinear-triangular pulse ($C_1 = 0.100$, $C_2 = 1.7$)



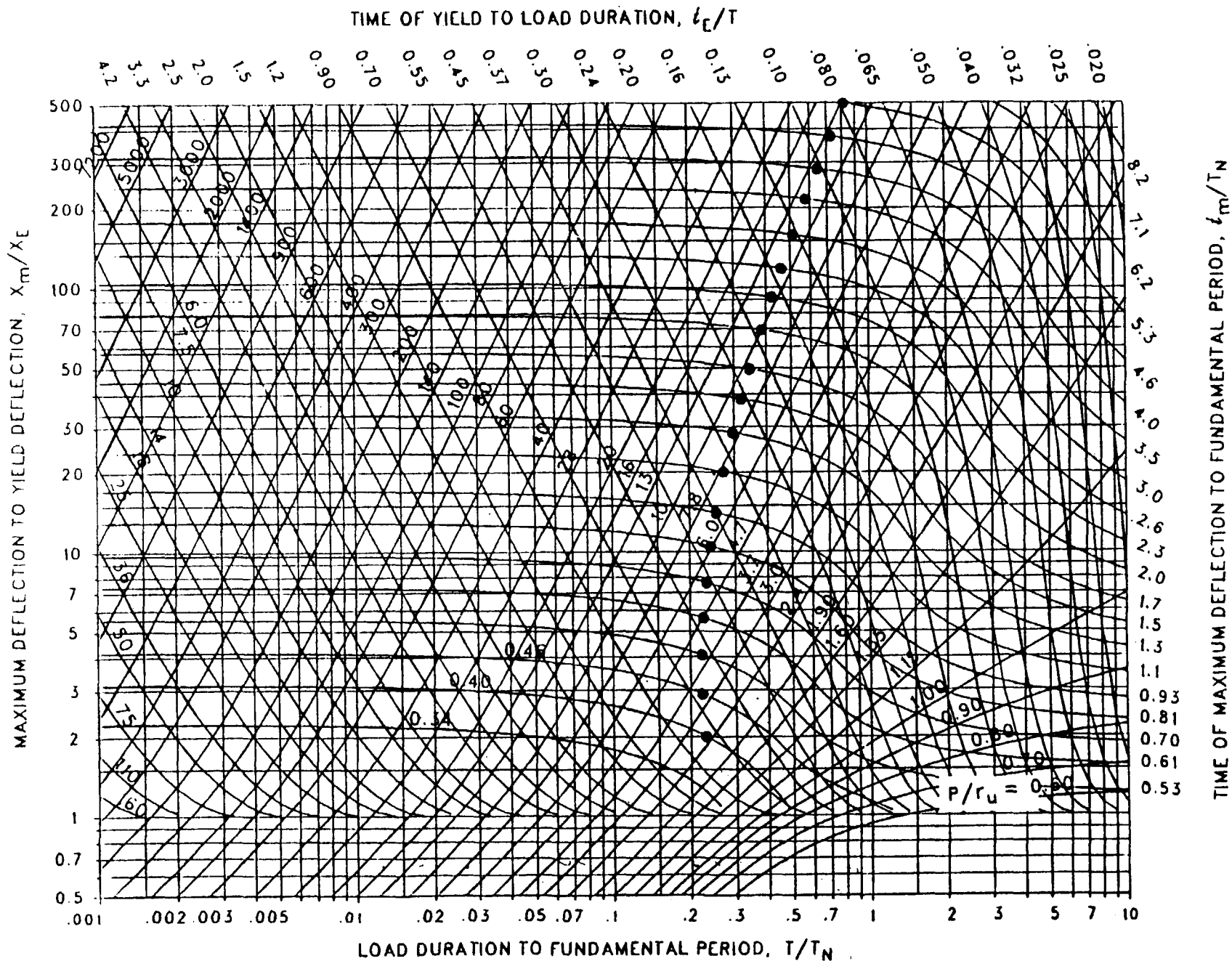


Figure 3-72

Maximum response of elasto-plastic, one-degree-of-freedom system for bilinear-triangular pulse ($C_1 = 0.032$, $C_2 = 1.7$)

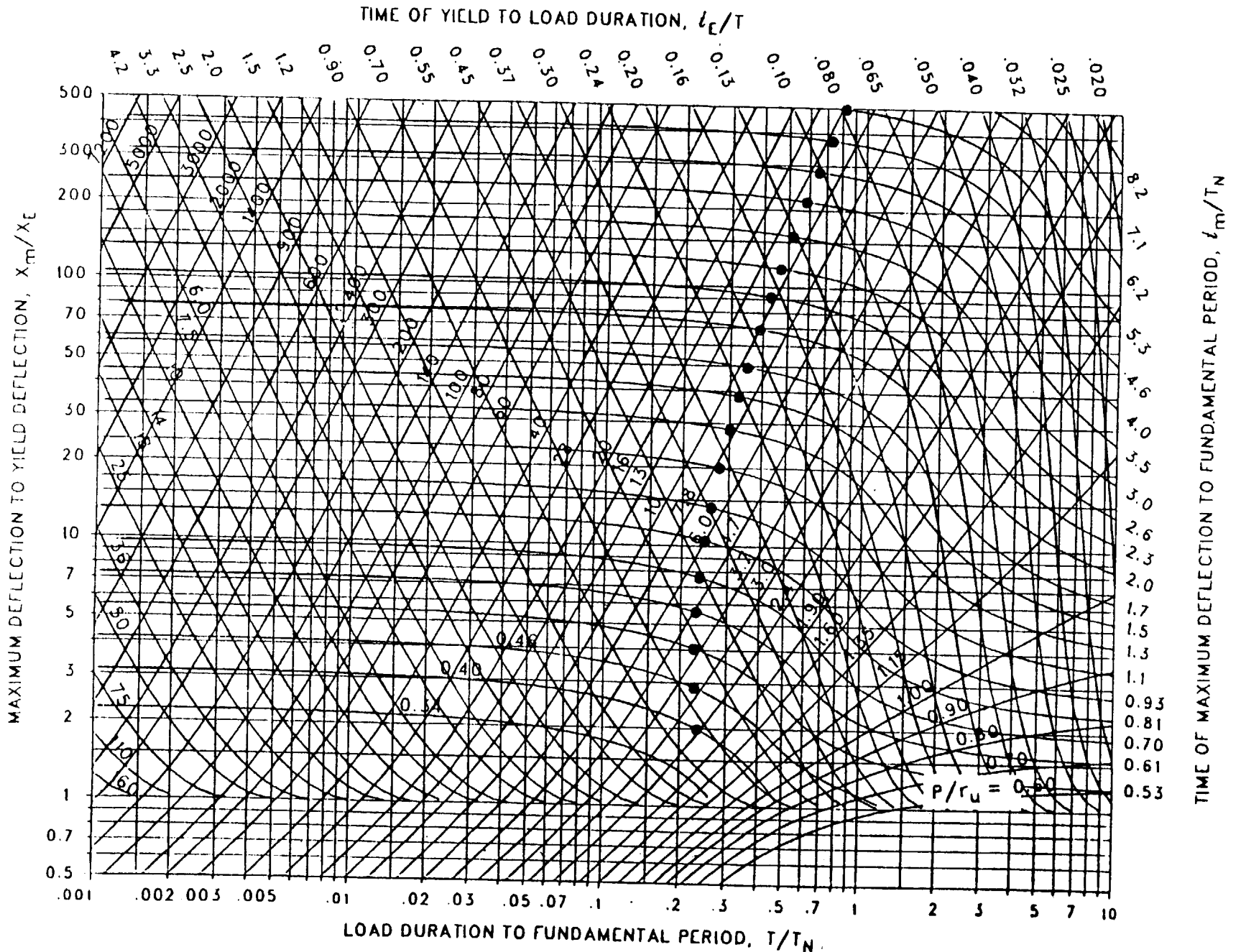


Figure 3-73 Maximum response of elasto-plastic, one-degree-of-freedom system for bilinear-triangular pulse ($C_1 = 0.018$, $C_2 = 1.7$)

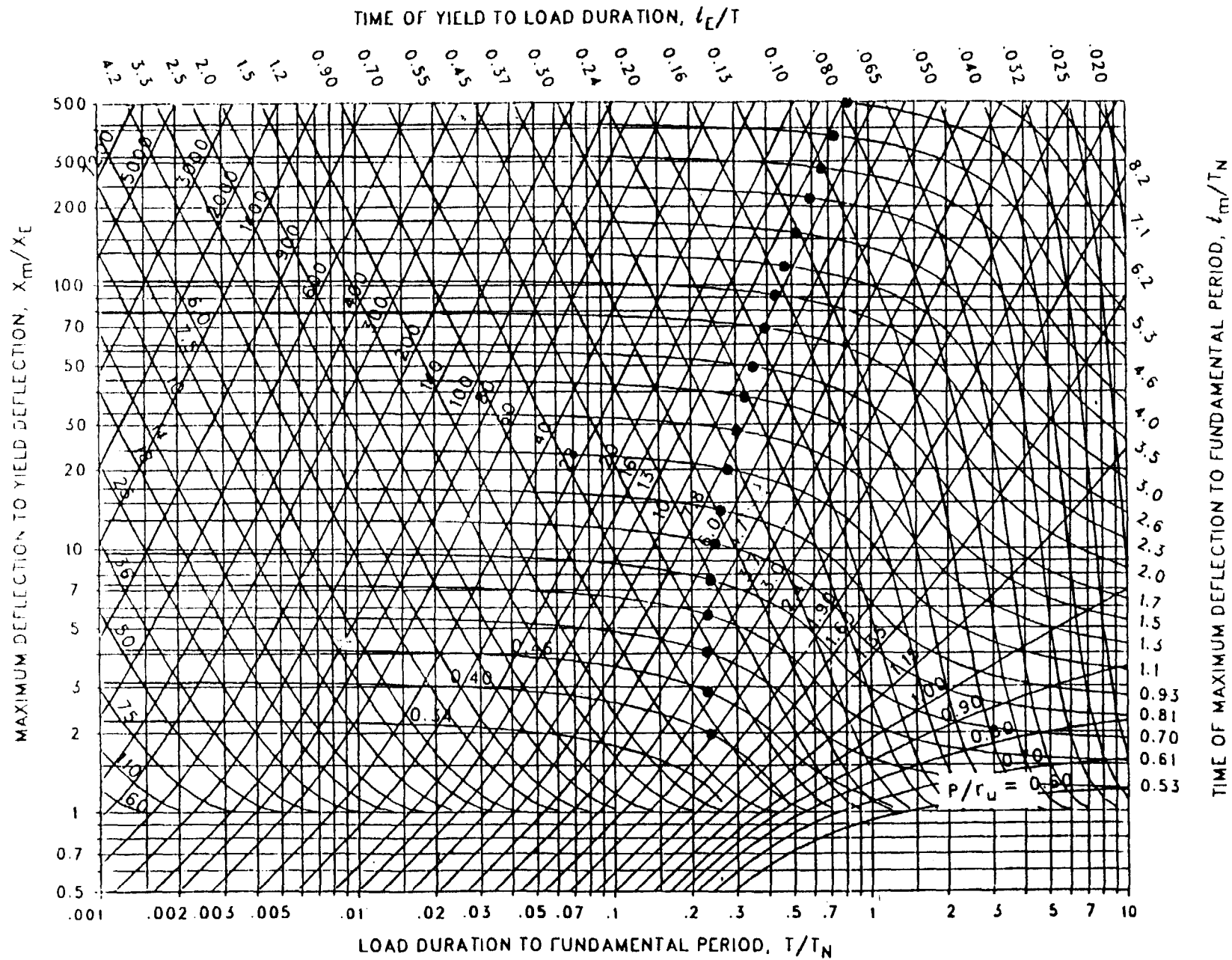


Figure 3-74 Maximum response of elasto-plastic, one-degree-of-freedom system for bilinear-triangular pulse ($C_1 = 0.010$, $C_2 = 1.7$)

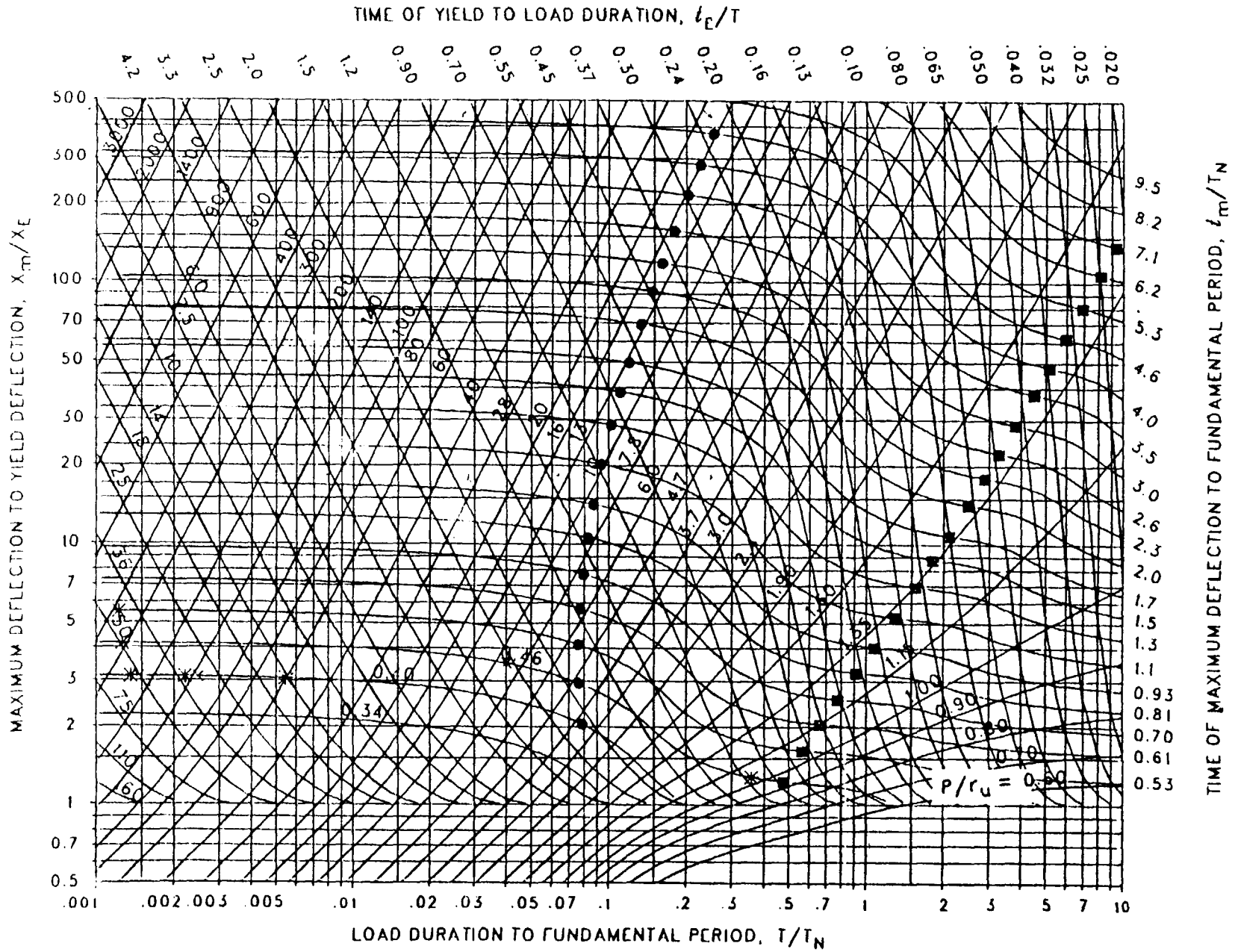


Figure 3-75 Maximum response of elasto-plastic, one-degree-of-freedom system for bilinear-triangular pulse ($C_1 = 0.681$, $C_2 = 3.0$)

3-134

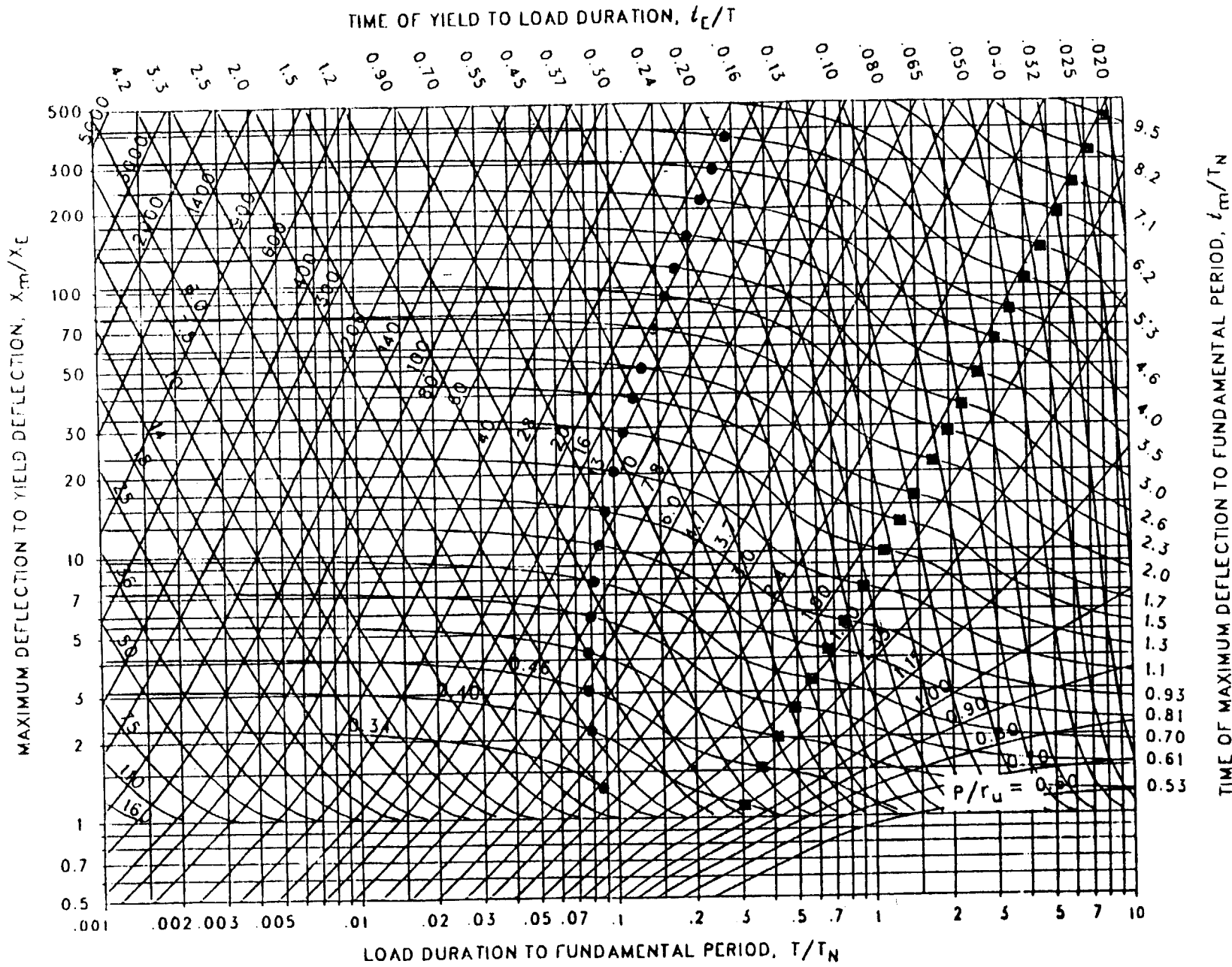


Figure 3-76 Maximum response of elasto-plastic, one-degree-of-freedom system for bilinear-triangular pulse ($C_1 = 0.464$, $C_2 = 3.0$)

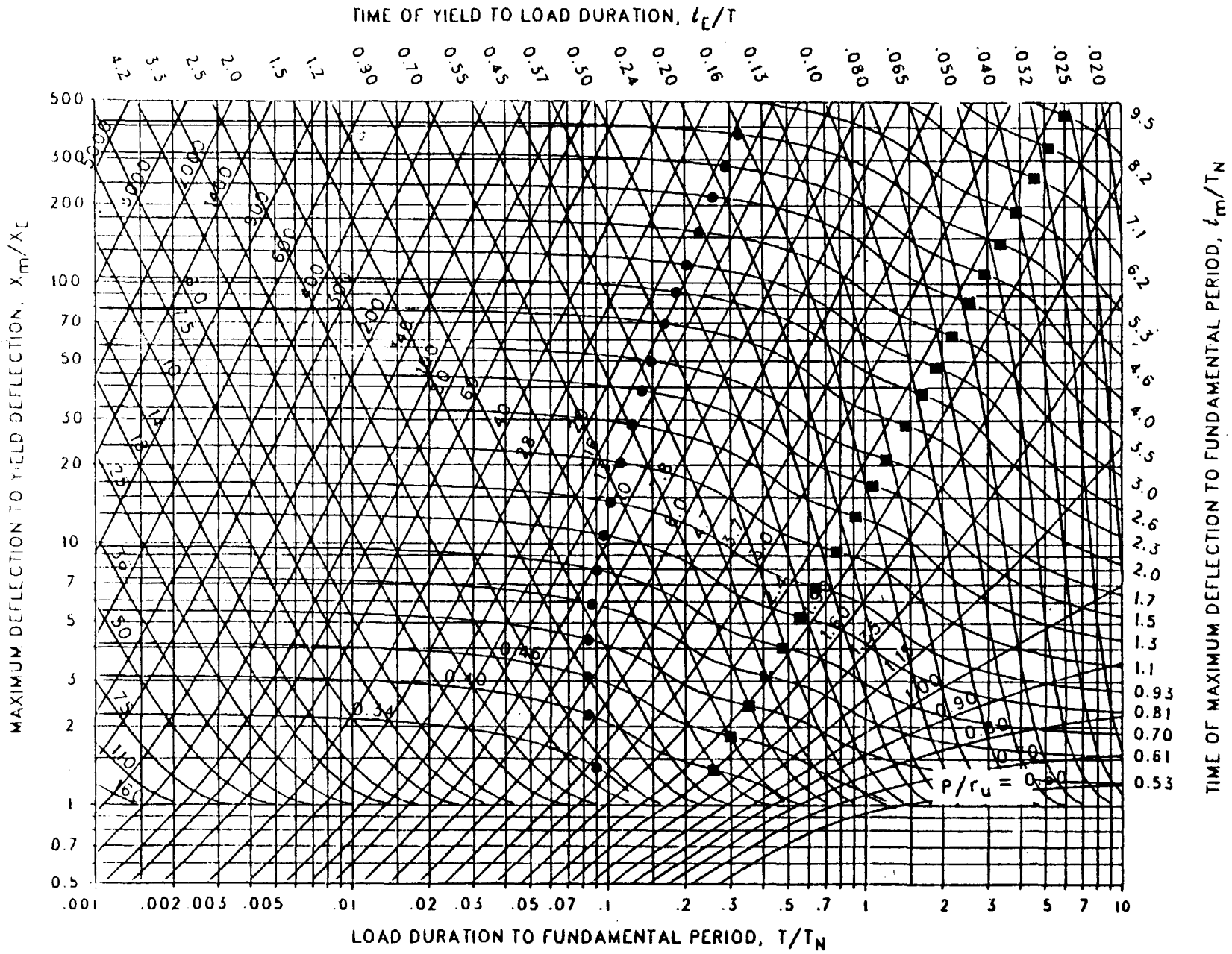


Figure 3-77 Maximum response of elasto-plastic, one-degree-of-freedom system for bilinear-triangular pulse ($C_1 = 0.316$, $C_2 = 3.0$)

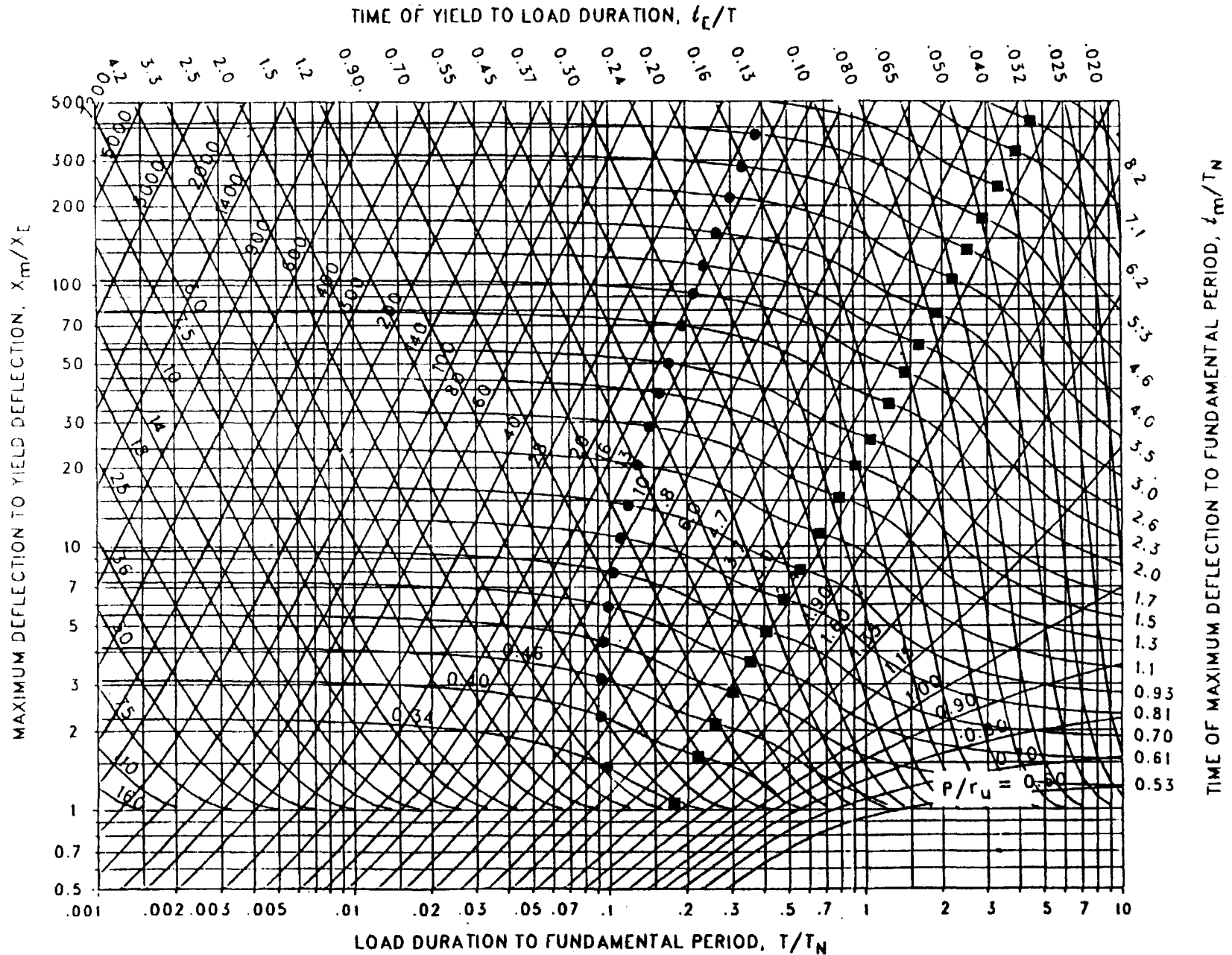


Figure 3-78 Maximum response of elasto-plastic, one-degree-of-freedom system for bilinear-triangular pulse ($C_1 = 1.215$, $C_2 = 3.0$)

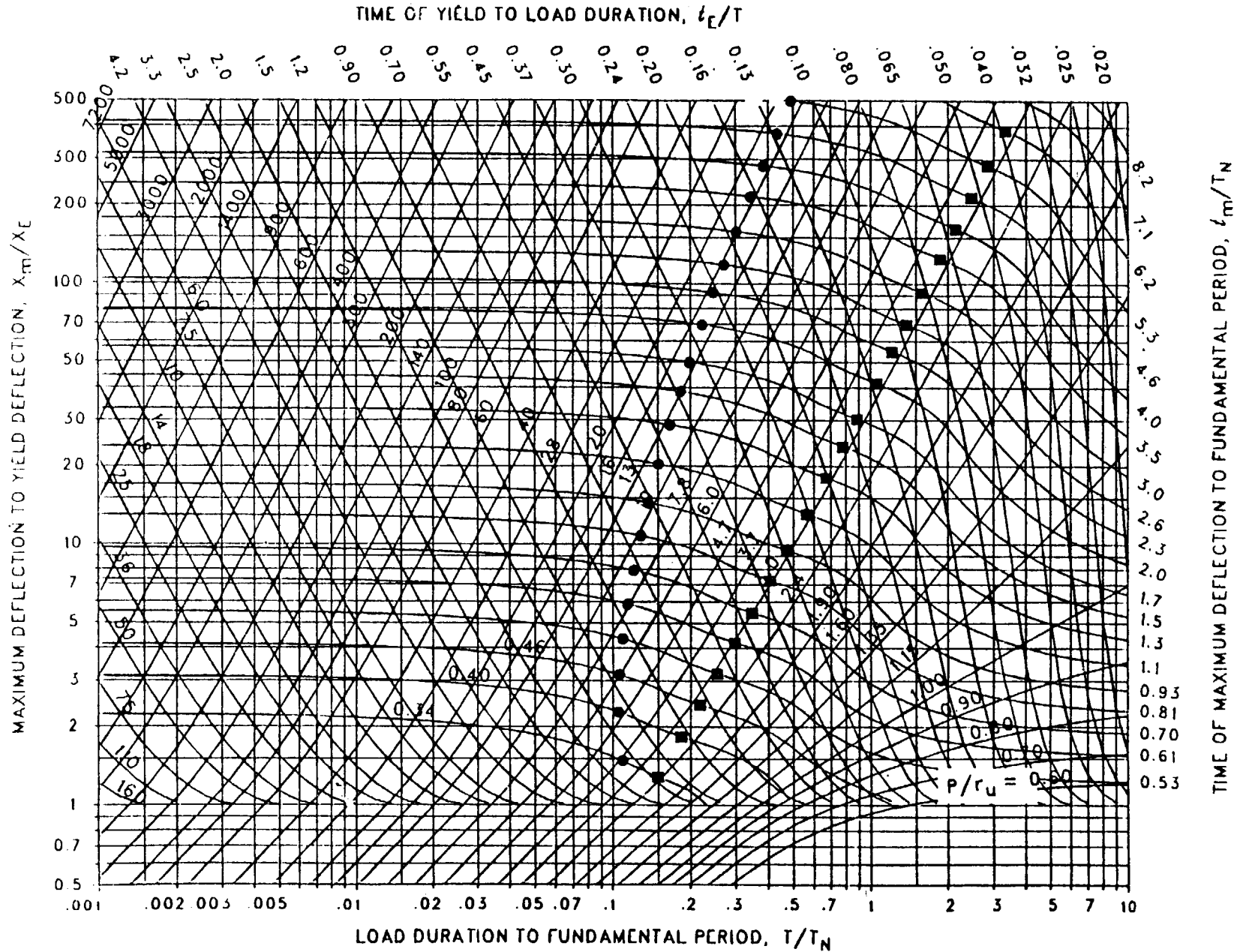


Figure 3-79 Maximum response of elasto-plastic, one-degree-of-freedom system for bilinear-triangular pulse ($C_1 = 0.147$, $C_2 = 3.0$)

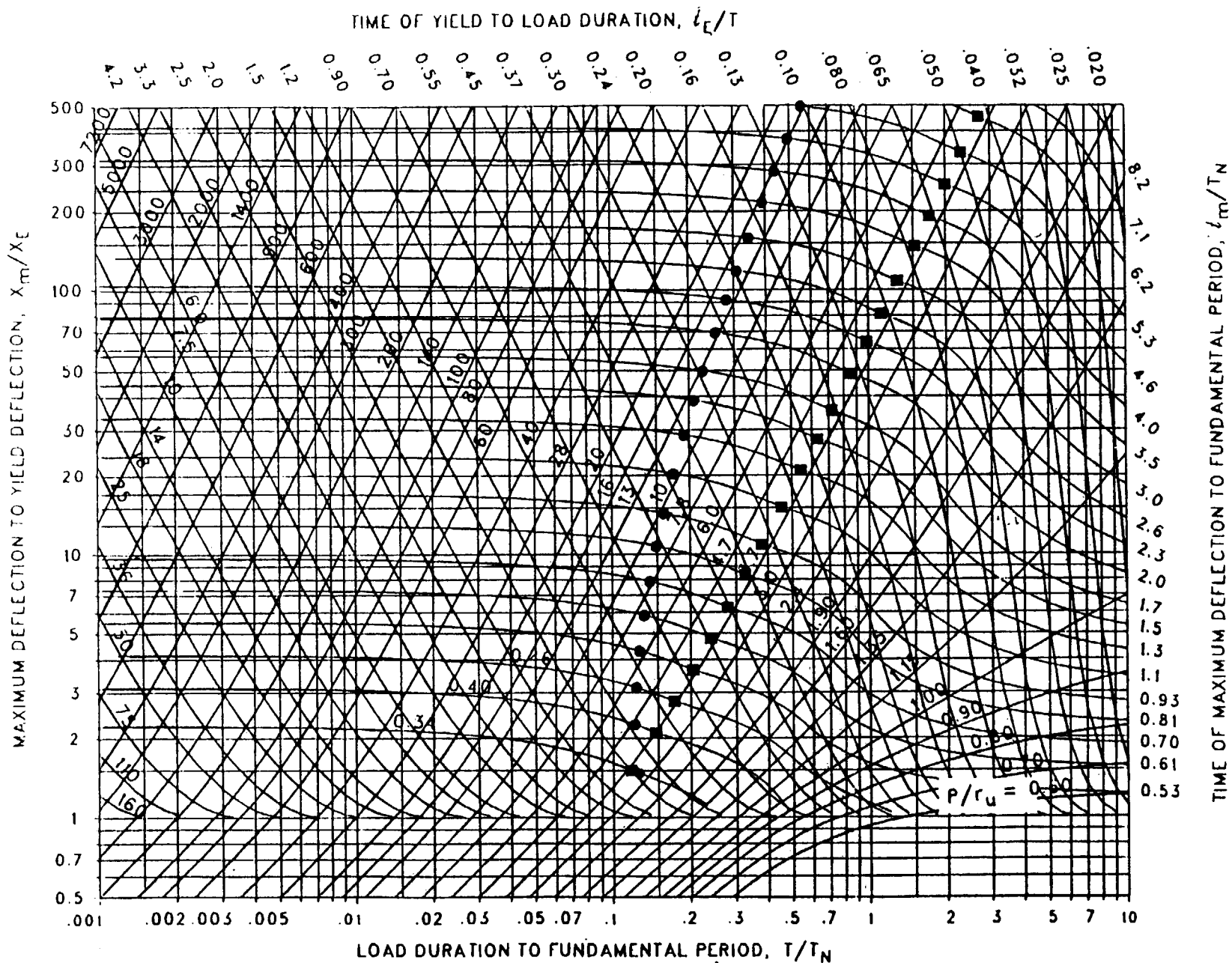


Figure 3-80 Maximum response of elasto-plastic, one-degree-of-freedom system for bilinear-triangular pulse ($C_1 = 0.100$, $C_2 = 3.0$)

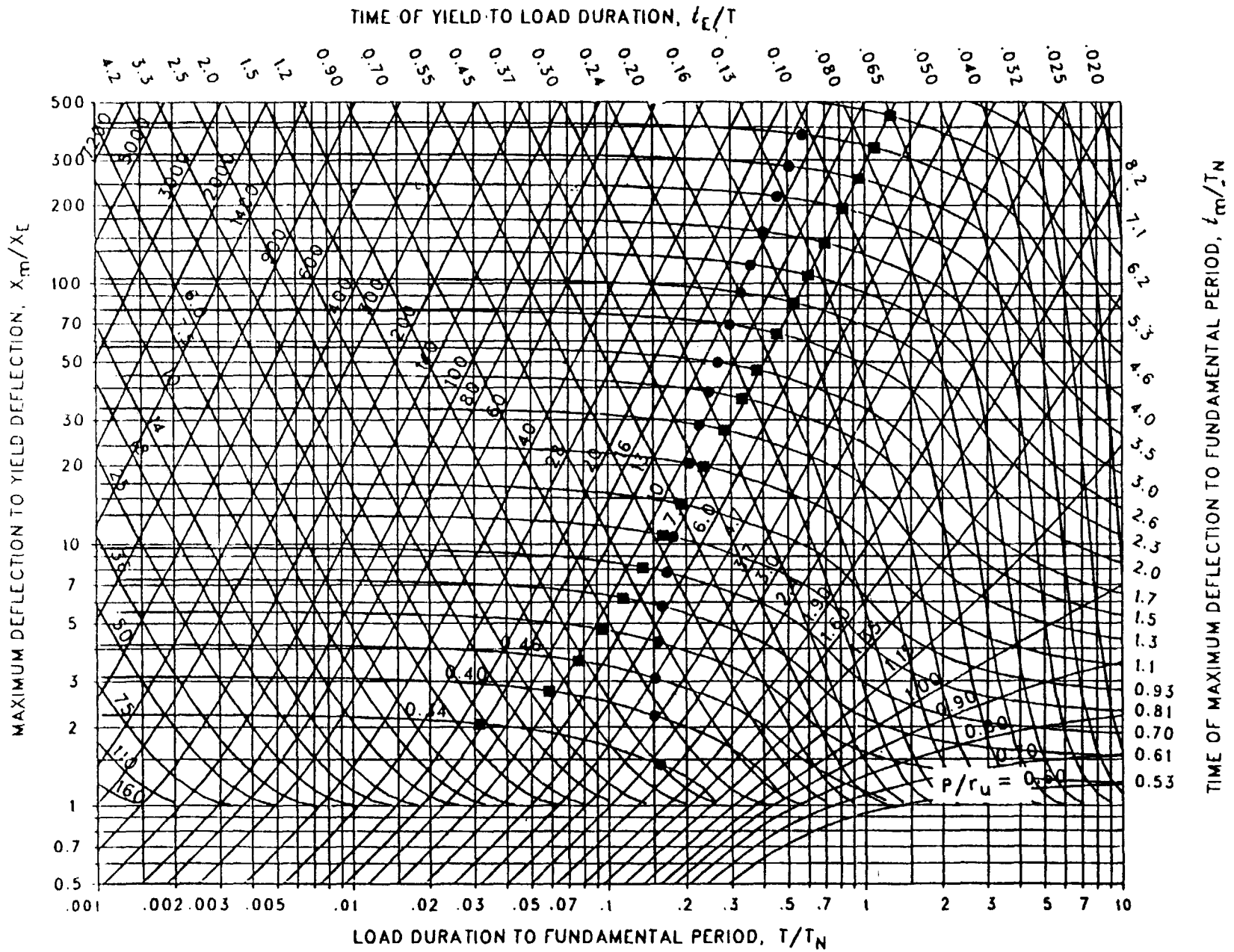


Figure 3-81 Maximum response of elasto-plastic, one-degree-of-freedom system for bilinear-triangular pulse ($C_1 = 0.056$, $C_2 = 3.0$)

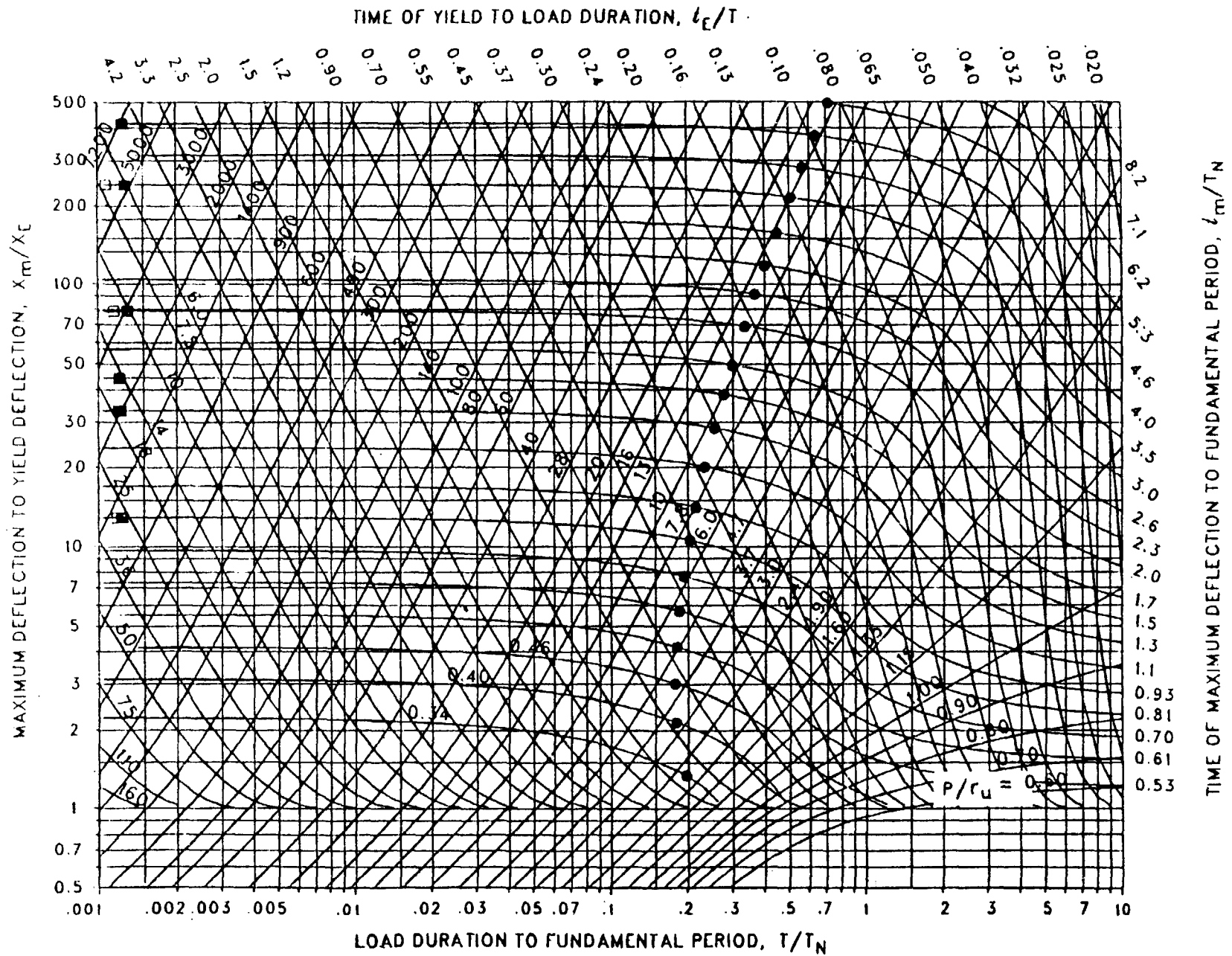


Figure 3-82 Maximum response of elasto-plastic, one-degree-of-freedom system for bilinear-triangular pulse ($C_1 = 0.032$, $C_2 = 3.0$)

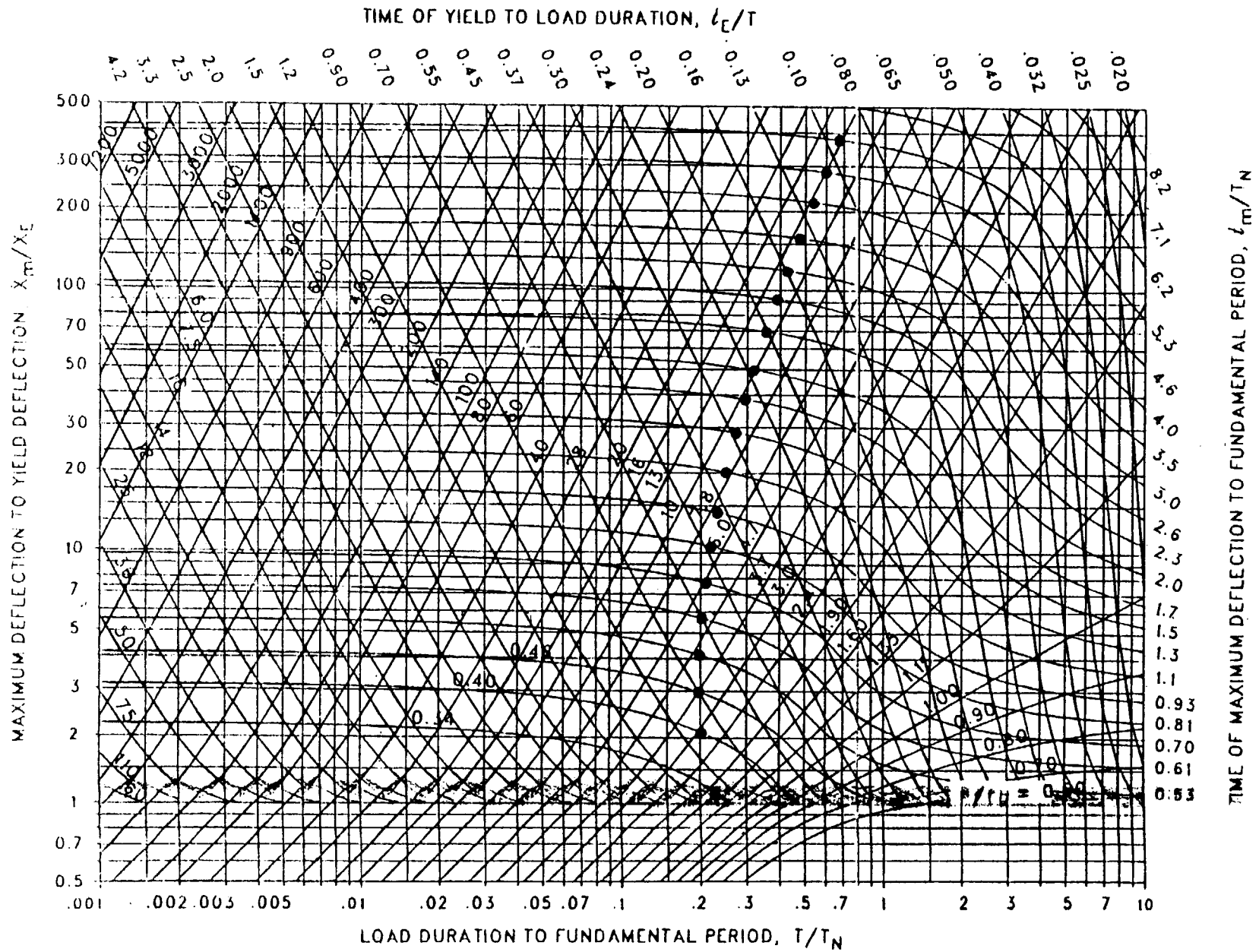


Figure 3-83 Maximum response of elasto-plastic, one-degree-of-freedom system for bilinear-triangular pulse ($C_1 = 0.018$, $C_2 = 3.0$)

3-142

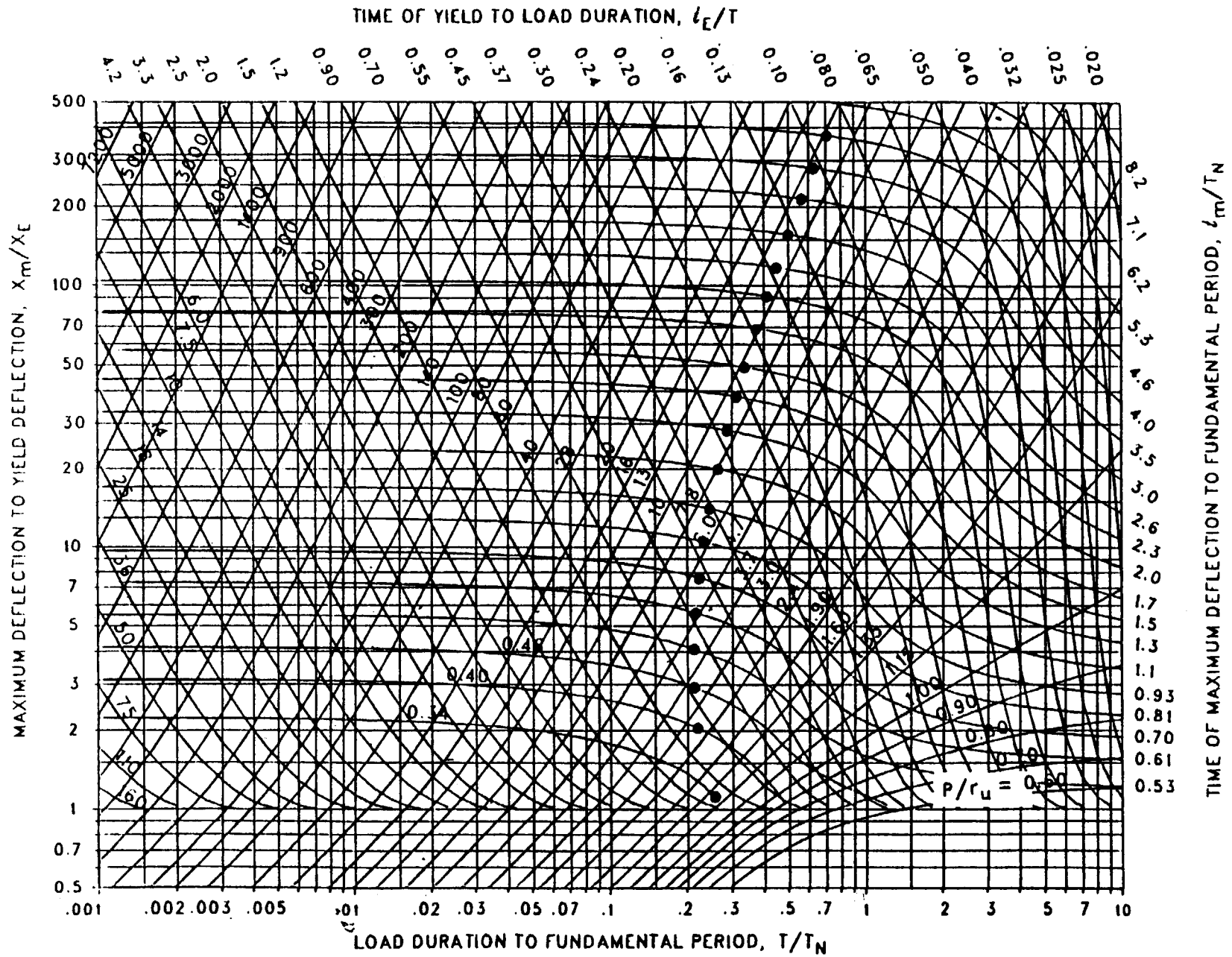


Figure 3-84

Maximum response of elasto-plastic, one-degree-of-freedom system for bilinear-triangular pulse ($C_1 = 0.010$, $C_2 = 3.0$)

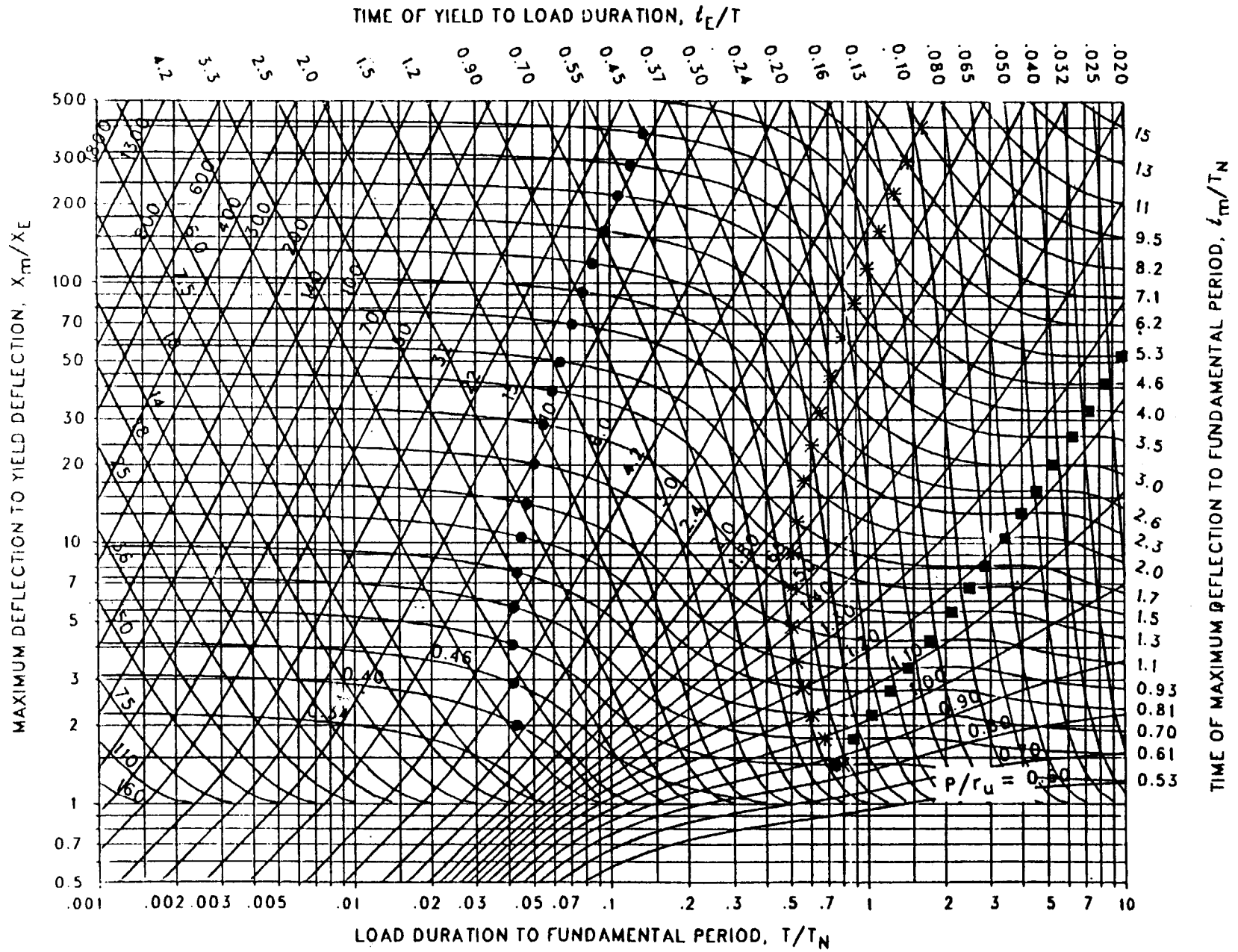


Figure 3-85 Maximum response of elasto-plastic, one-degree-of-freedom system for bilinear-triangular pulse ($C_1 = 0.750$, $C_2 = 5.5$)

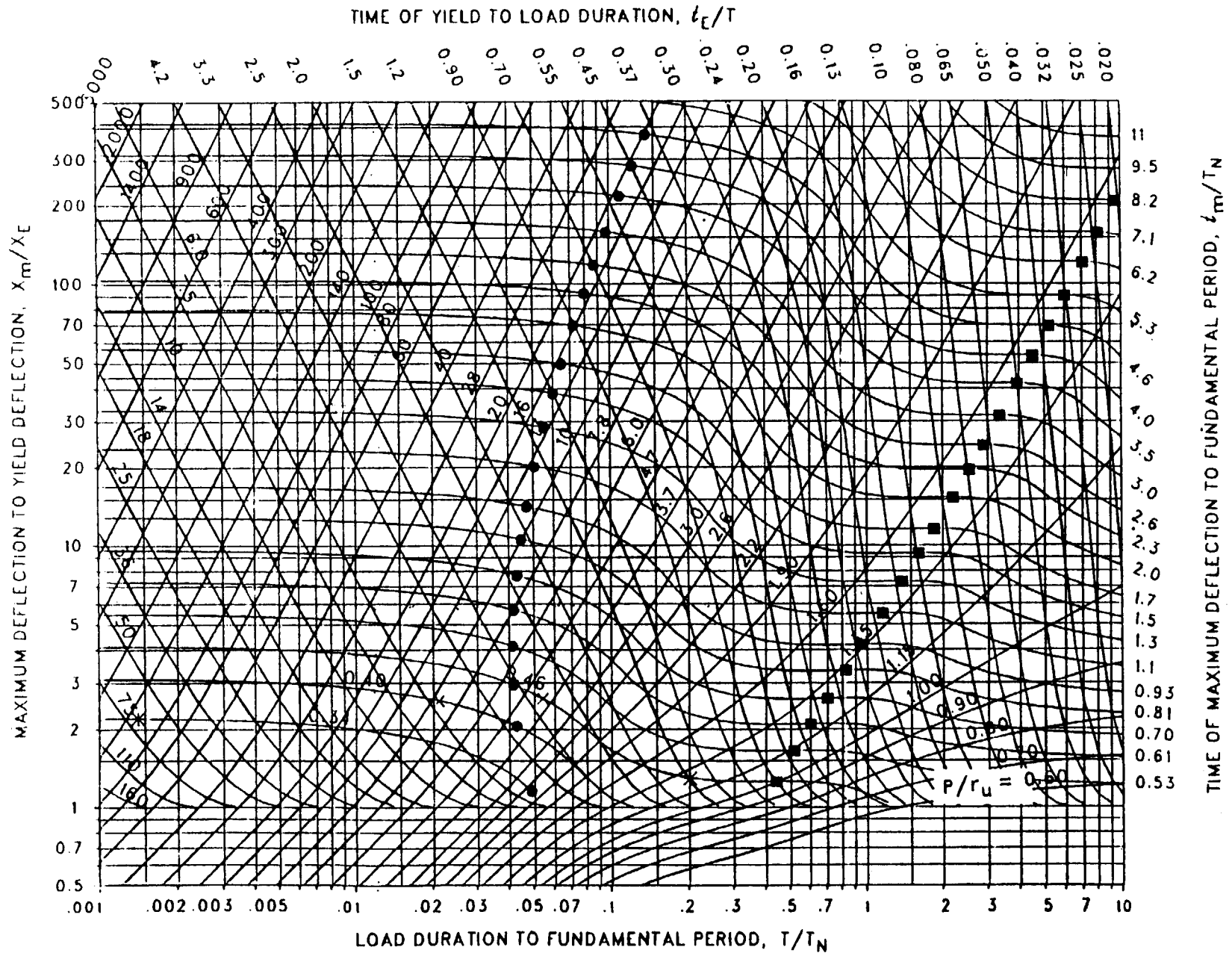


Figure 3-86 Maximum response of elasto-plastic, one-degree-of-freedom system for bilinear-triangular pulse ($C_1 = 0.562$, $C_2 = 5.5$)

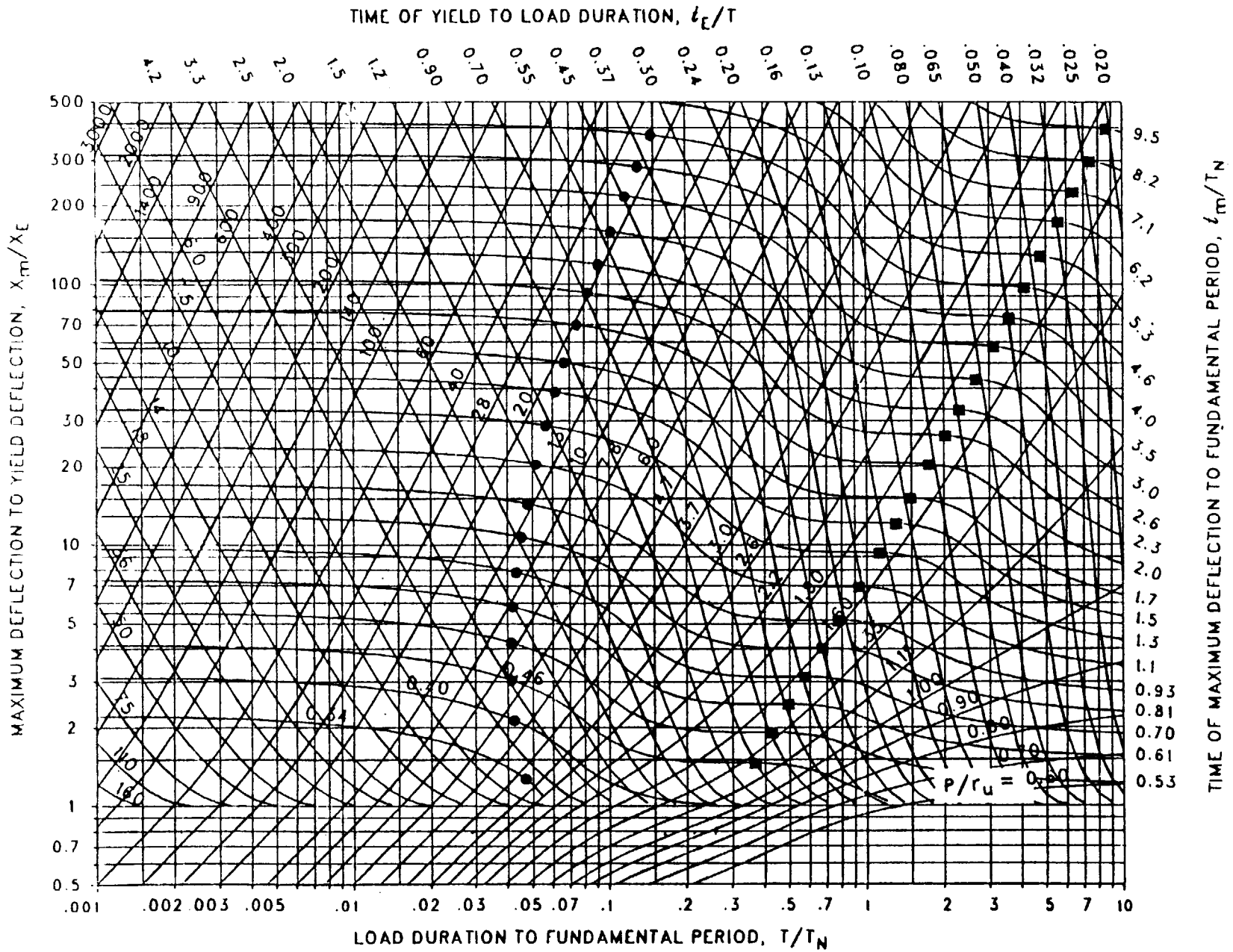


Figure 3-87 Maximum response of elasto-plastic, one-degree-of-freedom system for bilinear-triangular pulse ($C_1 = 0.422$, $C_2 = 5.5$)

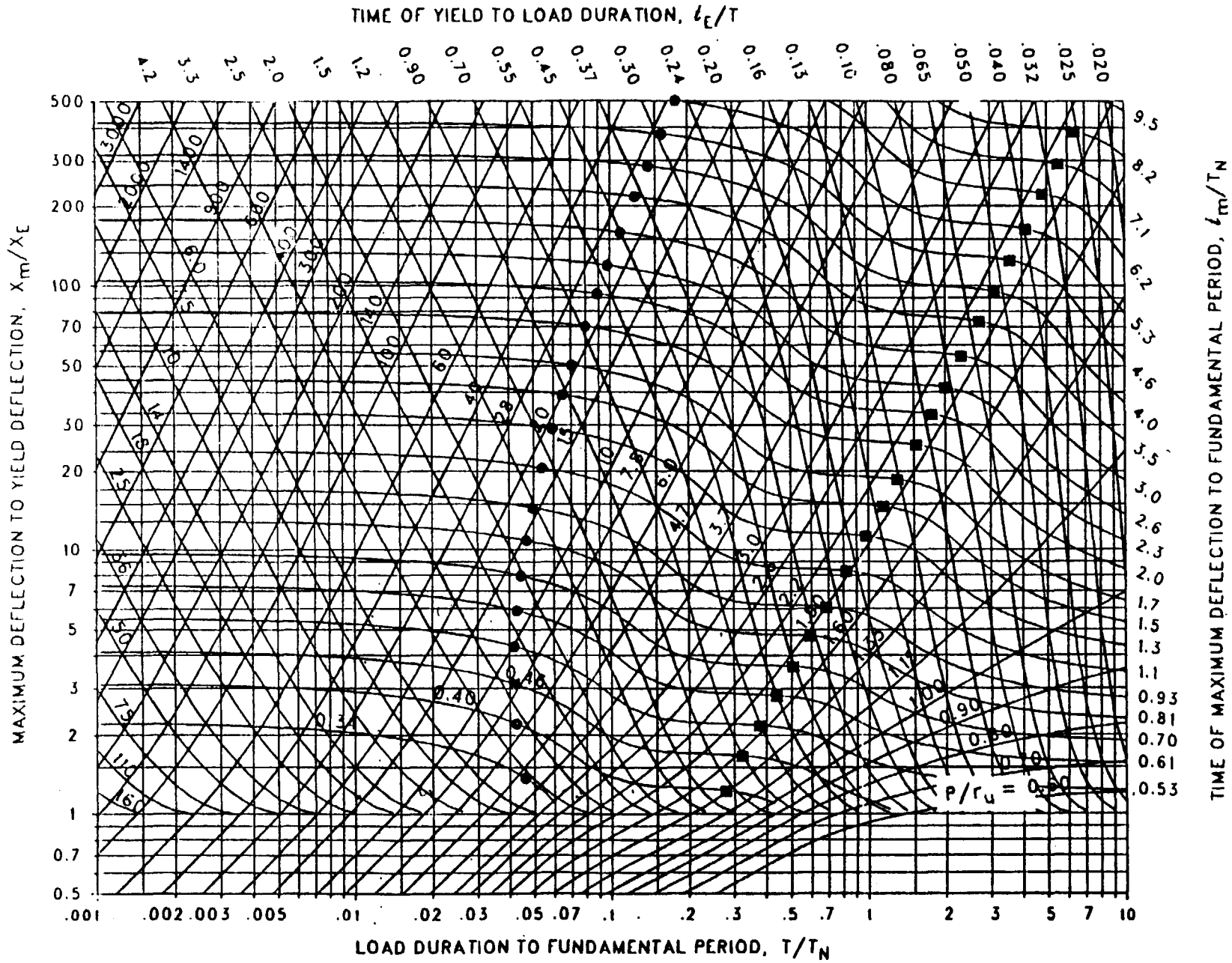


Figure 3-88 Maximum response of elasto-plastic, one-degree-of-freedom system for bilinear-triangular pulse ($C_1 = 0.316$, $C_2 = 5.5$)

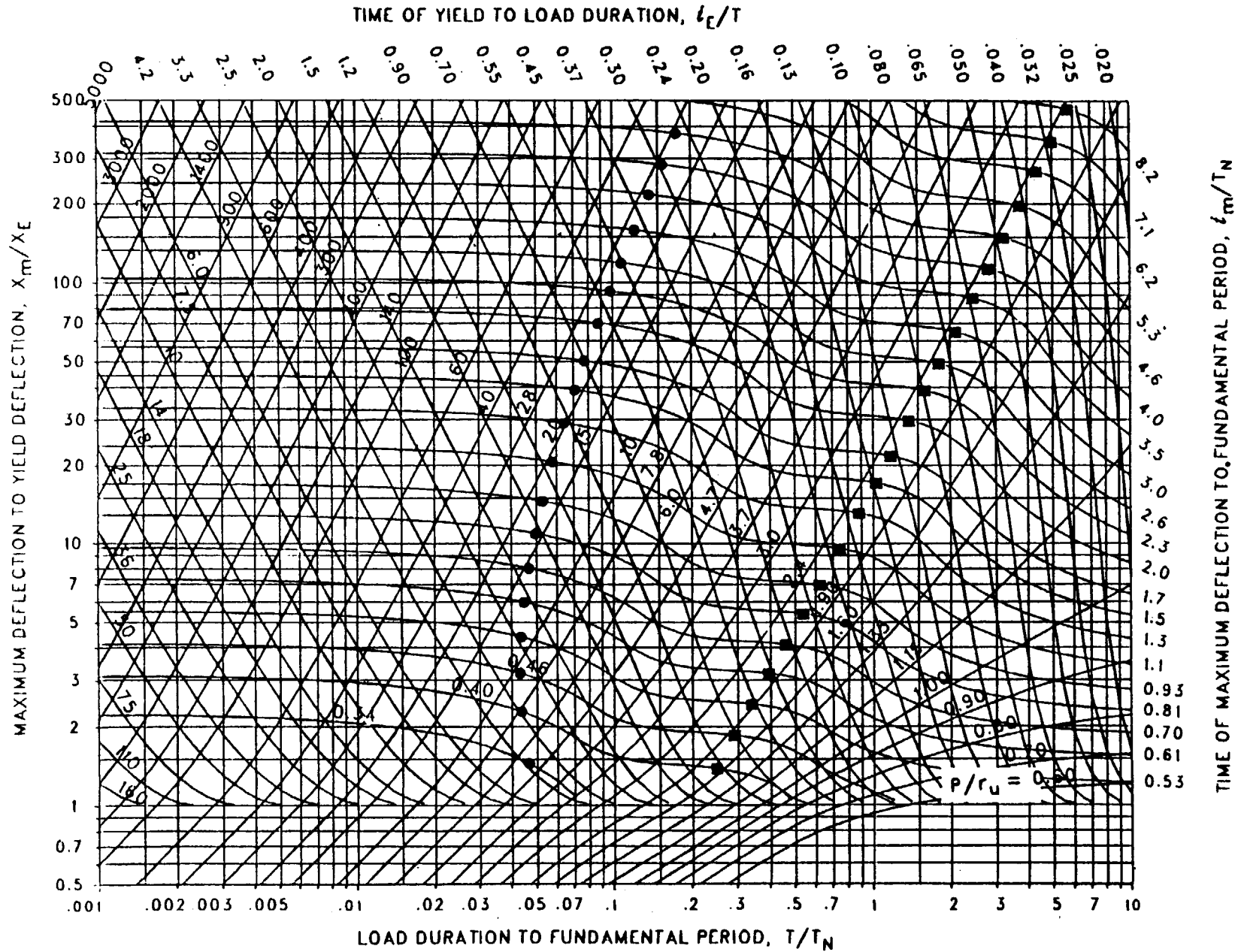


Figure 3-89 Maximum response of elasto-plastic, one-degree-of-freedom system for bilinear-triangular pulse ($C_1 = 0.237$, $C_2 = 5.5$)

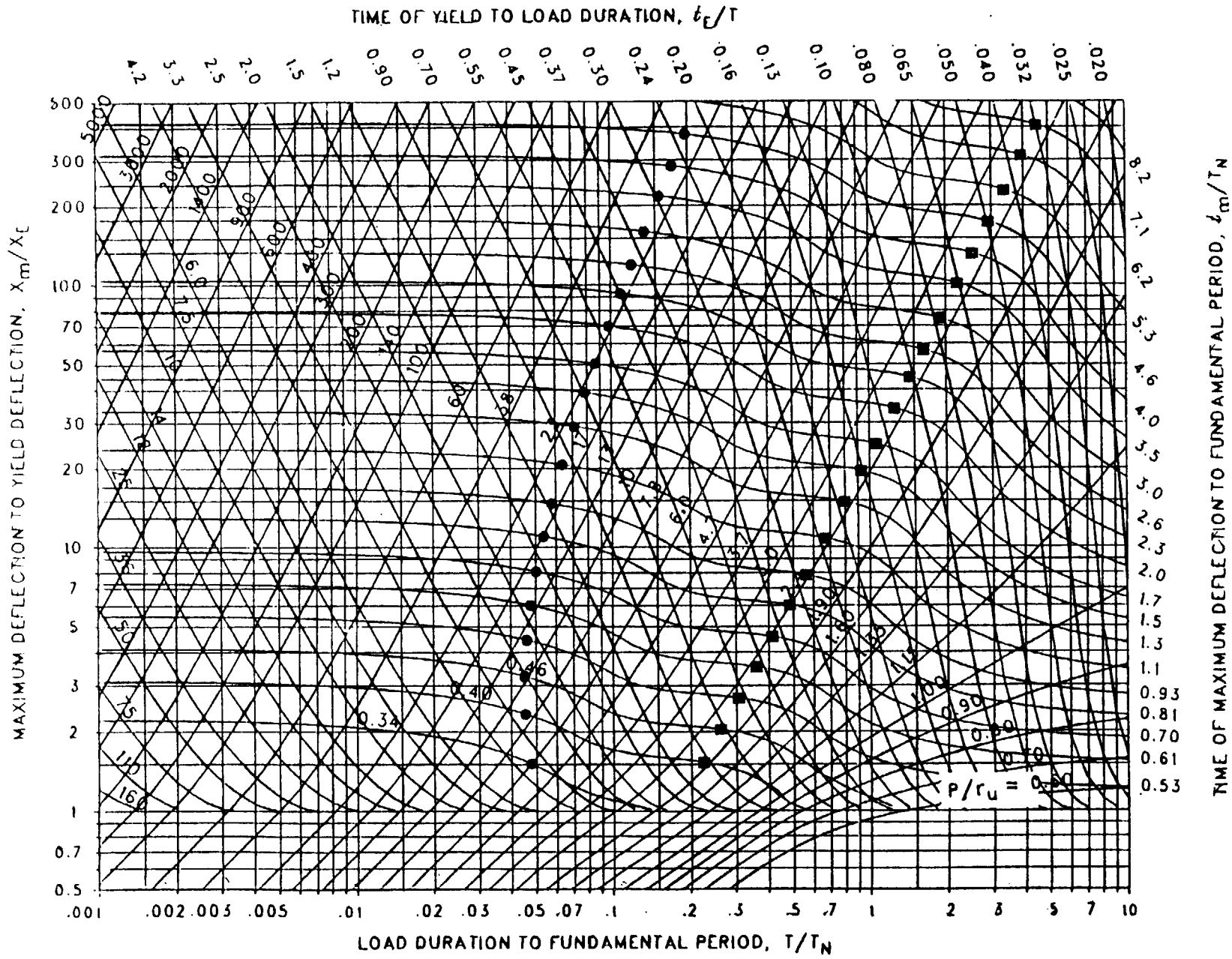


Figure 3-90 Maximum response of elasto-plastic, one-degree-of-freedom system for bilinear-triangular pulse ($C_1 = 0.178$, $C_2 = 5.5$)

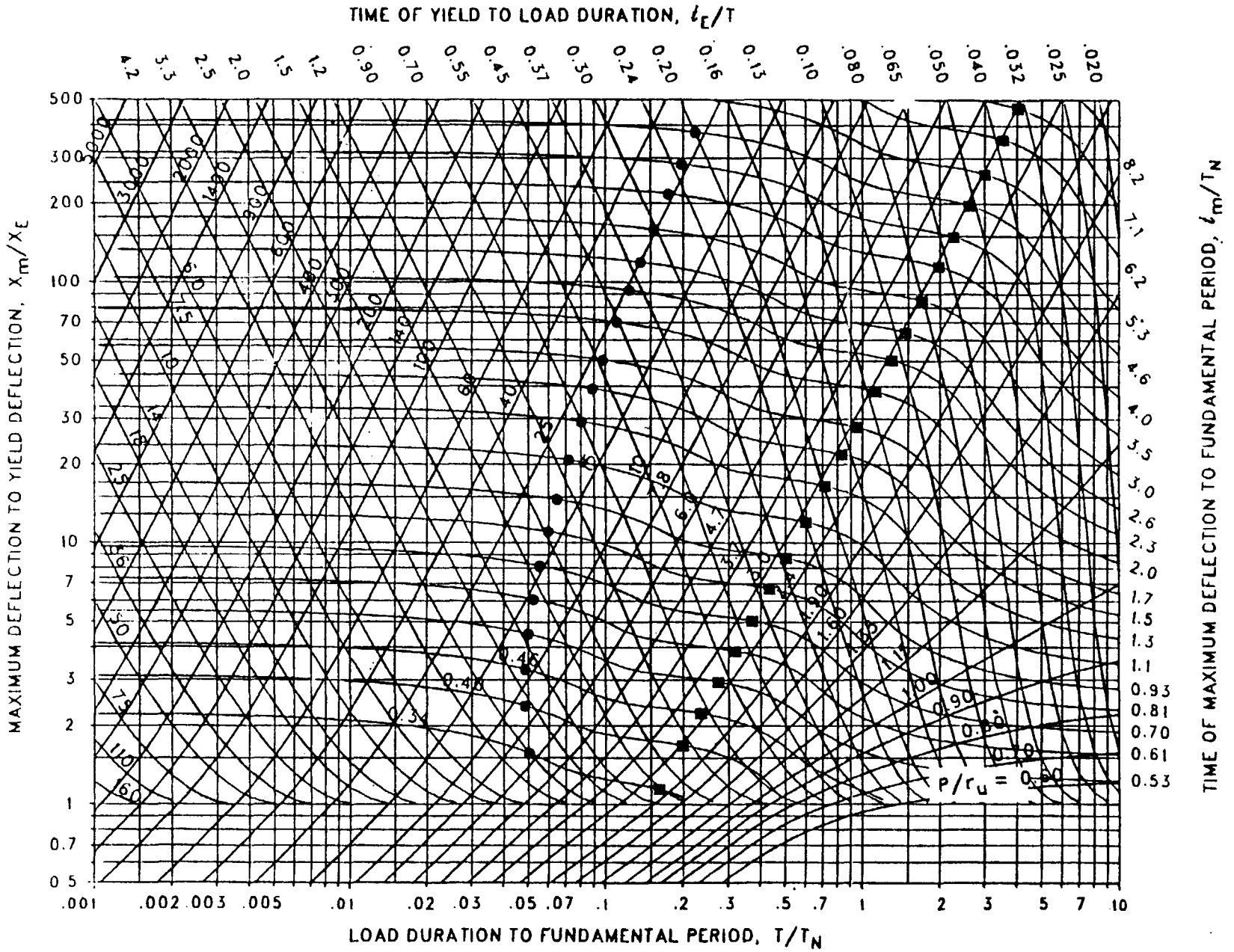


Figure 3-91 Maximum response of elasto-plastic, one-degree-of-freedom system for bilinear-triangular pulse ($C_1 = 0.133$, $C_2 = 5.5$)

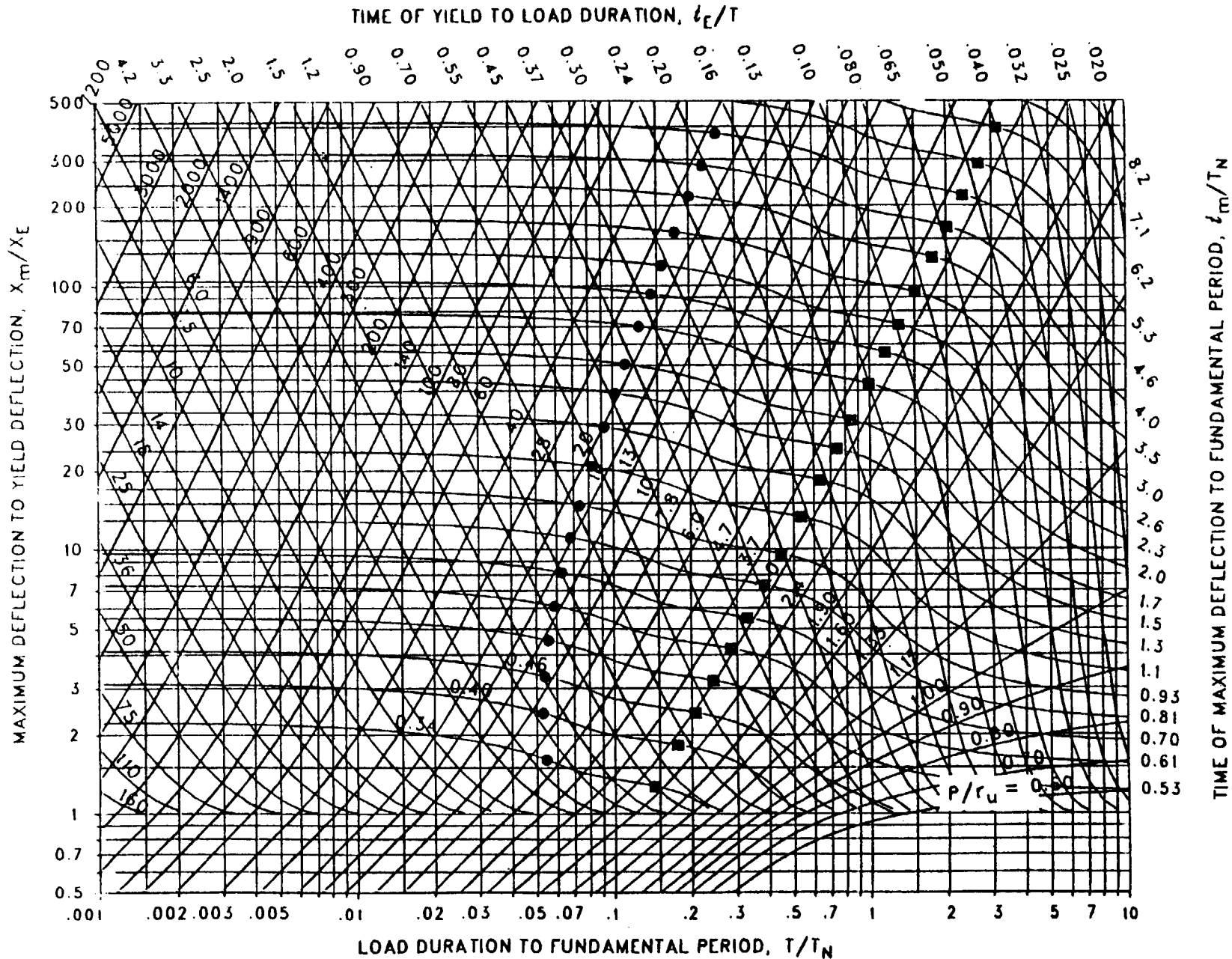


Figure 3-92 Maximum response of elasto-plastic, one-degree-of-freedom system for bilinear-triangular pulse ($C_1 = 0.100$, $C_2 = 5.5$)

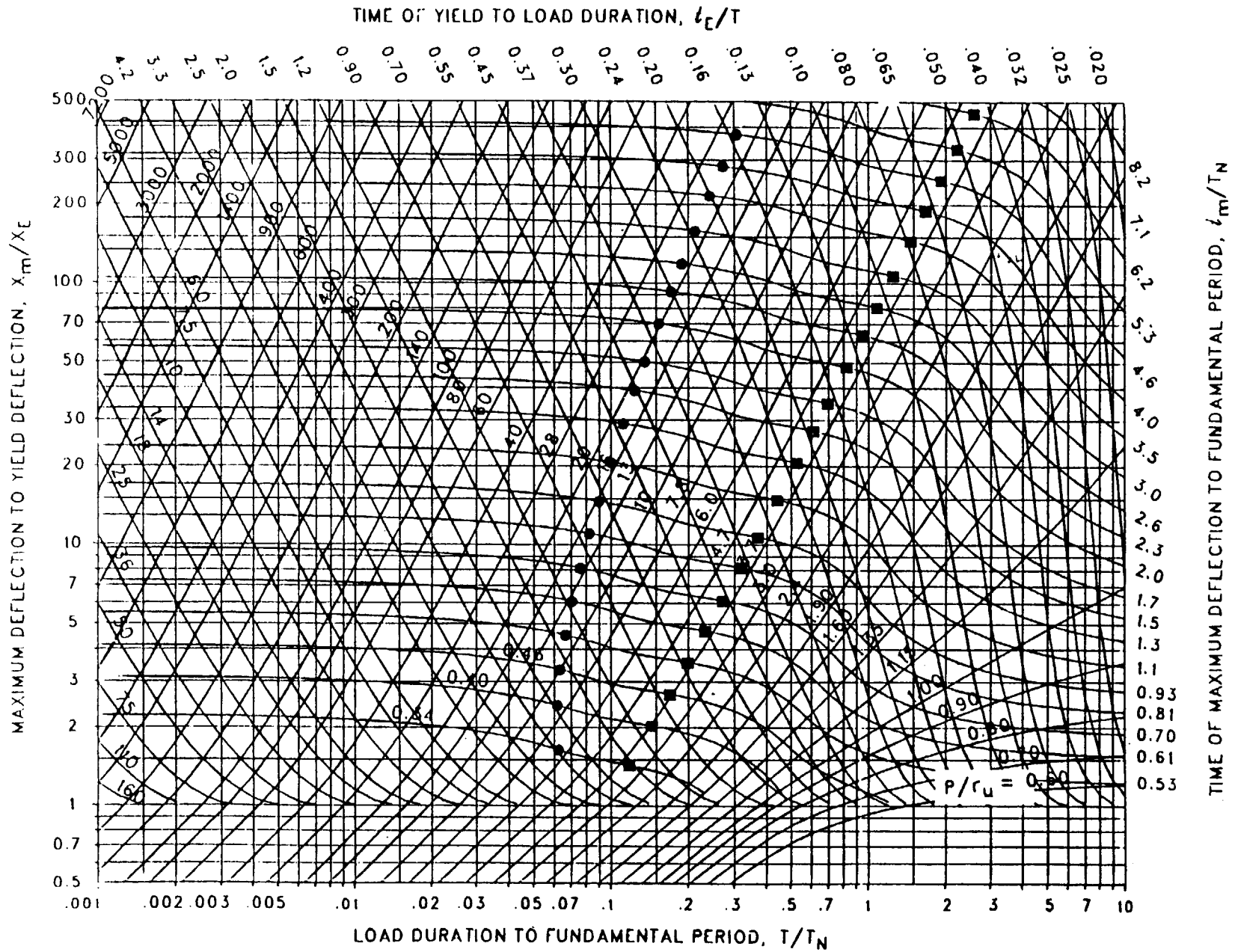


Figure 3-93 Maximum response of elasto-plastic, one-degree-of-freedom system for bilinear-triangular pulse ($C_1 = 0.068$, $C_2 = 5.5$)

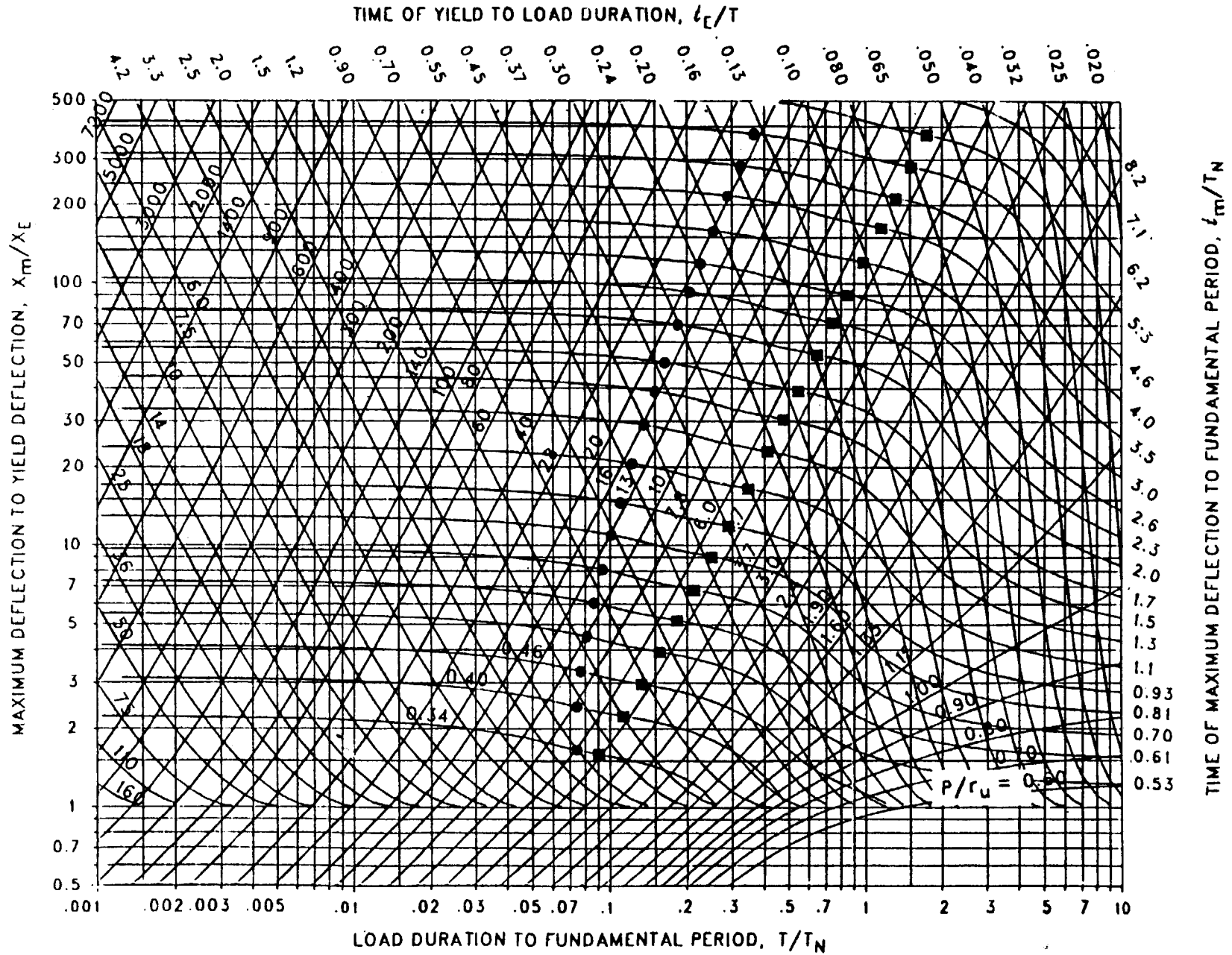


Figure 3-94 Maximum response of elasto-plastic, one-degree-of-freedom system for bilinear-triangular pulse ($C_1 = 0.046$, $C_2 = 5.5$)

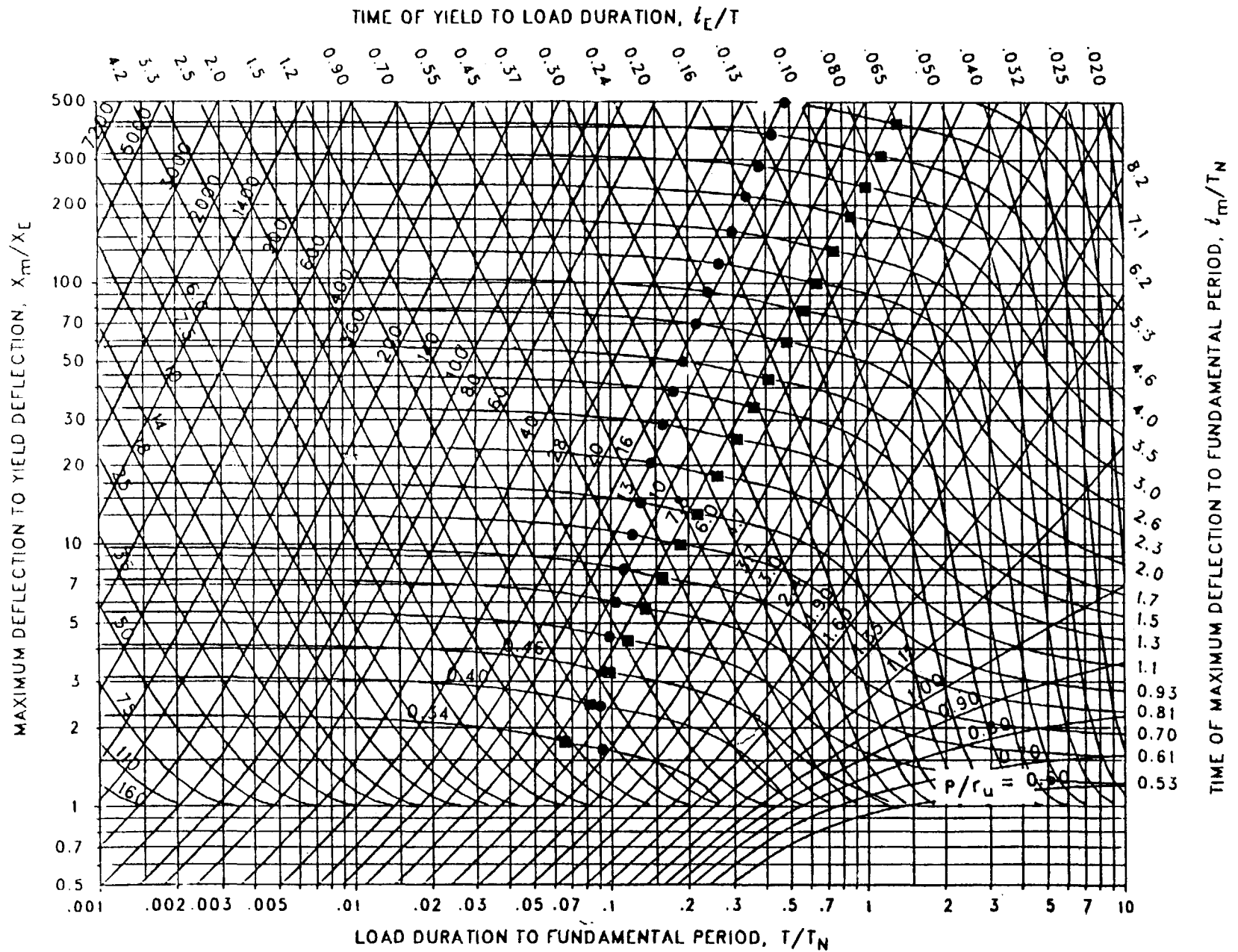


Figure 3-95 Maximum response of elasto-plastic, one-degree-of-freedom system for bilinear-triangular pulse ($C_1 = 0.032$, $C_2 = 5.5$)

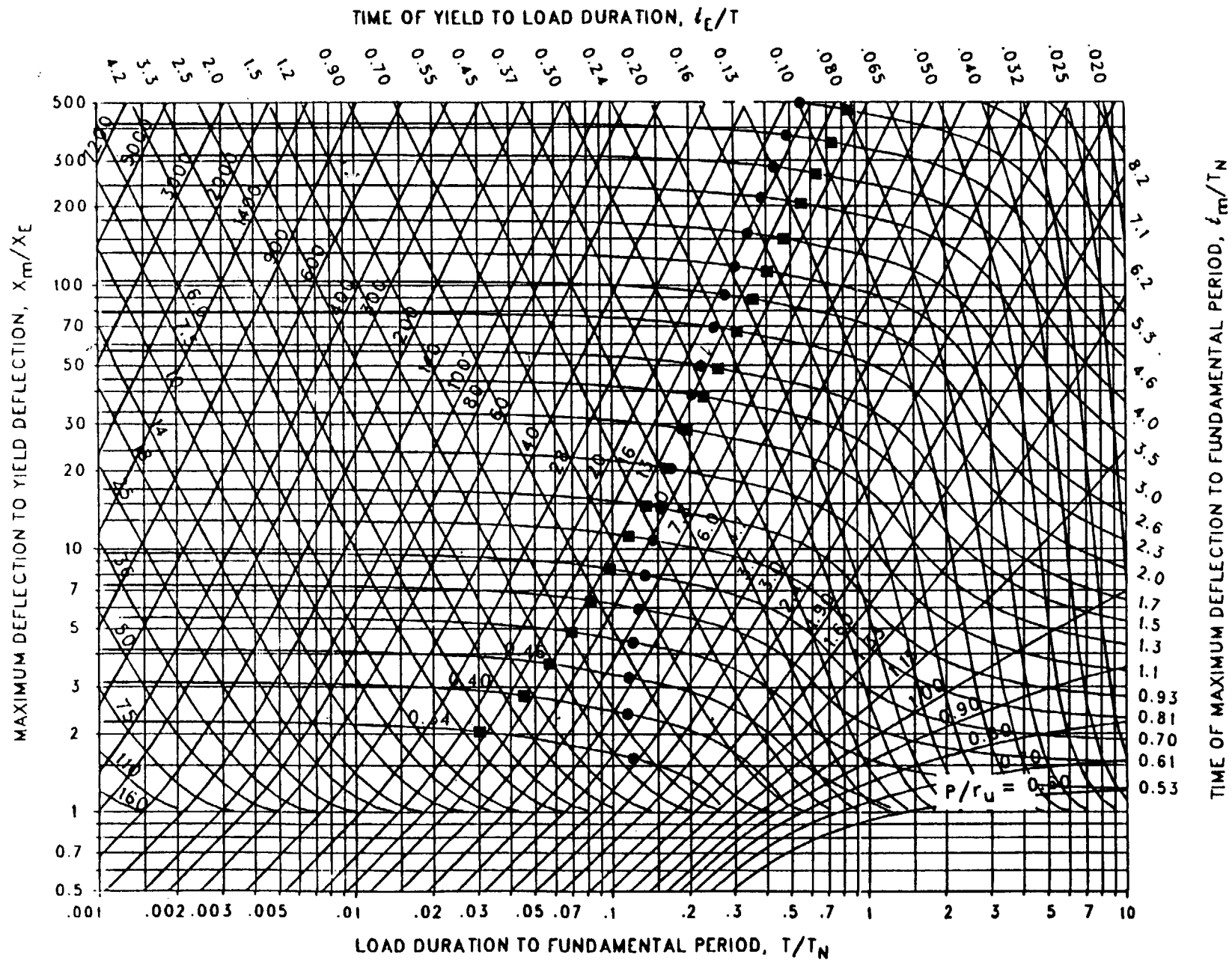


Figure 3-96 Maximum response of elasto-plastic, one-degree-of-freedom system for bilinear-triangular pulse ($C_1 = 0.022$, $C_2 = 5:5$)

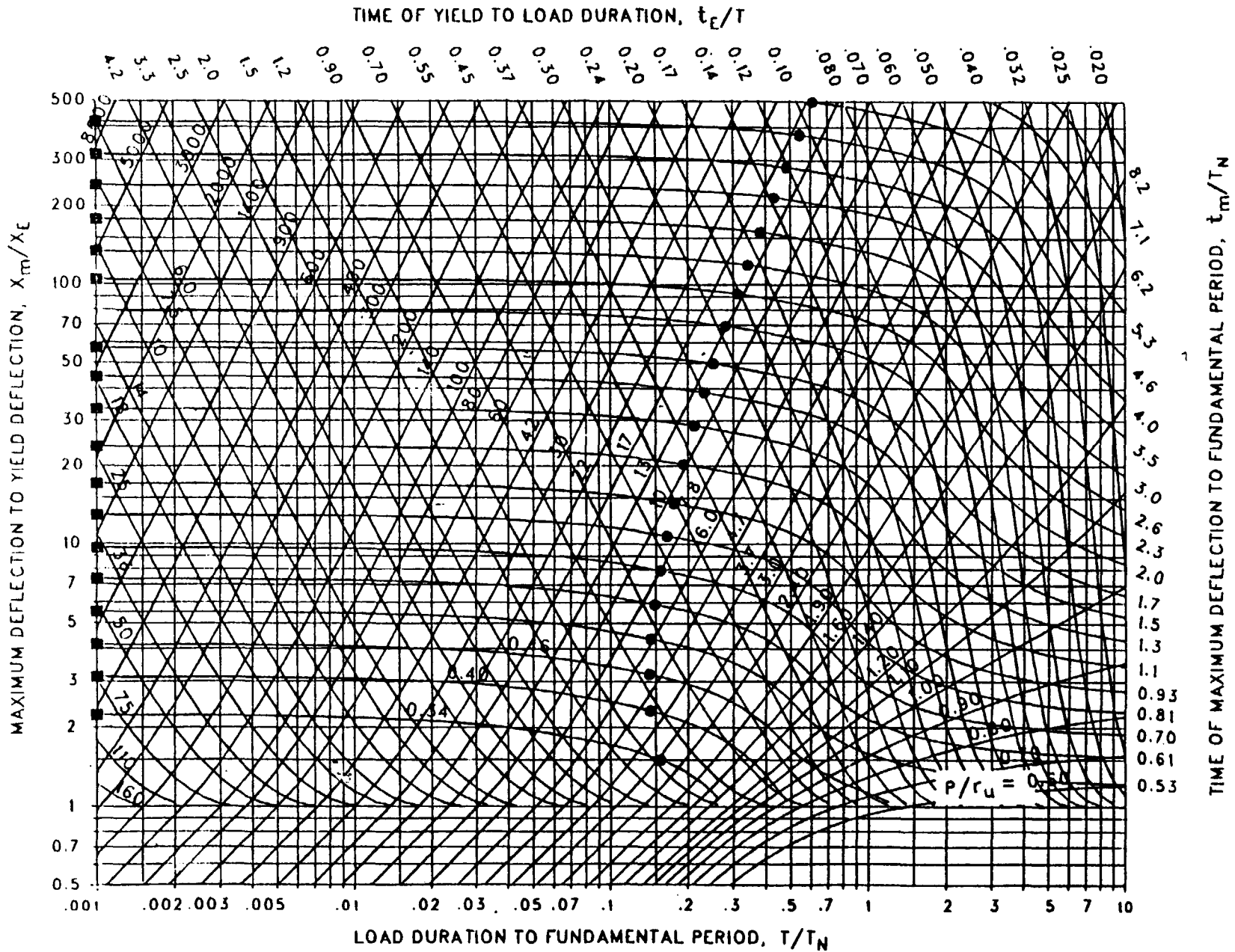


Figure 3-97 Maximum response of elasto-plastic, one-degree-of-freedom system for bilinear-triangular pulse ($C_1 = 0.015$, $C_2 = 6$)

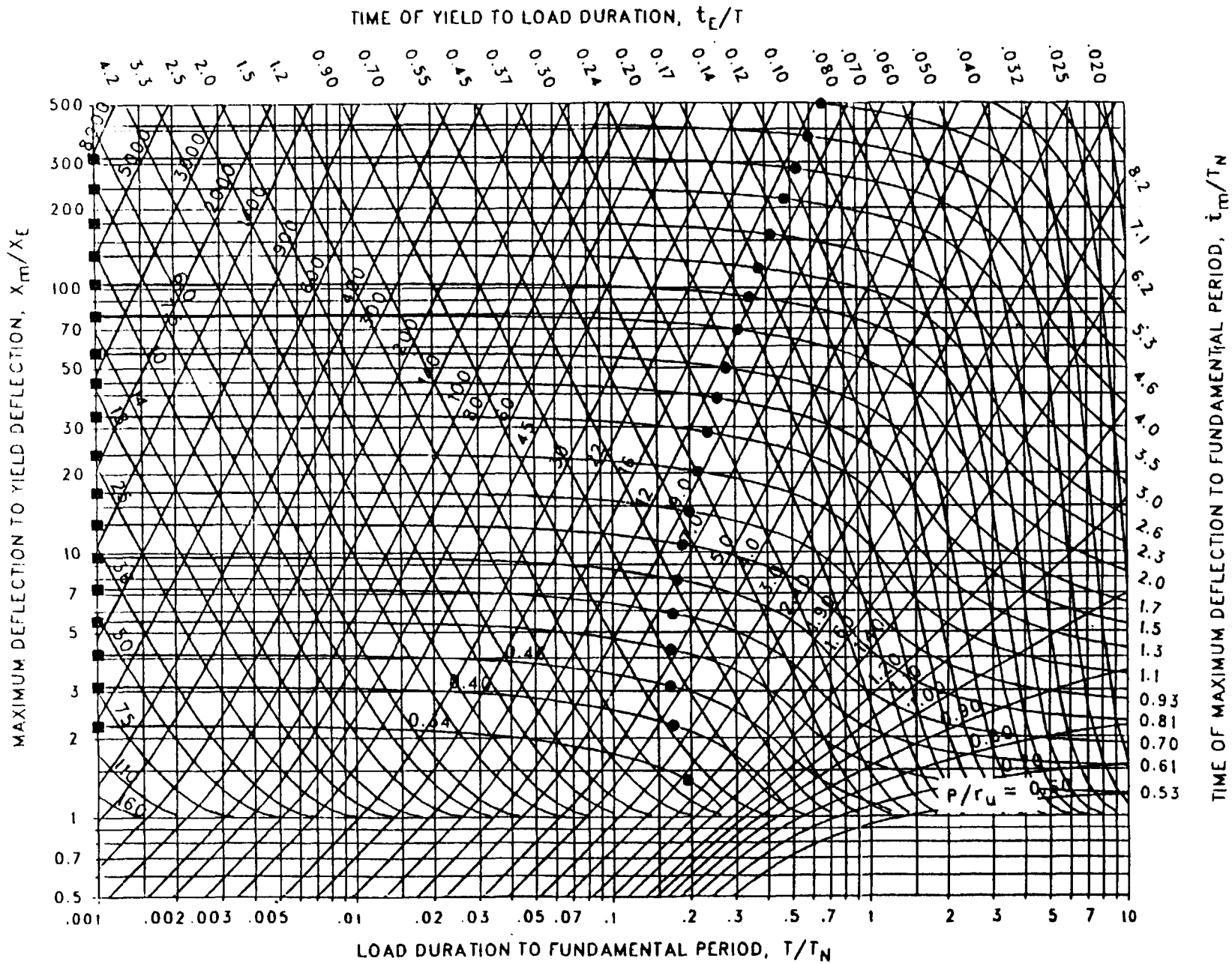


Figure 3-98 Maximum response of elasto-plastic, one-degree-of-freedom system for bilinear-triangular pulse ($C_1 = 0.010$, $C_2 = 6$)

3-157

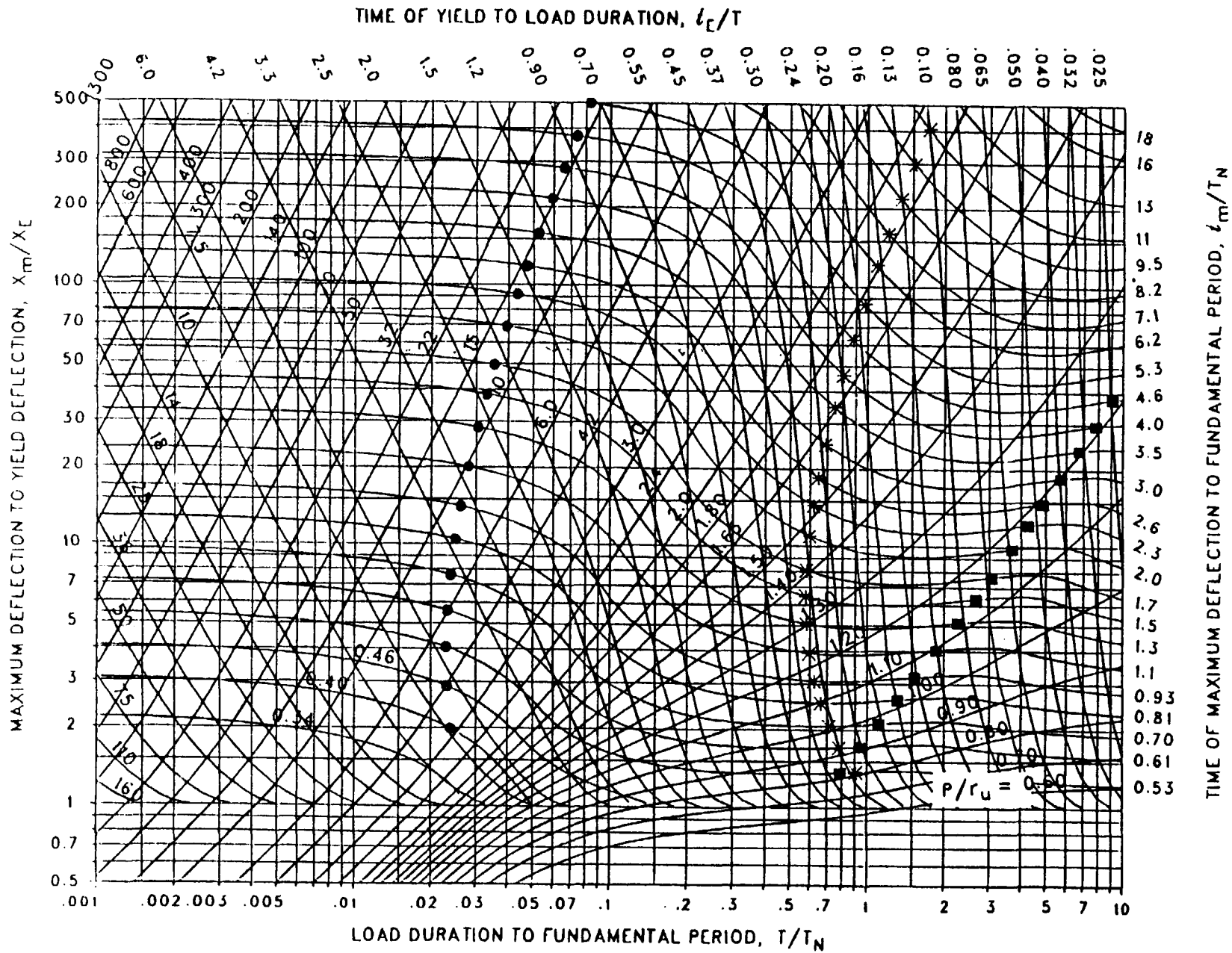


Figure 3-99 Maximum response of elasto-plastic, one-degree-of-freedom system for bilinear-triangular pulse ($C_1 = 0.750$, $C_2 = 10$)

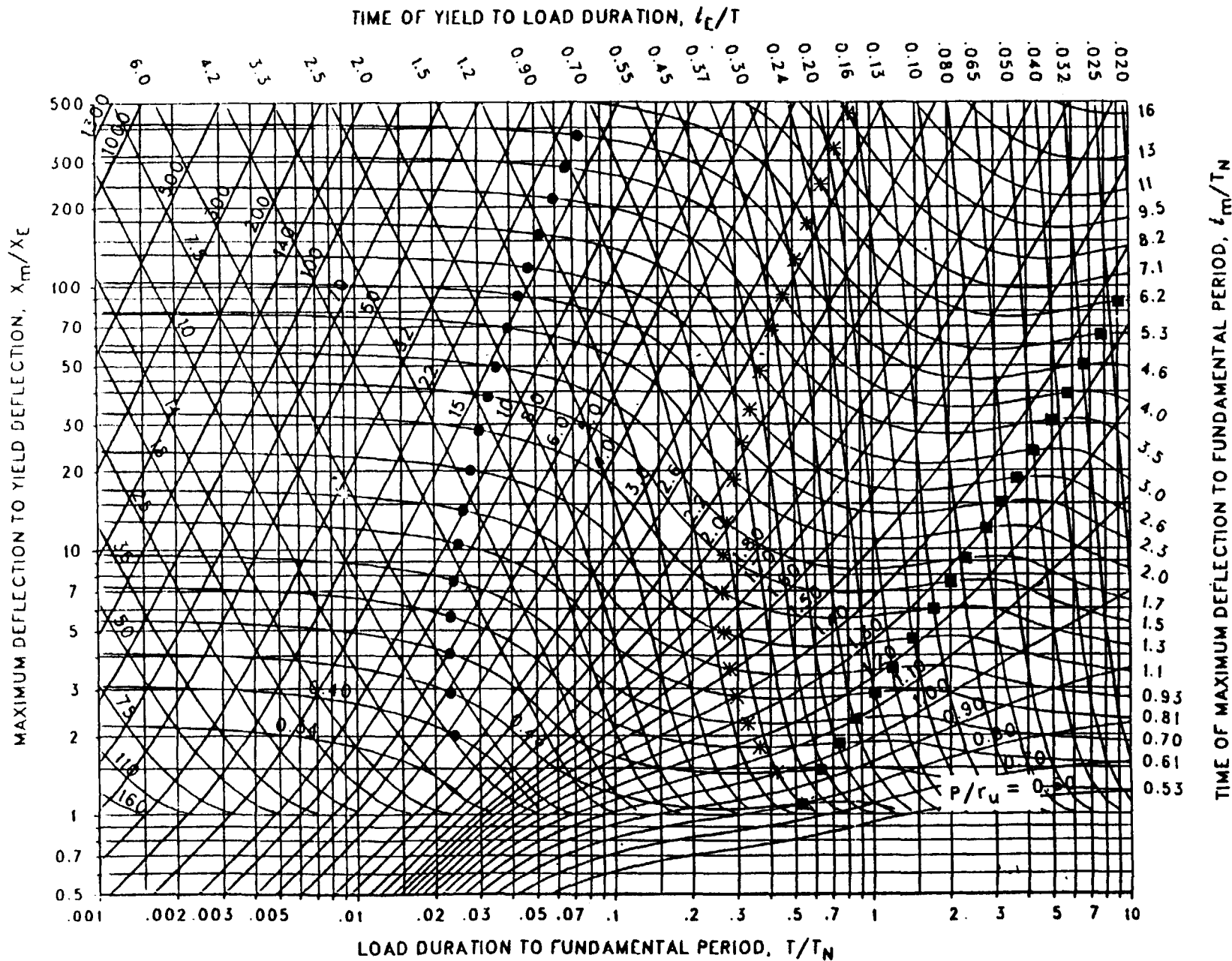


Figure 3-100 Maximum response of elasto-plastic, one-degree-of-freedom system for bilinear-triangular pulse ($C_1 = 0.648$, $C_2 = 10$)

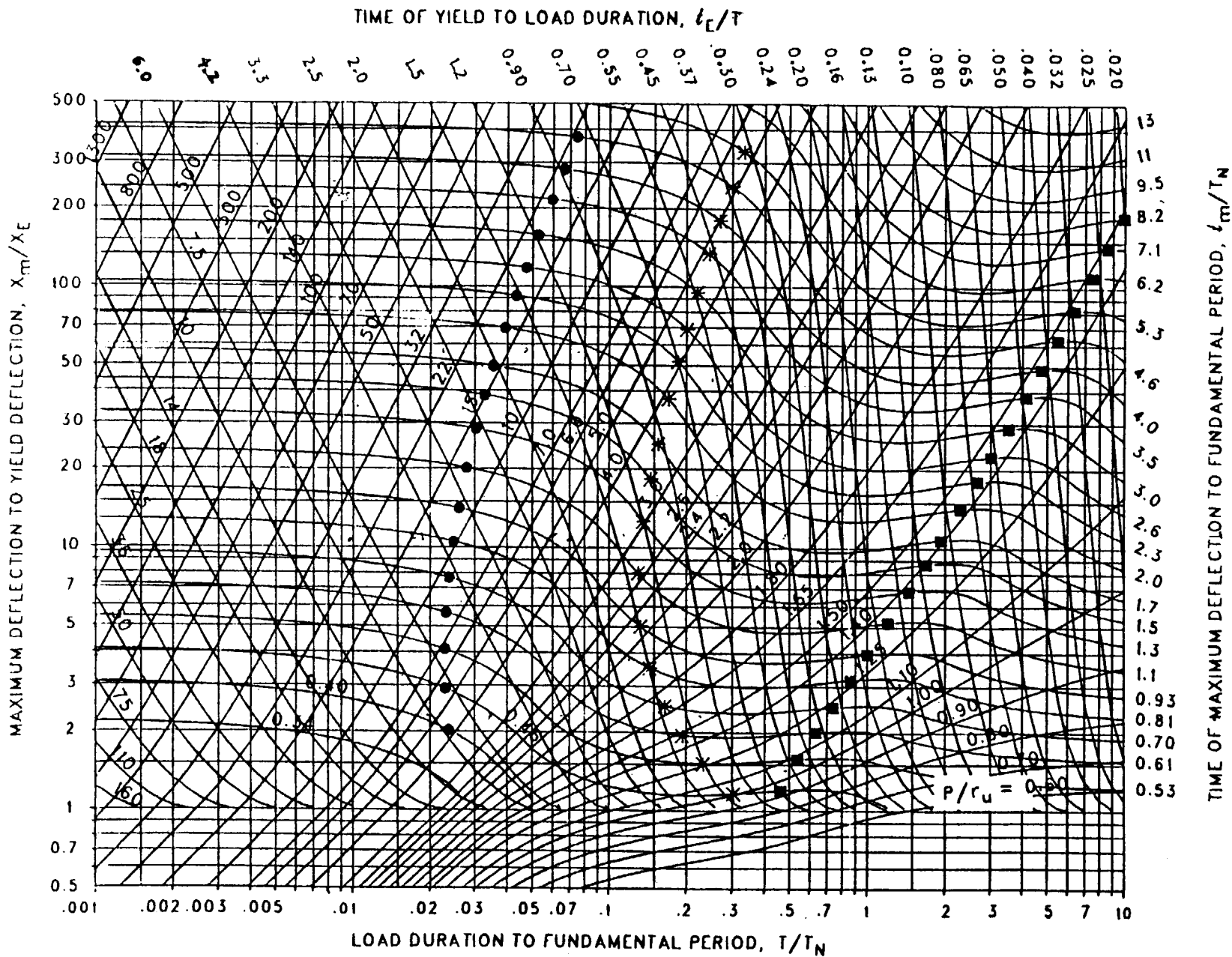


Figure 3-101 Maximum response of elasto-plastic, one-degree-of-freedom system for bilinear-triangular pulse ($C_1 = 0.562$, $C_2 = 10$)

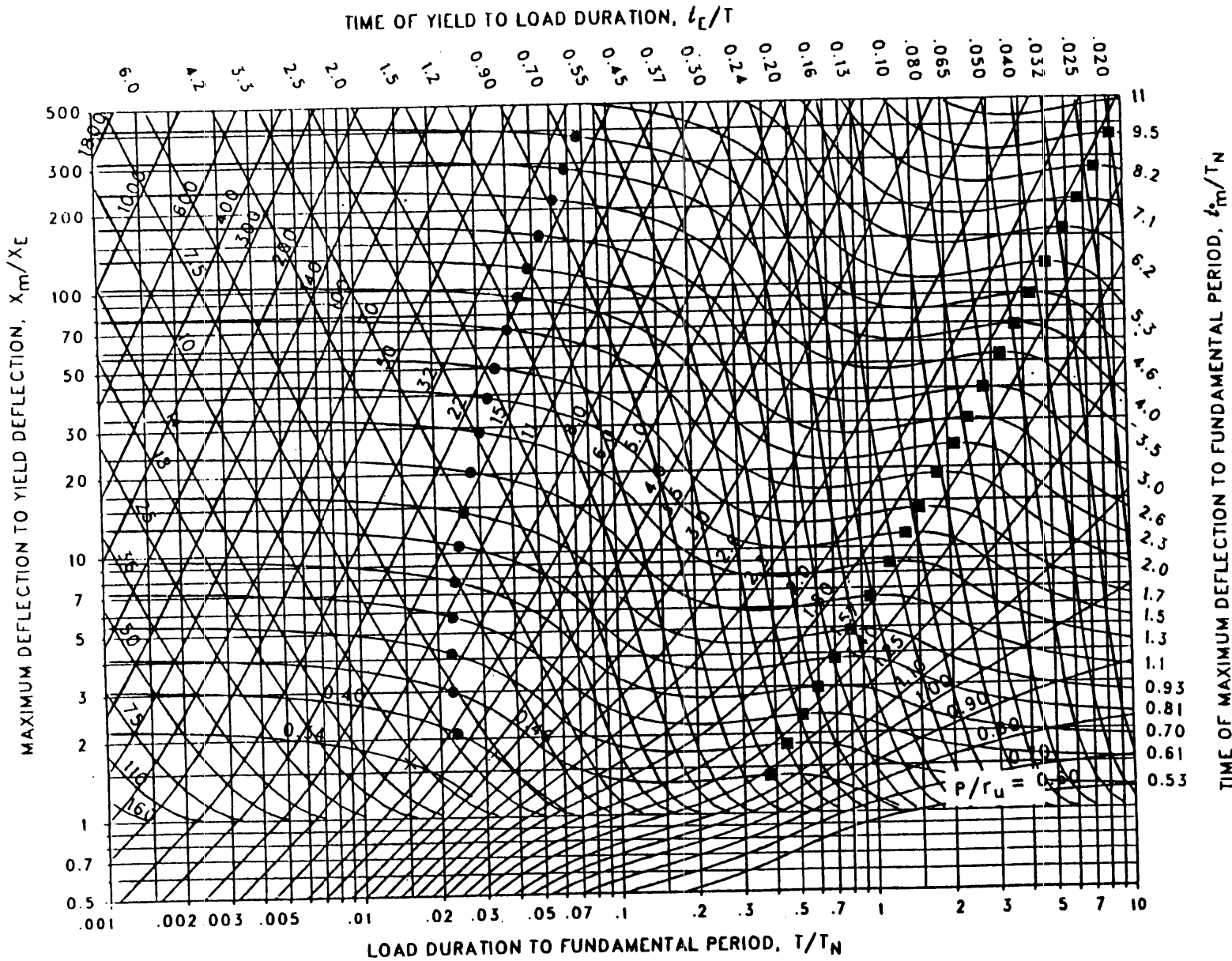


Figure 3-102 Maximum response of elasto-plastic, one-degree-of-freedom system for bilinear-triangular pulse ($C_1 = 0.422$, $C_2 = 10$)

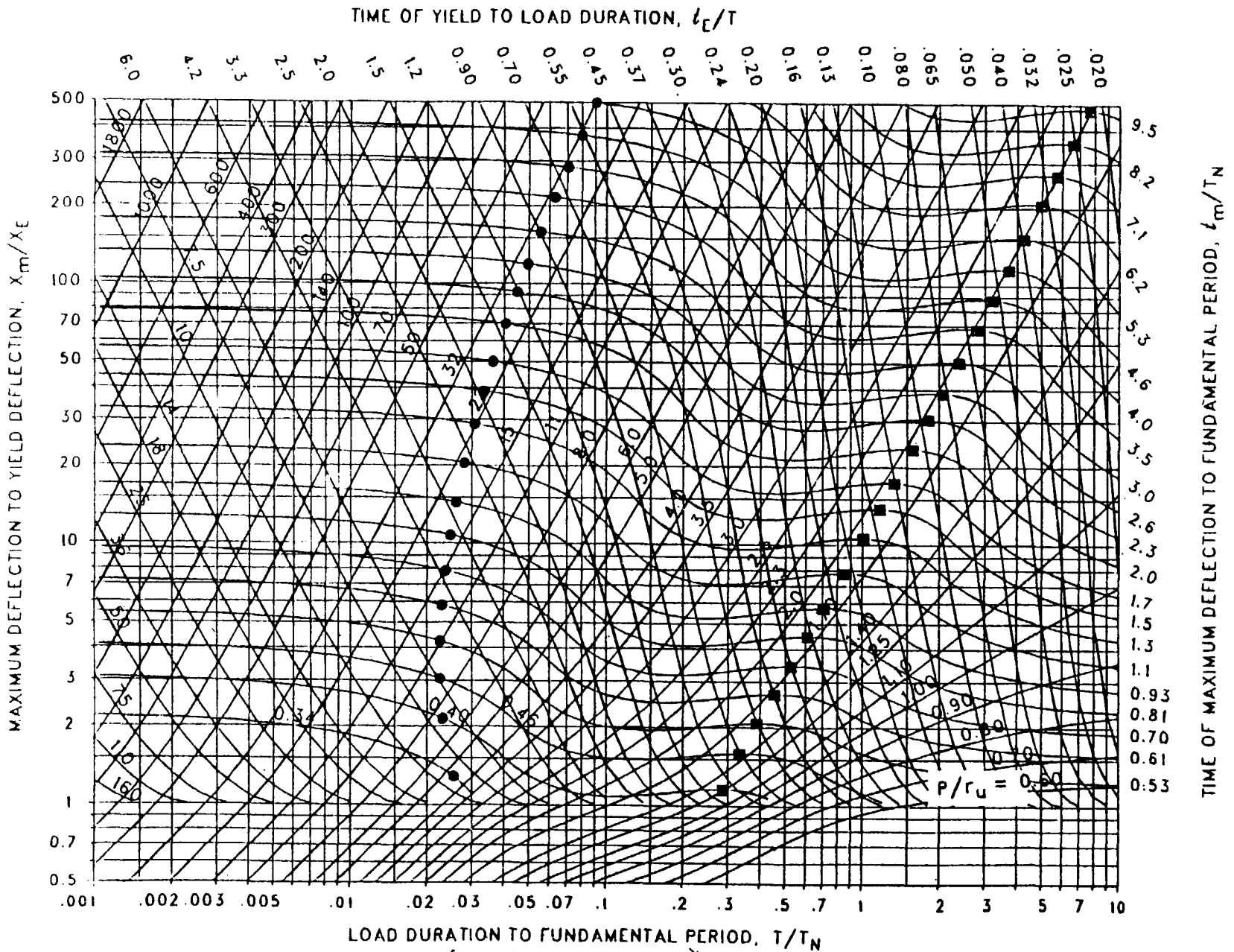


Figure 3-103 Maximum response of elasto-plastic, one-degree-of-freedom system for bilinear-triangular pulse ($C_1 = 0.316$, $C_2 = 10$)

3-162

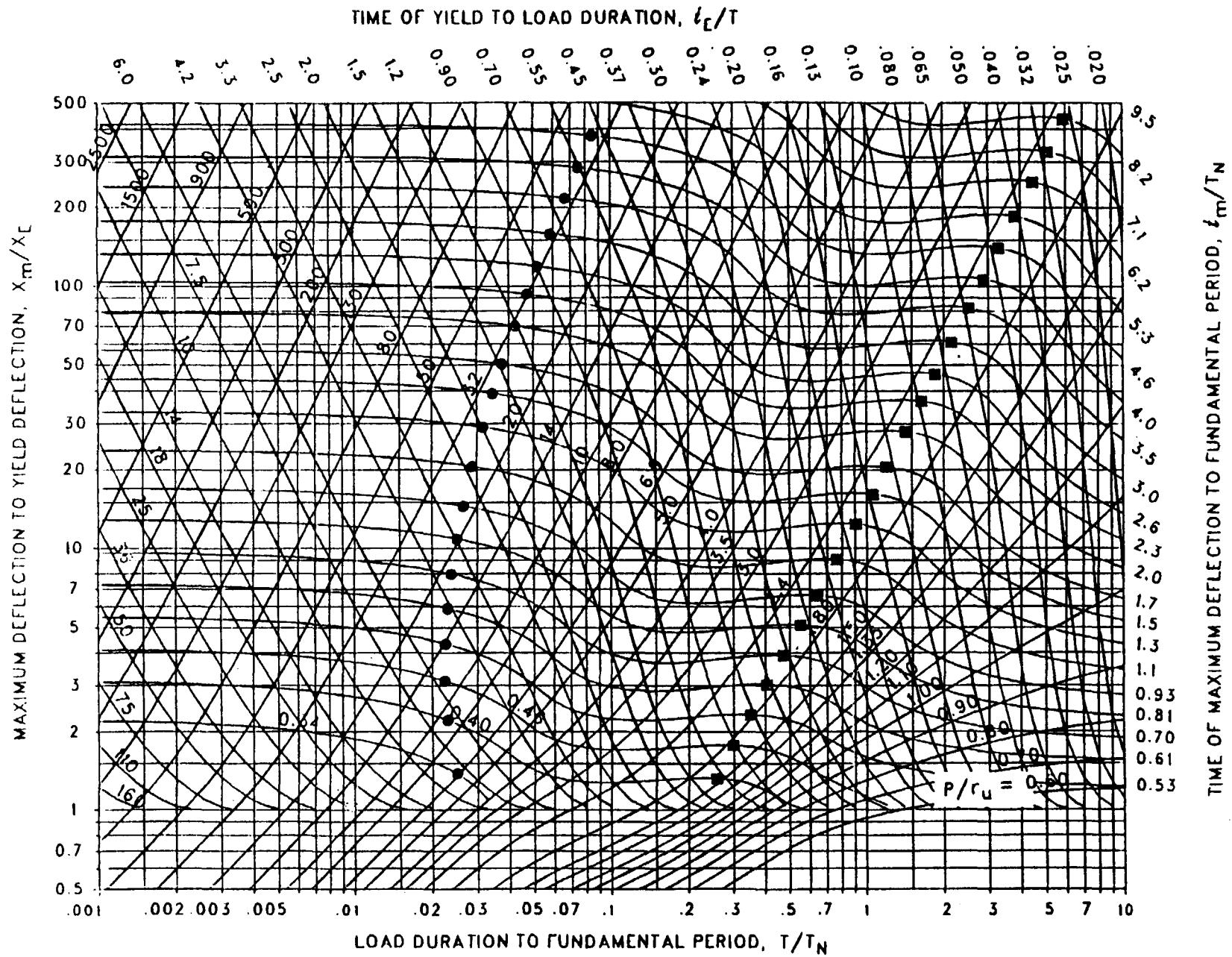


Figure 3-104 Maximum response of elasto-plastic, one-degree-of-freedom system for bilinear-triangular pulse ($C_1 = 0.237$, $C_2 = 10$)

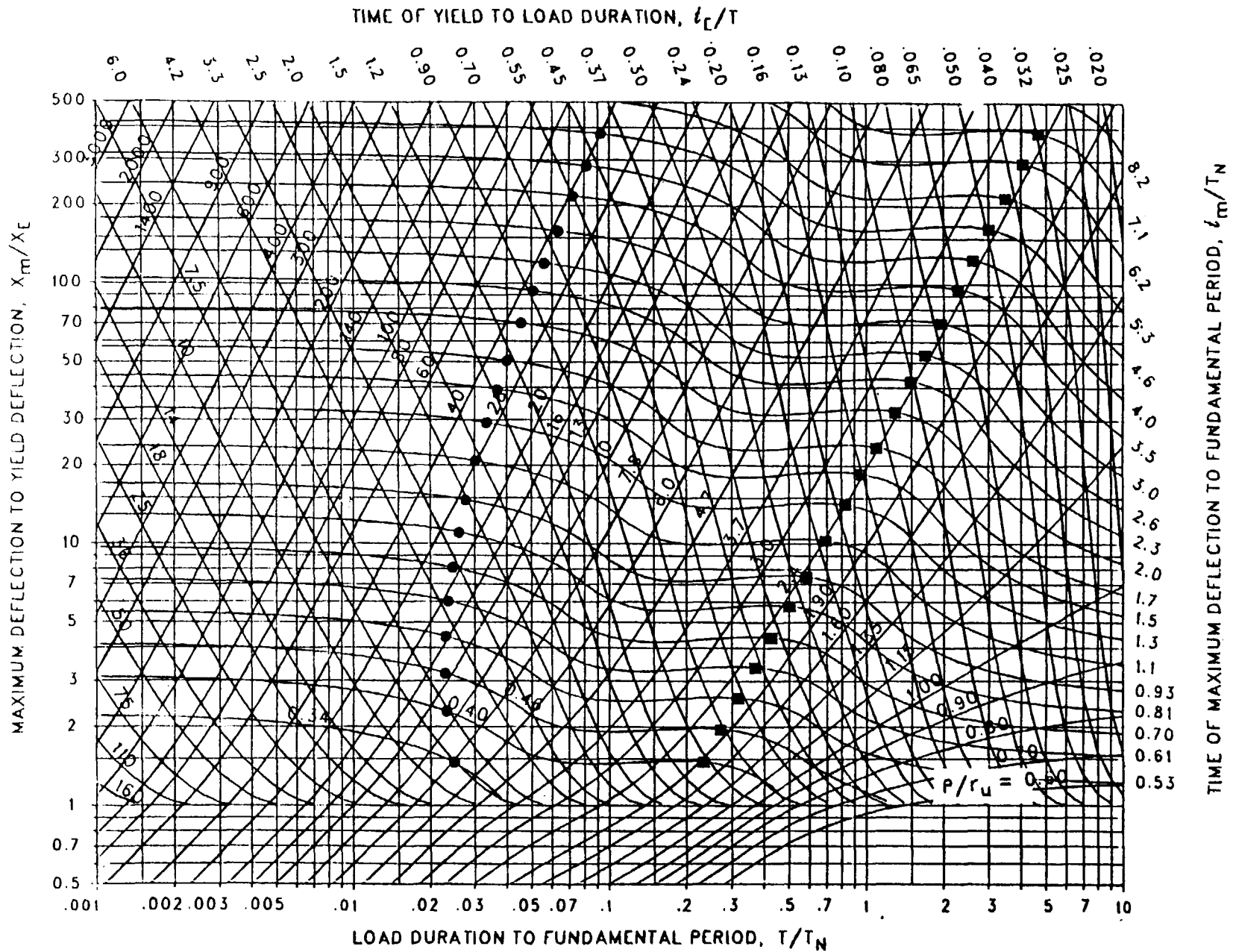


Figure 3-105 Maximum response of elasto-plastic, one-degree-of-freedom system for bilinear-triangular pulse ($C_1 = 0.178$, $C_2 = 10$)

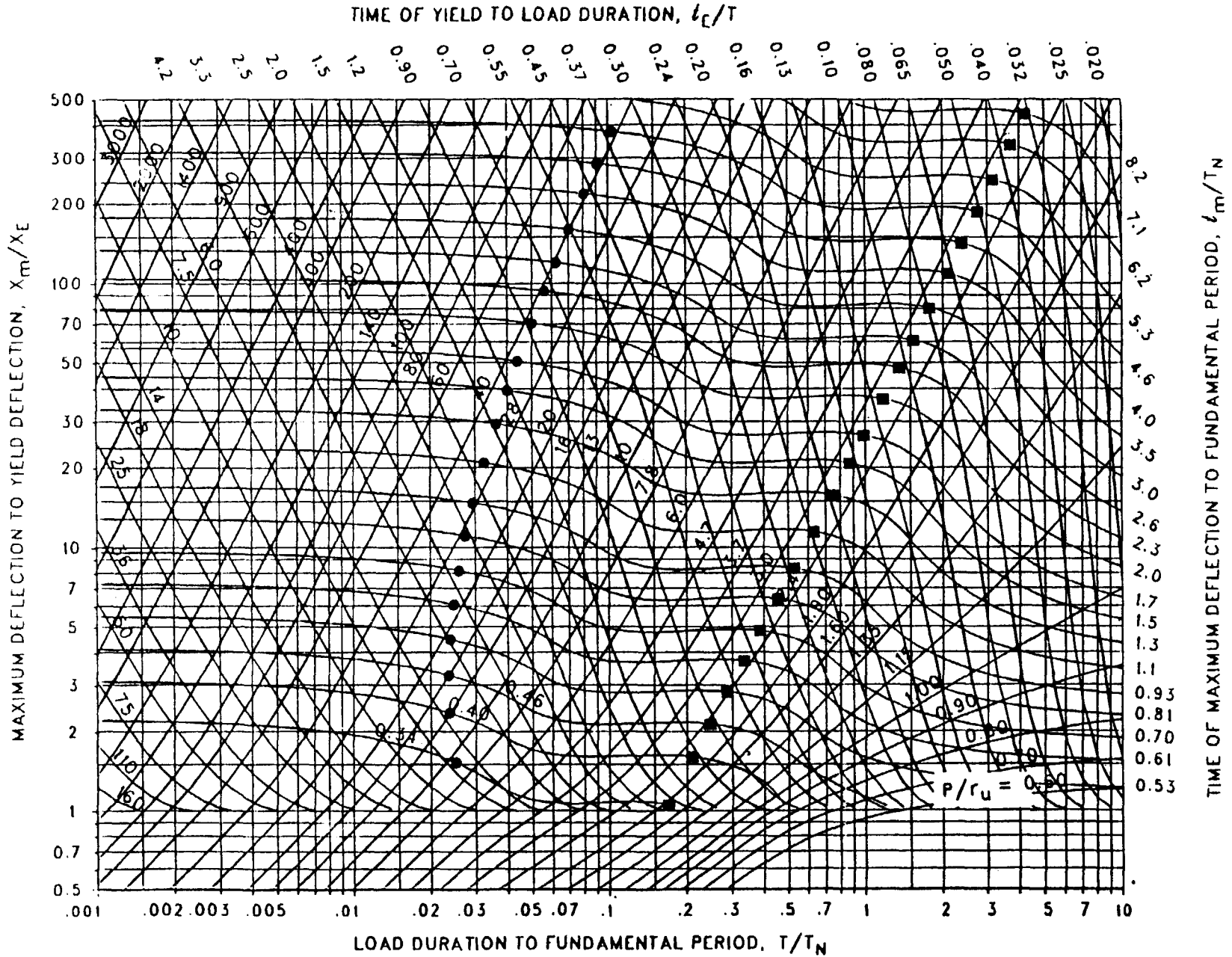


Figure 3-106 Maximum response of elasto-plastic, one-degree-of-freedom system for bilinear-triangular pulse ($C_1 = 0.133$, $C_2 = 10$)

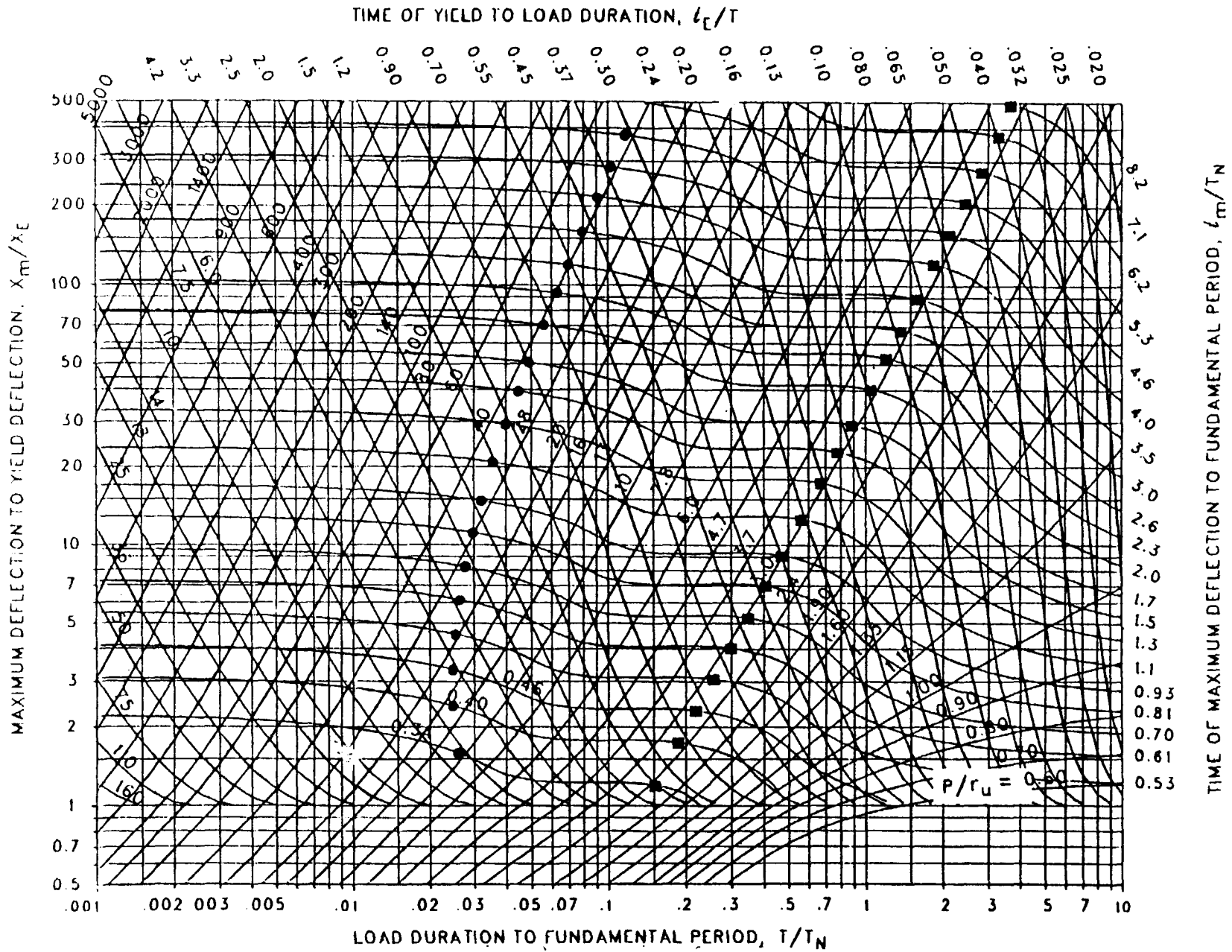


Figure 3-107 Maximum response of elasto-plastic, one-degree-of-freedom system for bilinear-triangular pulse ($C_1 = 0.100$, $C_2 = 10$)

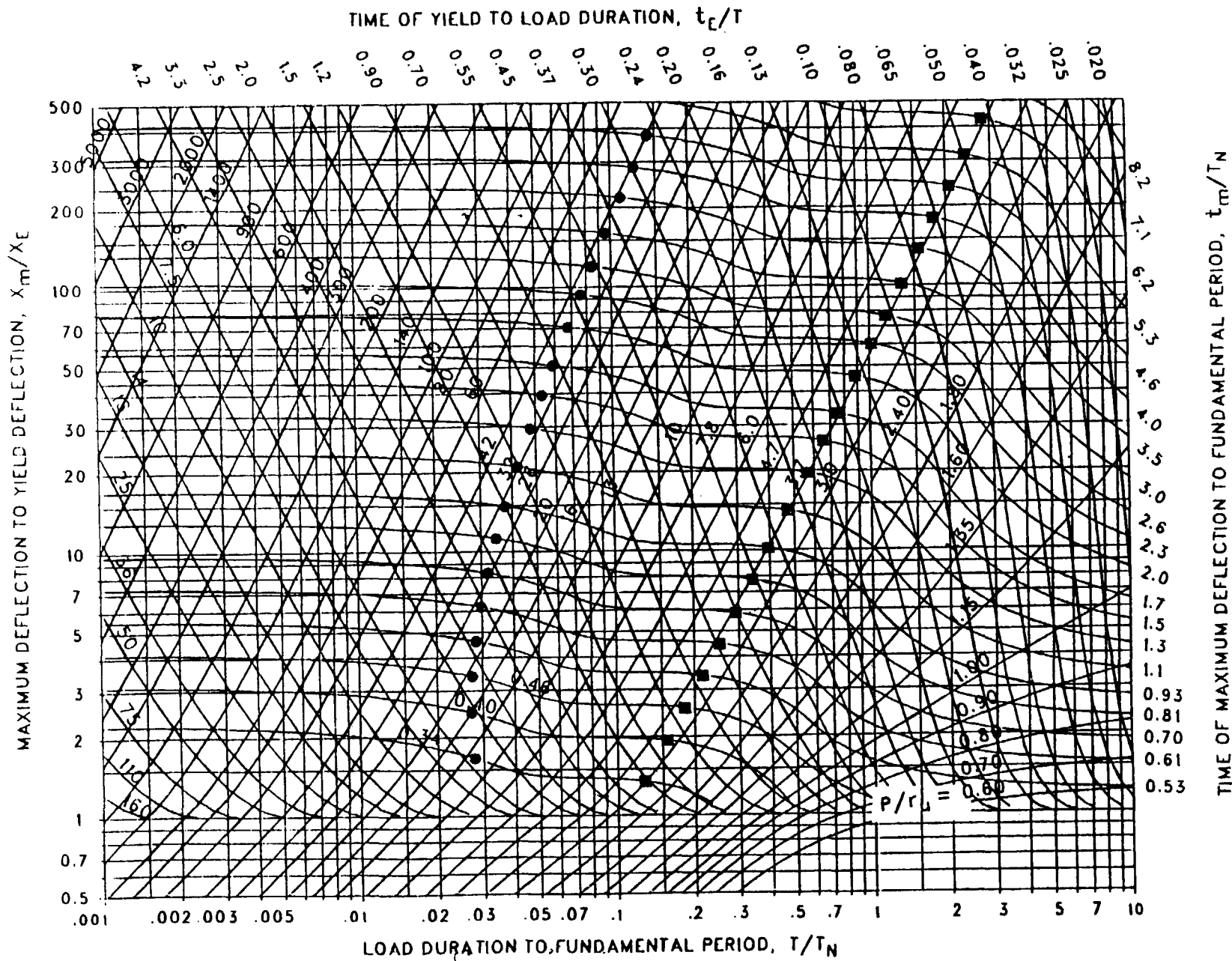


Figure 3-108 Maximum response of elasto-plastic, one-degree-of-freedom system for bilinear-triangular pulse ($C_1 = 0.068$, $C_2 = 10$)

3-167

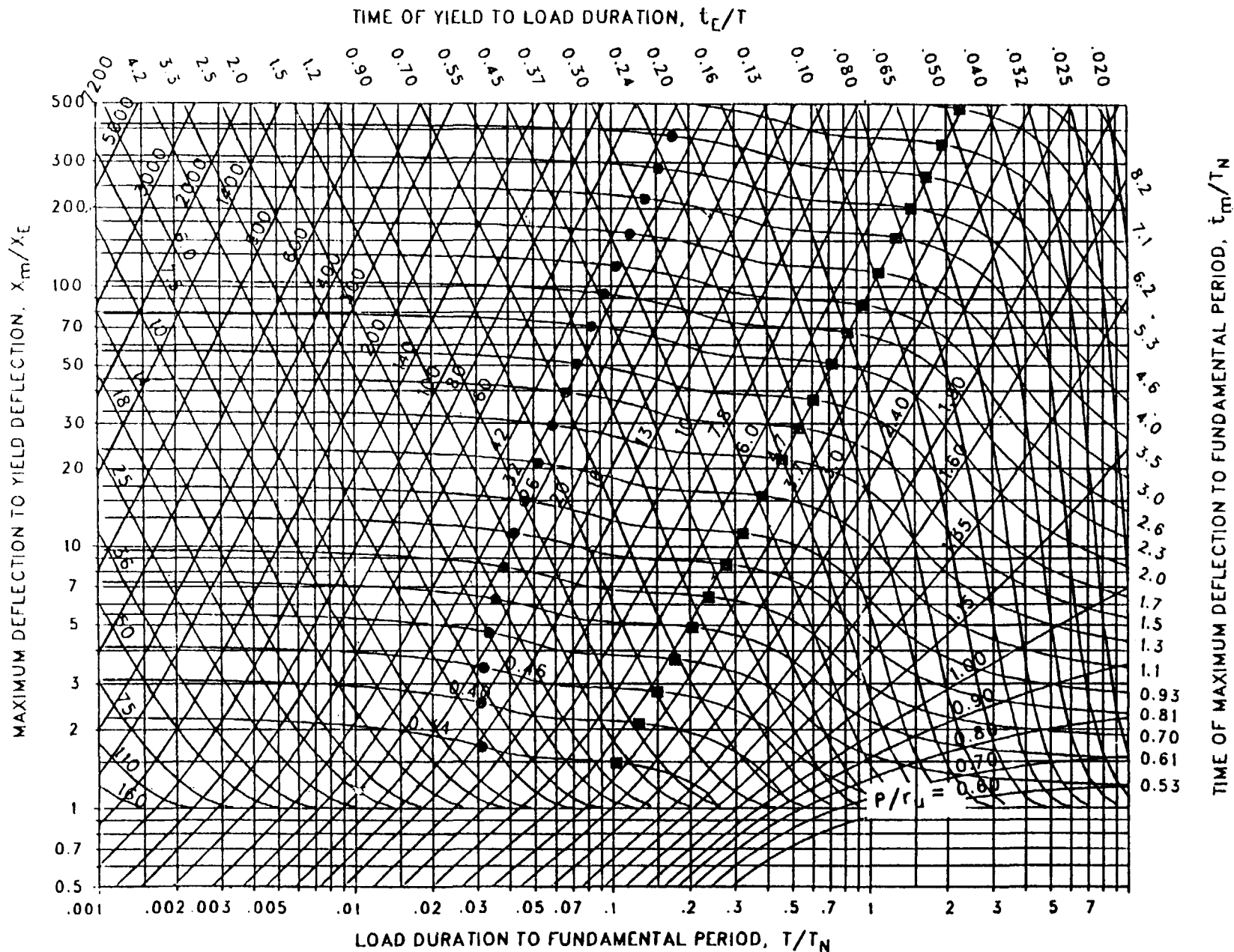


Figure 3-109 Maximum response of elasto-plastic, one-degree-of-freedom system for bilinear-triangular pulse ($C_1 = 0.046$, $C_2 = 10$)

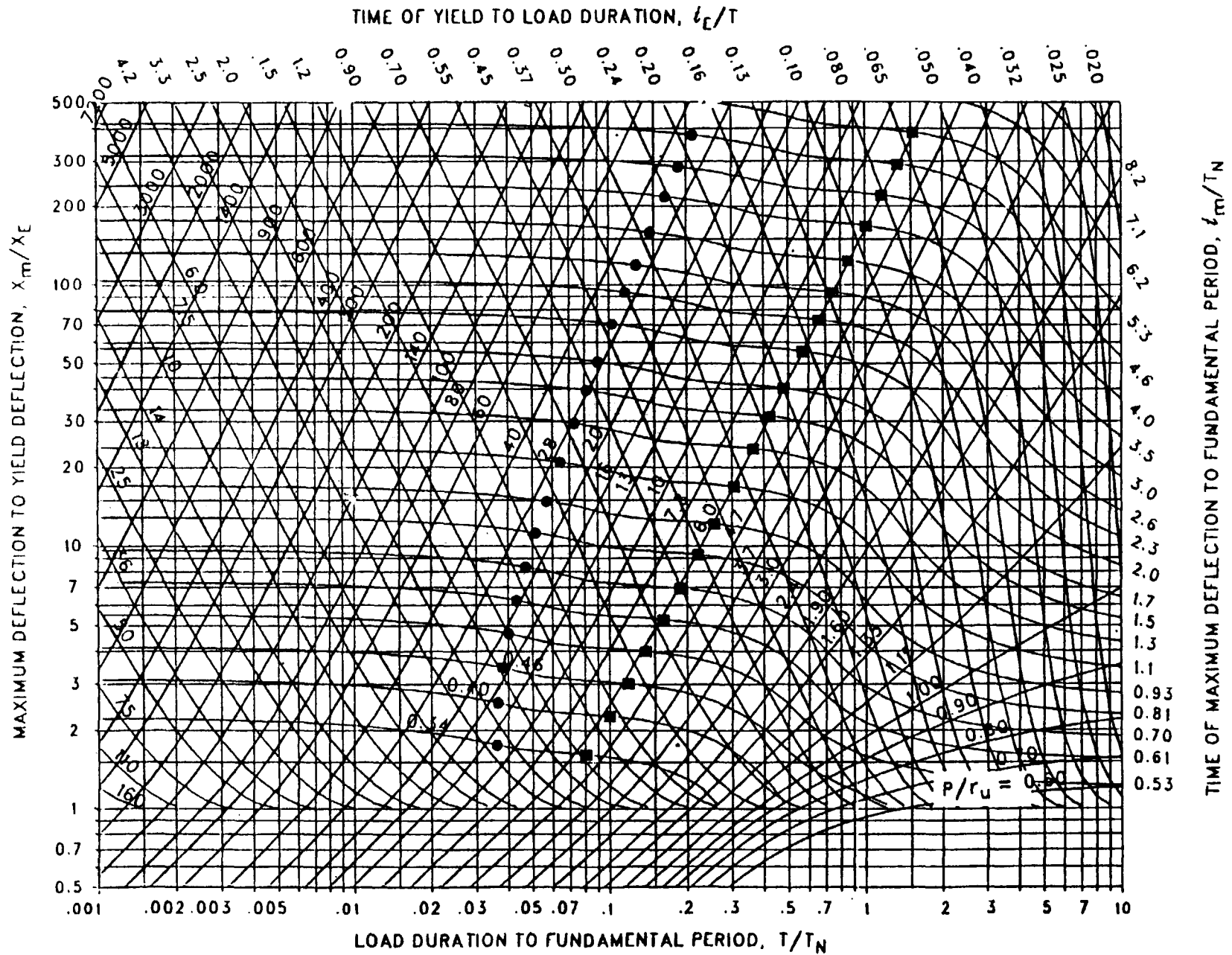


Figure 3-110 Maximum response of elasto-plastic, one-degree-of-freedom system for bilinear-triangular pulse ($C_1 = 0.032$, $C_2 = 10$)

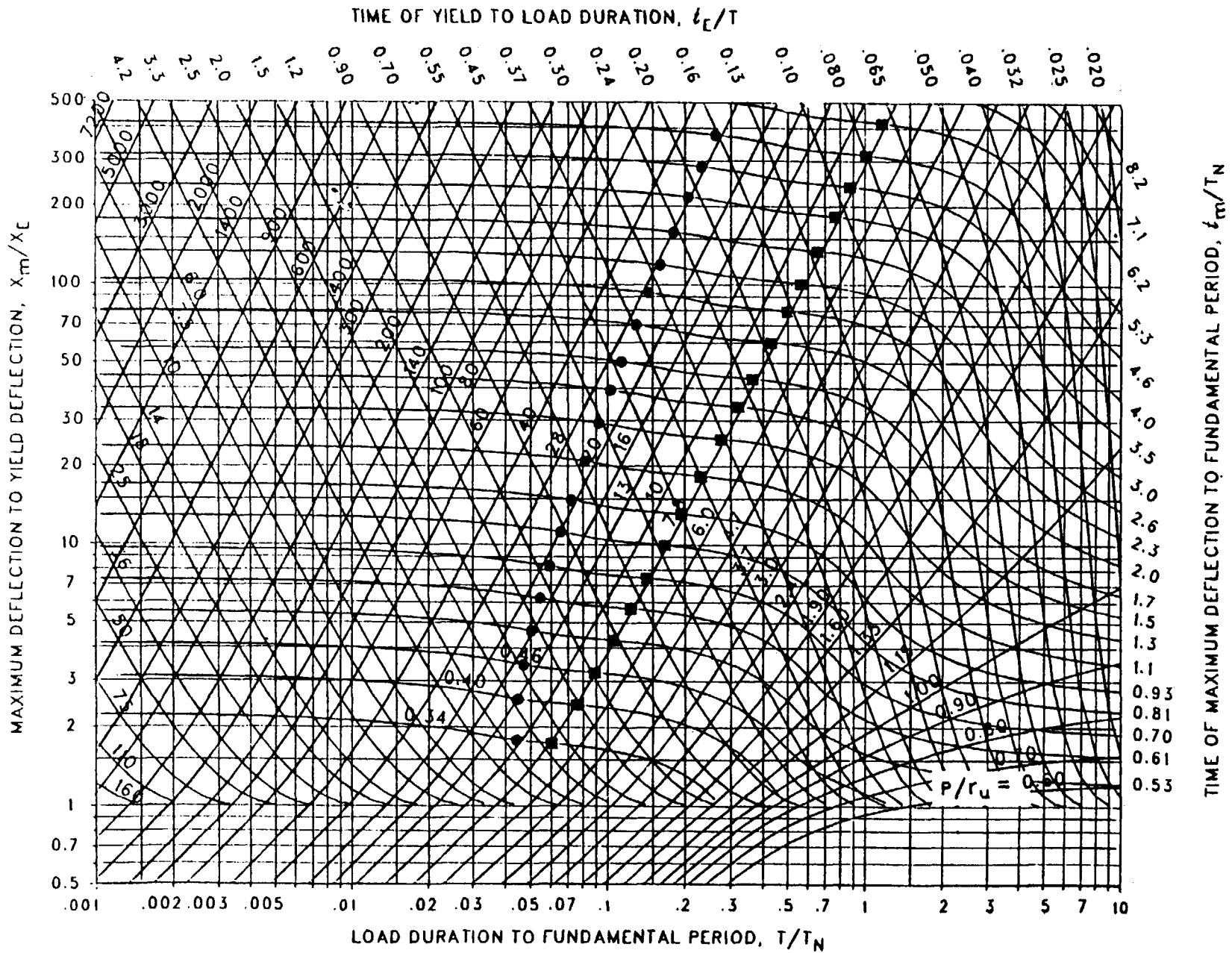


Figure 3-111 Maximum response of elasto-plastic, one-degree-of-freedom system for bilinear-triangular pulse ($C_1 = 0.022$, $C_2 = 10$)

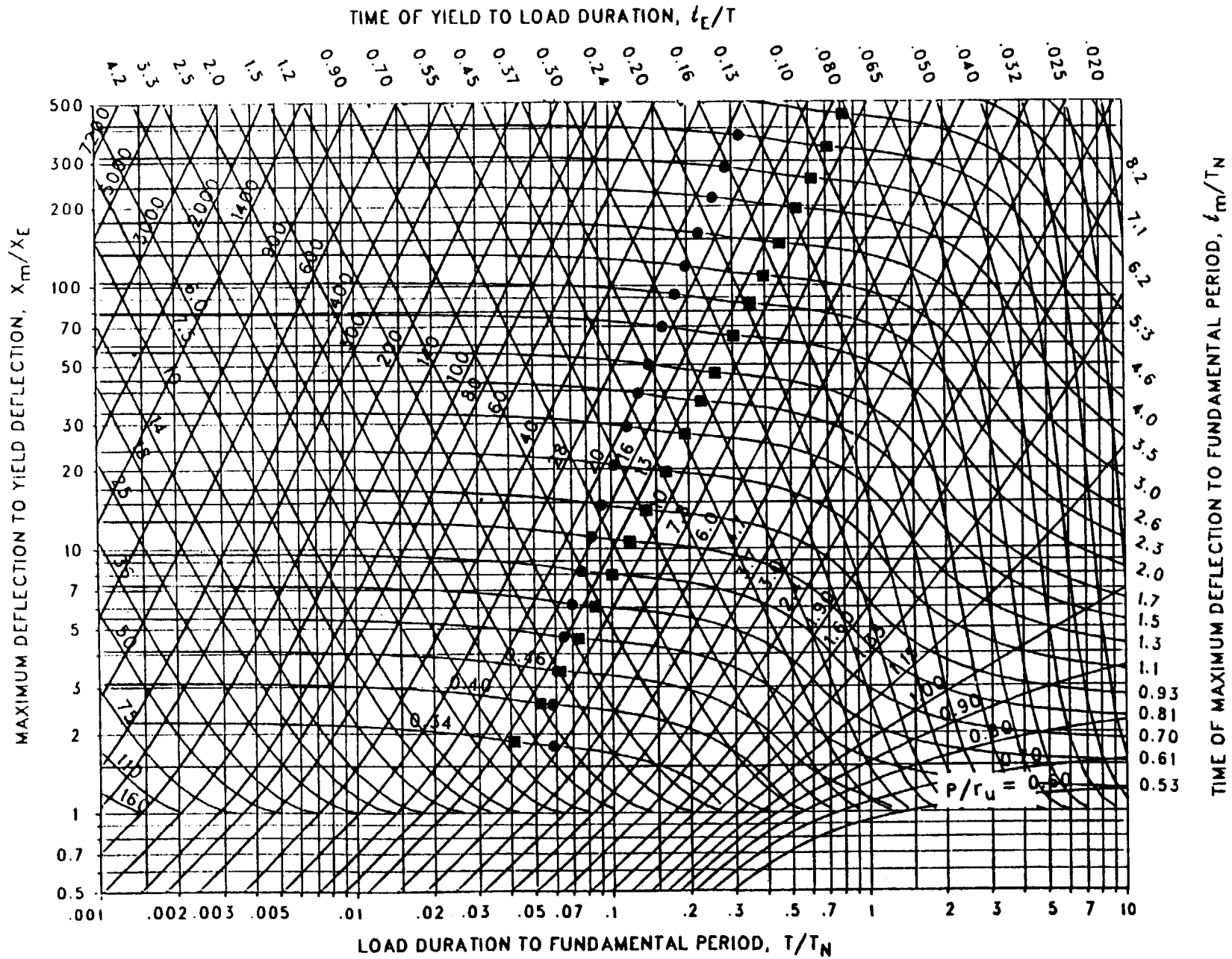


Figure 3-112 Maximum response of elasto-plastic, one-degree-of-freedom system for bilinear-triangular pulse ($C_1 = 0.015$, $C_2 = 10$)

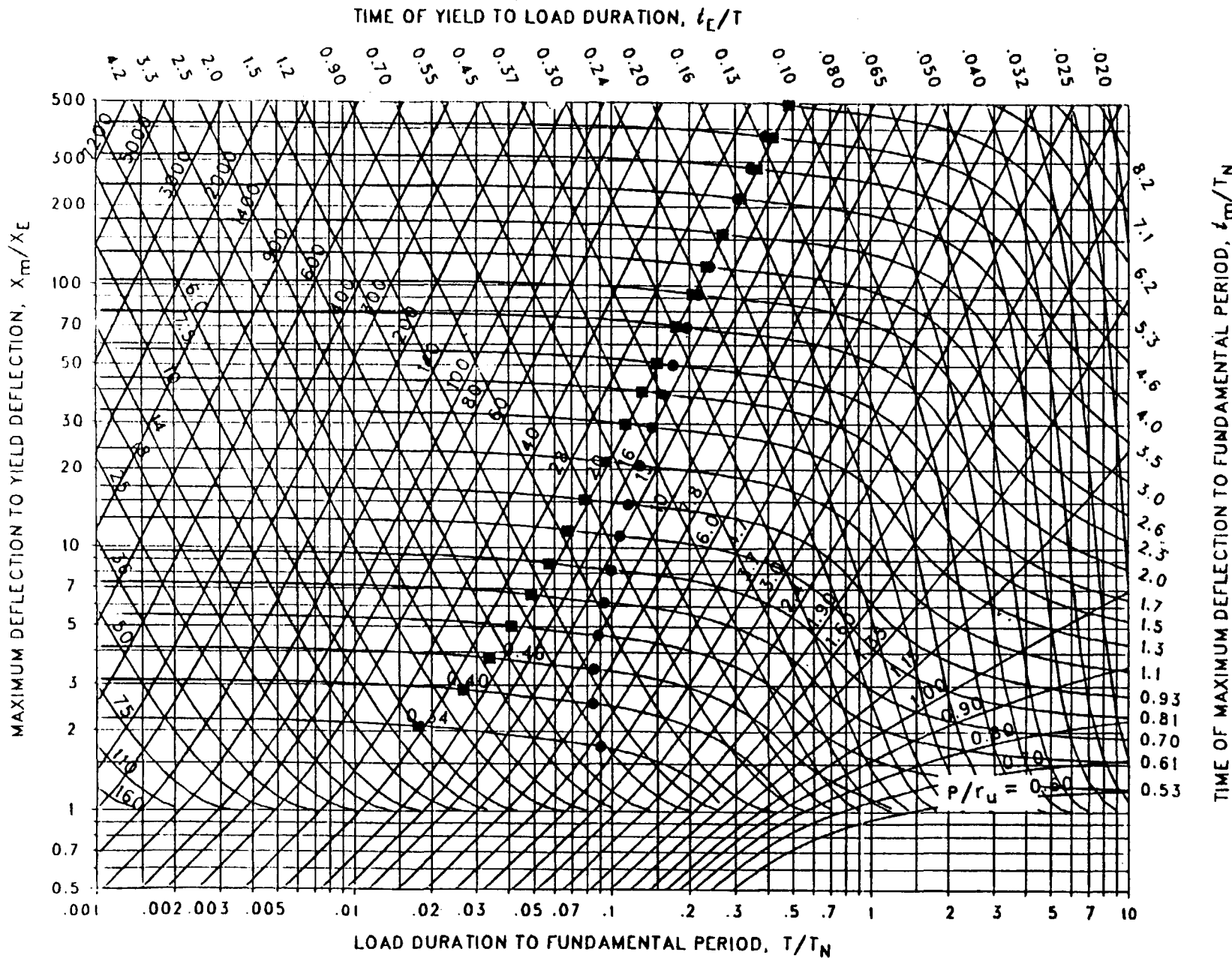


Figure 3-113 Maximum response of elasto-plastic, one-degree-of-freedom system for bilinear-triangular pulse ($C_1 = 0.010$, $C_2 = 10$)

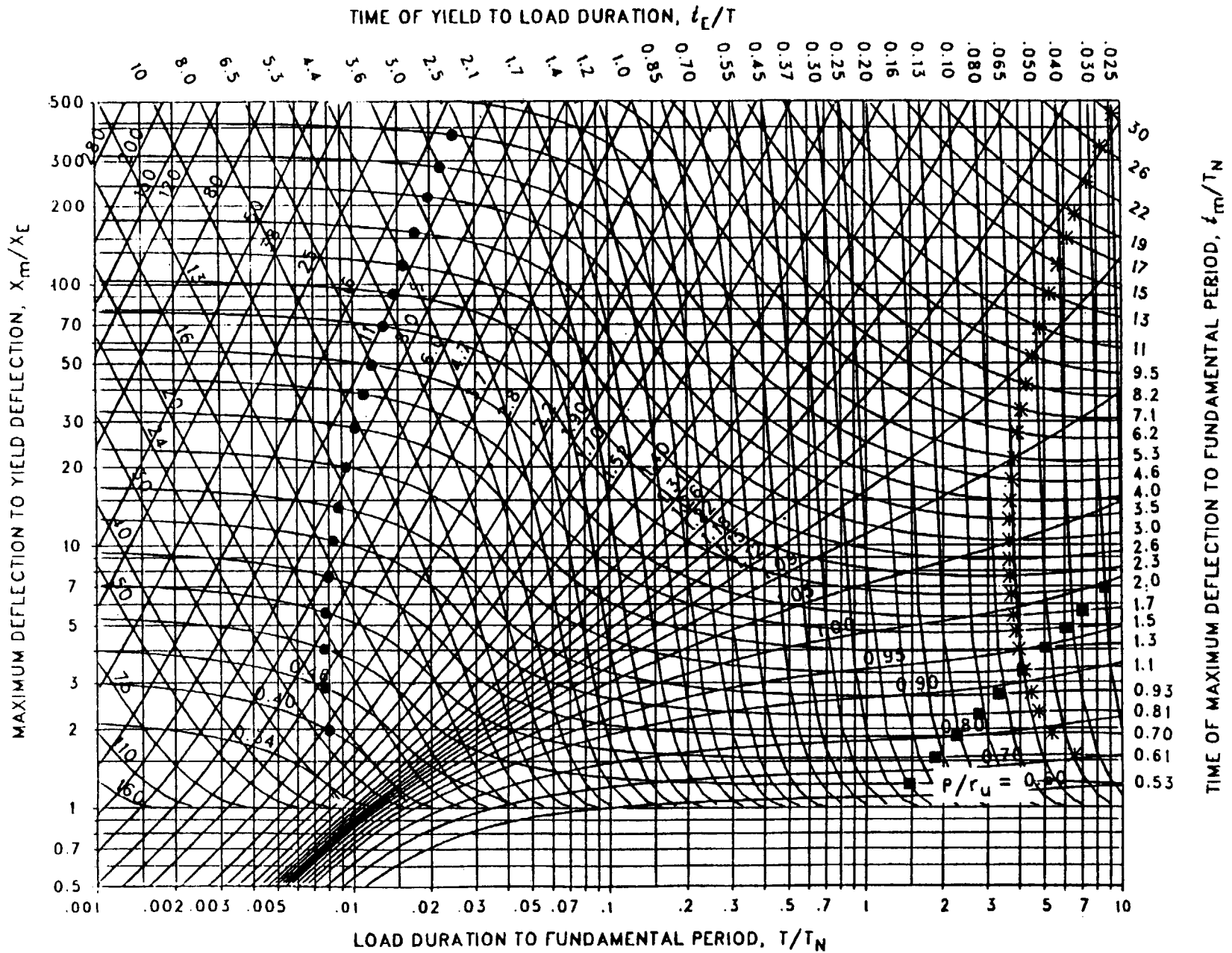


Figure 3-114 Maximum response of elasto-plastic, one-degree-of-freedom system for bilinear-triangular pulse ($C_1 = 0.909$, $C_2 = 30$)

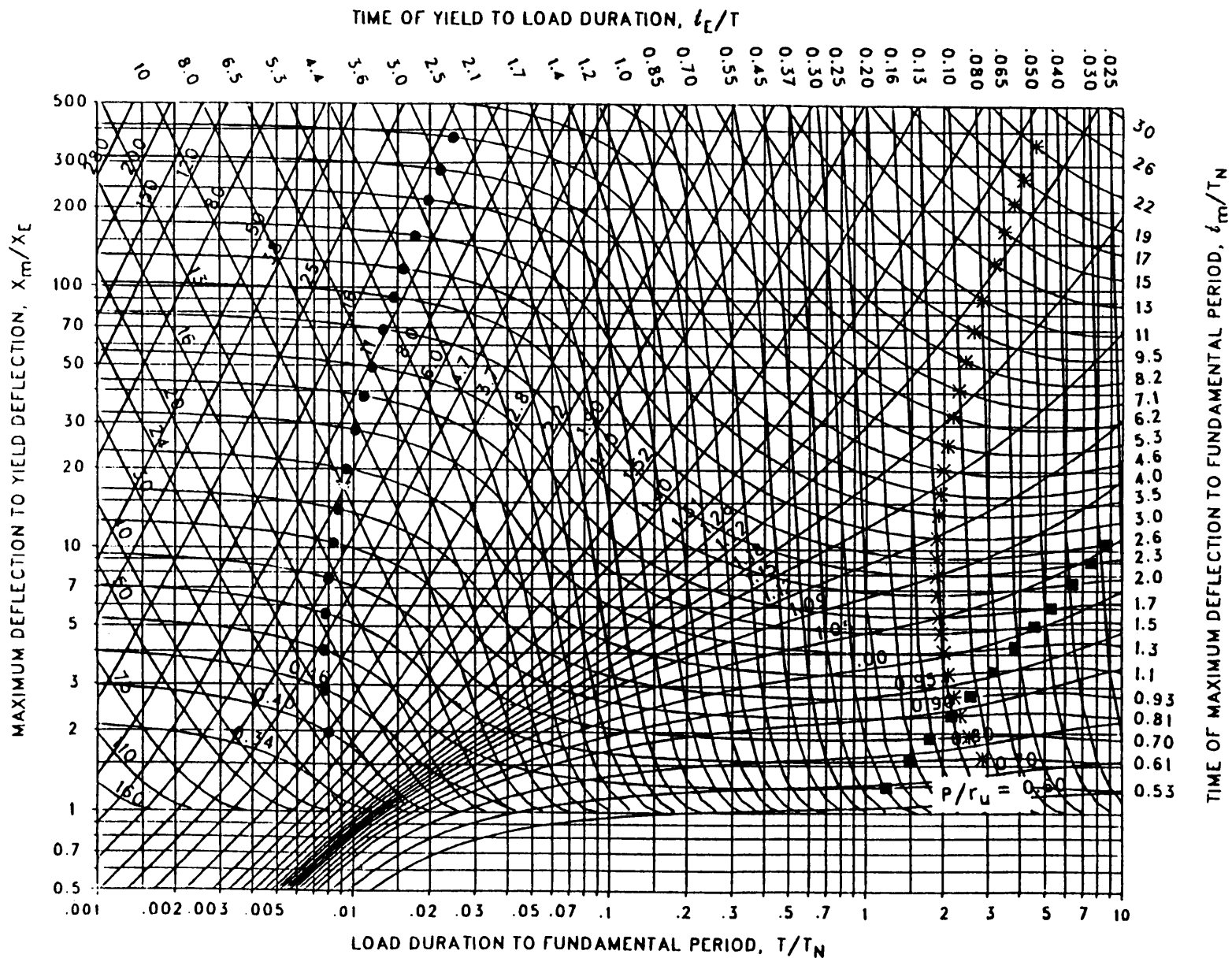


Figure 3-115 Maximum response of elasto-plastic, one-degree-of-freedom system for bilinear-triangular pulse ($C_1 = 0.866$, $C_2 = 30$)

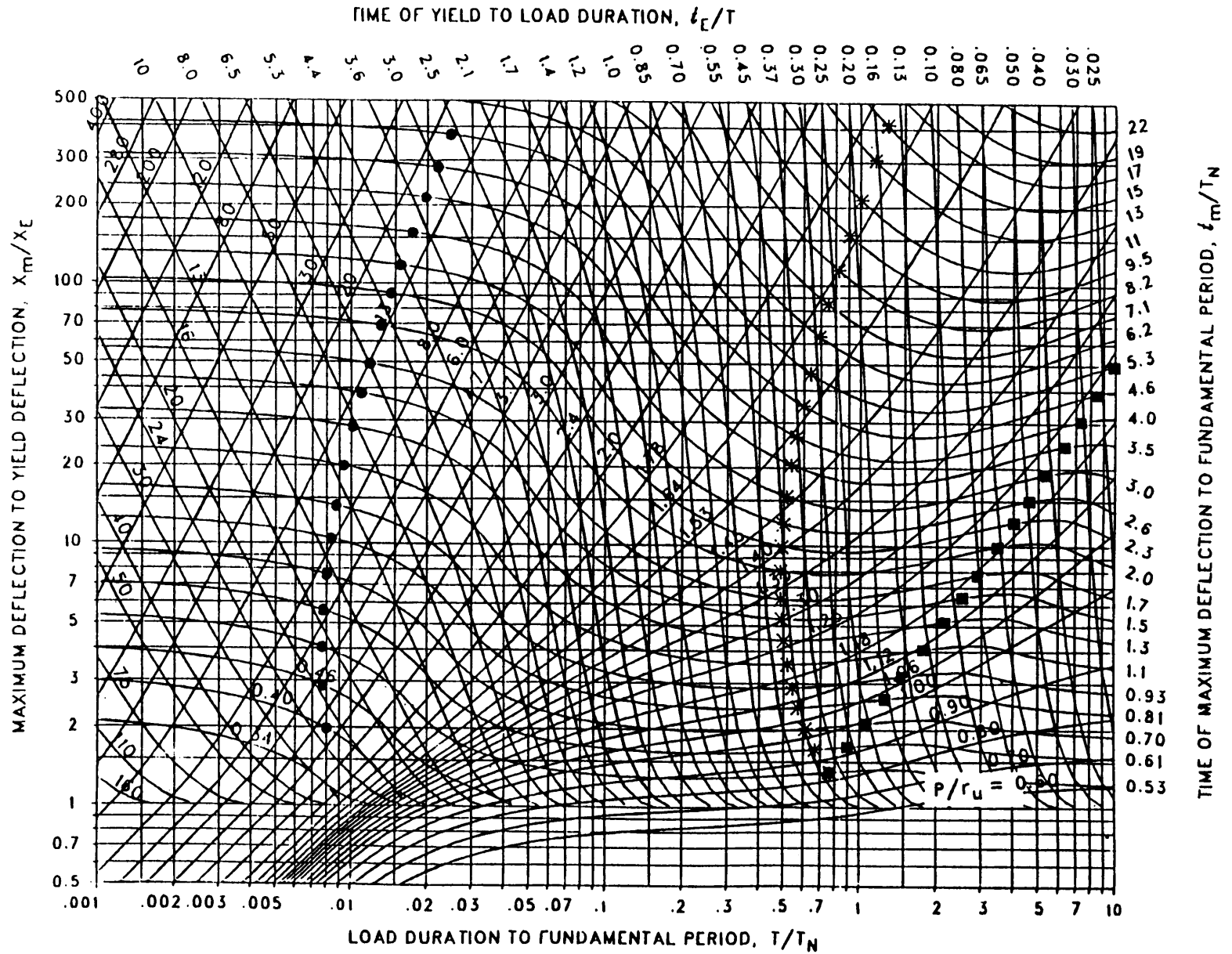


Figure 3-118 Maximum response of elasto-plastic, one-degree-of-freedom system for bilinear-triangular pulse ($C_1 = 0.715$, $C_2 = 30$)

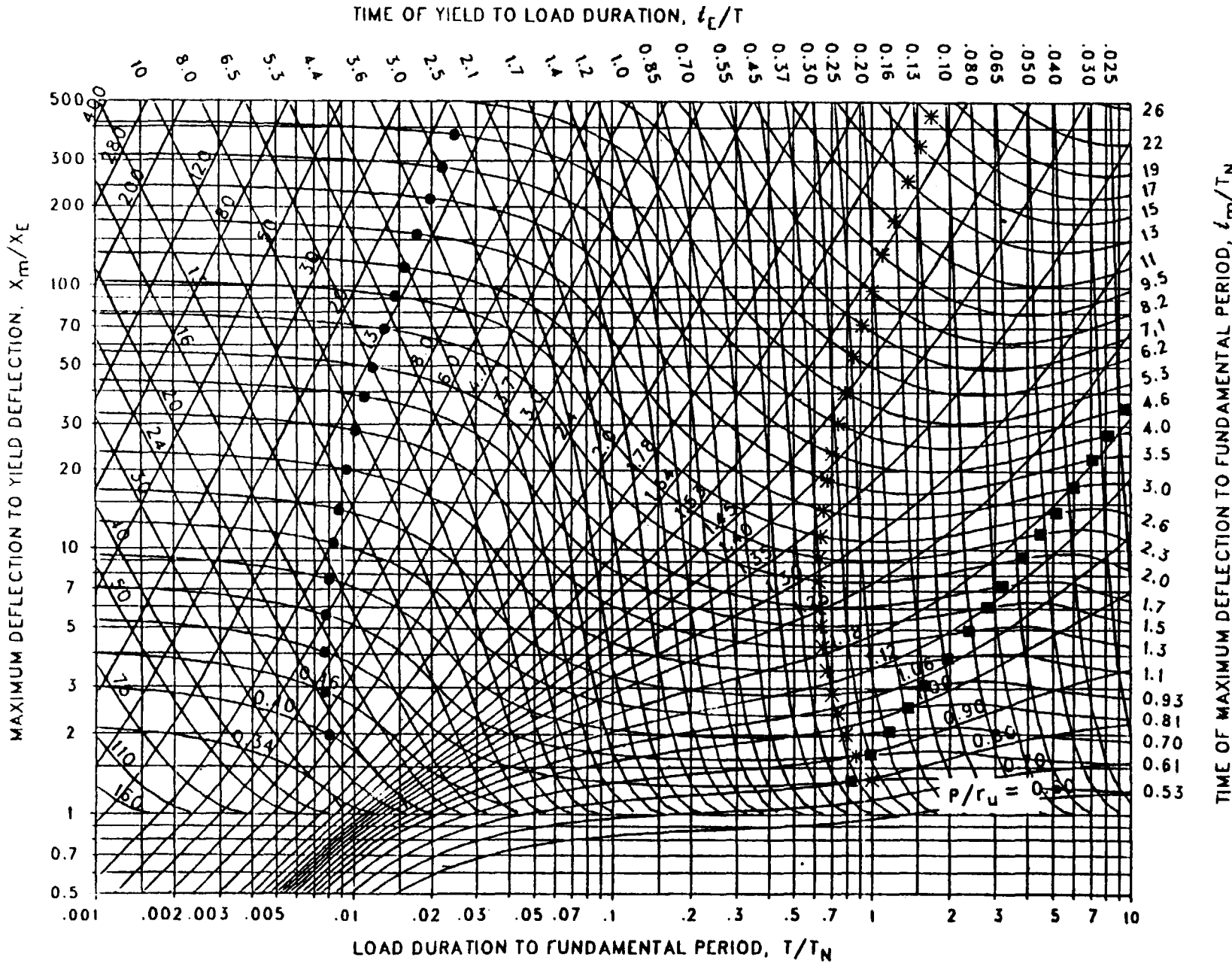


Figure 3-117 Maximum response of elasto-plastic, one-degree-of-freedom system for bilinear-triangular pulse ($C_1 = 0.750$, $C_2 = 30$)

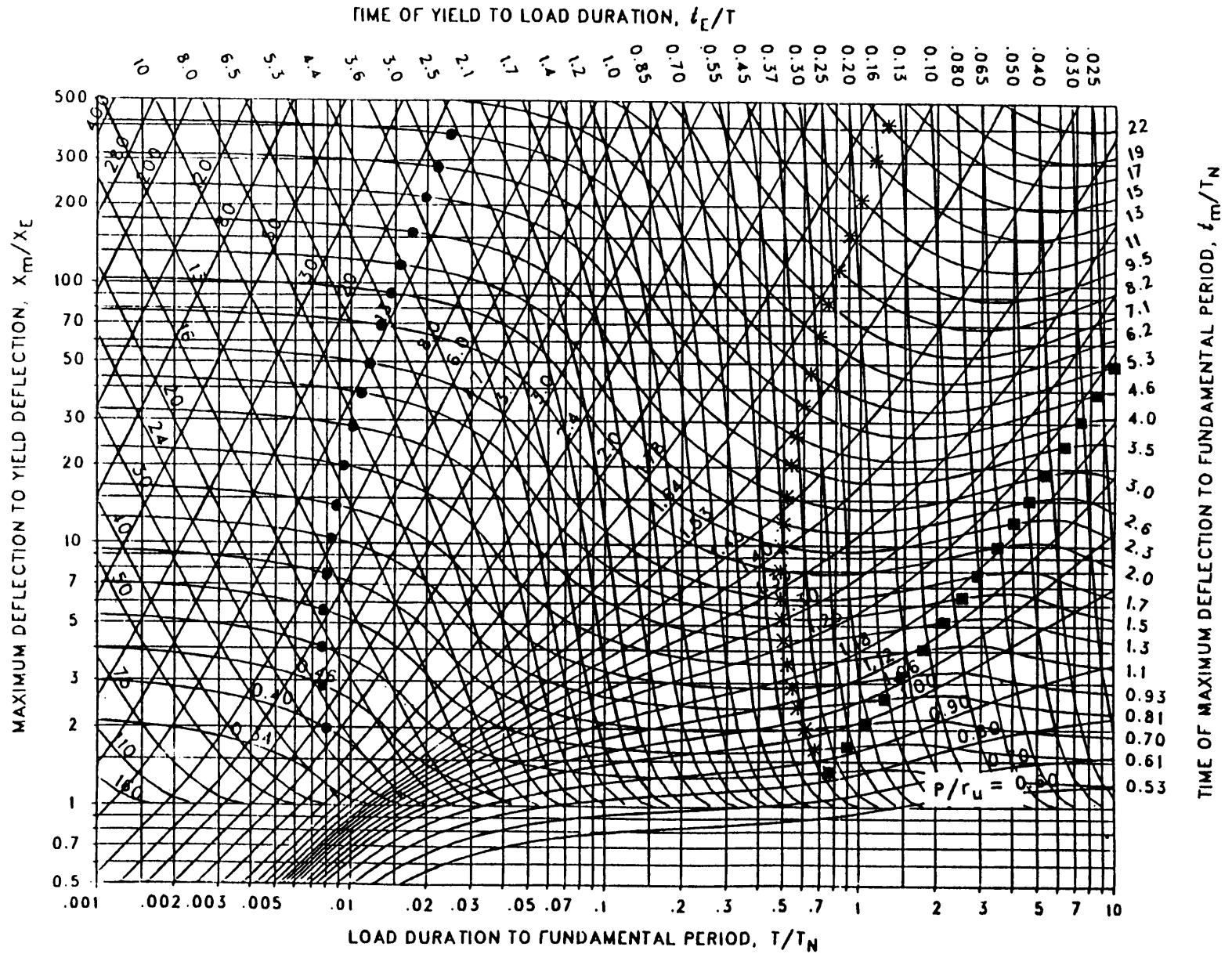


Figure 3-118 Maximum response of elasto-plastic, one-degree-of-freedom system for bilinear-triangular pulse ($C_1 = 0.715$, $C_2 = 30$)

3-177

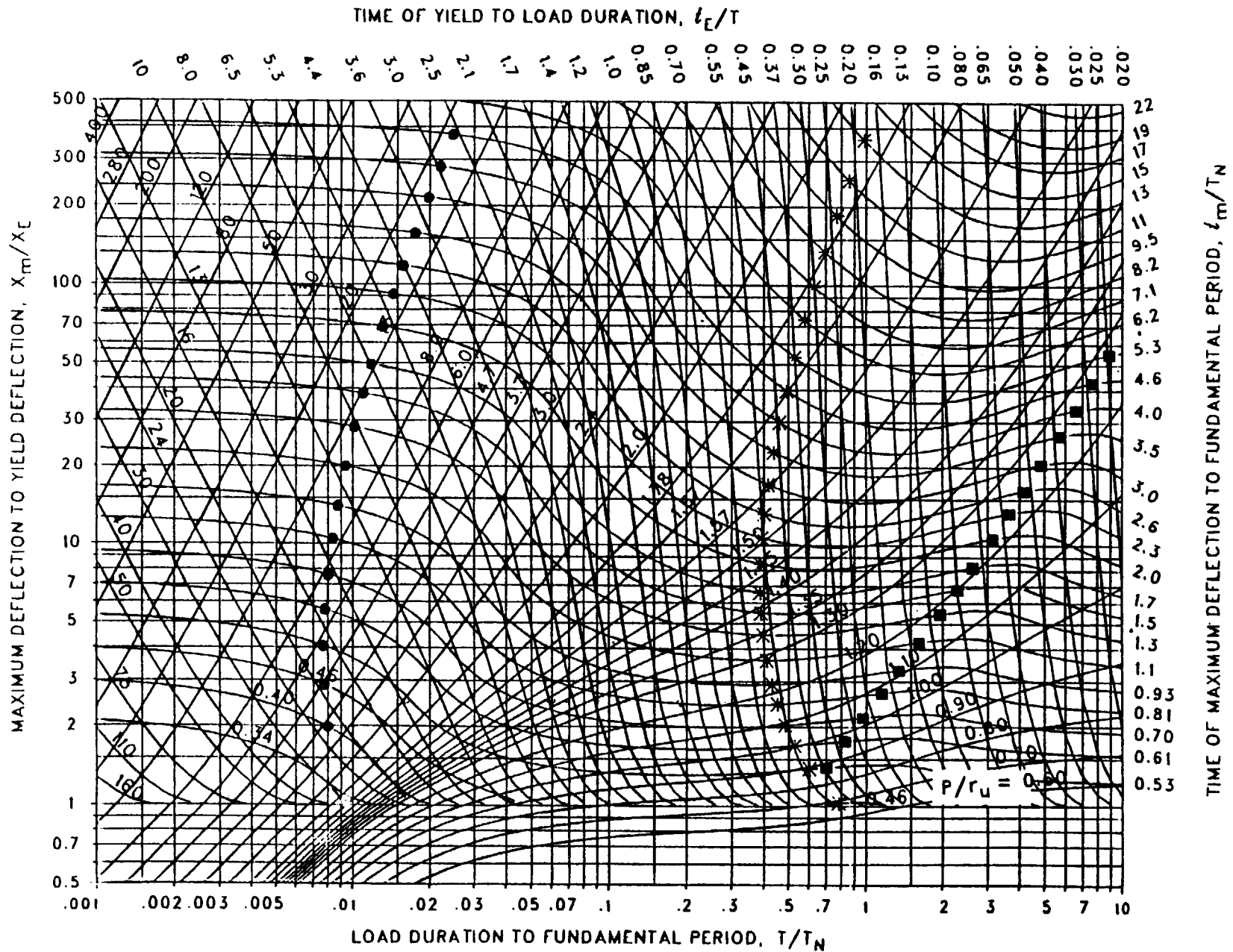


Figure 3-119 Maximum response of elasto-plastic, one-degree-of-freedom system for bilinear-triangular pulse ($C_1 = 0.681$, $C_2 = 30$)